Molecular Mechanisms of Natural Compounds : Compound Kushen Injection (CKI) in Cancer

By

THAZIN NWE AUNG

THE UNIVERSITY *of* ADELAIDE

Department of Molecular and Biomedical Science

School of Biological Sciences

A thesis presented for the degree of DOCTOR OF PHILOSOPHY

JANUARY 2019

Foreword

“The important thing is NOT TO STOP QUESTIONING. Curiosity has its own reason for existence. One cannot help but be in awe when he contemplates the mysteries of eternity, of life, of the marvellous structure of reality. It is enough if one tries merely to comprehend a little of this mystery each day.”

— Albert Einstein

"*Old Man’s Advice to Youth: ’Never Lose a Holy Curiosity’*."
LIFE Magazine (2 May 1955): p 64.

Abstract

Chemotherapy is a treatment that uses cytotoxic drugs to kill rapidly dividing cancer cells. There are many anti-cancer chemotherapeutic drugs used alone or in combination with others to kill cancerous cells, and some of these, are of plant origin. Naturally occurring compounds, such as Taxol, are used in chemotherapy and have very specific, unique, molecular targets. However, according to the World Health Organization (Ekor, 2014), approximately eighty percent of the world's population depends on natural compounds from traditional medicine and these compounds are widely used in complementary medicine as anti-cancer drugs (Foster et al., 2000). Traditional Chinese medicine (TCM) uses treatments that contain multiple natural compounds, a number of which have been claimed to be of therapeutic benefit to cancer sufferers (Chung et al., 2015). Some TCM preparations have shown anti-cancer, anti-migratory and anti-metastatic properties in laboratory settings (Wang et al., 2009;Pan et al., 2011;Qu et al., 2016). Research suggests that TCM natural compound mixtures might synergistically trigger therapeutic benefits through the action of multiple components affecting multiple regulatory signaling targets (Wang et al., 2008).

Compound Kushen injection (CKI) is a TCM anticancer agent which has been approved by the Chinese State Food and Drug Administration to treat solid tumors in combination with chemotherapy drugs in clinics for pain relief, cancer metastasis and enhancement of the immune system since 1995, and is used to treat approximately 30,000 patients daily. Although a large body of evidence has suggested CKI has anti-cancer properties (Xu et al., 2011;Gao et al., 2018) the anti-cancer mechanisms attributable to specific compounds within the mixture remain unknown. CKI contains multiple alkaloid and flavonoid compounds and the main bioactive compounds such as matrine and oxymatrine have shown to affect cancer cells in the lab. However, other medicinal herbs containing these two compounds as main components have demonstrated patient toxicity. It is therefore important to better understand the effects of CKI, particularly with respect the contributions of individual compounds within the mixture.

In this thesis, I describe a multi-disciplinary approach including analytical chemistry, cellular assays and transcriptome analysis to explore the effects of several major compounds present in CKI. Through the application of a subtractive fractionation method that removed individual compounds one, two or three at a time, I have been able to map these compounds and their interactions to specific pathways based on altered gene

expression profiles. This has illuminated the roles of several major compounds of CKI, that on their own, have no, or minimal, activity in our bioassay. This approach has enabled us to identify the interactions between compounds in a mixture as shown by the response of cancer cell cultures. Using a systems biology approach along with cellular migration and invasion assays, I have mapped the activity of related proteins and pathways which may contribute to the migrastatic activity of CKI.

Altogether, this thesis presents an initial characterization of the underlying mechanistic changes induced by CKI. First, by comparing differentially expressed genes across treatment combinations generated using our subtractive fractionation approach, I identified specific candidate pathways that were altered by the removal of compounds from the mixture. Second, by using transcriptome data of a breast cancer cell line, the effects of CKI on candidate anti-migratory pathways for six different cancer cell lines were assessed. These experiments identified specific candidate target pathways through which CKI might act. These approaches can be used to understand the roles and interactions of individual compounds from any complex natural compound mixture whose biological activity cannot be associated with purified compounds.

Keywords: *Systems biology , Natural Compounds, TCM, CKI, Multi-target medicine, Anticancer, Pathway/ network research, Cell Migration, Cell Invasion, Cell cycle, Cancer metabolism*

Dedication and Acknowledgements

First and foremost, I would like to express my appreciation to my supervisor David Adelson. It has been an honour to be his Ph.D. student. He has taught me, both consciously and un-consciously throughout my study. I appreciate all his contributions of time, ideas, and funding to make my Ph.D. experience productive. The joy and enthusiasm he has for his research was contagious and motivational for me, even during tough times in the Ph.D. pursuit. I have been extremely lucky to have Dave as my supervisor who cared so much about my work. Without his effort, help and guidance, I would have been nowhere. THANK YOU VERY MUCH DAVE!

I also would like to take an opportunity to thank my co-supervisor Dan Kortschak for his friendly guidance and expert advice throughout all stages of the work. His extended discussions, encouragements and valuable suggestions have contributed greatly to the improvement my Ph.D. work. I learnt many new things because of Dan and I could not have imagined a better co-supervisor for my Ph.D. study. Because of Dan, I came to realize that demonstrating is the most enjoyable experience I could ever have during my Ph.D. THANK YOU SO MUCH DAN!

The members of the Adelson group have contributed immensely to my personal and professional time at University of Adelaide. I am especially grateful to Zhipeng Qu for providing timely advice and support whenever I am in need. I am forever grateful for that. I would like to acknowledge Yuka Harata-Lee for patiently helping my experiments and making my learning process a fun and enjoyable experience. I also want to appreciate my friends and lab-mates Jian, Joy, Hanyuen, Lu, Catisha, Atma, Reuben, James, Carey, Urwah, Sydney and Chandler. We worked together, and the group has been a source of friendships as well as good advice and collaboration. I have had the pleasure to work with all of you.

Especially, I would like to thank Dr. Denis Scalon, Chemistry Department, for his help regarding to the usage of HPLC. Without his help, I would not have been able to successfully complete my projects. I would like to extend my special gratitude to Andrea Yool for providing new perspectives to my research. Your advice and help for my experiments have been invaluable. Special thanks to Merry Wickes for her warm friendship. Your presence was one of the reasons that makes my stay very enjoyable in Adelaide.

This work would not have been possible without the scholarship from The University of Adelaide. I am very grateful for the Beacon of Enlightenment Ph.D. scholarship which enabled me to complete my study and assist my future endeavours.

Lastly, I would like to thank my family for all their love and encouragement. For my parents, my brother and sister who raised me with a love of science and supported me in all my pursuits. And most of all for my loving, supportive, encouraging, and patient husband Saeed whose faithful support throughout all the stages of this Ph.D. is very much appreciated. THANK YOU SO MUCH!

Declaration

I certify that this work contains no material which has been accepted for the award of any other degree or diploma in my name in any university or other tertiary institution and, to the best of my knowledge and belief, contains no material previously published or written by another person, except where due reference has been made in the text. In addition, I certify that no part of this work will, in the future, be used in a submission in my name for any other degree or diploma in any university or other tertiary institution without the prior approval of the University of Adelaide and where applicable, any partner institution responsible for the joint award of this degree.

I give consent to this copy of my thesis when deposited in the University Library, being made available for loan and photocopying, subject to the provisions of the Copyright Act 1968.

The author acknowledges that copyright of published works contained within this thesis resides with the copyright holder(s) of those works.

I also give permission for the digital version of my thesis to be made available on the web, via the University's digital research repository, the Library Search and also through web search engines, unless permission has been granted by the University to restrict access for a period of time.

SIGNED: .... DATE: .....17/01/2019.....

Table of Contents

Chapter 1

Introduction: Understanding the Effectiveness of Natural Compound Mixtures in Cancer through Their Molecular Mode of Action

The work of this dissertation is two-fold. First, I have implemented a subtractive fractionation method through which I explore the effect of compounds in the CKI mixture on treated cancer cells. I have also applied cellular bioassays and transcriptomic analyses to determine the phenotypic and gene expression changes in cells treated with drug fractions. For the second part of the dissertation, I have performed transcriptome analysis of CKI treated breast cancer cells to study the role of CKI and its fractions on metastatic processes. This chapter provides an overview of the efficacy of traditional medicine natural compounds mixtures in the context of cancer. I also discuss the biased/flawed scientific evidence from natural products that suggests false positive therapeutic benefits during drug screening. This chapter is in the format of the manuscript that was published in the *International Journal of Molecular Life Sciences* as a review article.

Statement of Authorship

Title of Paper	Understanding the Effectiveness of Natural Compound Mixtures in Cancer through Their Molecular Mode of Action
Publication Status	☑ Published ☐ Accepted for Publication ☐ Submitted for Publication ☐ Unpublished and Unsubmitted w ork w ritten in manuscript style
Publication Details	Thazin Nwe Aung, Zhipeng Qu, R.Daniel Kortschak, David L. Adelson. "Understanding the Effectiveness of Natural Compound Mixtures in Cancer through Their Molecular Mode of Action". *Int. J. Mol. Sci.* 2017, *18*(3), 656; https://doi.org/10.3390/ijms18030656

Principal Author

Name of Principal Author (Candidate)	Thazin Nwe Aung		
Contribution to the Paper	Designed the study, performed the literature search and wrote the manuscript.		
Overall percentage (%)	70%		
Certification:	This paper reports on original research I conducted during the period of my Higher Degree by Research candidature and is not subject to any obligations or contractual agreements with a third party that would constrain its inclusion in this thesis. I am the primary author of this paper.		
Signature		Date	5/11/2018

Co-Author Contributions

By signing the Statement of Authorship, each author certifies that:

i. the candidate's stated contribution to the publication is accurate (as detailed above);

ii. permission is granted for the candidate in include the publication in the thesis; and

iii. the sum of all co-author contributions is equal to 100% less the candidate's stated contribution.

Name of Co-Author	Zhipeng Qu		
Contribution to the Paper	Generated Figure1, and assisted writing the manuscript.		
Signature		Date	5/11/2018

Name of Co-Author	R.Daniel Kortschak		
Contribution to the Paper	Assisted writing the manuscript.		
Signature		Date	5/11/2018

Please cut and paste additional co-author panels here as required.

Name of Co-Author	David L. Adelson		
Contribution to the Paper	Designed the study, and assisted writing the manuscript.		
Signature		Date	5/4/18

International Journal of
Molecular Sciences

MDPI

Review

Understanding the Effectiveness of Natural Compound Mixtures in Cancer through Their Molecular Mode of Action

Thazin Nwe Aung [1,2], Zhipeng Qu [1,2], R. Daniel Kortschak [1,2] and David L. Adelson [1,2,*]

[1] Department of Genetics and Evolution, School of Biological Sciences, The University of Adelaide, Adelaide, South Australia 5005, Australia; thazin.nweaung@adelaide.edu.au (T.N.A.); zhipeng.qu@adelaide.edu.au (Z.Q.); dan.kortschak@adelaide.edu.au (R.D.K.)

[2] Zhendong Australia China Centre for Molecular Chinese Medicine, The University of Adelaide, Adelaide, South Australia 5005, Australia

* Correspondence: david.adelson@adelaide.edu.au; Tel.: +61-8-8313-7555

Academic Editor: Toshio Morikawa
Received: 15 February 2017; Accepted: 15 March 2017; Published: 17 March 2017

Abstract: Many approaches to cancer management are often ineffective due to adverse reactions, drug resistance, or inadequate target specificity of single anti-cancer agents. In contrast, a combinatorial approach with the application of two or more anti-cancer agents at their respective effective dosages can achieve a synergistic effect that boosts cytotoxicity to cancer cells. In cancer, aberrant apoptotic pathways allow cells that should be killed to survive with genetic abnormalities, leading to cancer progression. Mutations in apoptotic mechanism arising during the treatment of cancer through cancer progression can consequently lead to chemoresistance. Natural compound mixtures that are believed to have multiple specific targets with minimal acceptable side-effects are now of interest to many researchers due to their cytotoxic and chemosensitizing activities. Synergistic interactions within a drug mixture enhance the search for potential molecular targets in cancer cells. Nonetheless, biased/flawed scientific evidence from natural products can suggest false positive therapeutic benefits during drug screening. In this review, we have taken these factors into consideration when discussing the evidence for these compounds and their synergistic therapeutic benefits in cancer. While there is limited evidence for clinical efficacy for these mixtures, in vitro data suggest that these preparations merit further investigation, both in vitro and in vivo.

Keywords: cancer; apoptosis; chemosensitization; microRNA; natural compound mixtures; metal derivatized natural compounds

1. Introduction

Cancer remains one of the highest causes of death globally. Various types of chemotherapies fail due to adverse reactions, drug resistance, and target specificity of some types of drugs. There is now emerging interest in developing drugs that overcome the problems stated above by using natural compounds, which may affect multiple targets with reduced side effects and which are effective against several cancer types. Natural compounds from various sources including plants, animals, and microorganisms offer a great opportunity for discovery of novel therapeutic candidates for the treatment of cancer [1]. Apoptosis is a self-destructive programmed sequence of signal transduction events that destroys cells that become a threat, or are no longer necessary to the organism [2]. When there is aberrant apoptosis, cells that should be killed instead become immortal, leading to the pathogenesis of many diseases including cancer.

Apoptosis falls into two categories: extrinsic and intrinsic apoptosis. Extrinsic apoptosis occurs when cell death is triggered by binding of extracellular stress ligands to transmembrane receptors such

as death receptors CD95 (APO-1/Fas) and tumor necrosis factor (receptor1) [3] as well as dependence receptors such as netrin-1 receptor UNC5H4 [4,5]. In contrast, intrinsic apoptosis occurs in the mitochondria through heterogeneous signaling cascades dependent or independent of caspases [4]. Failure to trigger complete apoptosis in the unhealthy cell population is a cause for cells to grow out of control, leading to cancer [6]. When apoptosis is defective in one of the main apoptotic pathways, it increases the likelihood of the cell becoming cancerous. Various well-established treatments have been designed to destroy cancer cells through apoptosis. Another important mechanism of cell death in cancer cells in response to chemotherapy is autophagy, which takes places in the lysosome by self-degrading intracellular proteins and organelles. It triggers cell death in the absence of apoptotic regulators, but in the presence of important autophagy-regulated genes such as *BECN1* [7] and *ATG5* [8]. In this review, we primarily confine our discussion to apoptotic cell death and autophagic cell death caused by natural chemotherapeutic agents in the context of cancer.

Resistance to treatments that target apoptotic cell death is indicative of treatment failure. Anti-apoptotic mutations during cancer progression reduce chemotherapy-induced apoptosis in spontaneous murine tumors [9] and produce multi-drug resistance [10]. Therefore, understanding how to induce cell cytotoxicity via chemosensitization is as important as how to trigger apoptosis in cancer cells with chemotherapies. It has been reported that natural compounds such as quercetin [11] and tetrandrine [12], known to have anti-tumor activities, are able to not only kill cancer cells but also restore drug sensitivity [13,14]. Moreover, there is evidence that natural compounds including rhamnetin and cirsiliol can radiosensitize in non-small cell lung cancer (NSCLC) [15]. This suggests that natural compounds can have therapeutic effects in cancer chemo-radiotherapy.

Effective development of an anti-cancer drug needs to consider different sets of upregulated, downregulated, and mutated genes and their regulatory pathways in cancer cells. Computational genomics is a powerful tool to identify differential gene expression based on cancer treatment, as it improves our understanding of challenging mechanistic changes in cancer cells and facilitates treatment with a wide range of molecular targets. Whole transcriptome sequencing comprehensively investigates messenger RNA (mRNA)-Seq and small/non-coding RNA-sequencing (RNA-Seq), analyzing tens of thousands of RNA transcripts to uncover their genetic functions. Transcriptomic results subjected to Gene Ontology (GO) clustering and annotation identify differentially expressed genes and can further identify candidate target pathways [16]. Here we highlight the efficacy of complex natural compound mixtures by using molecular approaches with specific emphasis on cancer apoptosis and chemosensitization.

2. Treatment of Cancer through Targeting Apoptosis

There are many therapies for treating cancer, including surgery, radiation therapy, hormone therapy, chemotherapy, and targeted therapies such as immunotherapy and monoclonal antibody therapy. Depending on the type of cancer and underlying biological conditions in the patient, therapy consists of either a single or combination of classical treatments such as surgery, chemotherapy, and/or radiotherapy.

Chemotherapy is a treatment that uses anti-cancer drugs to damage DNA in unhealthy and rapidly dividing cancer cells. Chemotherapy with a defined dosage is usually used to trigger cancer cell cytotoxicity at desirable apoptotic rates. The effectiveness of chemotherapeutic agents depends on their type, dosage, and any adverse reactions in patients. There are several anti-cancer drugs used alone or in combination with other agents to kill cancerous cells. Chemotherapeutic drugs that include synthetic, semi-synthetic, and naturally occurring compounds are cytotoxic, and can destroy both cancerous cells and rapidly dividing normal cells. These agents signal through both death receptors and mitochondrial pathways to induce one or more of the apoptotic pathways [17]. They are characterized based on their structure, derivation, and mechanism of action. Some affect parts of the cell cycle, while others are not phase specific. Depending on the mechanism of action, they are categorized into different groups including alkylating antineoplastic agents, kinase inhibitors, vinca alkaloids,

anthracyclines, antimetabolites, aromatase inhibitors, and topoisomerase inhibitors [18]. Nonetheless, the pharmacokinetic variability of synthetic drugs in patients often limits optimal effectiveness with minimal toxic side effects. On the other hand, treatment of cancer by natural compounds and their semi-synthetic analogues both in vitro and in vivo shows promising results against different malignancies [19,20]. Natural compounds such as sesquiterpenes, flavonoids, alkaloids, diterpenoids, saponins, and polyphenolic compounds [11,21] can be substituted for, or applied in combination with, existing drugs.

3. Natural Compounds as Anti-Cancer Agents

Natural compounds with potent anti-cancer activities are widely available from different plant tissues. Eighty percent of the population worldwide traditionally use natural compounds contained in medicinal plants [22] and are largely dependent on them. Naturally occurring compounds target tumor cells by regulating cell death pathways such as extrinsic and intrinsic apoptosis pathways and autophagic pathways. Evidence from in vitro and in vivo studies in prostate cancer treatment with isoflavones and phytoestrogens from soy showed NF-κB deactivation, apoptosis induction, and angiogenesis inhibition [23,24]. A collection of plant-derived natural anti-cancer compounds can be found at Naturally Occurring Plant-based Anti-cancer Compound-Activity-Target Database (NPACT, http://crdd.osdd.net/raghava/npact/) where approximately 1980 experimentally validated compound-target interactions are documented [25]. Millimouno et al. also reviewed promising natural compounds and their related natural sources, pharmacological actions, and molecular targets in details [21].

4. Traditional Chinese Medicines (TCMs) as Anti-Cancer Agents

Due to the complex etiology and pathophysiology of cancer, it is relatively difficult to treat the disease with just single target drugs. Moreover, regardless of the specificity and efficiency of single target therapy, it is difficult to achieve optimal cytotoxic effects on cancer cells because of their rapid molecular adaptations. In contrast, synergistic interactions within multi-component drug preparations allow us to broaden the search for potential molecular targets in cancer cells. Traditional Chinese Medicines (TCM) is formulated based on the compatibility and interrelationships between herbal ingredients that render synergistic therapeutic benefits [26]. TCM uses a combinatorial approach where the application of two or more agents at their respective effective concentrations achieves a synergistic effect that boosts cytotoxicity to cancer cells and can have additional effects on the tumor environment and the immune response to tumors. Therefore, TCM has been used as an alternative or complementary medicine worldwide, and has long been used to treat cancer in China. Chinese herbal medicinal products have been used for cancer prevention and treatment for many years [27], and there is evidence to suggest that TCMs are effective against cancer recurrence and metastasis and can enhance quality of life (QoL), and prolong survival time [27]. For instance, Bioactive polysaccharides with β-1,3, β-1,4, and β-1,6 side branches in TCM stimulate the immune system, thereby indirectly suppressing tumors [28]. TCM is also used to reduce the side effects of conventional chemotherapy for advanced pancreatic cancer, advanced colorectal cancer, and breast cancer [29–31]. There are a range of TCM extracts from *Anemarrhena asphodeloides*, *Artemisia argyi*, *Commiphora myrrha*, *Duchesnea indica*, *Gleditsia sinensis*, *Ligustrum lucidum*, *Rheum palmatum*, *Rubia cordifolia*, *Salvia chinensis*, *Scutellaria barbata*, and *Uncaria rhychophylla* that specifically inhibit cancer cell proliferation from breast, lung, pancreas, and prostate tissues of human and mouse, but show limited inhibition against normal human mammary epithelial cell growth [32]. Artemisinin derivatives artesunate (ART) and dihydroartemisinin have been shown to inhibit cancer cell proliferation and suppress angiogenesis in cervical, uterus chorion, embryo transversal cancer, and ovarian cancer [33]. Because naturally occurring compounds such as plant extracts in TCM are highly chemically diverse, they have become highly significant in the discovery and development of effective therapeutic anti-cancer drugs. TCM preparations can contain

alkaloids, flavonoids, saponins, terpenes, polyphenols, fatty acids, and essential oils as bioactive ingredients [34,35].

4.1. Natural Compounds from TCM as Cancer Therapeutics

The main components of TCM such as alkaloids, flavonoids, and saponins are used either individually or as mixtures to treat different types of cancer. Below we list compounds contained in various TCMs that have been found to have anti-cancer activities, including triggering apoptosis.

4.2. Alkaloids

Alkaloids are more abundantly found in broad ranges of the plant kingdom than other classes of natural plant products [36] and are active against various cancers. Alkaloids commonly consist of a nitrogen atom within a heterocyclic ring [37] and are of relatively low toxicity. Several alkaloids have a wide range of significant biological functions including anti-inflammatory, anti-bacterial, anti-diabetic, and anti-cancer activities [38–40]. Some well-developed semi-synthetic anti-cancer drugs are alkaloid derivatives including vinblastine, vinorelbine, vincristine, and vindesine. They are the most important active ingredients in traditional medicine and have been approved for cancer treatment in the United States and Europe [41].

Matrine is a major quinolizindine alkaloid found in the *Sophora flavescens* Aiton plant [42]. Matrine stimulates major apoptotic cascades by upregulating Fas/FasL and Bax, and downregulating Bcl-2 leading to the activation of caspase-3, -8, and -9 in MG-63, U-2OS, Saos-2, and MNNG/HOS human osteosarcoma cells [43]. It also represses cancer metastasis via vascular endothelial growth factor (VEGF)-Protein Kinase B (Akt)-nuclear factor kappa-light-chain-enhancer of activated B cells (NF-κB) signaling in MDA-MB-231 breast cancer cells. The reduction of Bcl-2/Bax protein and mRNA levels by matrine leads to an increase of cell cycle arrest in cancer cells [44]. In human medulloblastoma D341 cells, increased expression of Bcl-2 and decreased expression of Bax is triggered by matrine through caspase-3 and -9 mediated apoptotic pathways [45]. In HepG2 cells, matrine induces tumor suppressor transcription factor p53 through the adenosine monophosphate-activated protein kinase (AMPK) signal transduction pathway, resulting in autophagic cell death through the p53/AMPK signaling pathway [46]. Interestingly, this research reported that downregulation of AMPK leads to a switch to apoptotic cell death from autophagic cell death [46]. The sequential signal transduction leading from autophagy to apoptosis via the activation of p53 was discussed by Guillermo Mariño et al. [47]. Furthermore, metabolomics analysis of matrine treated HepG2 cells identified lipid droplet metabolites, which are substrates for macro autophagy that may partly drive immunity and apoptosis [48]. Li et al. also reported that matrine treatment reduced the level of glutathione (GSH), and the elevated level of GSH is related to chemoresistance in cancer [49]. The above results provide evidence that matrine alone can induce cell death and can be effective against various tumor types.

Oxymatrine is another major quinolizindine alkaloid found in the *Sophora flavescens* Aiton plant. It is cytotoxic to SW1116 human colon cancer cells by downregulating human telomerase reverse transcriptase (hTERT) and upregulating *p53* as well as *mad1* in a concentration dependent manner [50]. It also inhibits the growth of GBC-SD and SGC-996 gallbladder cancer cells via the activation of caspase-3 together with Bax and the suppression of Bcl-2 and NF-κB [51]. It is also known that a mixture of oxymatrine and micellar nanoparticles is an effective proliferation inhibitor of SMM7721 cells [52]. Oxymatrine treatment significantly induces apoptosis by increasing Bax protein expression and reducing Bcl-2 in human lung cancer A549 cells [53]. Proteomic analysis has shown that oxymatrine induces apoptosis in HeLa cells by inhibiting inosine monophosphate dehydrogenase type II (IMPDH2), mitochondrial related apoptotic protein [54]. These studies suggest that oxymatrine may be a useful drug candidate for cancer therapy.

Another type of natural alkaloid is tetrandrine, contained in the Chinese medicinal plant Hang-Fang-Chi, *Radix Stephania tetrandra* S. Moore. This compound has anti-inflammatory, immunosuppressive, and anti-cancer activities [55]. It was reported that a derivative (H1) of tetrandrine

has the ability to reverse multi-drug resistance [56]. It inhibits cancer cell proliferation and induces apoptosis in human esophageal cancer cell lines ECa109, Eca109-C3, and human monoblastic leukemic U937 cells. It is also effective in reversing multi-drug resistance in Adriamycin-resistant human breast cancer MCF-7/Adr and human nasopharyngeal cancer KB_{v200} [12]. The molecular mechanisms of action of tetrandrine in cancer cells include upregulation of Bax, Bak, Bad, and apaf-1, downregulation of Bcl-2 and Bcl-xl, releasing cytochrome *c*, and activation of caspase-3 and -9 in the apoptotic mitochondrial pathway [56]. The efficacy of tetrandrine with respect to activation of the intrinsic apoptosis pathway highlights its potential importance as a therapeutic agent.

The semi-synthetic alkaloid analogue vinblastine is an anti-mitotic drug that was originally isolated from the periwinkle plant *Catharanthus roseus* (L.) G. Don. It kills cancer cells by shortening microtubules, disrupting microtubule function resulting in the disappearance of the mitotic spindle, thereby inhibiting cell proliferation [57]. Low concentrations of vinblastine have been shown to slow down or block mitosis in HeLa and BSC cells [57]. Vinblastine is highly potent in relapsed/refractory anaplastic large-cell lymphoma (ALCL) with 65% five-year overall survival [58].

4.3. Flavonoids

Flavonoids are plant secondary metabolites, widely present in fruits and vegetables that are consumed daily. They generally have a sixteen-carbon skeleton and the structures vary around the heterocyclic oxygen ring [59]. Research has shown that flavonoids inhibit cell proliferation and angiogenesis, cause cell cycle arrest, induce cell apoptosis, and reverse multi-drug resistance and/or a combination of the aforementioned mechanisms [60].

Trifolirhizin, a pterocarpan flavonoid, is present in the *Sophora flavescens* Aiton plant. It was shown that trifolirhizin reduces the expression of pro-inflammatory cytokines such as TNF-α, cyclooxygenase-2 (COX-2) and IL6 in experimentally lipopolysaccharide (LPS)-stimulated mouse J774A.1 macrophage [61]. Zhou et al. also showed that it was able to inhibit the growth of human ovarian A2780 and lung H23 cancer cells in vitro. The compound also has anti-proliferative activity in oral carcinoma SCC2095 cells [62]. A combination of trifolirhizin together with maackiain (a constituent of *Trifolium pratense*) has been shown to induce apoptosis in human leukemia HL-60cells. This mixture of compounds resulted in the degradation of DNA into oligonucleosome-size fragments in a time- and dose- dependent manner [63]. These results suggest that trifolirhizin may possibly be developed as an anti-inflammatory nutraceutical for cancer prevention as well as for the mitigation of DNA damage through apoptosis.

Curcumin is a traditional medicine and main curcuminoid of *Curcuma longa* and has been implicated in the perturbation of several genetic pathways [64,65]. It was reported that it selectively targets tumor cells rather than normal cells in vitro and activates different apoptotic pathways including caspase, induction of death receptors and DNA fragmentation, mitochondrial activation, autophagy pathways, inhibition of NF-κB, and inhibition of COX-2 and 5 LOX [65]. In proteomic identification of curcumin treated MCF-7 cells, 3-PGDH and ERP29 were found to be upregulated and TDP-43, SF2/ASF, and eIF3i were downregulated, suggesting curcumin induced apoptosis in breast cancer [64]. However, due to its lack of aqueous solubility, high concentrations are required to demonstrate potential chemotherapeutic efficacy [66]. While many researchers are optimistic regarding curcumin's potential effectiveness against cancer, there is evidence to show that curcumin has no therapeutic benefits despite many published articles and clinical trials [67]. Skepticism about curcumin is based on both poor characterization of curcumin and pan-assay interference in many experiments that indicated that curcumin was a promising compound for cancer treatment. Yet, in spite of no significant effects in trials, researchers still think that because curcumin can interact with many proteins and because of suggestive trends in trial results, there is still justification for further study [68]. Until better experiments are carried out, the anti-cancer activity of curcumin remains unconfirmed.

A flavonoid, quercetin, is abundant in daily-consumed foods such as onions (*Allium cepa*) with a wide range of anecdotally reported health benefits that include anti-oxidant, anti-inflammatory,

and anti-cancer activities in vitro and is effective against various cancer cells [69]. Quercetin mainly targets the cell cycle at G1/S and G2/M check points by inducing the p21 CDK inhibitor while decreasing pRb phosphorylation, thereby blocking E2F1, which is an important transcription factor of DNA synthesis proteins [70]. Deng et al. reported that apoptosis-mediated cell death from quercetin treatment resulted from arresting the cell cycle at G0/G1 phase in MCF-7 breast cancer cells. They also showed that increasing concentrations of quercetin were directly proportional to the decreasing concentrations of survivin, a member of a protein family that negatively regulates apoptosis [71]. Proteomic analysis revealed that quercetin treatment suppressed cell proliferation while arresting mitosis leading to apoptosis by downregulating IQGAP1 and β-tubulin and their interactions with other proteins in HepG2 cells [72]. Despite the abundance of quercetin, it has not been investigated in cancer clinical trials.

4.4. Saponins

Saponins are found not only in a wide range of plants but also in animals, and have different carbon backbones that classify them as either steroids or triterpenes. They are secondary metabolites with potent biological functions. These compounds are active against several tumors not only as single compounds but also in combination with conventional therapies by causing cell cycle arrest and triggering apoptosis [73].

Chikusetsusaponin IVa butyl ester (CS-IVa-Be) is an apoptotic triterpenoid saponin extracted from *Acanthopanas gracilistylus* herb. The extract from this Chinese medicinal herb has been found to cause cell cycle arrest at G0/G1 stage in a variety of cancer cell lines including MT-2, Raji, HL-60, TMK-1, and HSC-2 [74]. The compound induces apoptosis in MDA-MB-231 cells by inhibiting IL-6 family induced STAT3 activity through the IL-6/JAK/STAT3 signaling pathway. It also sensitizes the Tumor necrosis factor (TNF)-related apoptosis-inducing ligand (TRAIL), a specific inducer of cancer cell apoptosis, in TRAIL resistant MDA-MB-231 cells by upregulating death receptor 5 (DR5) [75]. Because of this, CS-IVa-Be induces apoptosis upon treatment with TRAIL in TRAIL resistant MDA-MB-231 cells.

Polyphyllin D is a promising anti-proliferative steroidal saponin extracted from the traditional Chinese medicinal plant *Paris polyphylla*. The cytotoxic activity of polyphyllin D was observed via induction of DNA fragmentation and dissipation of mitochondrial membrane potential $\Delta\psi m$, resulting in mitochondrial dysfunction and loss of membrane integrity in MCF-7 and MDA-MB-231 cells [76]. A 50% reduction in tumor growth from 10 consecutive days of polyphyllin D administration in mice was also documented.

Diosgenin is effective against HCT-116 human colon cancer cells by reducing both mRNA and protein expression of 3-hydroxy-3-methylglutaryl CoA reductase, resulting in apoptosis [77]. It truncated the poly (ADP-ribose) polymerase protein from 116-kDa to an 85 kDA fragment, which leads to the induction of apoptosis. This indicates that Diosgenin is a potent apoptosis inducer in HCT-116 cancer cells. Diosgenin arrested the cell cycle at sub-G1 phase, suppressed FAS expression, and inhibited mammalian target of rapamycin (mTOR) phosphorylation in HER2 overexpressing human AU565 breast cancer cells, inhibiting cell proliferation [78].

Another apoptotic triterpenoid saponin is Macranthoside B (MB), extracted from *Lonicera macranthoids*. It is strongly effective in various tumors via mitochondrially mediated apoptosis resulting from an increased Bax/Bcl-2 ratio [79]. Furthermore, MB induced apoptosis via autophagy through the ROS/AMPK/mTOR pathway, while elevating reactive oxygen species (ROS) together with 5′ AMPK, and reducing mTOR in human ovarian cancer A2780 cells [80].

With respect to the cytotoxic properties of saponins, a wide range of these compounds has been tested, with some shown to be potent apoptotic inducers. Yet the potential of this class of compounds remains to be fully explored, and they may also be effective in combination with other agents to synergistically enhance their therapeutic effect in cancer.

4.5. Drugs Based on Mixtures of Compounds

Compound Kushen Injection (CKI), approved by the State Food and Drug Administration of China, has been used to treat different types of cancer, including liver, gastric, and non-small cell lung carcinoma in combination with Western anti-cancer agents [81]. It contains alkaloids, flavonoids, saccharides, and organic acids [82] and is extracted from two medical herbs including *Radix Sophorae flavescentis* and *Rhizoma Smilacis Glabrae* [83]. It modulates immunity, decreases inflammation, relieves cancer pain, and, most importantly, has anti-neoplastic activity [83]. For example, CKI downregulates β-catenin through the Wnt signaling pathway, which in turn targets the oncogenes *c-MYC* and *CyclinD1* [84], leading to suppression of MCF-7 cancer stem cell-like side population (SP) cells [85]. A systematic review and meta-analysis reported that CKI could reduce adverse effects in cancer patients and improved total pain relief and QoL [86]. Transcriptome analysis of CKI treated MCF-7 cells by Qu et al. revealed that the mixture inhibited cell proliferation and induced apoptosis in a concentration-dependent manner by primarily targeting the cell cycle in MCF-7 cells [87]. Qu et al. also showed that long non-coding RNA (lncRNA) *H19* was dramatically downregulated in MCF-7 cells treated with CKI [87]. *H19* is overexpressed in several cancer types and is associated with tumor metastasis, for example, where lncRNA *H19* suppresses miR-630, perturbing the inhibition of EZH2 in nasopharyngeal carcinoma [88]. The primary effect of CKI on cancer cells is through the cell cycle, but it also affects many other pathways and it may be useful as both an anticancer and anti-inflammatory agent. It was claimed that CKI is effective in inhibiting metastasis and reversing multi-drug resistance (MDR) as well [83]. Yet, there is currently no research evidence supporting the effectiveness of CKI on reversing MDR in English-language journals. Therefore, in vivo and clinical relevance of the drug should be researched to establish the effective usage of CKI with respect to chemosensitizing activities.

Anti-tumor B (ATB), known as Zeng Sheng Ping, is also an herbal medicine which is formulated from six different medicinal plants, and its main constituents are flavones, alkaloids, phytosterols, sapogenins, triterpenes, and triterpenoids [89]. ATB decreased lung tumor load by approximately 60% in both wild-type and Ink4a/Arf tumor suppressor gene-deficient mice and 90% in p53 transgenic mice [89]. The drug markedly reduced cell proliferation by inhibiting the mitogen-activated protein kinase (MAPK) pathway while increasing apoptosis by reducing Bcl-2 in oral cancer in hamsters [90]. Lim et al. also showed that the Notch2 receptor, which is an important signaling regulator of brain tumors, and its downstream effector gene *Hes1* were downregulated by ATB [91]. ATB induced apoptosis in both U87 glioblastoma and DAOY medulloblastoma cells [91], suggesting that ATB might be effective against multiple tumors. Based on the results from animal models, ATB has shown chemo-preventive activities in hamsters and mice with carcinogen-induced oral cancers [92]. Microarrays, combined with GenMAPP analysis of mouse lung tumor models, showed that multiple genes affected by herbal medicine ATB are members of different genetic pathways such as ubiquitin-proteasome, Notch, Ras-MAPK, and G13 pathways [89], which are important in mitogenesis, neoplastic transformation [93] and apoptosis [94]. This gene expression microarray study showed that ATB is a potential tumor suppressor capable of targeting cell proliferation, differentiation, and apoptosis [89].

The proteomic profile of MCF-7 cells treated with Zilongjin, an herbal antitumor medicine, showed the downregulation of HSP27, a blocker of apoptosis [95]. Zilongjin also suppressed the expression of eIF3I and eIF1AY proteins, which are important regulators of translation initiation [95]. Collectively, the proteomic approach can identify translational perturbations in cancer cells and protein-wide changes from these perturbations in response to stimuli. Microarray based gene expression analysis of four different lung cancer cell lines treated by Zilongjin showed that 170 genes were upregulated and 313 were downregulated by the drug. Of these 483 genes, eleven genes including *HELLS*, *JUN*, *XIAP*, *MCM6*, *CDKN2C*, *CCNE2*, *HN1L*, *TFDP2*, *CCNG2*, *GADD45A*, and *CDKN1A* were found to be involved in cancer-related pathways such as apoptosis, cell cycle, and MAPK cascade [96].

Taken together, the findings based on the molecular and '–omics approaches' suggest that natural compound mixtures have multiple targets in cancer cells. Combined compounds from two or more

sources are potential resources for the development of multi-targeted anti-cancer therapeutics and have a broader range of molecular targets in cancer cells. It is important to bear in mind that the clinical effectiveness of some of these combined drugs have only been reported in non-English language papers and these often lack compelling clinical data. Therefore, more work is needed to evaluate natural compound mixtures as cancer treatments. Figure 1 shows the molecular targets of two groups of single compounds, alkaloids and flavonoids, compared to a compound mixture, CKI, that contains both groups of natural compounds in an in vitro setting. Summaries of therapeutic effects from single or mixtures of natural compounds and their possible cellular mechanisms are shown in Table 1.

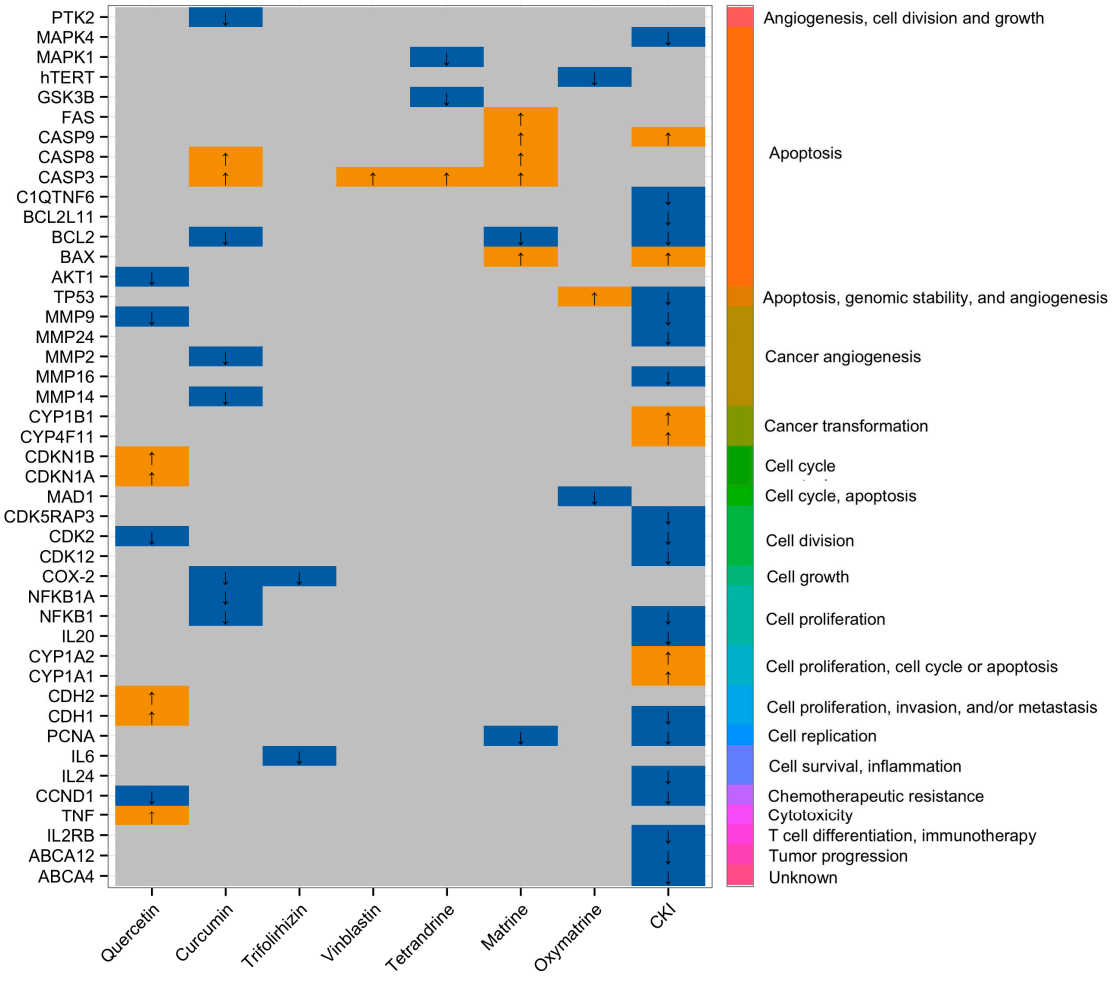

Figure 1. Differential gene expression in different cancer cell lines induced by flavonoids and alkaloids as well as Compound Kushen Injection (CKI). Left hand axis shows differentially expressed genes, bottom axis shows natural anti-cancer agent treatments (Quercetin, Curcumin, Trifolirhizin = flavonoids), (Vinblastine, Tetrandrine, Matrine, Oxymatrine = alkaloids), and (compound mixture = CKI) and the right hand axis shows Gene Ontology (GO) clustering and annotation of differentially expressed genes. Up and down-regulated genes (up = YELLOW and down = BLUE) known to be affected by natural compound anti-cancer agents were obtained from http://crdd.osdd.net/raghava/npact/browse.php and significantly differentially expressed genes from CKI treated MCF-7 cells were obtained from RNA-Seq experiments conducted by Qu et al. [87].

Table 1. Reported therapeutic effects by single or mixtures of natural compounds in different stages of cellular mechanisms.

Ref.	Herbal Medicines	Types of Cancer	Cell Lines/Model	Mechanisms of Actions
[97]	Curcumin	Colorectal	Colorectal cancer stem cells (CCSCs)	Apoptosis
[98]	Ginsenoside Rg3	Liver	Tumor bearing rats	Apoptosis, Immune responses
[99]	Curcumin	Breast	MCF-7	Anti-inflammation
[100]	Matrine	Lung	HepG2	Proliferation and metastasis chemosensitization
[72]	Quercetin	Lung	HepG2	Apoptosis
[95]	Zilongjin	Breast	MCF-7	Inhibits malignant proliferation, apoptosis
[101]	Triterpenes from *Ganoderma lucidum*	Cervical	HeLa	Cell death, oxidative stress, calcium signaling, and ER stress
[64]	Curcumin	Breast	MCF-7	Apoptosis
[102]	Triterpenes from *Patrinia heterophylla*	Leukemia	K562	Energy metabolism, oxidative stress, signal transduction, differential induction, protein biosynthesis, and apoptosis
[54]	Oxymatrine	Cervical	HeLa	Inhibits proliferation, apoptosis
[103]	Sanguinarine from Papaveraceae family	Pancreatic	BxPC-3, MIA PaCa-2	Decreases cellular hypoxia and cell proliferation, induces apoptosis leading to cancer cells inhibition
[89]	Zeng Sheng Ping (Antitumor B)	Lung	Mouse lung	Ubiquitin-proteasome, Notch, Ras-MAPK, G13 pathway, cell proliferation, differentiation, and apoptosis
[104]	Aidi injection	Breast	MCF-7	Inhibits proliferation, apoptosis
[96]	Zilongjin	Lung	A549, H446, H460, and H520	Cell cycle regulation, MAPK cascade, and apoptosis
[87]	Compound Kushen Injection	Breast	MCF-7	Cell cycle regulation, cell growth related pathway

5. Alternative Approach of Triggering Apoptosis Using Metal-Derivatized Natural Compounds

Structurally modified anti-cancer compounds can be highly effective in treating cancer due to their controlling chemo-, site- selectivity in cells. The heavy metal-based compound, cisplatin, has a broad spectrum of cytotoxicity that makes it among the most popular and effective chemotherapy drugs. Cisplatin and compounds of this type are used to treat approximately 50%–70% of all cancer patients [105]. Although metal-based anti-cancer drugs show significant effectiveness against cancer, they can also have severe adverse effects. Moreover, different mechanisms are used by cancer cells to resist cytotoxic drugs, complicating the development of novel potent anti-cancer drugs. Natural compounds have been shown to have low adverse reactions in normal cells of cancer patients, and natural compound-metal complexes have been confirmed as potential (pro) drugs [106]. The alkaloid liriodenine has anti-tumor activity and when combined with platinum (II) and ruthenium (II), the liriodenine-metal complexes covalently bind to DNA and enhance the cytotoxicity of liriodenine. When Gallium (III) and Tin (IV) are combined with matrine, these combinations further modulate cell cycle arrest at the G2/M phase, and Gold (III)-matrine complexes inhibit topoisomerase I [106], thereby causing DNA replication processes in cancer cells to malfunction. The actions of these different metal-based compounds vary depending on cell type. For instance, Gallium III-matrine and Gold III-matrine compounds have significant anti-proliferative activities in SW480 cells, HeLa cells, HepG2 cells, and MCF-7 cells, respectively [106]. It is worth noting that the efficacy of synthetic metal-natural compounds in vitro greatly exceeds those of cisplatin and matrine alone. These results indicate that metal-based cytotoxic natural compounds may hold promise as anti-cancer therapeutics, based on their multi-targeting effects on cancer cell regulatory networks. A summary of therapeutic effects by metal-derivatized natural compounds and their mechanisms of actions compared to their original forms and/or existing metal-based anticancer drugs are shown in Table 2.

Table 2. Mechanisms of action of metal-derivatized natural compounds compared to their original forms and/or existing metal-based anticancer drugs.

Groups of Natural Compounds	Metal Derivatized Natural Compounds	Source	Cell Lines/Model	Mechanisms of Actions	Remarks	Ref.
Alkaloids	GL331	**Compound**: Podophyllotoxin **Plant**: *Podophyllum* species	KB/VCR, MCF-7/ADR, and HL60/VCR	TOPO II inhibitor, cell cycle arrest at G2, cause DNA breakage and apoptosis via inhibiting protein tyrosine kinase	GL331 shows greater cytotoxicity in vitro and in vivo, and overcomes multi-drug resistance (MDR) compared to etoposide. GL331 is now in phase II clinical trial	[107]
	[H-MT][$GaCl_4$] [H-MT][$AuCl_4$] [Sn(H-MT)Cl_5]	**Compound**: *MT* (*Matrine*) **Plant**: *Sophora flavescens*	SW480, HeLa, HepG2, and MCF-7	Cell cycle arrest at the G_2/M phase	MT + Gallium ($GaCl_4$) and MT + Gold ($AuCl_4$) enhanced the cytotoxicity better than MT alone and cisplatin	[108]
	[Ru(N–N)$_2$ (Norharman)$_2$] $(SO_3CF_3)_2$	**Compound**: Norharman **Plant**: *Peganum harmala* L.	HepG2, HeLa, MCF-7, and MCF-10A	Cell cycle arrest at G0/G1, apoptosis via mitochondrial dysfunction and ROS accumulation	IC_{50} value of the complex is much lower and the anti-proliferative activity is much higher than those of Norharman and cisplatin	[109]
	[L+H][$AuCl_4$] [$AuCl_3$ L]	**Compound**: Liriodenine (L) **Plant**: *Zanthoxylum nitidum*	MCF-7	TOPO I inhibitor, cell cycle arrest at S phase	Higher anti-proliferative activity than cisplatin, Adriamycin, liriodenine alone, and NaAuCl4	[110]
Flavonoids	hesperetin $[CuL_2(H_2O)_2]nH_2O$	**Compound**: hesperetin, **Plant**: *Stilbella fimetaria*	HepG2, and SGC-7901	Growth inhibition	DNA binding affinity of hesperetin-Cu(II) complex is stronger than that of free hesperetin	[111]
	Zn(morin)$_2$.3H_2O Cu(morin)$_2$.2H_2O	**Compound**: Morin **Plant**: *Maclura pomifera*	Hep-2, BBHK-2, BHK21, and HL-60	In vitro antitumor activity	Higher anti-proliferative activity than morin alone	[106]
	Cu(Que)$_2$(H_2O)$_2$	**Compound**: quercetin, **Plant**: various fruits and vegetables	A549	DNA breakage, apoptosis via generation of ROS and intercalation into DNA	Higher cytotoxic activity than that of quercetin alone	[112]

6. Chemoresistance in Cancer and Chemosensitization by Natural Compounds

The main reason for cancer treatment failure by chemotherapy is the emergence of drug-resistance during cancer progression. Collectively, MDR occurs when ABC transporters become overexpressed. Out of 48 human ABC transporters, the mechanisms of actions of P-gp, MDR1, ABCB1, MRP1/ABCC1, and ABCG2 have been widely reported clinically [113]. However, additional ABC transporters have been explored as targets for cancer therapeutics in drug discovery. For instance, four ABC transporter genes (*ABCA4*, *ABCC3*, *ABCC5*, and *ABCC8*) were upregulated in resistant MCF-7/AdVp3000 cells, whereas complete or partial downregulation of these genes was observed in the revertant MCF-7/AdVpRev cells [114]. Overexpression of drug resistance associated genes *ABCA4* [113,114] and *ABCA12* [115,116] were observed in human pancreatic cancers and MCF-7 breast cancer cell lines, respectively. Therefore, it might be productive to scrutinize the mechanisms of actions of less commonly studied ABC transporters from drug resistant cancer cell lines when treated with natural compounds.

To overcome drug resistance, natural compounds such as sesquiterpenes, flavonoids, alkaloids, diterpenoids, saponins, and polyphenolic compounds [11,21] are substituted or applied in combination with existing drugs. These compounds are known to have anti-tumor activities and can not only kill cancer cells but also restore drug sensitivity. For example, tetrandrine (bioactive alkaloid) modulates P-gp-mediated drug efflux in vitro and has anti-neoplastic activity when given together with doxorubicin to mice bearing resistant MCF-1/DOX cells in vivo [13,14]. Another natural product is Quercetin (a flavonoid [11]), which blocks *MDR1* transcription, thereby suppressing P-gp expression [117] and restoring daunorubicin chemosensitivity in HL-60/DOX and K562/DOX cell lines [118,119].

A different flavonoid, curcumin, inhibits the main ABC transporters such as P-gp, MRP1, and ABCG2, and increases vincristine chemosensitivity in SGC7901/VCR cell lines [120,121]. 20(*S*)-Ginsenoside Rg3 (saponins) chemosensitizes vincristine, doxorubicin, etoposide, and colchicine

resistant KBV20 cell lines in a time- and dose-dependent manner [11]. Oxymatrine chemosensitizes cisplatin resistant HeLa/DDP cells by suppressing inosine monophosphate dehydrogenase type II (IMPDH2) levels and inducing apoptosis through the mitochondrial pathway [54]. CKI may also act as a stimulator of drug resistance reversal and chemosensitization in cancer. Transcriptome analysis from Qu et al. revealed that two drug resistant ABC transporter genes, *ABCA12* and *ABCA4*, were significantly downregulated in CKI treated MCF-7 cells [87]. These results support the assertion that natural compounds can reverse or alter chemoresistance.

7. Apoptosis in MDR Cells through Modulation of MicroRNA (miRNA) Networks by Natural Compounds

The compelling link between possible successful cancer chemotherapy and triggering apoptosis by chemosensitization is connected in this review by the involvement of microRNAs. miRNAs are highly conserved small non-coding RNA molecules that directly interact with their target mRNA, causing either mRNA transcriptional degradation or translational repression that results in the reduction of gene expression [122]. miRNAs have emerged as both potential therapeutic agents and biomarkers [123]. Some have oncogenic properties while others act as tumor suppressors. Miller et al. reported that eight upregulated miRNAs and seven downregulated miRNAs were found in tamoxifen resistant human breast cancer MCF-7 cells [124]. Moreover, increased expression of miR-415 is correlated with the decreased expression of *MDR1* genes and seems to elevate sensitivity to doxorubicin in DOX-resistant breast cancer cells [125]. In tumors, epithelial-to-mesenchymal transition (EMT) plays an important role of tumor invasion/migration and metastasis [126]. ZEB1 and ZEB2 repress E-cadherin expression [127,128] and downregulation of E-cadherin allows epithelial cells to undergo EMT, which contributes resistance to EGFR-directed therapy in cancer. Members of the miR-200 family, particularly miR-200c and miR-200b, target ZEB1 and ZEB2 and control EMT to sensitize EGFR therapy [129].

Growing evidence indicates that natural compounds are important regulators of miRNA mediated genetic pathways in cancer. For example, matrine significantly reduces the overexpression of miRNA-21 and stimulates apoptosis in HepG2 and Hep3B cells [130]. Matrine also downregulated 14 miRNAs and upregulated their target genes in the MAPK signaling pathway in SGC7901 human gastric cancer cells [131]. Another natural compound, oxymatrine, acts on human ovarian cancer OVCAR3 cells by upregulating miR-29b, which downregulates the expression level of matrix metalloproteinase-2 and induces apoptosis [132]. In the microarray analysis of MCF-7 cells, upregulation of 45 miRNAs was shown after treatment with TCM Aidi injection. Of these, miRNA-126 was found to be a suppressor of proliferation of MCF-7 cells [104]. Research showed that inhibition of miRNA-25 by a natural phenol, isoliquiritigenin, leads to autophagy in MCF-7/ADR cells via increased expression of autophagy regulator ULK1 [133]. In the transcriptome of CKI treated MCF-7 cells, the upregulation of hsa-miR-6879 and downregulation of its target drug resistant gene *ABCA12* were observed [87]. However, the prediction of the role of pre-miR-6879 in terms of the regulation of ABC transporters still needs to be experimentally confirmed. The link between natural compounds inducing miRNA mediated drug resistance reversal and chemosensitization, leading to cancer cells autophagy and apoptosis, supports the investigation of natural compounds in drug resistant cancer chemosensitization therapy. Whilst it is known that miRNAs are important in phytochemically mediated cancer cell death, little is known about full or partial reversal of MDR via the regulation of miRNAs by natural compounds. Hence, there is a gap between the use of natural compounds that regulate miRNA and MDR that is not well understood. A model of the regulatory interactions between drugs, miRNA, and target genes in the context of autophagy, drug resistance reversal, and apoptosis is shown in Figure 2.

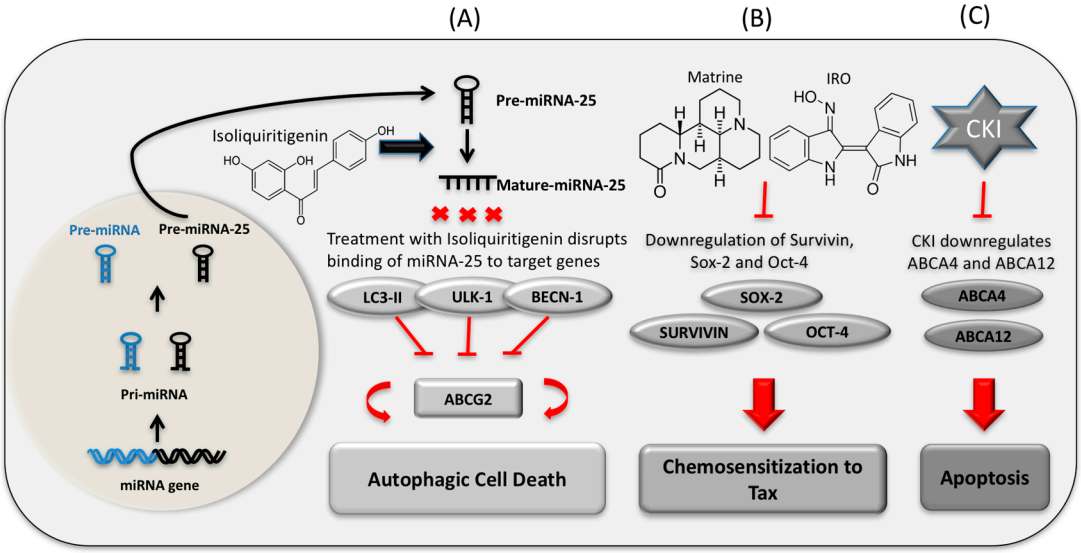

Figure 2. Three panels (**A**–**C**) show the influence of natural compounds on gene expression in terms of MDR regulation. (**A**) Treatment of Isoliquiritigenin blocks binding of autophagy-related miR-25 to the 3′ UTR region of *ULK-1*, *LC3-II*, and *BECN-1* in killing drug-resistant breast cancer cells [133]; (**B**) Matrine and indirubin-3′-monoxime (IRO) reverse chemoresistance of paclitaxel (TAX) by downregulating the expression of Sox-2, Survivin, and Oct-4 proteins in human squamous cell carcinoma [134]; (**C**) CKI suppresses the expression of the drug resistant related genes *ABCA12* and *ABCA4* in cancer cell apoptosis. The involvement of miRNAs in the regulation of these genes with respect to drug resistance has not yet been confirmed [87].

8. Conclusions

Despite significant progress in the fields of cancer diagnosis and chemotherapy, cancer remains one of the greatest causes of death worldwide. Novel approaches to cancer management often fail due to frequent genetic alterations and mutations in cancer genomes. Because of the high frequency of side effects caused by chemotherapy, metastatic cancers still need new, more effective chemotherapeutics. There is emerging interest in developing drugs to tackle these problems by using natural compounds, which may affect multiple targets with lower side effects and be effective against several cancer types. Despite attempts in chemotherapy using natural compounds, many questions remain regarding their efficacy and potential modes of action. From the medicinal chemistry point of view, an important fact when applying the natural compounds to consider is the impurities of the extracted herbal medicine that have their own biological activity which may provide false positive signal of the molecules during drug screening. In addition, flawed scientific evidence from natural product mixtures can suggest false positive therapeutic benefits. Therefore, careful examination to approve the molecular target engagement while researching drug discovery is necessary. The best possible drug combinations are based on the understanding of the cancer-specific context of mutated oncogenes, tumor suppressor genes, and their regulatory pathways. To evaluate novel treatment approaches involving the use of mixtures of natural compounds, we must understand how coding and non-coding RNAs, oncogenes, downregulated tumor suppressor genes, and mutated genes, as well as their signal transduction pathways, respond to these drugs. Systems biology can help characterize the roles of functionally cryptic elements such as long and short ncRNAs in cancer. We have reviewed the effectiveness of natural compounds in cancer cells in terms of triggering apoptosis and chemosensitization through the application of molecular genetic and "-omics" approaches. There is evidence to suggest that natural compounds might be effective and less toxic in some circumstances. Furthermore, metal-derivatized natural compounds can also trigger apoptosis and natural compound-metal complexes have been

confirmed as potential (pro) drugs [106]. This suggests that natural compounds and their derivatives merit further investigation as anti-cancer therapeutics.

The effect of multi-drug resistance during cancer progression is another important hurdle for chemotherapy. In resistance to chemotherapy-induced cancer cell death, genetic alterations in the drug-induced apoptotic program also cause MDR to biochemically unrelated drugs [135]. This is illustrated by the relationship between chemoresistance and targeted upregulation of apoptosis regulator *bcl-2* by multiple DNA damaging stimuli [135]. Therefore, it is important to study the role of natural compounds in chemosensitization, since this may create new avenues for novel drug development in cancer treatment. The investigation of natural compound mixtures as apoptosis-inducing and chemosensitizing cancer therapeutics will improve our understanding of the molecular changes in cancer cells and should provide clues about how the disease can be controlled. Our current knowledge of natural compounds' effects on cancer is mainly from cell-based experiments and partly from in vivo experiments. To date, the clinical effectiveness of some of these combined drugs has not been robustly demonstrated. As a result, additional research using in vivo systems and better clinical trials is needed to determine the safety and clinical usefulness of these drugs.

Acknowledgments: Thazin Nwe Aung acknowledges Saeed Nourmohammadi for valuable assistance and advice along with everyone in David L. Adelson's lab. Special thanks to Merry Wickes for her advice to improve the manuscript.

Author Contributions: Thazin Nwe Aung and David L. Adelson designed the study. Thazin Nwe Aung performed the literature review and wrote the manuscript. Zhipeng Qu prepared Figure 1. Zhipeng Qu, R. Daniel Kortschak, and David L. Adelson contributed to writing the paper. All authors read and approved the final manuscript.

Conflicts of Interest: The authors declare that the research was conducted in the absence of any commercial or financial relationships that could be construed as a potential conflict of interest. The Zhendong Centre is funded through a charitable donation of Zhendong Pharmaceutical Co., Ltd. Zhendong Pharmaceutical Co., Ltd. has had no control over the scientific research we carry out or the content of this article.

Abbreviations

CKI	Compound Kushen Injection
MDR	Multi-drug Resistance
ATB	Antitumor B
NPACT	Naturally Occurring Plant-based Anti-cancer Compound-Activity-Target Database
TCM	Traditional Chinese Medicine
QoL	Quality of Life
MT	Matrine
GO	Gene Ontology
IRO	Indirubin-3′-monoxime
CS-IVa-Be	Chikusetsusaponin IV a Butyl Ester
VEGF	Vascular Endothelial Growth Factor
Akt	Protein Kinase B
NF-κB	Nuclear Factor κ-light-chain-enhancer of activated B cells
ER	Endoplasmic Reticulum
MAPK	Mitogen Activated Protein Kinase

References

1. Newman, D.J.; Cragg, G.M.; Snader, K.M. Natural products as sources of new drugs over the period 1981–2002. *J. Nat. Prod.* **2003**, *66*, 1022–1037. [CrossRef] [PubMed]
2. Alberts, B.; Johnson, A.; Lewis, J.; Raff, M.; Roberts, K.; Walter, P. Programmed Cell Death (Apoptosis). In *Molecular Biology of the Cell*, 4th ed.; Garland Science: New York, NY, USA, 2002.
3. Wajant, H. The Fas signaling pathway: More than a paradigm. *Science* **2002**, *296*, 1635–1636. [CrossRef] [PubMed]

4. Galluzzi, L.; Vitale, I.; Abrams, J.; Alnemri, E.; Baehrecke, E.; Blagosklonny, M.; Dawson, T.M.; Dawson, V.; El-Deiry, W.; Fulda, S. Molecular definitions of cell death subroutines: Recommendations of the Nomenclature Committee on Cell Death 2012. *Cell. Death Differ.* **2012**, *19*, 107–120. [CrossRef] [PubMed]
5. Mehlen, P.; Bredesen, D.E. Dependence receptors: From basic research to drug development. *Sci. Signal.* **2011**, *4*, mr2. [CrossRef] [PubMed]
6. Wong, R. Apoptosis in cancer: From pathogenesis to treatment. *J. Exp. Clin. Cancer Res.* **2011**, *30*, 87. [CrossRef] [PubMed]
7. Chen, R.; Wang, H.; Liang, B.; Liu, G.; Tang, M.; Jia, R.; Fan, X.; Jing, W.; Zhou, X.; Wang, H. Downregulation of ASPP2 improves hepatocellular carcinoma cells survival via promoting BECN1-dependent autophagy initiation. *Cell Death Dis.* **2016**, *7*, e2512. [CrossRef] [PubMed]
8. Codogno, P.; Meijer, A.J. Atg5: More than an autophagy factor. *Nat. Cell Biol.* **2006**, *8*, 1045–1046. [CrossRef] [PubMed]
9. Schmitt, C.A.; McCurrach, M.E.; de Stanchina, E.; Wallace-Brodeur, R.R.; Lowe, S.W. INK4a/ARF mutations accelerate lymphomagenesis and promote chemoresistance by disabling p53. *Genes Dev.* **1999**, *13*, 2670–2677. [CrossRef] [PubMed]
10. Dive, C.; Hickman, J. Drug-target interactions: Only the first step in the commitment to a programmed cell death? *Br. J. Cancer* **1991**, *64*, 192. [PubMed]
11. Chai, S.; To, K.; Lin, G. Circumvention of multi-drug resistance of cancer cells by Chinese herbal medicines. *Chin. Med.* **2010**, *5*, 26. [CrossRef] [PubMed]
12. Yu-Jen, C. Potential role of tetrandrine in cancer therapy. *Acta Pharmacol. Sin.* **2002**, *23*, 1102–1106.
13. Tian, H.; Pan, Q. A comparative study on effect of two bisbenzylisoquinolines, tetrandrine and berbamine, on reversal of multidrug resistance. *Acta Pharm. Sin.* **1997**, *32*, 245–250.
14. Choi, S.-U.; Park, S.-H.; Kim, K.-H.; Choi, E.-J.; Kim, S.; Park, W.-K.; Zhang, Y.-H.; Kim, H.-S.; Jung, N.-P.; Lee, C.-O. The bis benzylisoquinoline alkaloids, tetrandine and fangchinoline, enhance the cytotoxicity of multidrug resistance-related drugs via modulation of P-glycoprotein. *Anti Cancer Drugs* **1998**, *9*, 255–262. [CrossRef] [PubMed]
15. Kang, J.; Kim, E.; Kim, W.; Seong, K.M.; Youn, H.; Kim, J.W.; Kim, J.; Youn, B. Rhamnetin and cirsiliol induce radiosensitization and inhibition of epithelial-mesenchymal transition (EMT) by miR-34a-mediated suppression of Notch-1 expression in non-small cell lung cancer cell lines. *J. Biol. Chem.* **2013**, *288*, 27343–27357. [CrossRef] [PubMed]
16. Graw, S.; Meier, R.; Minn, K.; Bloomer, C.; Godwin, A.K.; Fridley, B.; Vlad, A.; Beyerlein, P.; Chien, J. Robust gene expression and mutation analyses of RNA-sequencing of formalin-fixed diagnostic tumor samples. *Sci. Rep.* **2015**, *5*, 12335. [CrossRef] [PubMed]
17. Kaufmann, S.H.; Earnshaw, W.C. Induction of apoptosis by cancer chemotherapy. *Exp. Cell Res.* **2000**, *256*, 42–49. [CrossRef] [PubMed]
18. Espinosa, E.; Zamora, P.; Feliu, J.; Barón, M.G. Classification of anticancer drugs—A new system based on therapeutic targets. *Cancer Treat. Rev.* **2003**, *29*, 515–523. [CrossRef]
19. Manson, M.M. Cancer prevention–the potential for diet to modulate molecular signalling. *Trends Mol. Med.* **2003**, *9*, 11–18. [CrossRef]
20. Prakash, O.; Kumar, A.; Kumar, P. Anticancer potential of plants and natural products: A review. *Am. J. Pharmacol. Sci.* **2013**, *1*, 104–115. [CrossRef]
21. Millimouno, F.M.; Dong, J.; Yang, L.; Li, J.; Li, X. Targeting apoptosis pathways in cancer and perspectives with natural compounds from Mother Nature. *Cancer Prev. Res.* **2014**, *7*, 1081–1107. [CrossRef] [PubMed]
22. Fulda, S. Evasion of apoptosis as a cellular stress response in cancer. *Int. J. Cell Biol.* **2010**. [CrossRef] [PubMed]
23. Davis, J.N.; Kucuk, O.; Sarkar, F.H. Genistein inhibits NF-κB activation in prostate cancer cells. *Nutr. Cancer* **1999**, *35*, 167–174. [CrossRef] [PubMed]
24. Stephens, F.O. The rising incidence of breast cancer in women and prostate cancer in men. Dietary influences: A possible preventive role for nature's sex hormone modifiers-the phytoestrogens (review). *Oncol. Rep.* **1999**, *6*, 865–935. [CrossRef] [PubMed]
25. Mangal, M.; Sagar, P.; Singh, H.; Raghava, G.P.; Agarwal, S.M. NPACT: Naturally occurring plant-based anti-cancer compound-activity-target database. *Nucleic Acids Res.* **2013**, *41*, D1124–D1129. [CrossRef] [PubMed]

26. Zhou, X.; Seto, S.W.; Chang, D.; Kiat, H.; Razmovski-Naumovski, V.; Chan, K.; Bensoussan, A. Synergistic effects of Chinese herbal medicine: A comprehensive review of methodology and current research. *Front. Pharmacol.* **2016**, *7*, 201. [CrossRef] [PubMed]
27. Liu, J.; Wang, S.; Zhang, Y.; Fan, H.T.; Lin, H.S. Traditional Chinese medicine and cancer: History, present situation, and development. *Thorac. Cancer* **2015**, *6*, 561–569. [CrossRef] [PubMed]
28. Chang, R. Bioactive polysaccharides from traditional Chinese medicine herbs as anticancer adjuvants. *J. Altern. Complement. Med.* **2002**, *8*, 559–565. [CrossRef] [PubMed]
29. Ni, Y.H.; Li, X.; Xu, Y.; Liu, J.P. Chinese herbal medicine for advanced pancreatic cancer. *Cochrane Libr.* **2012**. [CrossRef]
30. Zhang, M.; Liu, X.; Li, J.; He, L.; Tripathy, D. Chinese medicinal herbs to treat the side-effects of chemotherapy in breast cancer patients. *Cochrane Libr.* **2007**. [CrossRef]
31. Guo, Z.; Jia, X.; Liu, J.P.; Liao, J.; Yang, Y. Herbal medicines for advanced colorectal cancer. *Cochrane Libr.* **2012**. [CrossRef]
32. Shoemaker, M.; Hamilton, B.; Dairkee, S.H.; Cohen, I.; Campbell, M.J. In vitro anticancer activity of twelve Chinese medicinal herbs. *Phytother. Res.* **2005**, *19*, 649–651. [CrossRef] [PubMed]
33. Chen, H.-H.; Zhou, H.-J.; Fang, X. Inhibition of human cancer cell line growth and human umbilical vein endothelial cell angiogenesis by artemisinin derivatives in vitro. *Pharmacol. Res.* **2003**, *48*, 231–236. [CrossRef]
34. Sun, M.; Cao, H.; Sun, L.; Dong, S.; Bian, Y.; Han, J.; Zhang, L.; Ren, S.; Hu, Y.; Liu, C. Antitumor activities of kushen: Literature review. *Evid. Based Complement. Altern. Med.* **2012**. [CrossRef] [PubMed]
35. Liu, J.; Henkel, T. Traditional Chinese medicine (TCM): Are polyphenols and saponins the key ingredients triggering biological activities? *Curr. Med. Chem.* **2002**, *9*, 1483–1485. [CrossRef] [PubMed]
36. Hartwell, J. Types of anticancer agents isolated from plants. *Cancer Treat. Rep.* **1976**, *60*, 1031–1067. [PubMed]
37. Lu, J.-J.; Bao, J.-L.; Chen, X.-P.; Huang, M.; Wang, Y.-T. Alkaloids isolated from natural herbs as the anticancer agents. *Evid. Based Complement. Altern. Med.* **2012**. [CrossRef] [PubMed]
38. Yu, H.-H.; Kim, K.-J.; Cha, J.-D.; Kim, H.-K.; Lee, Y.-E.; Choi, N.-Y.; You, Y.-O. Antimicrobial activity of berberine alone and in combination with ampicillin or oxacillin against methicillin-resistant Staphylococcus aureus. *J. Med. Food* **2005**, *8*, 454–461. [CrossRef] [PubMed]
39. Han, J.; Lin, H.; Huang, W. Modulating gut microbiota as an anti-diabetic mechanism of berberine. *Med. Sci. Monit. Basic Res.* **2011**, *17*, RA164–RA167. [CrossRef]
40. Ji, Y. *Active Ingredients of Traditional Chinese Medicine: Pharmacology and Application*; People's Medical Publishing House Cp., LTD: Shelton, CT, USA, 2011.
41. Moudi, M.; Go, R.; Yien, C.Y.S.; Nazre, M. Vinca alkaloids. *Int. J. Prev. Med.* **2013**, *4*, 1231–1235. [PubMed]
42. Liu, Y.; Xu, Y.; Ji, W.; Li, X.; Sun, B.; Gao, Q.; Su, C. Anti-tumor activities of matrine and oxymatrine: Literature review. *Tumor Biol.* **2014**, *35*, 5111–5119. [CrossRef] [PubMed]
43. Liang, C.Z.; Zhang, J.K.; Shi, Z.; Liu, B.; Shen, C.Q.; Tao, H.M. Matrine induces caspase-dependent apoptosis in human osteosarcoma cells in vitro and in vivo through the upregulation of Bax and Fas/FasL and downregulation of Bcl-2. *Cancer Chemother. Pharmacol.* **2012**, *69*, 317–331. [CrossRef] [PubMed]
44. Yu, P.; Liu, Q.; Liu, K.; Yagasaki, K.; Wu, E.; Zhang, G. Matrine suppresses breast cancer cell proliferation and invasion via VEGF-Akt-NF-κB signaling. *Cytotechnology* **2009**, *59*, 219–229. [CrossRef] [PubMed]
45. Zhou, K.; Ji, H.; Mao, T.; Bai, Z. Effects of matrine on the proliferation and apoptosis of human medulloblastoma cell line D341. *Int. J. Clin. Exp. Med.* **2014**, *7*, 911–918. [PubMed]
46. Xie, S.-B.; He, X.-X.; Yao, S.-K. Matrine-induced autophagy regulated by p53 through AMP-activated protein kinase in human hepatoma cells. *Int. J. Oncol.* **2015**, *47*, 517–526. [CrossRef] [PubMed]
47. Mariño, G.; Niso-Santano, M.; Baehrecke, E.H.; Kroemer, G. Self-consumption: The interplay of autophagy and apoptosis. *Nat. Rev. Mol. Cell Biol.* **2014**, *15*, 81–94. [CrossRef] [PubMed]
48. Rambold, A.S.; Cohen, S.; Lippincott-Schwartz, J. Fatty acid trafficking in starved cells: Regulation by lipid droplet lipolysis, autophagy, and mitochondrial fusion dynamics. *Dev. Cell* **2015**, *32*, 678–692. [CrossRef] [PubMed]
49. Estrela, J.M.; Ortega, A.; Obrador, E. Glutathione in cancer biology and therapy. *Crit. Rev. Clin. Lab. Sci.* **2006**, *43*, 143–181. [CrossRef] [PubMed]
50. Zou, J.; Ran, Z.H.; Xu, Q.; Xiao, S.D. Experimental study of the killing effects of oxymatrine on human colon cancer cell line SW1116. *Chin. J. Dig. Dis.* **2005**, *6*, 15–20. [CrossRef] [PubMed]

51. Wu, X.-S.; Yang, T.; Gu, J.; Li, M.-L.; Wu, W.-G.; Weng, H.; Ding, Q.; Mu, J.-S.; Bao, R.-F.; Shu, Y.-J. Effects of oxymatrine on the apoptosis and proliferation of gallbladder cancer cells. *Anti Cancer drugs* **2014**, *25*, 1007–1015. [CrossRef] [PubMed]
52. Jin, N.; Zhao, Y.-X.; Deng, S.-H.; Sun, Q. Preparation and in vitro anticancer activity of oxymatrine mixed micellar nanoparticles. *Die Pharm. Int. J. Pharm. Sci.* **2011**, *66*, 506–510.
53. Wang, B.; Han, Q.; Zhu, Y. Oxymatrine inhibited cell proliferation by inducing apoptosis in human lung cancer A549 cells. *Bio Med. Mater. Eng.* **2015**, *26*, 165–172. [CrossRef] [PubMed]
54. Li, M.; Su, B.-S.; Chang, L.-H.; Gao, Q.; Chen, K.-L.; An, P.; Huang, C.; Yang, J.; Li, Z.-F. Oxymatrine induces apoptosis in human cervical cancer cells through guanine nucleotide depletion. *Anti Cancer Drugs* **2014**, *25*, 161–173. [CrossRef] [PubMed]
55. Wu, J.-M.; Chen, Y.; Chen, J.-C.; Lin, T.-Y.; Tseng, S.-H. Tetrandrine induces apoptosis and growth suppression of colon cancer cells in mice. *Cancer Lett.* **2010**, *287*, 187–195. [CrossRef] [PubMed]
56. Qin, R.; Shen, H.; Cao, Y.; Fang, Y.; Li, H.; Chen, Q.; Xu, W. Tetrandrine induces mitochondria-mediated apoptosis in human gastric cancer BGC-823 cells. *PLoS ONE* **2013**, *8*, e76486. [CrossRef] [PubMed]
57. Panda, D.; Jordan, M.A.; Chu, K.C.; Wilson, L. Differential effects of vinblastine on polymerization and dynamics at opposite microtubule ends. *J. Biol. Chem.* **1996**, *271*, 29807–29812. [CrossRef] [PubMed]
58. Brugières, L.; Pacquement, H.; Le Deley, M.-C.; Leverger, G.; Lutz, P.; Paillard, C.; Baruchel, A.; Frappaz, D.; Nelken, B.; Lamant, L. Single-drug vinblastine as salvage treatment for refractory or relapsed anaplastic large-cell lymphoma: A report from the French Society of Pediatric Oncology. *J. Clin. Oncol.* **2009**, *27*, 5056–5061. [CrossRef] [PubMed]
59. Yao, L.H.; Jiang, Y.; Shi, J.; Tomas-Barberan, F.; Datta, N.; Singanusong, R.; Chen, S. Flavonoids in food and their health benefits. *Plant Foods Hum. Nutr.* **2004**, *59*, 113–122. [CrossRef] [PubMed]
60. Chahar, M.K.; Sharma, N.; Dobhal, M.P.; Joshi, Y.C. Flavonoids: A versatile source of anticancer drugs. *Pharmacogn. Rev.* **2011**, *5*, 1. [PubMed]
61. Zhou, H.; Lutterodt, H.; Cheng, Z.; Yu, L. Anti-inflammatory and antiproliferative activities of trifolirhizin, a flavonoid from Sophora flavescens roots. *J. Agric. Food Chem.* **2009**, *57*, 4580–4585. [CrossRef] [PubMed]
62. Yin, T.; Yang, G.; Ma, Y.; Xu, B.; Hu, M.; You, M.; Gao, S. Developing an activity and absorption-based quality control platform for Chinese traditional medicine: Application to Zeng-Sheng-Ping (Antitumor B). *J. Ethnopharmacol.* **2015**, *172*, 195–201. [CrossRef] [PubMed]
63. Aratanechemuge, Y.; Hibasami, H.; Katsuzaki, H.; Imai, K.; Komiya, T. Induction of apoptosis by maackiain and trifolirhizin (maackiain glycoside) isolated from sanzukon (Sophora Subprostrate Chen et T. Chen) in human promyelotic leukemia HL-60 cells. *Oncol. Rep.* **2004**, *12*, 1183–1188. [CrossRef] [PubMed]
64. Fang, H.; Chen, S.; Guo, D.; Pan, S.; Yu, Z. Proteomic identification of differentially expressed proteins in curcumin-treated MCF-7 cells. *Phytomedicine* **2011**, *18*, 697–703. [CrossRef] [PubMed]
65. Ravindran, J.; Prasad, S.; Aggarwal, B.B. Curcumin and cancer cells: How many ways can curry kill tumor cells selectively? *AAPS J.* **2009**, *11*, 495–510. [CrossRef] [PubMed]
66. Jordan, B.C.; Mock, C.D.; Thilagavathi, R.; Selvam, C. Molecular mechanisms of curcumin and its semisynthetic analogues in prostate cancer prevention and treatment. *Life Sci.* **2016**, *152*, 135–144. [CrossRef] [PubMed]
67. Nelson, K.M.; Dahlin, J.L.; Bisson, J.; Graham, J.; Pauli, G.F.; Walters, M.A. The Essential Medicinal Chemistry of Curcumin: Miniperspective. *J. Med. Chem.* **2017**, *60*, 1620–1637. [CrossRef] [PubMed]
68. Baker, M.M. Deceptive curcumin offers cautionary tale for chemists. *Nature* **2017**, *541*, 144–145. [CrossRef] [PubMed]
69. Sak, K. Site-specific anticancer effects of dietary flavonoid quercetin. *Nutr. Cancer* **2014**, *66*, 177–193. [CrossRef] [PubMed]
70. Jeong, J.H.; An, J.Y.; Kwon, Y.T.; Rhee, J.G.; Lee, Y.J. Effects of low dose quercetin: Cancer cell-specific inhibition of cell cycle progression. *J. Cell. Biochem.* **2009**, *106*, 73–82. [CrossRef] [PubMed]
71. Deng, X.-H.; Song, H.-Y.; Zhou, Y.-F.; Yuan, G.-Y.; Zheng, F.-J. Effects of quercetin on the proliferation of breast cancer cells and expression of survivin in vitro. *Exp. Ther. Med.* **2013**, *6*, 1155–1158. [PubMed]
72. Zhou, J.; Liang, S.; Fang, L.; Chen, L.; Tang, M.; Xu, Y.; Fu, A.; Yang, J.; Wei, Y. Quantitative proteomic analysis of HepG2 cells treated with quercetin suggests IQGAP1 involved in quercetin-induced regulation of cell proliferation and migration. *OMICS J. Integr. Biol.* **2009**, *13*, 93–103. [CrossRef] [PubMed]

73. Man, S.; Gao, W.; Zhang, Y.; Huang, L.; Liu, C. Chemical study and medical application of saponins as anti-cancer agents. *Fitoterapia* **2010**, *81*, 703–714. [CrossRef] [PubMed]
74. Shan, B.E.; Zeki, K.; Sugiura, T.; Yoshida, Y.; Yamashita, U. Chinese medicinal herb, Acanthopanax gracilistylus, extract induces cell cycle arrest of human tumor cells in vitro. *Jpn. J. Cancer Res.* **2000**, *91*, 383–389. [CrossRef] [PubMed]
75. Yang, J.; Qian, S.; Cai, X.; Lu, W.; Hu, C.; Sun, X.; Yang, Y.; Yu, Q.; Gao, S.P.; Cao, P. Chikusetsusaponin IVa butyl ester (CS-IVa-Be), a novel IL-6R antagonist, inhibits IL-6/STAT3 signaling pathway and induces cancer cell apoptosis. *Mol. Cancer Ther.* **2016**, *15*, 1190–1200. [CrossRef] [PubMed]
76. Lee, M.-S.; Chan, J.Y.-W.; Kong, S.-K.; Yu, B.; Eng-Choon, V.O.; Nai-Ching, H.W.; Mak Chung-Wai, T.; Fung, K.-P. Effects of polyphyllin D, a steroidal saponin in Paris polyphylla, in growth inhibition of human breast cancer cells and in xenograft. *Cancer Biol. Ther.* **2005**, *4*, 1248–1254. [CrossRef] [PubMed]
77. Raju, J.; Bird, R.P. Diosgenin, a naturally occurring furostanol saponin suppresses 3-hydroxy-3-methylglutaryl CoA reductase expression and induces apoptosis in HCT-116 human colon carcinoma cells. *Cancer Lett.* **2007**, *255*, 194–204. [CrossRef] [PubMed]
78. Chiang, C.-T.; Way, T.-D.; Tsai, S.-J.; Lin, J.-K. Diosgenin, a naturally occurring steroid, suppresses fatty acid synthase expression in HER2-overexpressing breast cancer cells through modulating Akt, mTOR and JNK phosphorylation. *FEBS Lett.* **2007**, *581*, 5735–5742. [CrossRef] [PubMed]
79. Wang, J.; Zhao, X.-Z.; Qi, Q.; Tao, L.; Zhao, Q.; Mu, R.; Gu, H.-Y.; Wang, M.; Feng, X.; Guo, Q.-L. Macranthoside B, a hederagenin saponin extracted from Lonicera macranthoides and its anti-tumor activities in vitro and in vivo. *Food Chem. Toxicol.* **2009**, *47*, 1716–1721. [CrossRef] [PubMed]
80. Shan, Y.; Guan, F.; Zhao, X.; Wang, M.; Chen, Y.; Wang, Q.; Feng, X. Macranthoside B Induces Apoptosis and Autophagy Via Reactive Oxygen Species Accumulation in Human Ovarian Cancer A2780 Cells. *Nutr. Cancer* **2016**, *68*, 280–289. [CrossRef] [PubMed]
81. Tan, C.-J.; Zhao, Y.; Goto, M.; Hsieh, K.-Y.; Yang, X.-M.; Morris-Natschke, S.L.; Liu, L.-N.; Zhao, B.-Y.; Lee, K.-H. Alkaloids from Oxytropis ochrocephala and Antiproliferative Activity of Sophoridine Derivatives Against Cancer Cell Lines. *Bioorganic Med. Chem. Lett.* **2015**, *26*, 1495–1497. [CrossRef] [PubMed]
82. Ma, Y.; Gao, H.; Liu, J.; Chen, L.; Zhang, Q.; Wang, Z. Identification and determination of the chemical constituents in a herbal preparation, Compound Kushen injection, by HPLC and LC-DAD-MS/MS. *J. Liq. Chromatogr. Relat. Technol.* **2014**, *37*, 207–220. [CrossRef]
83. Wang, W.; You, R.-L.; Qin, W.-J.; Hai, L.-N.; Fang, M.-J.; Huang, G.-H.; Kang, R.-X.; Li, M.-H.; Qiao, Y.-F.; Li, J.-W. Anti-tumor activities of active ingredients in Compound Kushen Injection. *Acta Pharmacol. Sin.* **2015**, *36*, 676–679. [CrossRef] [PubMed]
84. Polakis, P. Wnt signaling and cancer. *Genes Dev.* **2000**, *14*, 1837–1851. [CrossRef] [PubMed]
85. Xu, W.; Lin, H.; Zhang, Y.; Chen, X.; Hua, B.; Hou, W.; Qi, X.; Pei, Y.; Zhu, X.; Zhao, Z. Compound Kushen Injection suppresses human breast cancer stem-like cells by down-regulating the canonical Wnt/b-catenin pathway. *J. Exp. Clin. Cancer Res.* **2011**, *30*, 103. [CrossRef] [PubMed]
86. Guo, Y.-M.; Huang, Y.-X.; Shen, H.-H.; Sang, X.-X.; Ma, X.; Zhao, Y.-L.; Xiao, X.-H. Efficacy of Compound Kushen Injection in Relieving Cancer-Related Pain: A Systematic Review and Meta-Analysis. *Evid. Based Complement. Altern. Med.* **2015**. [CrossRef] [PubMed]
87. Qu, Z.; Cui, J.; Harata-Lee, Y.; Aung, T.N.; Feng, Q.; Raison, J.; Kortschak, R.D.; Adelson, D.L. Identification of Candidate Anti-Cancer Molecular Mechanisms Of Compound Kushen Injection Using Functional Genomics. *Oncotarget* **2016**, *7*, 66003–66019. [CrossRef] [PubMed]
88. Xudong, L.; Yan, L.; Xi, Y.; Xiaoguang, W.; Xiaoguang, H. Long noncoding RNA H19 regulates EZH2 expression by interacting with miR-630 and promotes cell invasion in nasopharyngeal carcinoma. *Biochem. Biophys. Res. Commun.* **2016**, *473*, 913–919.
89. Zhang, Z.; Wang, Y.; Yao, R.; Li, J.; Yan, Y.; La Regina, M.; Lemon, W.L.; Grubbs, C.J.; Lubet, R.A.; You, M. Cancer chemopreventive activity of a mixture of Chinese herbs (antitumor B) in mouse lung tumor models. *Oncogene* **2004**, *23*, 3841–3850. [CrossRef] [PubMed]
90. Guan, X.; Sun, Z.; Chen, X.; Wu, H.; Zhang, X. Inhibitory effects of Zengshengping fractions on DMBA-induced buccal pouch carcinogenesis in hamsters. *Chin. Med. J.* **2012**, *125*, 332–337. [CrossRef] [PubMed]
91. Lim, K.J.; Rajan, K.; Eberhart, C.G. Effects of Zeng Sheng Ping/ACAPHA on Malignant Brain Tumor Growth and Notch Signaling. *Anticancer Res.* **2012**, *32*, 2689–2696. [PubMed]

92. Sun, Z.; Guan, X.; Li, N.; Liu, X.; Chen, X. Chemoprevention of oral cancer in animal models, and effect on leukoplakias in human patients with ZengShengPing, a mixture of medicinal herbs. *Oral Oncol.* **2010**, *46*, 105–110. [CrossRef] [PubMed]
93. Voyno-Yasenetskaya, T.A.; Pace, A.M.; Bourne, H.R. Mutant alpha subunits of G12 and G13 proteins induce neoplastic transformation of Rat-1 fibroblasts. *Oncogene* **1994**, *9*, 2559–2565. [PubMed]
94. Berestetskaya, Y.V.; Faure, M.P.; Ichijo, H.; Voyno-Yasenetskaya, T.A. Regulation of apoptosis by α-subunits of G12 and G13 proteins via apoptosis signal-regulating kinase-1. *J. Biol. Chem.* **1998**, *273*, 27816–27823. [CrossRef] [PubMed]
95. Tian, Z.H.; Li, Z.F.; Zhou, S.B.; Liang, Y.Y.; He, D.C.; Wang, D.S. Differentially expressed proteins of MCF-7 human breast cancer cells affected by Zilongjin, a complementary Chinese herbal medicine. *Proteom. Clin. Appl.* **2010**, *4*, 550–559. [CrossRef] [PubMed]
96. Zhang, P.; Wang, X.; Xiong, S.; Wen, S.; Gao, S.; Wang, L.; Cao, B. Genome wide expression analysis of the effect of the Chinese patent medicine zilongjin tablet on four human lung carcinoma cell lines. *Phytother. Res.* **2011**, *25*, 1472–1479. [CrossRef] [PubMed]
97. Huang, L.-C.; Clarkin, K.C.; Wahl, G.M. Sensitivity and selectivity of the DNA damage sensor responsible for activating p53-dependent G1 arrest. *Proc. Natl. Acad. Sci. USA* **1996**, *93*, 4827–4832. [CrossRef] [PubMed]
98. Wang, Y.; Wang, J.; Yao, M.; Zhao, X.; Fritsche, J.; Schmitt-Kopplin, P.; Cai, Z.; Wan, D.; Lu, X.; Yang, S. Metabonomics study on the effects of the ginsenoside Rg3 in a β-cyclodextrin-based formulation on tumor-bearing rats by a fully automatic hydrophilic interaction/reversed-phase column-switching HPLC-ESI-MS approach. *Anal. Chem.* **2008**, *80*, 4680–4688. [CrossRef] [PubMed]
99. Bayet-Robert, M.; Morvan, D. Metabolomics reveals metabolic targets and biphasic responses in breast cancer cells treated by curcumin alone and in association with docetaxel. *PLoS ONE* **2013**, *8*, e57971. [CrossRef] [PubMed]
100. Li, Z.; Zheng, L.; Shi, J.; Zhang, G.; Lu, L.; Zhu, L.; Zhang, J.; Liu, Z. Toxic Markers of Matrine Determined Using ^{1}H-NMR-Based Metabolomics in Cultured Cells In Vitro and Rats In Vivo. *Evid. Based Complement. Altern. Med.* **2015**. [CrossRef]
101. Yue, Q.-X.; Song, X.-Y.; Ma, C.; Feng, L.-X.; Guan, S.-H.; Wu, W.-Y.; Yang, M.; Jiang, B.-H.; Liu, X.; Cui, Y.-J. Effects of triterpenes from Ganoderma lucidum on protein expression profile of HeLa cells. *Phytomedicine* **2010**, *17*, 606–613. [CrossRef] [PubMed]
102. Wei, D.-F.; Wei, Y.-X.; Cheng, W.-D.; Yan, M.-F.; Su, G.; Hu, Y.; Ma, Y.-Q.; Han, C.; Lu, Y.; Hui-Ming, C. Proteomic analysis of the effect of triterpenes from Patrinia heterophylla on leukemia K562 cells. *J. Ethnopharmacol.* **2012**, *144*, 576–583. [CrossRef] [PubMed]
103. Singh, C.K.; Kaur, S.; George, J.; Nihal, M.; Hahn, M.C.P.; Scarlett, C.O.; Ahmad, N. Molecular signatures of sanguinarine in human pancreatic cancer cells: A large scale label-free comparative proteomics approach. *Oncotarget* **2015**, *6*, 10335. [CrossRef] [PubMed]
104. Zhang, H.; Zhou, Q.-M.; Lu, Y.-Y.; Jia, D.; Su, S.-B. Aidi Injection () Alters the Expression Profiles of MicroRNAs in Human Breast Cancer Cells. *J. Tradit. Chin. Med.* **2011**, *31*, 10–16. [CrossRef]
105. Dyson, P.J.; Sava, G. Metal-based antitumour drugs in the post genomic era. *Dalton Trans.* **2006**, 1929–1933. [CrossRef] [PubMed]
106. Chen, Z.-F.; Liang, H.; Liu, Y.-C. *Traditional Chinese Medicine Active Ingredient-Metal Based Anticancer Agents*; INTECH Open Access Publisher: Rijeka, Croatia, 2012.
107. Dholwani, K.; Saluja, A.; Gupta, A.; Shah, D. A review on plant-derived natural products and their analogs with anti-tumor activity. *Indian J. Pharmacol.* **2008**, *40*, 49–58. [CrossRef]
108. Chen, Z.-F.; Mao, L.; Liu, L.-M.; Liu, Y.-C.; Peng, Y.; Hong, X.; Wang, H.-H.; Liu, H.-G.; Liang, H. Potential new inorganic antitumour agents from combining the anticancer traditional Chinese medicine (TCM) matrine with Ga (III), Au (III), Sn (IV) ions, and DNA binding studies. *J. Inorg. Biochem.* **2011**, *105*, 171–180. [CrossRef]
109. Tan, C.; Wu, S.; Lai, S.; Wang, M.; Chen, Y.; Zhou, L.; Zhu, Y.; Lian, W.; Peng, W.; Ji, L. Synthesis, structures, cellular uptake and apoptosis-inducing properties of highly cytotoxic ruthenium-Norharman complexes. *Dalton Trans.* **2011**, *40*, 8611–8621. [CrossRef] [PubMed]
110. Chen, Z.-F.; Liu, Y.-C.; Huang, K.-B.; Liang, H. Alkaloid-metal based anticancer agents. *Curr. Top. Med. Chem.* **2013**, *13*, 2104–2115. [CrossRef]

111. Tan, M.; Zhu, J.; Pan, Y.; Chen, Z.; Liang, H.; Liu, H.; Wang, H. Synthesis, cytotoxic activity, and DNA binding properties of copper (II) complexes with hesperetin, naringenin, and apigenin. *Bioinorg. Chem. Appl.* **2009**. [CrossRef] [PubMed]
112. Tan, J.; Wang, B.; Zhu, L. DNA binding and oxidative DNA damage induced by a quercetin copper (II) complex: Potential mechanism of its antitumor properties. *JBIC J. Biol. Inorg. Chem.* **2009**, *14*, 727–739. [CrossRef] [PubMed]
113. Glavinas, H.; Krajcsi, P.; Cserepes, J.; Sarkadi, B. The role of ABC transporters in drug resistance, metabolism and toxicity. *Curr. Drug Deliv.* **2004**, *1*, 27–42. [CrossRef] [PubMed]
114. Liu, Y.; Peng, H.; Zhang, J.-T. Expression profiling of ABC transporters in a drug-resistant breast cancer cell line using AmpArray. *Mol. Pharmacol.* **2005**, *68*, 430–438. [CrossRef] [PubMed]
115. Park, S.; Shimizu, C.; Shimoyama, T.; Takeda, M.; Ando, M.; Kohno, T.; Katsumata, N.; Kang, Y.-K.; Nishio, K.; Fujiwara, Y. Gene expression profiling of ATP-binding cassette (ABC) transporters as a predictor of the pathologic response to neoadjuvant chemotherapy in breast cancer patients. *Breast Cancer Res. Treat.* **2006**, *99*, 9–17. [CrossRef] [PubMed]
116. Sasaki, N.; Ishii, T.; Kamimura, R.; Kajiwara, M.; Machimoto, T.; Nakatsuji, N.; Suemori, H.; Ikai, I.; Yasuchika, K.; Uemoto, S. Alpha-fetoprotein-producing pancreatic cancer cells possess cancer stem cell characteristics. *Cancer Lett.* **2011**, *308*, 152–161. [CrossRef] [PubMed]
117. Kioka, N.; Hosokawa, N.; Komano, T.; Hirayoshi, K.; Nagate, K.; Ueda, K. Quercetin, a bioflavonoid, inhibits the increase of human multidrug resistance gene (MDR1) expression caused by arsenite. *FEBS Lett.* **1992**, *301*, 307–309. [CrossRef]
118. Cai, X.; Chen, F.; Han, J.; Gu, C.; Zhong, H.; Ouyang, R. Restorative effect of quercetin on subcellular distribution of daunorubicin in multidrug resistant leukemia cell lines K562/ADM and HL-60/ADM. *Chin. J. Cancer* **2004**, *23*, 1611–1615.
119. Cai, X.; Chen, F.; Han, J.; Gu, C.; Zhong, H.; Teng, Y.; Ouyang, R. Reversal of multidrug resistance of HL-60 adriamycin resistant leukemia cell line by quercetin and its mechanisms. *Chin. J. Oncol.* **2005**, *27*, 326–329.
120. Tang, X.-Q.; Bi, H.; Feng, J.-Q.; Cao, J.-G. Effect of curcumin on multidrug resistance in resistant human gastric carcinoma cell line SGC7901/VCR. *Acta Pharmacol. Sin.* **2005**, *26*, 1009–1016. [CrossRef] [PubMed]
121. Ganta, S.; Amiji, M. Coadministration of paclitaxel and curcumin in nanoemulsion formulations to overcome multidrug resistance in tumor cells. *Mol. Pharm.* **2009**, *6*, 928–939. [CrossRef] [PubMed]
122. Fix, L.N.; Shah, M.; Efferth, T.; Farwell, M.A.; Zhang, B. MicroRNA expression profile of MCF-7 human breast cancer cells and the effect of green tea polyphenon-60. *Cancer Genom. Proteom.* **2010**, *7*, 261–277.
123. Kasinski, A.L.; Slack, F.J. MicroRNAs en route to the clinic: Progress in validating and targeting microRNAs for cancer therapy. *Nat. Rev. Cancer* **2011**, *11*, 849–864. [CrossRef] [PubMed]
124. Miller, T.E.; Ghoshal, K.; Ramaswamy, B.; Roy, S.; Datta, J.; Shapiro, C.L.; Jacob, S.; Majumder, S. MicroRNA-221/222 confers tamoxifen resistance in breast cancer by targeting p27Kip1. *J. Biol. Chem.* **2008**, *283*, 29897–29903. [CrossRef] [PubMed]
125. Kovalchuk, O.; Filkowski, J.; Meservy, J.; Ilnytskyy, Y.; Tryndyak, V.P.; Vasyl'F, C.; Pogribny, I.P. Involvement of microRNA-451 in resistance of the MCF-7 breast cancer cells to chemotherapeutic drug doxorubicin. *Mol. Cancer Ther.* **2008**, *7*, 2152–2159. [CrossRef] [PubMed]
126. Mani, S.A.; Guo, W.; Liao, M.-J.; Eaton, E.N.; Ayyanan, A.; Zhou, A.Y.; Brooks, M.; Reinhard, F.; Zhang, C.C.; Shipitsin, M. The epithelial-mesenchymal transition generates cells with properties of stem cells. *Cell* **2008**, *133*, 704–715. [CrossRef] [PubMed]
127. Angst, B.D.; Marcozzi, C.; Magee, A.I. The cadherin superfamily. *J. Cell Sci.* **2001**, *114*, 625–626. [PubMed]
128. Hurteau, G.J.; Carlson, J.A.; Spivack, S.D.; Brock, G.J. Overexpression of the microRNA hsa-miR-200c leads to reduced expression of transcription factor 8 and increased expression of E-cadherin. *Cancer Res.* **2007**, *67*, 7972–7976. [CrossRef] [PubMed]
129. Adam, L.; Zhong, M.; Choi, W.; Qi, W.; Nicoloso, M.; Arora, A.; Calin, G.; Wang, H.; Siefker-Radtke, A.; McConkey, D. miR-200 expression regulates epithelial-to-mesenchymal transition in bladder cancer cells and reverses resistance to epidermal growth factor receptor therapy. *Clin. Cancer Res.* **2009**, *15*, 5060–5072. [CrossRef] [PubMed]
130. Lin, Y.; Lin, L.; Jin, Y.; Zhang, Y.; Wang, D.; Tan, Y.; Zheng, C. Combination of Matrine and Sorafenib Decreases the Aggressive Phenotypes of Hepatocellular Carcinoma Cells. *Chemotherapy* **2014**, *60*, 112–118. [CrossRef] [PubMed]

131. Li, H.; Xie, S.; Liu, X.; Wu, H.; Lin, X.; Gu, J.; Wang, H.; Duan, Y. Matrine alters microRNA expression profiles in SGC-7901 human gastric cancer cells. *Oncol. Rep.* **2014**, *32*, 2118–2126. [CrossRef] [PubMed]
132. Li, J.; Jiang, K.; Zhao, F. Oxymatrine suppresses proliferation and facilitates apoptosis of human ovarian cancer cells through upregulating microRNA-29b and downregulating matrix metalloproteinase-2 expression. *Mol. Med. Rep.* **2015**, *12*, 5369–5374. [CrossRef] [PubMed]
133. Wang, Z.; Wang, N.; Liu, P.; Chen, Q.; Situ, H.; Xie, T.; Zhang, J.; Peng, C.; Lin, Y.; Chen, J. MicroRNA-25 regulates chemoresistance-associated autophagy in breast cancer cells, a process modulated by the natural autophagy inducer isoliquiritigenin. *Oncotarget* **2014**, *5*, 7013–7026. [CrossRef] [PubMed]
134. Luo, S.; Deng, W.; Wang, X.; Lü, H.; Han, L.; Chen, B.; Chen, X.; Li, N. Molecular mechanism of indirubin-3′-monoxime and Matrine in the reversal of paclitaxel resistance in NCI-H520/TAX25 cell line. *Chin. Med. J.* **2013**, *126*, 925–929. [PubMed]
135. Schmitt, C.A.; Lowe, S.W. Apoptosis and chemoresistance in transgenic cancer models. *J. Mol. Med.* **2002**, *80*, 137–146. [CrossRef] [PubMed]

Chapter 2

Fractional deletion of Compound Kushen Injection, a natural compound mixture, indicates cytokine signaling pathways are critical for its perturbation of the cell cycle

CKI is a mixture of compounds containing several major and minor components. Accumulating evidence suggests that CKI has anti-cancer activity. However, the exact molecular mechanism by which each or a group of single compounds exerts its anti-cancer activity remains poorly understood. The work for this chapter addressed this question by using analytical chemistry coupled with cellular and molecular assays. Results here indicate that the experimental approach for this work has enabled the association of specific compounds with alterations in specific pathway gene expression. This novel approach of depleting components from a mixture and observing the effects using both phenotypic and gene expression studies is likely to be a powerful tool for future research on the mechanism of action of complex mixtures of compounds. This chapter is in the format of the manuscript submitted to *Protein and Cell*. Specific Aim1: To fractionate and reconstitute CKI in order to examine the functions and interactions of reconstituted compounds in MDA-MB-231 breast cancer cell line. Specific Aim2: To determine how specific compounds are responsible for specific aspects of CKI's effects on cancer cell gene expression in order to identify genes/pathways that are associated with specific fractions/components of CKI.

Statement of Authorship

Title of Paper	Fractional deletion of Compound Kushen Injection, a natural compound mixture, indicates cytokine signaling pathways are critical for its perturbation of the cell cycle
Publication Status	☐ Published ☐ Accepted for Publication ☑ Submitted for Publication ☐ Unpublished and Unsubmitted w ork w ritten in manuscript style
Publication Details	

Principal Author

Name of Principal Author (Candidate)	Thazin Nwe Aung		
Contribution to the Paper	Designed and carried out the experiments, analysed data and wrote the manuscript.		
Overall percentage (%)	60%		
Certification:	This paper reports on original research I conducted during the period of my Higher Degree by Research candidature and is not subject to any obligations or contractual agreements with a third party that would constrain its inclusion in this thesis. I am the primary author of this paper.		
Signature		Date	5/11/2018

Co-Author Contributions

By signing the Statement of Authorship, each author certifies that:

i. the candidate's stated contribution to the publication is accurate (as detailed above);

ii. permission is granted for the candidate in include the publication in the thesis; and

iii. the sum of all co-author contributions is equal to 100% less the candidate's stated contribution.

Name of Co-Author	Saeed Nourmohammadi		
Contribution to the Paper	Designed and carried out the experiments, analysed data and wrote the manuscript.		
Signature			06-11-2018

Name of Co-Author	Zhipeng Qu		
Contribution to the Paper	Experimental design, assisted with experiments, assisted with data analysis and manuscript writing		
Signature		Date	5/11/2018

Please cut and paste additional co-author panels here as required.

Name of Co-Author	Yuka Harata-Lee		
Contribution to the Paper	Experimental design, assisted with experiments, assisted with data analysis and manuscript writing		
Signature		Date	5/11/2018

Name of Co-Author	Jian Cui		
Contribution to the Paper	Assisted with experiments		
Signature		Date	5/11/2018

Name of Co-Author	Hanyuen Shen		
Contribution to the Paper	Assisted with experiments		
Signature		Date	6/11/2018

Name of Co-Author	Andrea J Yool		
Contribution to the Paper	Assisted with experiments and manuscript writing		
Signature		Date	5/11/18

Name of Co-Author	Tara Pukala		
Contribution to the Paper	Assisted with experiments and manuscript writing		
Signature		Date	1/11/2018

Name of Co-Author	Hong Du		
Contribution to the Paper	Experimental Design		
Signature		Date	Oct. 31, 2018

Name of Co-Author	Robert Danial Kortschak		
Contribution to the Paper	Experimental design and assisted with manuscript writing		
Signature		Date	5/4/2018

Name of Co-Author	David L. Adelson		
Contribution to the Paper	Supervised the research, assisted the research with the funding, experimental design and wrote the manuscript.		
Signature		Date	5/4/2018

Fractional Deletion of Compound Kushen Injection Indicates Cytokine Signaling Pathways are Critical for its Perturbation of the Cell Cycle

Running title: Fractional deletion of Compound Kushen Injection

Keywords : *Sophora flavescens*, *Smilax glabra*, alkaloid, matrine

Aung TN[1]†, Nourmohammadi S[2]†, Qu Z [1], Harata-Lee Y [1], Cui J[1], Shen HY[1], Yool AJ[2], Pukala T[3], Hong Du[4], Kortschak RD[1], and Adelson DL*[1].

[1] Department of Molecular and Biomedical Science, School of Biological Sciences, University of Adelaide, Adelaide, South Australia, 5005.

[2] Adelaide Medical School, University of Adelaide, Adelaide, South Australia, 5005.

[3] School of Physical Sciences, University of Adelaide, Adelaide, South Australia, 5005.

[4] School of Chinese Materia Medica, Beijing University of Chinese Medicine, Beijing, 100029, P.R.China.

†Co-1st authors: Aung TN and Nourmohammadi S

Thazin NweAung ORCID ID : 0000-0003-4150-0426

Saeed Nourmohammadi ORCID ID : 0000-0002-9469-2874

***Corresponding author: Adelson DL**

Department of Molecular and Biomedical Science, School of Biological Sciences, University of Adelaide, Adelaide, South Australia, 5005.

Telephone : +61 8 8303 7555

Email: david.adelson@adelaide.edu.au

Abstract

We have used computational and experimental biology approaches to identify candidate mechanisms of action of a traditional Chinese medicine; Compound Kushen Injection (CKI), in a breast cancer cell line in which CKI has been shown to cause apoptosis. Because CKI is a complex mixture of plant secondary metabolites, we used a high-performance liquid chromatography (HPLC) fractionation and reconstitution approach to define chemical fractions required for CKI to induce apoptosis in MDA-MB-231 cells. Our initial fractionation separated major from minor compounds, and showed that the major compounds accounted for little of the activity of CKI. By systematically perturbing the major compounds in CKI we found that removal of no single major compound could alter the effect of CKI on cell viability and apoptosis. However, simultaneous removal of two major compounds identified oxymatrine and oxysophocarpine as critical compounds with respect to CKI activity. We then used RNA sequencing and transcriptome analysis to correlate compound removal with gene expression and phenotype data. We determined that many compounds in CKI are required for its effectiveness in triggering apoptosis but that significant modulation of its activity is conferred by a small number of compounds. In conclusion, CKI may be typical of many plant based extracts that contain many compounds in that no single compound is responsible for all of the bioactivity of the mixture and that many compounds interact in a complex fashion to influence a network containing many targets.

Introduction

Natural compounds are chemically diverse and have long served as resources for the identification of drugs (Harvey et al., 2015). However, the standard approach of fractionating natural product extracts to identify a single compound's biological activity can fail because the original activity of the mixture is not present in single compounds after fractionation. This failure to identify single compounds implies that some natural product mixtures derive their activity from the interaction of several bioactive compounds within the mixture. Characterising the mode of action of natural product mixtures has remained a difficult task as the combinatorial complexity of such mixtures makes it unfeasible to screen all combinations of the compounds in the mixture.

We introduce here a "subtractive fractionation approach" using high performance liquid chromatography (HPLC) that can pinpoint significant interacting compounds within a mixture when coupled with a suitable bioassay. We combined this approach with RNA sequencing (RNAseq) characterisation of our bioassay, correlating the removal of interacting compounds with concomitant alterations in gene expression. This allows us to identify specific combinations of compounds associated with specific pathways and regulatory interactions. In this report, we have applied this approach for the first time to a particular Traditional Chinese Medicine formulation: CKI, which is used to treat approximately 30,000 cancer patients/day in China in conjunction with Western chemotherapy.

CKI is composed primarily of alkaloids and flavonoids extracted from two herbal medicinal plants: Kushen (*Sophora flavescens*) and Baituling (*Heterosmilax chinensis*). Twenty-one chromatographic peaks have been identified from CKI with eight compounds being recognized as major components on the basis of their abundance (Ma et al., 2014). The extract containing the most abundant compounds in CKI is derived from Kushen herb which has a long history in the treatment of patients suffering immune function disorders (Xu et al., 2005; Cheng et al., 2006). The main component of CKI, macrozamin, is a derivative of baituling which has been

a suggested therapeutic agent for the treatment of inflammatory disease (Jiang et al., 1997). Gao and colleagues showed that treatment with each of four of the main compounds of CKI (oxymatrine, matrine, sophoridine and Nmethycytisine) at 4 mg/ml significantly decreased cell viability (Gao et al., 2018). However, these concentrations are relatively high when compared to the contributing concentration of these four main compounds in CKI (Ma et al., 2014). The two main components of CKI, matrine and oxymatrine, may have significant anti-cancer activities in various types of solid tumors including breast cancer, non small lung cancer, cervical cancer, prostate cancer, synovial sarcoma, and hepatocellular carcinoma (Yu et al., 2009; Li et al., 2015; Wu et al., 2015; Cai et al., 2016; Wu et al., 2016; Aung et al., 2017; Gao et al., 2018; Zhou et al., 2018). In contrast, toxicity of medicinal herbs containing matrine and oxymatrine as main components has also been reported (Wang and Yang, 2003). Administration of matrine 150 mg/kg and oxymatrine 360 mg/kg significantly increased cytochrome P450 family protein CYPB1/2 in rats demonstrating a potential therapeutic drawback of these two compounds (Yuan et al., 2010). Overall, understanding the effects of CKI based on the effects of single compounds present in CKI has been at best, partially successful.

Alternatively, by removing one, two or three compounds, we have been able to map the effects of these compounds and their interactions to effects on specific pathways based on altered gene expression profiles in a cell-based assay. This has illuminated the roles of several major compounds of CKI, which on their own have little or no activity in our bioassay. This approach can be used to dissect the roles and interactions of individual compounds from complex natural compound mixtures whose biological activity cannot be attributed to single purified compounds.

Results

Subtractive fractionation overview

Well resolved chromatographic separation of CKI was used to collect all of the major components of CKI as individual fractions (Fig. 1A). We then reconstituted all of the separated fractions except for those we wished to subtract. We tested the reconstituted combination of compounds/peaks to see if removal of a single (N-1) or multiple compounds, (N-2 or N-3, where N represents the total number of compounds in CKI), or removal of all major peaks (minor, MN) or depletion of all minor peaks (major, MJ) significantly altered the effect of CKI in our cell based assays. Our cell based assays (Qu et al., 2016) measured MDA-MB-231 (human breast adenocarcinoma) cell viability, cell cycle phase and cell apoptosis. A summary of the subtractive fractions used in the cell based assays is shown in Table 1. We then carried out RNA isolation of cells treated with CKI, individual compounds or CKI deletions for RNAseq. Differentially expressed (DE) genes in these samples allowed the association of specific compounds with cell phenotype and underlying alterations in gene regulation. By comparing DE genes across treatment combinations we identified specific candidate pathways that were altered by removal of single or multiple compounds, as detailed below.

HPLC fractions and content identification using LC-MS/MS

HPLC fractionation and reconstitution was used to generate a number of N-1, N-2, N-3, MJ and MN mixtures, (Fig. 1A, 1B, 1C and Sup. Fig. 1) with specific combinations and their components shown in Table 1. The concentrations of known compounds in CKI and reconstituted subtractive fractions were determined from standard curves (Sup. Data. 1) for nine available reference compounds, using cytisine as an internal standard (Table 2). The combined concentration of 9 reference compounds from CKI was approximately 10.8 mg/ml, whereas subtractive fractions N-OmtOspc and N-MacOmtOspc had concentrations of reference compounds of 3.8 mg/ml and 2.1 mg/ml which were equivalent to the concentrations

of these compounds in unfractionated CKI. The depleted OmtOspc and MacOmtOspc were not observed in the N-OmtOspc and N-MacOmtOspc respectively. These collectively suggested any effects observed after the treatments of N-OmtOspc and N-MacOmtOspc were not influenced by the concentrations. A total of 9 (N-1), 4 (N-3) and 9 (N-2) combinations, along with MJ and MN deletions were tested in our cell based assays (Table 1).

Phenotypic changes associated with compound deletion

Fractionation and full reconstitution caused no changes in cell viability compared to original CKI (see methods) at either 24- or 48-hours in MDA-MB-231 cells. Both reconstituted CKI and CKI caused significantly reduced viability compared to untreated (UT) cells (Sup. Fig. 2A). The MJ subtractive fraction contained a total of 9 compounds including eight previously identified MJ peaks (Ma et al., 2014) and adenine (unpublished data from Ma Yue) (Fig. 1A) and the MN fraction contained the remaining peaks (Fig. 1C). MJ had no effect on cell viability, while MN reduced cell viability to the same extent as CKI (Fig. 2A). The 9 major compounds were individually depleted from CKI and tested as 9 (N-1) subtractive fractions, with no significant alterations in cell viability compared to CKI (Fig. 2B). We then assessed the interaction effects of single MJ compounds by adding them back to the MN subtractive fraction. No change in cell viability compared to MN was observed (Sup. Fig. 2B). Sets of 3 compounds from the 9 major/standard compounds of CKI were depleted to generate 3 (N-3) subtractive fractions. The nine reference compounds were allocated into three groups, one of which contained structurally similar compounds (Omt, Ospc, Spc) and two other groups ([Mac, Ade, Tri] and [Nme, Mt, Spr]) that contained structurally different compounds. Of these three fractions, N-OmtOspcSpc decreased cell viability significantly ($P < 0.05$) more than CKI after 48 hours (Fig. 2C) while none of the sets of three compounds on their own had any effect on cell viability (Sup. Fig. 2). We then generated 9 (N-2) subtractive fractions based on the N-3 subtractive fractions (Table 1). Out of 9 (N-2)

subtractive fractions (Sup. Fig. 2), only N-OmtOspc significantly decreased proliferation compared to CKI ($P < 0.05$) (Fig. 2C). We then depleted macrozamin, the only major compound derived from Baituling, together with OmtOspc as N-3 (N-MacOmtOspc) in order to determine if there was an additional effect when compared to CKI. N-OmtOspc and N-MacOmtOspc both decreased cell proliferation to the same extent (Fig. 2C and 2D).

While no change in cell viability was found across all N-1 treatments, cell cycle analysis was performed to identify more subtle differences. There was no statistically significant difference in phases of the cell cycle of MDA-MB-231 cells for many of the N-1 treatments compared to CKI except for a statistically significant change in G1 phase by N-Omt after 48 hours (Fig. 3A). On the other hand, N-OmtOspc treatment significantly altered the cell cycle for MDA-MB-231 cells and induced significant higher apoptosis from 0.25 mg/ml through 2 mg/ml treatments as compared to CKI at both timepoints (Fig. 3B and Sup. Fig. 3). N-MacOmtOspc treatment also significantly altered the cell cycle at both timepoints with generally similar effects to N-OmtOspc (Fig. 3C).

Annexin V/PI apoptosis assays were performed using subtractive fractions on MDA-MB-231, HEK-293 (human embryonic kidney cells) and HFF (primary human foreskin fibroblasts) cell lines. While CKI at 2 mg/ml caused increased apoptosis in MDA-MB-231 cells at both 24- and 48-hour after treatment, N-OmtOspc and N-MacOmtOspc subtractive fractions at concentrations equivalent to CKI 2 mg/ml significantly increased the percentage of apoptotic cells at 24-hour with increasing apoptosis at the 48-hour timepoint, indicating that N-OmtOspc and N-MacOmtOspc significantly enhanced apoptosis compared to CKI (Fig. 4A, 4E and Sup. Fig. 3A). Although CKI did not generally cause apoptosis in HEK-293 or HFF cells, N-OmtOspc and N-MacOmtOspc subtractive fractions significantly induced apoptosis ($P*** < 0.001$) at 24-hour and 48-hour ($P**** < 0.0001$) in both HEK-293 and HFF cells. CKI only induced apoptosis of HEK-293 ($P* < 0.05$) at 48-hour and showed no significant apoptotic induction in HFF (Fig. 4B, 4C and Sup. Fig. 3B and 3C). These results indicated that the N-

OmtOspc and N-MacOmtOspc subtractive fractions induced apoptosis not only in cancerous cells but also in non-cancerous cell lines. In contrast to this, no significant apoptosis was triggered by CKI on HFF cells. A small but significant apoptotic induction was observed for HEK-293.

Because of the significant decreased viability accompanied by increased apoptosis triggered by subtractive fractions, cytotoxicity tests were carried out for all three cell lines using CKI (2 mg/ml) and N-OmtOspc and N-MacOmtOspc subtractive fractions at concentrations equivalent to CKI 2 mg/ml. N-OmtOspc and N-MacOmtOspc at equivalent concentration to CKI 2 mg/ml were significantly cytotoxic to both non-cancerous cell lines (Fig. 4D).

Overall, these results indicated that removal of combinations of specific compounds from CKI had unpredictable effects on the ability of CKI to kill cells. While removal of all major compounds from CKI caused no loss of activity and removal of all minor compounds caused total loss of activity, removal of selected major compounds (N-OmtOspc) paradoxically caused major, significant increases in the ability of CKI to reduce viability and killed cells.

Differential gene expression

In order to understand the interactions of the components in CKI as a result of depletion, we carried out RNAseq of MDA-MB-231 cells treated with CKI and subtractive fractions. Four out of nine (N-1) subtractive fractions, four, namely N-Omt, N-Mac, N-Tri and N-Nme, were selected due to their structural differences to determine their effects on transcript levels. N-OmtOspc and N-MacOmtOspc, OmtOspc, MacOmtOspc and CKI treated cells were sequenced at 24 and 48-hour timepoints.

After normalization, clear clustering of the replicates was observed (Fig. 5A and Sup. Fig. 4, 5, 6 and 7), indicating that all 4 (N-1) treatments show comparable downstream gene expression patterns. Likewise, OmtOspc and MacOmtOspc groups and N-OmtOspc and N-

MacOmtOspc groups showed similar changes in gene expression, except for one replicate (N-MacOmtOspc, 24-hour) that clustered with UT, OmtOspc and MacOmtOspc.

The number of DE genes associated with each treatment was calculated using pairwise comparative analysis. CKI treatment was used as a baseline to compare all other treatments in order to emphasize the effect of depleted compounds and CKI treatment was compared to UT. There were thousands of upregulated and downregulated genes at 24 and 48 hours in most pairwise comparisons (Fig. 5B). However DE genes between OmtOspc and MacOmtOspc treatments were not observed and there were almost no DE genes between N-Mac, N-Nme and N-Tri treatments (Fig. 5B) indicating that these three subtractive fractions had very similar effects on gene expression.

When we compared the DE genes found between treatments, there were a large number of DE genes (~71.3 %) shared between all four (N-1) treatments (Sup. Fig. 8 and 9 and Sup. Table. 1). A similar number of shared DE genes (~24.6 %) between four (N-1), OmtOspc and MacOmtOspc and between four (N-1), N-OmtOspc and N- MacOmtOspc as compared to CKI at 48-hours indicated that gene expression patterns from N-1 treatments were mostly different from N-OmtOspc, N- MacOmtOspc, OmtOspc and MacOmtOspc treated cells. 55 % of the DE genes between UT, OmtOspc and MacOmtOspc were shared. When the four (N-1) treatments were compared to CKI treatment, 42.8 % of DE genes were shared, and when N-OmtOspc and N- MacOmtOspc treatments were compared to CKI, 50.1 % DE genes were shared, indicating that N-OmtOspc and N-MacOmtOspc treatments appeared to be more similar to CKI than N-1 treatments.

The overall levels of similarity in DE genes were as follows: 1) All N-1 treatments had approximately 70 % similar gene expression patterns, 2) OmtOspc and MacOmtOspc treatments were approximately 50 % similar to UT and 33 % similar to N-1 treatments, 3) downstream gene expression patterns between N-1, N-OmtOspc and N-MacOmtOspc were approximately 37 % similar.

Gene ontology and pathway annotation of DE genes

DE genes were analysed for over-representation in our data sets with respect to biological function using Gene Ontology (GO) annotation. We looked for shared DE genes between treatments and identified over-represented genes in these shared genes. The only common function enriched across all comparisons was for "cell cycle checkpoint" (Fig. 6A). This confirmed earlier results (Qu et al., 2016) and was consistent with the phenotype data for CKI.

Subtracted fractionation altered pathways

We also performed pathway based analysis to look for pathway level perturbation by comparing DE genes within Kyoto Encyclopedia of Genes and Genomes (KEGG) pathways between treatments. We used Signaling Pathway Impact Analysis (SPIA) to identify pathways with statistically significant perturbation values expected to alter pathway flux. We identified 86 pathways (Sup. Fig. 11) with statistically significant ($P < 0.05$) perturbations of gene expression and of these, 15 pathways were most obviously linked to our phenotypes of cell viability, cell cycle and apoptosis (Fig. 6B). By comparing the pathway gene expression global perturbation scores (pG) between treatments three specific observations could be made: 1) N-1 fractional deletions vs CKI had significant effects on flux in some pathways without phenotypic effects, 2) N−OmtOspc vs CKI which had a pronounced phenotypic effect at both 24- and 48-hours, had a significant effect on reducing estimated pathway flux for Cytokine-Cytokine Receptor, Cell Cycle and TGF-Beta signaling pathways, 3) comparison of N-1 fractional deletions vs fractional deletions of N−OmtOspc/N−MacOmtOspc showed consistent pathway perturbations for Cytokine-Cytokine Receptor and p53 signaling pathways. On this basis, we inferred that different major compounds could be deleted with very similar effects, indicating that they may have similar targets. In contrast, deleting Omt and Ospc simultaneously caused a significant shift in phenotype and was accompanied by specific perturbations in pathways that regulate inflammation, cell cycle and apoptosis. The combined

deletion of Omt and Ospc had a synergistic effect on viability, cell-cycle and apoptosis and a synergistic effect on gene expression, consistent with the observed changes in pathway specific perturbation of gene expression. Because this double compound deletion potentiated the cell killing effect of CKI we hypothesised that the compounds in CKI have multiple targets leading to a phenotypic effect that reflects the integration of stimulation and inhibition across all those targets. Removal of Omt and Ospc alter the balance of stimulation and inhibition leading to an integrated effect for the remaining compounds in the mixture that caused more cell death than CKI.

More detailed examination of some of these interactions within significantly perturbed pathways highlighted the gene-specific changes in expression for some key regulators of inflammation and the cell-cycle. Most effects on gene expression from deletion of single vs two compounds were similar, suggesting that the enhanced cell killing by N-OmtOspc was due to additive effects of the compound deletions. However, by comparing differences in pairwise comparisons between treatments at the gene level within the Cytokine-Cytokine Receptor Interaction and Cell Cycle pathways we identified a subset of genes that had opposite changes in gene expression when comparing single compound deletions to N-OmtOspc deletion. In the Cytokine-Cytokine Receptor Interaction pathway (Fig. 7), these genes are *IL1-R1* (Interleukin-1 Receptor), *IL-27RA* (Interleukin-27 Receptor alphasubunit), *TNFRSF1B* (Tumor Necrosis Factor Receptor Superfamily Member 1B), *TNFRSF14* (Tumor Necrosis Factor Receptor Superfamily, Member 14) and *OSMR* (Oncostatin M Receptor/IL-31 Receptor Subunit Beta) and they all transduce inflammatory ligand signals to the NF_kB pathway and/or the apoptosis pathway. In the Cell-Cycle pathway (Fig. 8), these genes are *CDKN1C* (Cyclin-Dependent Kinase Inhibitor 1C (P57, Kip2)), *CDC25B* (Cell Division Cycle 25B), *ATR* (ATR Serine/Threonine Kinase), *CDKN1B* (Cyclin-Dependent Kinase Inhibitor 1B (P27, Kip1)), *CDKN2D* (Cyclin-Dependent Kinase Inhibitor 2D (P19, Inhibits CDK4)), *TGFB1*

(Transforming Growth Factor Beta 1), *FZR1* (Fizzy And Cell Division Cycle 20 Related 1), *CDC20* (Cell Division Cycle 20), *CDC27* (Cell Division Cycle 27), *ORC2* (Origin Recognition Complex Subunit 2), *ANAPC4* (Anaphase Promoting Complex Subunit 4), *ZBTB17* (Zinc Finger And BTB Domain Containing 17) and *, ABL1* (ABL Proto-Oncogene 1, Non-Receptor Tyrosine Kinase). The opposite changes in gene expression stimulated by N-OmtOspc compared to N-1 subfractions provide support for the idea that multiple major compounds can have similar effects on specific genes but that the combination of Omt and Ospc can have synergistic and opposite effects on those same genes. This means that multiple compounds with overlapping targets (based on their structural similarities) can either reinforce a single outcome or exhibit unpredictable and opposite effects when combined.

Overall our results support the concept of multi-compound/multi-target interactions for plant extract based drugs that contain many plant secondary metabolites. Biological effects of complex plant extracts may result from interactions of multiple compounds, with negligible effects from single compounds alone. This has implications for how we assess the functional evidence for such extracts.

Discussion

Previous studies have demonstrated that CKI can alter the cell cycle, induce apoptosis and reduce proliferation in various cancer cell lines (Xu et al., 2011; Qu et al., 2016; Gao et al., 2018). CKI also killed leukaemia cells via the Prdxs/ROS/Trx1 signalling pathway in an acute myeloid leukaemia patient-derived xenograft model and caused cell cycle arrest in U937 leukaemia derived cells (Jin et al., 2018). Cell cycle arrest by CKI at checkpoints is correlated with the induction of double strand breaks by CKI treatment (Cui et al., 2018). In contrast to our experiments reported above, oxymatrine was previously shown to arrest the cell cycle and induce apoptosis in human glioblastoma cells through EGFR/PI3K/Akt/mTOR signaling pathway (Dai et al., 2018) and inhibit the proliferation of laryngeal squamous cell carcinoma Hep-2 cells (Ying et al., 2015). As shown in this report, oxymatrine or oxysophocarpine or combined OmtOspc treatment caused no significant change in cell viability, the cell cycle or apoptosis, in agreement with prior work that showed oxymatrine and oxysophocarpine exerting no significant effect on apoptosis, cell cycle or cell proliferation in HCT116 human colon cancer cells (Zhang et al., 2014).

The paradoxical result that removal of OmtOspc caused a striking increase in apoptosis is most simply explained by a model based on integrating effects of multiple compounds on many targets. The interactions between compounds in the mixture can be synergistic and antagonistic such that if two compounds are removed that have a synergistic effect that is antagonistic to the remainder of the mixture, the resulting depleted mixture will be dis-inhibited compared to CKI. This is illustrated by our studies and others that show single compounds alone had no or little effect compared to CKI. For instance, while CKI treatment resulted in increased DNA double strand breaks and affected the cell cycle resulting in decreased cancer cell proliferation, oxymatrine alone exhibited only a small effect in the same assay (Cui et al., 2018). Gao and colleagues also reported that oxysophocarpine at 4 mg/ml had no effect, oxymatrine at 4 mg/ml

(*P < 0.05) and CKI at 2 mg/ml (***P < 0.001) significantly reduced the proliferation of hepatocellular carcinoma SMMC-7721 cells *in vitro* (Gao et al., 2018). Although significant inhibition of proliferation by oxymatrine occurred, the concentration used in this experiment was ~ 8x times higher than that of oxymatrine in 2 mg/ml of CKI. These studies agree with our experimental outcomes that oxymatrine and oxysophocarpine individually had no or little effect compared to CKI treatment.

At the level of gene expression in our study, gene ontology analysis indicated that genes for "cell cycle checkpoint" were significantly enriched in cells treated with all fractionated mixtures or mixtures of Omt and Ospc. Consistent with other studies, our results also demonstrated that these compounds had little or no phenotypic effect on their own, but that when both were deleted, the remaining compounds unexpectedly had significantly greater effects on phenotype and gene expression. When examined in the context of specific pathways, treatment with OmtOspc or N-OmtOspc which had strikingly different effects on phenotype, had similar effects on the perturbation of the "Cytokine-Cytokine Receptor Interaction" pathway, the most commonly perturbed pathway seen in our analysis, that interestingly did not show up when comparing CKI to UT. This is consistent with previous work showing that CKI induced cytokines IL4 and IL10 in cancer patients with acute leukaemia (Tu et al., 2016). In contrast to this observation, IL4 and IL10 levels were significantly decreased in transgenic mice treated with oxymatrine at a dose of 200 mg/kg (Dong et al., 2002). In our experiment, we also observed that while CKI and many of the depleted fractions had significant effect on the genes in the "Cytokine-Cytokine Receptor Interaction" pathway, OmtOspc and MacOmtOspc had little effect on the genes in that pathway. The observation that many genes in the "Cytokine-Cytokine Receptor Interaction" pathway were not affected by OmtOspc and MacOmtOspc compared to deletion fractions confirmed that removal of compounds rather than

treatment with single or a few compounds can be more informative of the role and significance of individual compounds as part of mixtures/extracts.

In summary, Our approach allowed the identification of both synergistic and antagonistic interactions within the drug mixture. Viewed as a network where the compounds and the targets are nodes and the interactions between compounds and targets, and between targets are edges, it is clear that the edges (interactions) determine the overall effect of the compound mixture. By removing one or two compounds from a mixture, we can potentially perturb the target network(s) to either reduce the effect of the mixture for some outcome or potentiate it for another. We believe this approach may be of general use for the study of herbal medicines/extracts, avoiding failures that stem from exclusive reliance on the identification of a single compound that accounts for most of the biological activity in mixtures.

Materials and Methods

Cell lines

MDA-MB-231 cells were purchased from the American Type Culture Collection (ATCC, VA, USA). HEK-293 and HFF were kindly provided by Prof. Andrea Yool (Medical School, University of Adelaide). Cells were cultured in Dulbecco's Modified Eagle's Medium (Thermo Fisher Scientific) with 10 % Fetal bovine serum (Thermo Fisher Scientific) at 37^0C with 5 % CO_2.

Compound fractionation by HPLC

CKI (Batch No: 20170322, total alkaloid concentration of 26.5 mg/ml) was provided by Zhendong Pharmaceutical Co.Ltd (China). CKI (N) was processed to deplete Single (N-1), double (N-2) and triple (N-3) compounds using HPLC by standardizing using nine compounds, namely Oxymatrine (Omt), Oxysophocarpine (Ospc), N-methylcytisine (Nme), Matrine (Mt), Sophocarpine (Spc), Trifolirhizin (Tri), Adenine (Ade), Sophoridine (Spr) (Beina Biotechnology Institute Co., Ltd, China), and macrozamin (Zhendong Pharmaceutical Co.Ltd, China) which were previously reported to be found in published and unpublished data (Ma et al., 2014). HPLC fractionation separated Minor (MN) and Major (MJ) peaks to determine the principle and secondary components. The MJ mixture contained the nine standard compounds mentioned above and MN contained the remaining CKI components. In addition, nine N-1 fractional deletions, nine N-2 fractional deletions and three N-3 fractional deletions were produced.

HPLC separation was achieved using an Shimadzu HPLC instrument (Japan) equipped with a photodiode-array UV-Vis detector with preparative C_{18} column (5 µm, 250 x 10 mm) (CA, USA). The following mobile phase was used to fractionate the CKI mixture: 0.01 M ammonium acetate (adjusted to pH 8.0, solvent A) and acetonitrile + 0.09 % trifluroacetic acid (solvent B). The flow rate was 2 ml/min and linear gradient was adopted as follows; 0 min, 100

% A; 60 min, 65 % A, 70 min, 100 % A. The chromatogram was recorded from 200 nm to 280 nm, with monitoring at 215 nm. Samples were frozen and lyophilised using a Christ Alpha 1-2 LD lyophilizer (Martin Christ Gefriertrocknungsanlagen GmbH, Germany). Several cycles of lyophilisation and resuspension were used to remove all remaining HPLC solvents and final reconstitution was carried out using MilliQ H_2O buffered with 10 mM HEPES (Gibco, Life technologies, USA) and adjusted to pH 6.8-7.0. Lyophilised samples were resuspended to create an equivalent dilution for compounds in the sample compared to CKI.

Identification of reconstituted mixtures by Liquid Chromatography/Mass Spectrometry (LC-MS/MS)

Agilent 6230 TOF mass spectrometer was used to determine the concentration of the known compounds from the CKI and reconstituted N-OmtOspc and N-MacOmtOspc mixtures. 10 µl sample was injected with the flow rate of 0.8 ml/min, a gradient program of 0 min, 100 % A; 40 % B; 25 min, 60 % B, 35 min, and solvents MilliQ H_2O + 0.1 % formic acid (solvent A) and acetonitrile + 0.1 % formic acid (solvent B). The column used was C_{18} (5 µm, 150 x 4.6 mm, Diamosnsil, Dkimatech, China). The recovered contents of the samples were measured by spike-in compound cytosine. Gas phase ions were generated with an electrospray source, with key instrument parameters: gas temperature, 325; sheath gas temperature, 350; vCap, 3500; fragmentor, 175; acquisition range (m/z) 60-17000. Calibration curves for 9 standard compounds containing various concentrations were shown in Supplementary Data.

Cell viability Assay

2,3-bis-(2-methoxy-4-nitro-5-sulfophenyl)-2H-tetrazolium-5-carboxanilide (XTT) and N-methyl dibenzopyrazine methyl sulfate (PMS) (50 : 1, Sigma-Aldrich, St. Louis, MO, USA) assay was used to assess cell viability as described in Qu et al (Qu et al., 2016). Briefly, 8,000 cells in 50 µl of medium were plated in 96 wells trays overnight prior to drug treatments in

triplicate. Cells were subsequently treated with 50 µl of drug mixtures to provide final concentrations of 0.25, 0.5, 1 and 2 mg/ml of total alkaloids in 100 µl. Cell viability was then measured at 24-and 48-hours after drug treatment by the addition of 50 µl of XTT:PMS mixture (50 : 1 ratio). An equal volume of medium and treating agents plus XTT:PMS was used to subtract the background optical density. The absorbance of each well was recorded using a Biotrack II microplate reader at 492 nm.

Annexin V/PI apoptosis assay

Apoptosis resulting from treatment was determined using an Annexin V-FITC apoptosis detection kit (Thermofisher Scientific) according to the manufacturer's protocol. Briefly, $4x10^5$ cells were seeded in 6-well plates in triplicate overnight prior to treatment. On the following day, cells were treated with the agents as described for 24-and 48-hours. Data were acquired with a BD LSR Fortessa X20 (BD Bio Sciences, NJ, USA) flow cytometer, and FlowJo software (TreeStar Inc., OR, USA) was used to analyse the acquired data and produce percent apoptosis values.

Cell cycle assay

Cell culture and drug treatments were performed as described above for cell cycle analysis. A Propidium Iodide (PI) staining protocol (Riccardi and Nicoletti, 2006) was used to detect the changes in cell cycle as a result of treatment after 24- and 48-hours. The characteristics of stained cells were measured using a BD LSR Fortessa flow cytometer, and acquired data were analysed using FlowJo software.

Cytotoxicity assay

Cells were seeded in 96-well plates at a density of 2.5 x 10^3 cells per well in triplicate. CKI and fractionated mixtures at final concentrations of 1 mg/ml and 2 mg/ml were added to each

well and after 24-hours of incubation and viable cells were measured using the Alamar Blue assay (Thermo Fisher Scientific). 5 μM of Mercuric chloride (Sigma-Aldrich) was used as a positive control and wells without cells were set as a negative control in the same plate.

Sample preparation and RNA sequencing

Cells were plated in 6 well plates with a density of $2x10^5$ cells/ml overnight prior to drug treatments. On the following day, CKI (at a final concentration of 2 mg/ml) and fractionated mixtures (equivalent dilutions of CKI) were added. Total RNA was isolated by using an RNA extraction kit (Thermo Fisher Scientific) according to the manufacturer's instructions and RNA samples were quantified and quality determined using a Bioanalyzer at the Cancer Genome Facility of the Australian Cancer Research Foundatin (Australia). RNA samples with RNA integrity number (RINs) > 7.0 were sent to be sequenced at Novogene (China). Briefly, after QC procedures were performed, mRNA was isolated using oligo(dT) beads and randomly fragmented by adding fragmentation buffer, followed by cDNA synthesis primed with random hexamers. Next, a custom second-strand synthesis buffer (Illumina) , dNTPs, RNase H and DNA polymerase I were added for second-strand synthesis. After end repair, barcode ligation and sequencing adaptor ligation, the double-stranded cDNA library was size selected and PCR amplified. Sequencing was carried out on an Illumina HiSeq platform PE150 with paired-end 150 bp reads.

Transcriptome data processing

FastQC (v0.11.4, Babraham Bioinformatics) was used to check the quality of raw reads before proceeding with downstream analysis. Trim_galore (v0.3.7, Babraham Bioinformatics) with the parameters: --stringency 5 --paired --fastqc_args was used to trim adaptors and low-quality sequences. STAR (v2.5.3a) was then applied to align the trimmed reads to the reference genome (hg19, UCSC) with the parameters: --outSAMstrandField intronMotif --

outSAMattributes All --outFilterMismatchNmax 10 --seedSearchStartLmax 30 --outSAMtype BAM SortedByCoordinate (Dobin et al., 2013). Then, subread (v1.5.2) was used to generate read counts data with the following parameters featureCounts -p -t exon -g gene_id (Liao et al., 2013). Significantly differentially expressed genes between treatments were analysed and selected using edgeR (v3.22.3) with false discovery rate (FDR) < 0.05 (Robinson et al., 2010). Removal of unwanted variance (RUVs) package in R was applied to two different batches of transcriptome datasets to eliminate batch variance (Risso et al., 2014). APE was used to cluster the treatments (Paradis et al., 2004) followed by RUVs. Gene Ontology (GO) overrepresentation analyses were performed using clusterProfiler with the parameter ont = "BP"(Biological Process), pAdjustMethod = "BH", pvalueCutoff = 0.01, and qvalueCutoff = 0.05 (Yu et al., 2012). Signalling Pathway Impact Analysis (SPIA) was carried out to identify the commonly perturbed pathways within the treatments using the SPIA R package (Tarca et al., 2008). Significantly perturbed pathways were visualized using Pathview package in R (Luo and Brouwer, 2013).

Statistical analysis

Statistical analyses were carried out using GraphPad Prism 8.0 (GraphPad Software Inc., CA, USA). Student's t-test or ANOVA (one-way or two-way) was used when there were two or three groups to compare respectively. Post hoc "Bonferroni's multiple comparisons test" was performed when ANOVA results were significant. Statistically significant results were represented as $p < 0.05$ (*) or $p < 0.01$ (**) $p < 0.001$ (***), or $p < 0.0001$ (****); ns (not significant). All data were shown as mean ± standard deviation (SD).

FOOTNOTES

Acknowledgements

This work was supported by the special international corporation project of traditional Chinese medicine (GZYYGJ2017035) and The University of Adelaide, Zendong Australia China Centre for Molecular Chinese Medicine. The authors would like to thank Dr. Denis Scanlon and Associate Prof. Stephen Bell for the assistance with HPLC usage and Jue Zeng for her valuable discussions.

Abbreviations

CKI, Compound Kushen Injection; RNA-Seq, RNA Sequencing; KEGG, Kyoto Encyclopedia of Genes and Genomes; SPIA, Signaling Pathway Impact Analysis; GO, Gene Ontology; FDR, False Discovery Rate; DE, Differentially Expressed; MDS, Multiple Dimensional Scaling; RUVs, Removal of unwanted variance; SD, Standard Deviation; PI, Propidium Iodide; HPLC, High Perfromance Liquid Chromatography; LC-MS/MS, Liquid Chromatography/Mass Spectrometry; Mac, Macrozamin; Ade, Adenine; Nme, N-methylcytisine; Spr, Sophoridine; Mt, Matrine; Spc, Sophocarpine; Ospc, Oxysophocarpine; Omt, Oxymatrine; Tri, Trifolirhizin; MJ, Major; MN, Minor.

Author contributions

T.N.A, S.N, Z.Q and D.L.A designed the study, analysed the data and wrote the manuscript. T.N.A and S.N conducted the experiments. Y.H-L, J.C, H.S, T.P, and H.D assisted the experiments and analysed the data. A.J.Y and D.K assisted in writing the manuscript.

Conflict of interest

The authors declare no conflicts of interest.

Declaration of transparency and scientific rigour

This declaration acknowledges that this paper adheres to the principles for transparent reporting and scientific rigour of preclinical research recommended by funding agencies, publishers and other organisations engaged with supporting research.

Reference:

Aung, T.N., Qu, Z., Kortschak, R.D., and Adelson, D.L. (2017). Understanding the effectiveness of natural compound mixtures in cancer through their molecular mode of action. International journal of molecular sciences 18, 656.

Cai, Y., Xu, P., Yang, L., Xu, K., Zhu, J., Wu, X., Jiang, C., Yuan, Q., Wang, B., and Li, Y. (2016). HMGB1-mediated autophagy decreases sensitivity to oxymatrine in SW982 human synovial sarcoma cells. Scientific reports 6, 37845.

Cheng, H., Xia, B., Zhang, L., Zhou, F., Zhang, Y.-X., Ye, M., Hu, Z.-G., Li, J., Li, J., and Wang, Z.-L. (2006). Matrine improves 2, 4, 6-trinitrobenzene sulfonic acid-induced colitis in mice. Pharmacological research 53, 202-208.

Cui, J., Qu, Z., Harata-Lee, Y., Aung, T.N., Shen, H., Wang, W., and Adelson, D.L. (2018). Cell Cycle, Energy Metabolism and DNA Repair Pathways in Cancer Cells are Suppressed by Compound Kushen Injection. bioRxiv, 348102.

Dai, Z., Wang, L., Wang, X., Zhao, B., Zhao, W., Bhardwaj, S.S., Ye, J., Yin, Z., Zhang, J., and Zhao, S. (2018). Oxymatrine induces cell cycle arrest and apoptosis and suppresses the invasion of human glioblastoma cells through the EGFR/PI3K/Akt/mTOR signaling pathway and STAT3. Oncology reports 40, 867-876.

Dobin, A., Davis, C.A., Schlesinger, F., Drenkow, J., Zaleski, C., Jha, S., Batut, P., Chaisson, M., and Gingeras, T.R. (2013). STAR: ultrafast universal RNA-seq aligner. Bioinformatics 29, 15-21.

Dong, Y., Xi, H., Yu, Y., Wang, Q., Jiang, K., and Li, L. (2002). Effects of oxymatrine on the serum levels of T helper cell 1 and 2 cytokines and the expression of the S gene in hepatitis B virus S gene transgenic mice: A study on the anti-hepatitis B virus mechanism of oxymatrine. Journal of gastroenterology and hepatology 17, 1299-1306.

Gao, L., Wang, K.-x., Zhou, Y.-z., Fang, J.-s., Qin, X.-m., and Du, G.-h. (2018). Uncovering the anticancer mechanism of Compound Kushen Injection against HCC by integrating quantitative analysis, network analysis and experimental validation. Scientific reports 8, 624.

Harvey, A.L., Edrada-Ebel, R., and Quinn, R.J. (2015). The re-emergence of natural products for drug discovery in the genomics era. Nature Reviews Drug Discovery 14, 111.

Jiang, J., Wu, F., Lu, J., Lu, Z., and Xu, Q. (1997). Anti-inflammatory activity of the aqueous extract fromrhizoma smilacis glabrae. Pharmacological research 36, 309-314.

Jin, Y., Yang, Q., Liang, L., Ding, L., Liang, Y., Zhang, D., Wu, B., Yang, T., Liu, H., and Huang, T. (2018). Compound kushen injection suppresses human acute myeloid leukaemia by regulating the Prdxs/ROS/Trx1 signalling pathway. Journal of Experimental & Clinical Cancer Research 37, 277.

Li, H., Li, X., Bai, M., Suo, Y., Zhang, G., and Cao, X. (2015). Matrine inhibited proliferation and increased apoptosis in human breast cancer MCF-7 cells via upregulation of Bax and downregulation of Bcl-2. International journal of clinical and experimental pathology 8, 14793.

Liao, Y., Smyth, G.K., and Shi, W. (2013). featureCounts: an efficient general purpose program for assigning sequence reads to genomic features. Bioinformatics 30, 923-930.

Luo, W., and Brouwer, C. (2013). Pathview: an R/Bioconductor package for pathway-based data integration and visualization. Bioinformatics 29, 1830-1831.

Ma, Y., Gao, H., Liu, J., Chen, L., Zhang, Q., and Wang, Z. (2014). Identification and determination of the chemical constituents in a herbal preparation, Compound Kushen injection, by HPLC and LC-DAD-MS/MS. Journal of Liquid Chromatography & Related Technologies 37, 207-220.

Paradis, E., Claude, J., and Strimmer, K. (2004). APE: analyses of phylogenetics and evolution in R language. Bioinformatics 20, 289-290.

Qu, Z., Cui, J., Harata-Lee, Y., Aung, T.N., Feng, Q., Raison, J.M., Kortschak, R.D., and Adelson, D.L. (2016). Identification of candidate anti-cancer molecular mechanisms of compound kushen injection using functional genomics. Oncotarget 7, 66003.

Riccardi, C., and Nicoletti, I. (2006). Analysis of apoptosis by propidium iodide staining and flow cytometry. Nature protocols 1, 1458.

Risso, D., Ngai, J., Speed, T.P., and Dudoit, S. (2014). Normalization of RNA-seq data using factor analysis of control genes or samples. Nature biotechnology 32, 896.

Robinson, M.D., McCarthy, D.J., and Smyth, G.K. (2010). edgeR: a Bioconductor package for differential expression analysis of digital gene expression data. Bioinformatics 26, 139-140.

Tarca, A.L., Draghici, S., Khatri, P., Hassan, S.S., Mittal, P., Kim, J.-s., Kim, C.J., Kusanovic, J.P., and Romero, R. (2008). A novel signaling pathway impact analysis. Bioinformatics 25, 75-82.

Tu, H., Lei, B., Meng, S., Liu, H., Wei, Y., He, A., Zhang, W., and Zhou, F. (2016). Efficacy of compound kushen injection in combination with induction chemotherapy for treating adult patients newly diagnosed with acute leukemia. Evidence-Based Complementary and Alternative Medicine 2016.

Wang, X., and Yang, R. (2003). Movement disorders possibly induced by traditional Chinese herbs. European neurology 50, 153-159.

Wu, C., Huang, W., Guo, Y., Xia, P., Sun, X., Pan, X., and Hu, W. (2015). Oxymatrine inhibits the proliferation of prostate cancer cells in vitro and in vivo. Molecular medicine reports 11, 4129-4134.

Wu, L., Wang, G., Liu, S., Wei, J., Zhang, S., Li, M., Zhou, G., and Wang, L. (2016). Synthesis and biological evaluation of matrine derivatives containing benzo-α-pyrone structure as potent anti-lung cancer agents. Scientific reports 6, 35918.

Xu, G., Yao, L., Rao, S., Gong, Z., Zhang, S., and Yu, S. (2005). Attenuation of acute lung injury in mice by oxymatrine is associated with inhibition of phosphorylated p38 mitogen-activated protein kinase. Journal of ethnopharmacology 98, 177-183.

Xu, W., Lin, H., Zhang, Y., Chen, X., Hua, B., Hou, W., Qi, X., Pei, Y., Zhu, X., and Zhao, Z. (2011). Compound Kushen Injection suppresses human breast cancer stem-like cells by down-regulating the canonical Wnt/b-catenin pathway. J Exp Clin Cancer Res 30, 103.

Ying, X.-J., Jin, B., Chen, X.-W., Xie, J., Xu, H.-M., and Dong, P. (2015). Oxymatrine downregulates HPV16E7 expression and inhibits cell proliferation in laryngeal squamous cell carcinoma Hep-2 cells in vitro. BioMed research international 2015.

Yu, G., Wang, L.-G., Han, Y., and He, Q.-Y. (2012). clusterProfiler: an R package for comparing biological themes among gene clusters. Omics: a journal of integrative biology 16, 284-287.

Yu, P., Liu, Q., Liu, K., Yagasaki, K., Wu, E., and Zhang, G. (2009). Matrine suppresses breast cancer cell proliferation and invasion via VEGF-Akt-NF-κB signaling. Cytotechnology 59, 219-229.

Yuan, F., Chen, J., Wu, W.j., Chen, S.z., Wang, X.d., Su, Z., and Huang, M. (2010). Effects of matrine and oxymatrine on catalytic activity of cytochrome P450s in rats. Basic & clinical pharmacology & toxicology 107, 906-913.

Zhang, L., Zheng, Y., Deng, H., Liang, L., and Peng, J. (2014). Aloperine induces G2/M phase cell cycle arrest and apoptosis in HCT116 human colon cancer cells. International journal of molecular medicine 33, 1613-1620.

Zhou, Y.J., Guo, Y.J., Yang, X.L., and Ou, Z.L. (2018). Anti-Cervical Cancer Role of Matrine, Oxymatrine and Sophora Flavescens Alkaloid Gels and its Mechanism. Journal of Cancer 9, 1357.

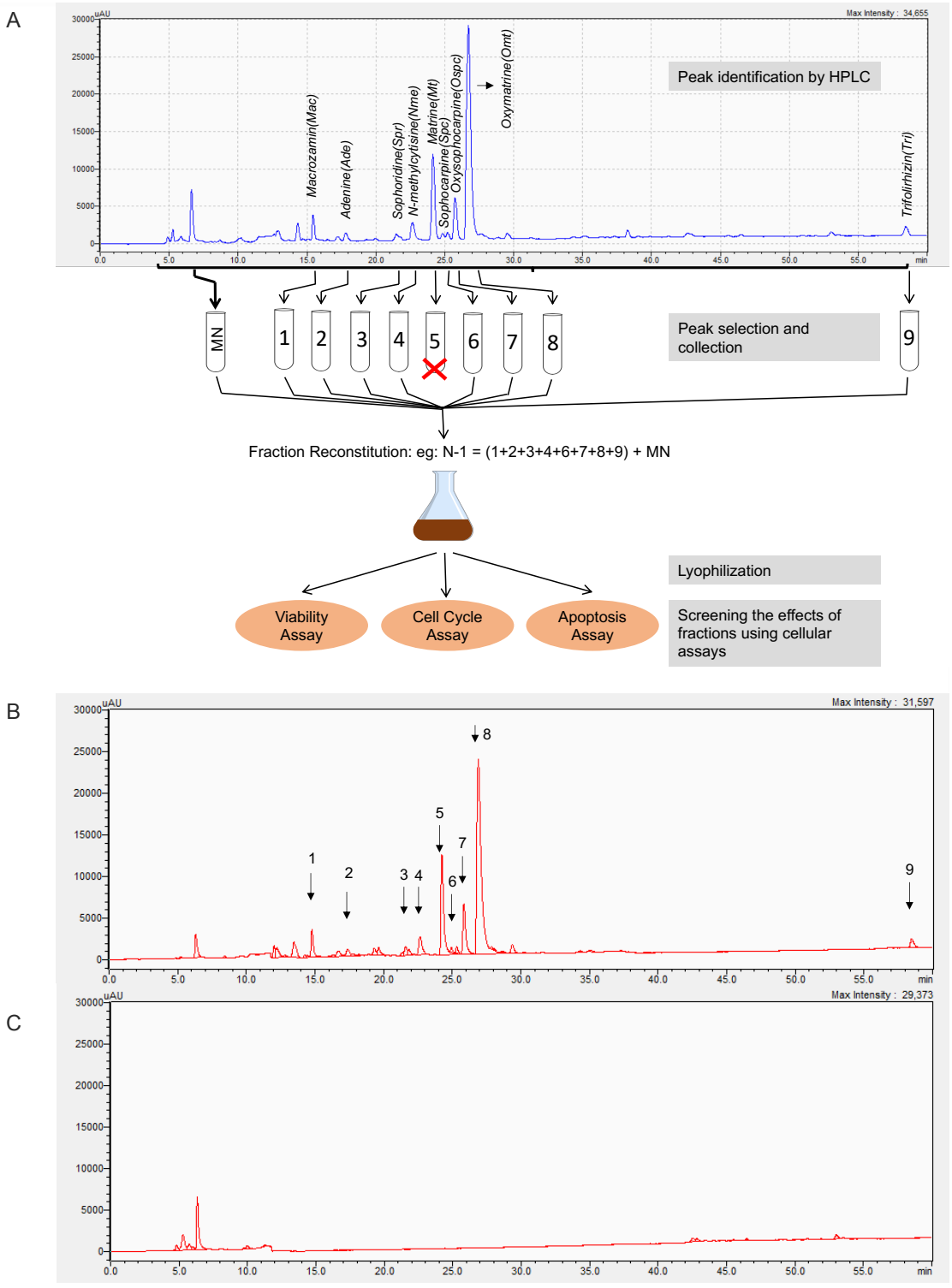

Fig. 1: Fractionation of CKI. (A) Diagram illustrating the process of subtractive fractionation, reconstitution, and screening of fractionated compounds using three cell-based assays. (B) HPLC profile of the 9 purified and reconstituted major peaks (MJ) demonstrating nine major compounds. (C) HPLC profile of reconstituted fractions not containing the 9 major compounds (MN) showing the remaining peaks with no remaining major compounds.

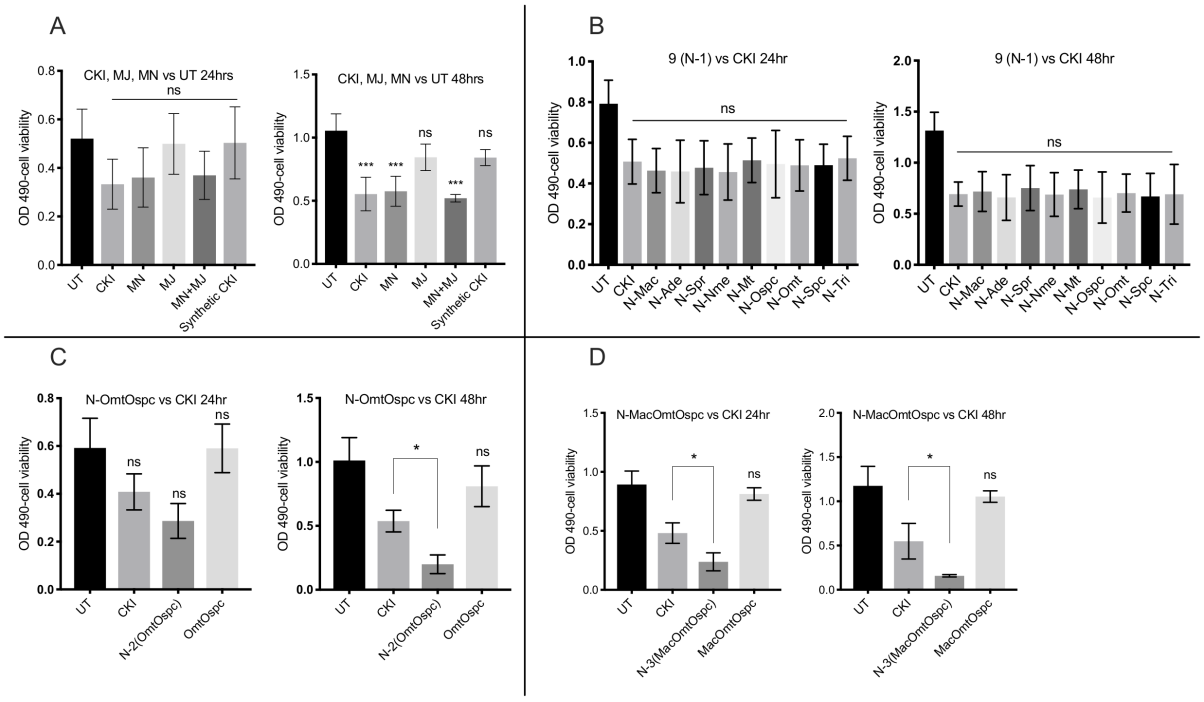

Fig. 2: XTT cell viability assays of subtractive fractions in MDA-MB-231 cells at 24- and 48-hour timepoints treated with 2 mg/ml of CKI and 2 mg/ml equivalent concentrations of all other treating agents. (A) Suppression of cell viability from the following fractions: UT (untreated), MJ, MN, MJ+MN (combination of MJ and MN) and Syn_CKI (synthetic CKI generated using nine major compounds). (B) Effect of 9 (N-1) subtractive fractions compared to CKI. (C) Effect of N-OmtOspc subtractive fraction and OmtOspc compared to CKI. (D) Effect of N-MacOmtOspc subtractive fraction and MacOmtOspc, compared to CKI. Statistically significant results relative to CKI treatment shown as $p < 0.05$ (*) or ns (not significant), all data were shown as mean ± SD.

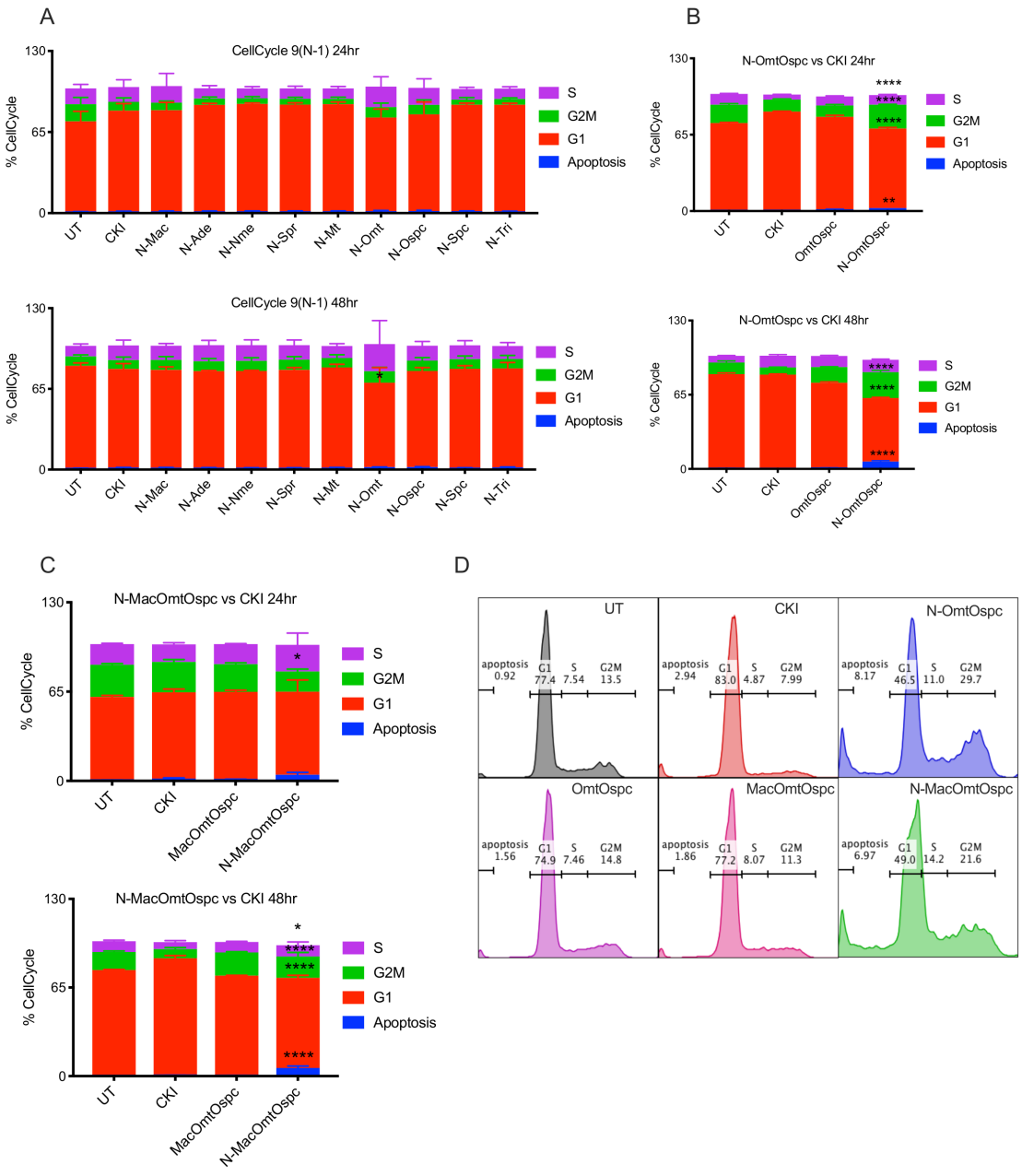

Fig. 3: Cell cycle assay of subtractive fractions at 24- and 48-hour timepoint treatments. (A) Effect of 9 (N-1) subtractive fractions on cell cycle in MDA-MB-231 cells as determined by PI staining assay. (B) Effect of N-OmtOspc subtractive fraction and OmtOspc on cell cycle in MDA-MB-231 cells as determined by PI staining assay. (C) Effect of N-MacOmtOspc subtractive fraction and MOO on cell cycle in MDA-MB-231 cells as determined by PI staining assay. (D) The representative histograms of cell cycle analysis by the treatments as compared to UT. Statistically significant results shown as $p < 0.05$ (*) or $p < 0.01$ (**) $p < 0.001$ (***), or $p < 0.0001$ (****). All data were shown as mean ± SD.

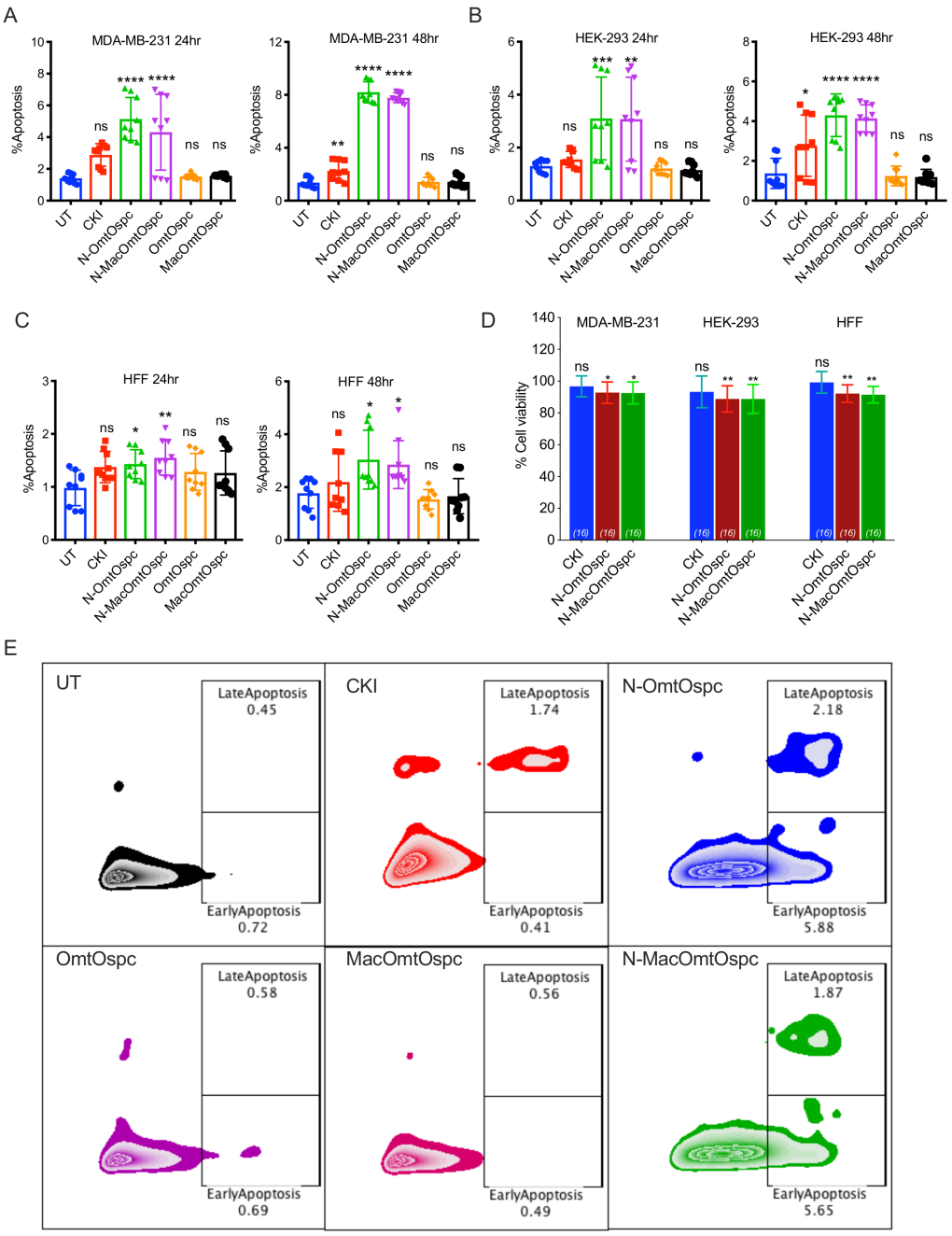

Fig. 4: Apoptosis and cytotoxicity assays of subtractive fractions at 24- and 48-hour timepoint treatments. Apoptotic effect of N-OmtOspc, N-MacOmtOspc subtractive fractions, OmtOspc and MacOmtOspc in (A) MDA-MB-231 cells, (B) HEK-293 cells, and (C) HFF cells as determined by AnnexinV/PI assay. (D) Cytotoxic effect of CKI, N-OmtOspc and N-MacOmtOspc subtractive fractions was determined using Alamar Blue cytotoxicity assay. Statistically significant results shown as $p < 0.05$ (*) or $p < 0.01$ (**) $p < 0.001$ (***), or $p < 0.0001$ (****); ns (not significant). All data were shown as mean ± SD.

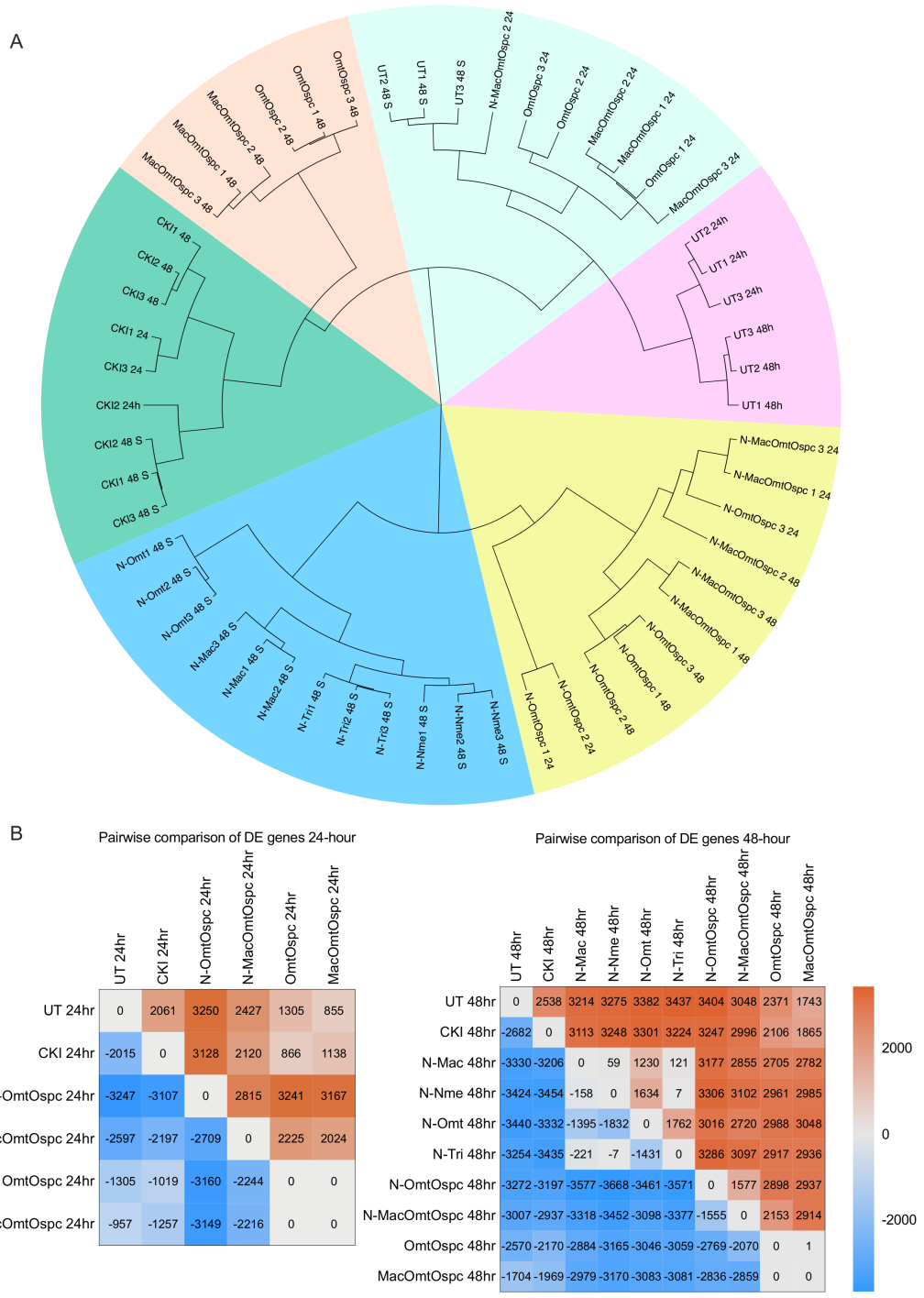

Fig. 5: Gene expression clustering and summary of differential gene expression (A) Clustering of treated samples based on gene expression, calculated as transcripts per million using Ward's hierarchical cluster analysis (Ward.D2) method. Number of DE genes (FDR < 0.05 according to edgeR) associated with each treatment was calculated using pair-wise comparison at (B) 24 hours and (C) 48 hours timepoint. Treatments were compared column versus row. Up-regulated genes are shown in shades of red and down-regulated genes are shown in shades of blue.

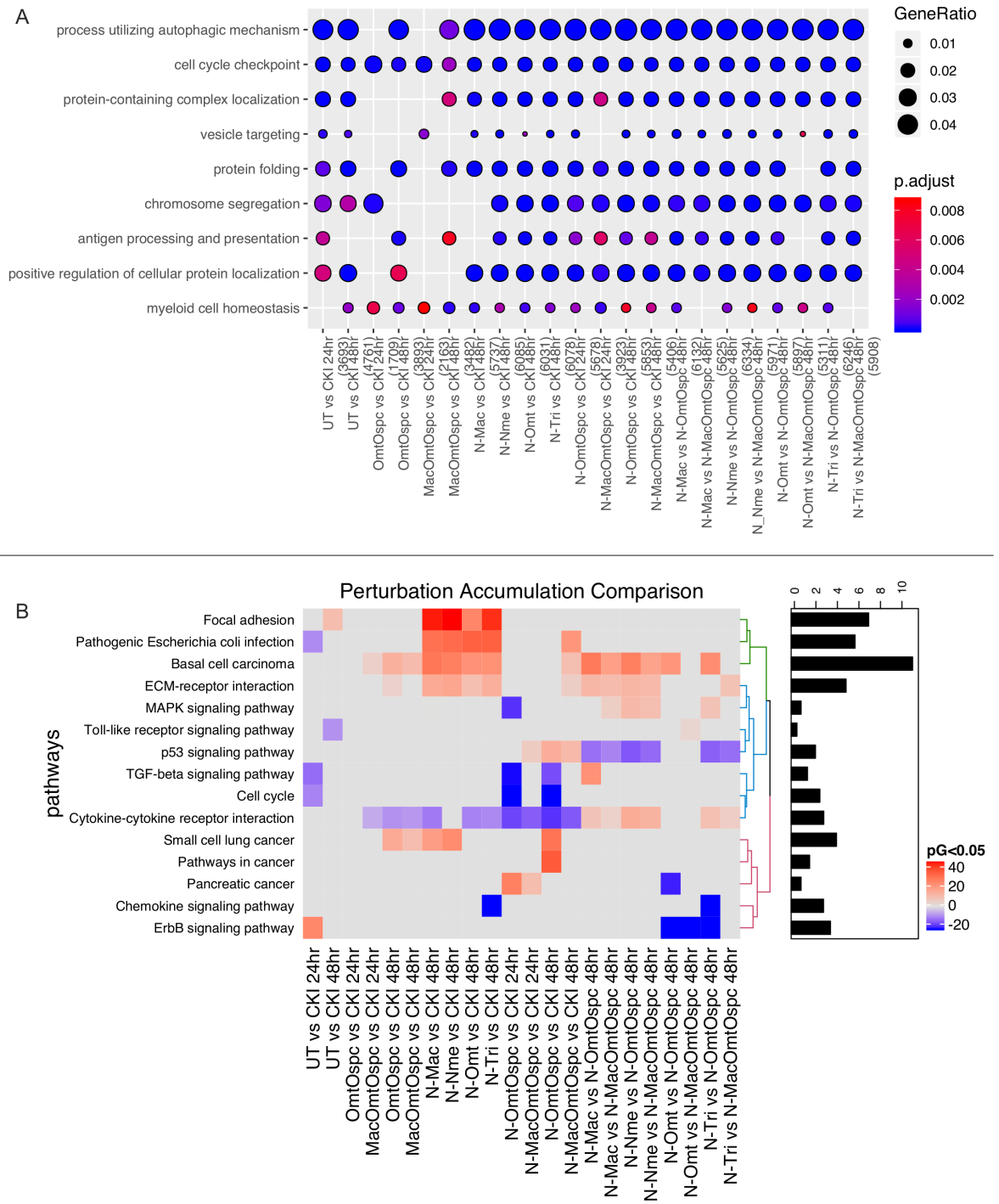

Fig. 6: Over-representation analysis of GO functional annotation and KEGG pathway perturbation analysis. (A) Over-represented GO terms (Biological Process, BP=3) for DE genes identified from comparison of subtractive fraction treated cells against CKI treatment in order to show the relative change from depleting compounds. Gene ratio of each term calculated from Cluster Profiler was plotted based on the adjusted p-values. Top 5 most significant categories of GO terms were plotted by default. Colour gradient of adjusted p-values

ranging from red to blue in order of increasing p-values (high to low significance). Number of identified genes in each treatment (numbers in parentheses) were shown in the bottom and the sizes of the dots correspond to the ratio of gens out of all significant DE gene from each treatment involved in the particular terms. (B) Identification of significantly perturbed pathways using SPIA ($pG < 0.05$) analysis. Eighty-six significantly perturbed pathways from twenty-two comparisons were found (Sup. Fig. 10). Only 15 pathways most obviously linked to our phenotypes of cell viability, cell cycle and apoptosis were shown here. Positive (overall increase in gene expression for pathway) and negative (overall decrease in gene expression for pathway) perturbation accumulation values of the pathways were shown in red and blue respectively. Mean perturbation values of each pathway were shown in bar plot.

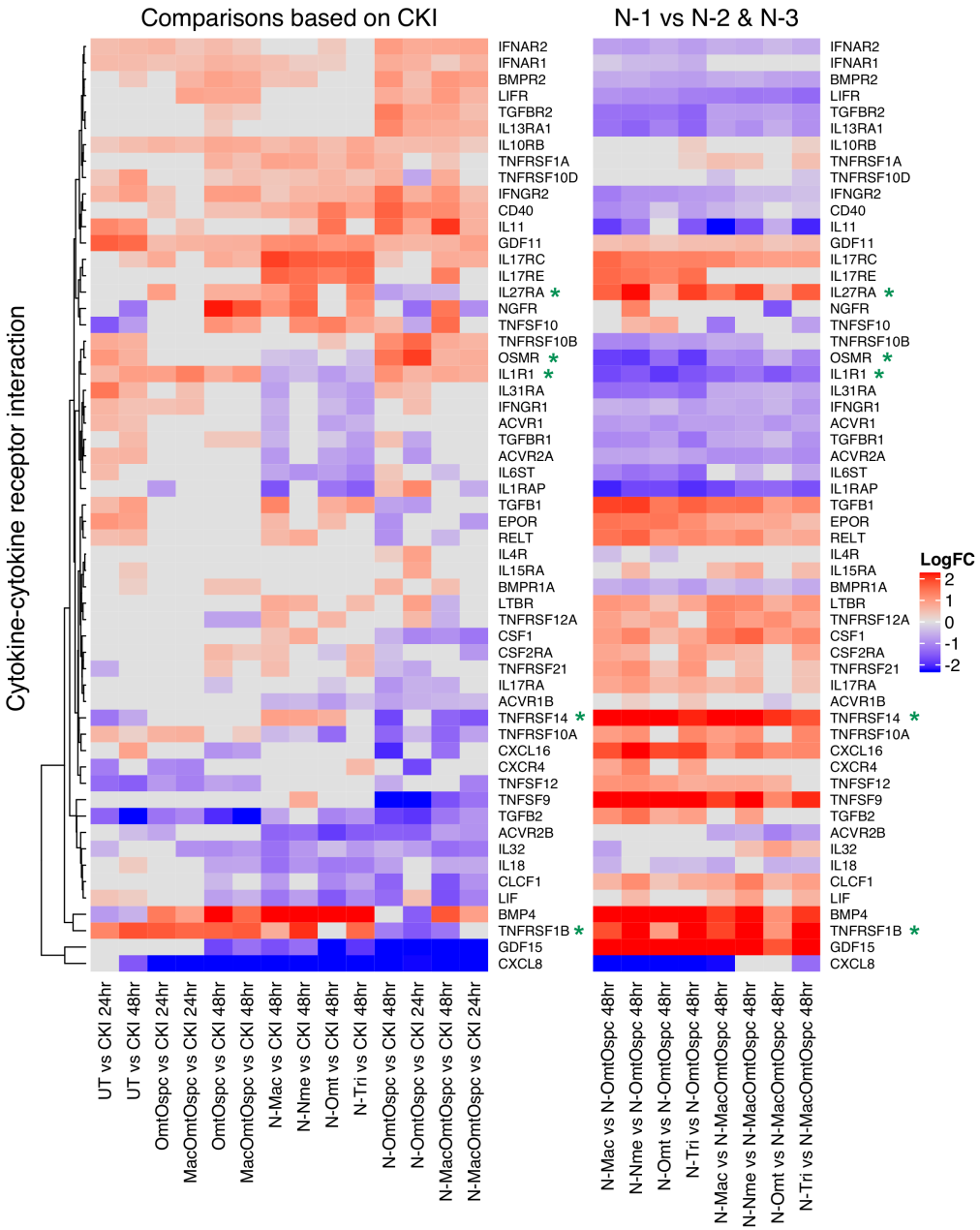

Fig. 7: Differential gene expression profiles of all treatments for Cytokine-Cytokine Receptor pathway. The left panel shows comparison of subtractive fraction treated cells against CKI treatment and the right panel shows comparison of single compound subtractive fraction treated cells against the treatments for two and three compound subtractive fractions. Asterisks in green show a subset of genes that had opposite changes in gene expression across treatments.

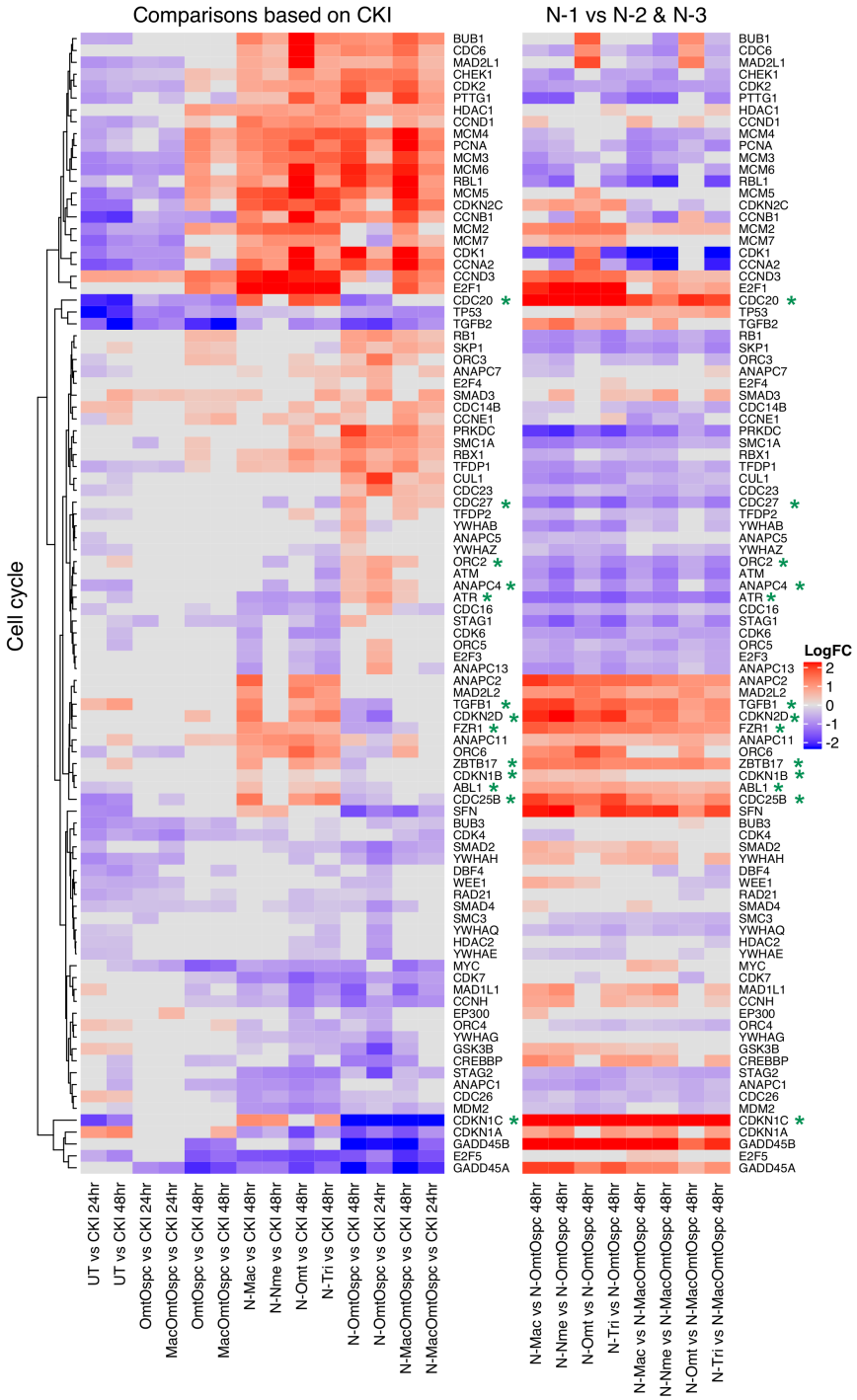

Fig. 8: Differential gene expression profiles of all treatments for Cell Cycle pathway. The left panel shows comparison of subtractive fraction treated cells against CKI treatment and the right panel shows comparison of single compound subtractive fraction treated cells against the treatments for two and three compound subtractive fractions. Asterisks in green show a subset of genes that have opposite changes in gene expression across treatments.

Table 1: Summarized results of HPLC fractionation and treatments using three cell-based assays. N represents the number of all compounds contained in CKI. Significant results of CKI treatment were calculated based on UT whereas those of other treatments were calculated based on CKI treatments. Statistically significant results were represented as $P < 0.05$ (*) or $P < 0.01$ (**) $P < 0.001$ (***), or $P < 0.0001$ (****).

HPLC Fractionation	Treatments	Proliferation Assay (MDA-MB-213)	Cell Cycle Assay (MDA-MB-213)	Apoptosis Assay in three cell lines		
				MDA-MB-231	HEK-293	HFF
9 known + small unknown (N)	Original CKI	*	*			
9known major compounds	MJ					
Small unknown minor compounds	MN	*				
N-1	N-Mac					
	N-Ade					
	N-Tri					
	N-Nme					
	N-Spr					
	N-Mt					
	N-Omt					
	N-Ospc					
	N-Spc					
N-3	N-MacAdeTri					
	N-MtNmeSpr					
	N-OmtOspcSpc					
	N-MacOmtOspc	*	****	****	****	**
N-2	N-MacAde					
	N-MacTri					
	N-AdeTri					
	N-MtNme					
	N-MtSpr					
	N-NmeSpr					
	N-OmtOspc	*	****	****	****	**
	N-OmtSpc					
	N-OspcSpc					
3 compounds	MacAdeTri					
	MtNmeSpr					
	OmtOspcSpc					
	MacOmtOspc					
2 compounds	MacAde					
	MacTri					
	AdeTri					
	MtNme					
	MtSpr					
	NmeSpr					
	OmtOspc					
	OmtSpc					
	OspcSpc					

Table 2: Concentration of 9 major compounds in CKI (N) (Batch No:20170322), remaining major compounds in N-OmtOspc, and remaining major compounds in N-MacOmtOspc.

Mixtures	Compounds	Regression Line	Regression coefficient	concentration (mg/ml) (n=2)	% Contribution
CKI (N)	Macrozamin	y = 6E-05x + 6E-05	0.996	1.1 ± 0.03	4.4
	Adenine	y = 0.021x + 0.0074	0.994	0.09 ± 0.09	0.4
	N-methylcytisine	y = 0.0937x + 0.042	0.9895	0.17 ± 0.02	0.7
	Sophoridine	y = 0.1443x + 0.2679	0.987	0.4 ± 0.08	1.6
	Matrine	y = 0.0132x + 0.7512	0.993	1.26 ± 0.06	5.04
	Sophocarpine	y = 0.0343x + 0.3974	0.994	0.54 ± 0.02	2.2
	Oxysophocarpine	y = 0.0371x - 0.0108	0.999	1.1 ± 0.1	4.4
	Oxymatrine	y = 0.0132x + 0.6226	0.992	6.1 ± 0.09	24.4
	Trifolirhizin	y = 0.0026x - 0.0002	0.990	0.08 ± 0.002	0.3
	Total			**10.8**	**43.4**
N-OmtOspc	Macrozamin	y = 6E-05x + 6E-05	0.996	1.1 ± 0.04	4.4
	Adenine	y = 0.021x + 0.0074	0.994	0.3 ± 0.5	1.2
	N-methylcytisine	y = 0.0937x + 0.042	0.9895	0.03 ± 0.03	0.1
	Sophoridine	y = 0.1443x + 0.2679	0.987	0.3 ± 0.07	1.2
	Matrine	y = 0.0132x + 0.7512	0.993	1.7 ± 0.1	6.8
	Sophocarpine	y = 0.0343x + 0.3974	0.994	0.3 ± 0.01	1.2
	Trifolirhizin	y = 0.0026x - 0.0002	0.990	0.07 ± 0.01	0.3
	Total			**3.8**	**15.2**
N-MacOmtOspc	Adenine	y = 0.021x + 0.0074	0.994	0.06 ± 0.09	0.2
	N-methylcytisine	y = 0.0937x + 0.042	0.9895	0.02 ± 0.01	0.1
	Sophoridine	y = 0.1443x + 0.2679	0.987	0.04 ± 0.02	0.2
	Matrine	y = 0.0132x + 0.7512	0.993	1.7 ± 0.06	6.8
	Sophocarpine	y = 0.0343x + 0.3974	0.994	0.2 ± 0.02	0.8
	Trifolirhizin	y = 0.0026x - 0.0002	0.990	0.08 ± 0.003	0.3
	Total			**2.1**	**8.4**

*Total alkaloid content in CKI = 26.5mg/ml based on manufacturer's assay.

Chapter 3

Compound Kushen Injection, a natural compound mixture, and its identified chemical components differentially slow migration and invasion in colon, brain and breast cancer cell lines

As a result of previous work that showed that CKI significantly disrupted the cell cycle and induced apoptosis in breast cancer cells, I hypothesized that CKI might also cause a previously unrecognized inhibition of cancer cell migration and invasion. Effects of CKI on migration were tested using the complete mixture, fractionated subsets, and single identified chemical components in various cell lines. Fractionation and reconstitution experiments showed that multiple compounds in CKI are required to inhibit cell migration. Transcriptomic analyses of the cancer cells after CKI-treatment indicated down-regulation of gene expression for actin cytoskeleton and focal adhesion pathways, consistent with the observed impairment of cell migration by CKI. Work here identifies the pharmacological complexity of CKI as an important feature of its effectiveness in blocking migration and invasion of cancer cells. This chapter is in the format of the manuscript that was submitted to *Molecular Cancer*. Specific Aim1: To fractionate and reconstitute CKI in order to determine the effects on cell migration of reconstituted mixtures as compared to complete CKI in various cancer and non-cancer cell lines. Specific Aim2: To identify the molecular pathways associated with the inhibition of cell migration by CKI and CKI fractions.

Statement of Authorship

Title of Paper	Compound Kushen Injection, a natural compound mixture, and its identified chemical components differentially slow migration and invasion in colon, brain and breast cancer cell lines.
Publication Status	☐ Published ☐ Accepted for Publication ☐ Submitted for Publication ☑ Unpublished and Unsubmitted work written in manuscript style
Publication Details	will be submitted in two weeks for publication.

Principal Author

Name of Principal Author (Candidate)	Thazin Nwe Aung and Saeed Nourmohammadi
Contribution to the Paper	Co-first authors: Designed and carried out the experiments, analysed data and wrote the manuscript.
Overall percentage (%)	75%
Certification:	This paper reports on original research I conducted during the period of my Higher Degree by Research candidature and is not subject to any obligations or contractual agreements with a third party that would constrain its inclusion in this thesis. I am the primary author of this paper.
Signature	Date 30/10/2018

5/11/2018

Co-Author Contributions

By signing the Statement of Authorship, each author certifies that:

i. the candidate's stated contribution to the publication is accurate (as detailed above);

ii. permission is granted for the candidate in include the publication in the thesis; and

iii. the sum of all co-author contributions is equal to 100% less the candidate's stated contribution.

Name of Co-Author	Jian Cui
Contribution to the Paper	Assisted with data analysis
Signature	Date 5/11/2018

Please cut and paste additional co-author panels here as required.

Name of Co-Author	Jinxin Victor Pei
Contribution to the Paper	Assisted with experiments
Signature	Date 30/10/2018

Name of Co-Author	Michael Lucio De Ieso
Contribution to the Paper	Assisted with experiments
Signature	Date 30/10/18

Name of Co-Author	Yuka Harata-Lee
Contribution to the Paper	Assisted with experiments
Signature	Date 5/11/2018

Name of Co-Author	Zhipeng Qu
Contribution to the Paper	Experimental Design
Signature	Date 5/11/2018

Name of Co-Author	David L Adelson
Contribution to the Paper	Supervised the research, assisted the research with the funding, experimental design and wrote the manuscript.
Signature	Date 5/11/18

Name of Co-Author	Andrea J Yool
Contribution to the Paper	Supervised the research, assisted the research with the funding, experimental design and wrote the manuscript.
Signature	Date 5/11/18

Compound Kushen Injection, a natural compound mixture, and its identified chemical components differentially slow migration and invasion in colon, brain and breast cancer cell lines.

Saeed Nourmohammadi (S.N) [(1)] †, Thazin Nwe Aung (T.N.A) [(2)] †, Jian Cui (J.C) [(2)], Jinxin V. Pei (J.V.P) [(1)], Michael Lucio De Ieso (M.L.D) [(1)], Yuka Harata-Lee (Y.H.L) [(2)], Zhipeng Qu (Z.Q) [(2)], David L Adelson (D.L.A) * [(2)], Andrea J Yool (A.J.Y) * [(1)].

[(1)] Adelaide Medical School and the [(2)] Department of Molecular and Biomedical Science, School of Biological Sciences, The University of Adelaide, Adelaide, SA, Australia

†Co 1st authors: Nourmohammadi S and Aung TN

***Co-Corresponding authors: Yool AJ [(1)] and Adelson DL[(2)]**

[(1)] Adelaide Medical School, University of Adelaide, Adelaide SA 5000, Australia;

T: +61 8 8313 3359, andrea.yool@adelaide.edu.au

[(2)] Department of Molecular and Biomedical Science, School of Biological Sciences, University of Adelaide, Adelaide SA 5000, Australia;

T: +61 8 8303 7555, david.adelson@adelaide.edu.au

Authors: Saeed Nourmohammadi, saeed.nourmohammadi@adelaide.edu.au

Thazin NweAung, thazin.nweaung@adelaide.edu.au

Jian Cui, jian.cui@adelaide.edu.au

Jinxin V Pei, jinxin.pei@adelaide.edu.au

Michael L De Ieso, michael.deieso@adelaide.edu.au

Yuka Harata-Lee, yuka.harata-lee@adelaide.edu.au

Zhipeng Qu, zhipeng.qu@adelaide.edu.au

Abstract

Background

Metastatic secondary tumors are a major cause of cancer-related deaths worldwide. Traditional Chinese medicines (TCM) are promising sources of new agents with anti-metastatic activities. Compound Kushen Injection (CKI), extracted from two traditional medicinal plants, Kushen *(Sophora flavescens)* and Baituling *(Heterosmilax chinensis),* contains a mixture of alkaloids and flavonoids. Prior work has shown that CKI disrupts the cell cycle and induces apoptosis in breast cancer MCF7 cells, but effects on cancer cell migration and invasion remained unknown.

Methods

We tested effects of CKI, fractionated subsets, and single identified chemical components on migration in colon (HT-29, SW-480, DLD-1), brain (U-87 MG, U-251 MG), and breast (MDA-MB-231) cancer cell lines. Cell lines from human embryonic kidney (HEK-293) and Human Foreskin Fibroblasts (HFF) were used as non-cancerous controls.

Results

Circular wound closure, transwell invasion, and live cell imaging assays showed that CKI significantly reduced migration and invasion in all eight cell lines. The greatest inhibition of migration (as measured by wound closure rates) was seen in HT-29 and MDA-MB-231 cells, and the smallest effect in HEK-293. Fractionation of CKI and selective reconstitution showed that multiple compounds in combination were required to inhibit cell migration. Live cell imaging confirmed that CKI was highly effective in reducing migration of HT-29 colon and MDA-MB-231 breast cancer cells, and was moderately effective on brain cancer cells, as compared with no effect on non-cancerous HEK-293. CKI robustly blocked cell invasion through extracellular matrix across all cell types. Apoptosis measured by an annexinV/PI assay was significantly increased by CKI treatment in MDA-MB-231 cells but not in the non-cancerous cells. Cytotoxicity measured by Alamar Blue assay showed CKI had no effect on

cell viability for any cell lines. Transcriptomic analyses comparing MDA-MB-231 with and without CKI-treatment indicated that actin cytoskeletal and focal adhesion gene expression were down-regulated, consistent with the observed impairment of cell migration by CKI.

Conclusions

Work here identifies the pharmacological complexity of CKI as an important feature of its effectiveness in blocking migration and invasion of cancer cells.

Keywords: Traditional Chinese Medicine (TCM), Compound Kushen Injection (CKI), Cell migration, Invasion, Cancer.

Background

Cancer progression results from uncontrolled migration of cells away from the primary tumor, intravasation into lymphatic or vascular circulation, invasion into secondary tissues and the formation of metastasized tumors [1, 2] which are the main cause of cancer-related deaths [3-5]. Migrating cells generate a driving force for cell motility based on the extension of filipodia and lamellipodia using actin polymerization at the leading edges of the cell [6]. New approaches for enhancing cancer treatment by impairing cell migration and metastasis might offer promise for curing patients with malignancies. Combinations of anticancer therapeutic regimens that not only reduce cell proliferation but also limit metastasis would be advantageous [7-9].

Herbal medicines are used in complementary and traditional medicines [10-12]. TCM relies on natural product extracts containing complex mixtures of components, suggested to deliver therapeutic benefit to individuals suffering from non-small cell lung cancer, liver, breast, and colorectal cancers [12-14]. The inherent complexity of TCM suggests principle components might act in concert with adjuvant components, explaining an apparent synergy in therapeutic benefits seen from the whole extract as compared to individual compounds [15]. Modulation of multiple regulatory signaling targets has been proposed as essential for the anti-proliferative, anti-migratory and anti-metastatic properties of TCMs [16, 17].

Compound Kushen Injection (CKI) has been used in combination with chemotherapies such as oxaliplatin and 5-fluorouracil in China since 1995 for the treatment of gastric, liver and non-small cell lung carcinomas [18]. Composed of alkaloids, flavonoids, organic acids and saccharides [19], CKI has been reported to boost immunity, decrease inflammation, and decrease metastasis [20], for example by repressing RNA markers associated with tumor metastasis in MCF-7 cells [17, 18], and impairing migration in hepatocellular carcinoma cells [21]. The challenge for defining mechanisms of action of TCMs such as CKI is to understand the differential activities of chemical components not only singly but in combination,

89 recognizing the likely involvement of multiple gene expression and signaling pathways in the
90 beneficial outcomes [22].
91 Work here is the first to show that CKI and defined chemical fractions slow cancer cell
92 migration and invasion, and to use systems biology to identify sets of genes linked to cell
93 migration that are regulated by CKI treatment. Differential expression of genes in the actin
94 cytoskeleton and focal adhesion pathways supports the idea that the therapeutic activity of CKI
95 in humans involves a serendipitous combination of effects on cancer cell properties.
96

Methods

Cell lines

MDA-MB-231, HT-29, SW-480, DLD-1, U-87 MG, U-251 MG and HEK-293 were purchased from the American Type Culture Collection (ATCC, Manassas, VA) and HFF was kindly provided by Dr. Eric Smith (Basil Hetzel Institute, The Queen Elizabeth Hospital, SA, Australia). DLD-1 cells were grown in RPMI (Roswell Park Memorial Institute) culture medium (Thermo Fisher Scientific, MA, USA) with 10 % fetal bovine serum (FBS, Thermo Fisher Scientific). All other cell lines were cultured in Dulbecco Modified Eagle Medium (DMEM, Thermo Fisher Scientific) with 10 % FBS, except for HFF (which contained 15 % FBS), at 37^0C in 5 % CO_2.

CKI preparation and other chemicals

CKI (Batch No: 20170322, total alkaloid concentration of 25 mg/ml) was obtained from Zhendong Pharmaceutical Co. Ltd (Shanxi, China). High performance liquid chromatography (HPLC) fractionation and liquid chromatography-mass spectrometry (LC-MS/MS) were used to analyse single compounds and confirm their concentrations in CKI. Fractionation of CKI was done by using Shimadzu HPLC SPC-M20A photodiode-array UV-Vis detector (Japan) equipped with a C_{18} column (5 µm, 250 x 10 mm; Phenomenex, CA, USA), with methods for fractionation and concentration determinations as described previously [23] (Supplementary Figs. 2 and 3). The nine compounds comprising the major fraction (MJ): oxymatrine, oxysophocarpine, n-methylcytisine, matrine, sophocarpine, trifolirhizin, adenine, and sophoridine were purchased as isolated compounds from Beina Biotechnology Institute Co., Ltd (Shanxi, China), and macrozamin was obtained from Zhendong Pharmaceutical Co. Ltd (Beijing, China). Two-fold serial dilutions from 2 mg/ml through to 0.25 mg/ml of total alkaloids in CKI, as well as equivalent dilutions of the MJ and minor (MN) fractions were used for bioassay experiments on the cancer and non-cancerous cell lines and compared with effects

of vehicle control treatments; 0.25 % Tween 80 (Sigma-Aldrich, MO, USA) and 10 mM HEPES (Thermo Fisher Scientific) in the same cell lines.

Circular wound closure assay

Two-dimensional (2D) cell migration was measured using circular wound closure rates [24]. CKI-based and vehicle control treatments were applied in low serum DMEM, with the mitotic inhibitor 5-fluoro-2'-deoxyuridine (FUDR). Initial wound areas were imaged at 0 hour (10x objective) with a Canon EOS 6D camera (Canon, Tokyo, Japan) on an Olympus inverted microscope (Olympus Corp., Tokyo, Japan); XnConvert software was used to standardize the images. NIH ImageJ software (U.S. National Institutes of Health, MD, USA) was used to quantify wound areas at 0 hour and at a second timepoint (18 to 24 hours), set for each cell line to ensure wounds were not completely closed. Experiments were independently repeated three times, with four to eight replicates.

Transwell invasion assay

Invasion assays were performed in 24-well transwell inserts (6.5 mm, 8 μm pore size; Corning® Transwell polycarbonate; Sigma-Aldrich). The upper surface of the filter was layered with extracellular matrix (ECM) gel from Sigma-Aldrich (at dilutions empirically optimized for each cell line; Additional file 9: TableS1), allowed to dry overnight, and rehydrated with 50 μl of serum-free media per insert for 1 hour prior to cell seeding. Cultures were grown to 40 % confluence and then starved in medium with 2 % FBS serum for 24 hours prior to seeding. Cells were detached (at ≤ 80 % confluency) and resuspended in serum-free culture media (Additional file 9: TableS1). Cells were then seeded in transwell inserts (total 150 μl of cell suspension per transwell, including 50 μl of rehydration medium added earlier) at appropriate number of cells per well in the presence of CKI, MN or MJ at 2 mg/ml, or vehicle control medium. The chemoattractant gradient was created with 700 μl of culture medium (containing

149 the relevant CKI-based or vehicle treatment), with 5 %, 10 %, or 15 % FBS for HEK-293,
150 cancerous cells, or HFF, respectively. Depending on invasion characteristics, cells from each
151 line were incubated for an optimized time period ranging from 5 to 24 hours at 37°C in 5 %
152 CO_2. Non-invasive cells were scraped from the upper surface of the filter with a cotton swab;
153 migrated cells on the bottom surface were counted after staining with crystal violet (Sigma-
154 Aldrich). The average number of invasive cells was calculated from three randomly selected
155 fields (x100 magnification). Cell counts were normalized to numbers in the vehicle control
156 treatment. Three independent experiments were carried out with two replicates.
157
158 **Cytotoxicity assay**
159 Cell viability was measured with the Alamar Blue assay [25] according to the manufacturer's
160 instructions (Thermo Fisher Scientific). Cells were seeded in 96-well plates in media with 2 %
161 FBS and FUDR. After overnight incubation, treatments were applied, and cultures were
162 incubated for 24 hours. After application of 10 % Alamar Blue solution (30-90 minutes),
163 fluorescence was measured by using FLUOstar Optima microplate reader. Mercuric chloride
164 (2.5 mM) served as a positive control, inducing cytotoxic cell death. A control sample with
165 medium and treatment agent only (no cells) was included for background color subtraction.
166
167 **Apoptosis assay**
168 Apoptosis assays based on annexin V and propidium iodide staining were performed as
169 described previously [17]. Briefly, MDA-MB-231, HEK-293 and HFF cells were seeded in 6-
170 well trays and treated with 2 mg/ml of CKI. After 24 hours of treatment, cells were harvested,
171 and levels of apoptotic cells were measured using the Annexin V-FITC detection kit (Thermo
172 Fisher Scientific) according to the manufacturer's guidelines. Cells were acquired on a
173 LSRFortessa X-20 (BD Biosciences, NJ, USA) and data were analyzed using FlowJo software
174 (TreeStar Inc., OR, USA).

Live cell imaging

Cells in 96 well plates were cultured to 80 % confluency, then serum-starved for 12-18 hours in optimal culture media with 2 % FBS and 400 nM FUDR. Wounds were created as circular lesions in the confluent monolayers, and treatments were added as described for the circular wound closure assay above. Plates were placed in an enclosed humidified chamber at 37°C with 5 % CO_2 for 20 hours, and images were acquired at 15-minute intervals with a Nikon Ti E Live Cell Microscope (Nikon, Tokyo, Japan) using Nikon NIS-Elements software. Time-lapse movies as AVI files were exported from NIS-Elements. ImageJ (U.S. National Institutes of Health) was used to convert the exported files into TIFF files and converted files were then analyzed using Fiji software [26].

Immunofluorescence labelling and confocal microscopy

Cells were plated in µ-Plate 8 Well dishes (Ibidi, Munich, Germany), in 2 % FBS with FUDR 400 nM in optimal culture media and incubated 12-18 hours at 37°C in 5 % CO_2. The following day, 2 mg/ml of CKI, MN, MJ or vehicle control treatments were applied, and cells were incubated for 24 hours. After washing with phosphate-buffered saline (PBS), cells were fixed in 4 % paraformaldehyde (at room temperature for 10-30 min), rinsed 2-3 times with PBS, and permeabilized with 200 µl of 0.1 % Triton X-100 in PBS (3-5 minutes at room temperature). After 2-3 washes with PBS, Phalloidin-iFluor 488 Reagent CytoPainter (ab176753; Abcam, MA, USA) at 200 µl per well was used to stain F-actin cytoskeleton (room temperature in the dark for 1-2 hours) and washed again 2-3 times with PBS. Cell nuclei were labelled with 200 µl of 1:1000 Hoechst stain (cat # 861405; Sigma-Aldrich) for 5-10 minutes. Cells were visualized using a SP5 laser scanning confocal microscope (Leica, Germany).

Pathway enrichment analysis of migratory genes affected by CKI

RNA-sequencing (RNA-seq) data [23] of MDA-MB-231 cells treated with CKI were used to identify cell migration genes affected by CKI. Gene Ontology (GO) enrichment analyses were carried out with R package clusterProfiler 3.8.0 [27]. The following parameters for GO enrichment analysis were used: biological process at the third level; right-sided hypergeometric test; and Benjamini-Hochberg method to correct p values. Pvalue cutoff 0.05 and false discovery rate 0.1 values were used to identify significantly over-represented GO terms. Pathways that were significantly perturbed by CKI treatment were identified with Signaling Pathway Impact Analysis (SPIA) [28], and visualized using the pathview package in R [29]. KEGG (Kyoto Encyclopedia of Genes and Genomes) functional analysis was performed with R package clusterProfiler 3.8.0 [27] and OmicCircos v 1.18.0 [30]. Venn diagrams were generated using an online tool (http://bioinformatics.psb.ugent.be/webtools/Venn/).

Intracellular protein staining and quantification by flow cytometry

Cells cultured in 6-well trays were treated with CKI, MN or MJ as described above, harvested after 24 hours, fixed and permeabilized using Nuclear Factor Fixation and Permeabilization Buffer Set (Biolegend, CA, USA) according to the manufacturer's instructions. 2×10^5 cells were labelled with rabbit anti-Cyclin D1 (CCND1) (92G2, Cell Signaling Technologies, MA USA), rabbit anti-β-actin (ACTB) (D6A8, Cell Signaling Technologies), rabbit anti-protein kinase B (AKT1, 2, 3) (Ab32505, Abcam) or rabbit IgG isotype control (Cell Signaling Technologies), and these antibodies were detected with anti-rabbit IgG-PE (Cell Signaling Technologies). For detection of β-catenin, rabbit anti-β-catenin (CTNNB1)-Alexa Fluor 647 and isotype control for CTNNB1 rabbit IgG-Alexa Fluor 647 (Abcam) were used. The cells were then sorted, and the data were acquired on a BD LSRFortessa X-20. Sorting parameters were set to gate and exclude small particles such as cell debris and large duplex cells. The data were analysed using FlowJo software.

227 **Statistical tests**

228 Statistical analyses were carried out using GraphPad Prism 8 software (San Diego, CA, USA)
229 with one-way ANOVA. Statistically significant results were represented as $p < 0.05$ (*) or $p <$
230 0.01 (**) $p < 0.001$ (***), or $p < 0.0001$ (****); ns (not significant). All data are shown as
231 mean ± standard deviation (SD); n values for independent samples are indicated in italics above
232 the x-axes in histogram figures, unless otherwise stated.

233

Results

Functional annotation of MDA-MB-231 transcriptome treated by CKI

Transcriptome [23] analyses were performed to identify over-represented Gene Ontology (GO) terms and Kyoto Encyclopedia of Genes and Genomes (KEGG) for all differentially expressed (DE) genes by comparing MDA-MB-231 gene expression profiles with and without CKI treatment (Fig. 1 and Additional file1: FigureS1). Differences in gene expression levels were used to identify migration related GO terms and pathways of interest, which were classified by functional roles via GO and KEGG over-representation analyses. Enriched GO terms connected to cell migration such as "positive regulation of locomotion", "tissue migration "and "leucocyte migration" emerged from analyses of DE genes in CKI-treated MDA-MB-231 cells (Additional file 1: FigureS1 and Additional file 6: DataS1). Integration of DE genes associated with CKI treatment into KEGG pathways showed that some of the most over-represented pathways were "focal adhesion", "regulation of actin cytoskeleton", "pathways in cancer", "TGF-β signaling pathway" and "adherens junction" (Fig. 1). These results indicated that many of the genes affected by CKI treatment were involved in cell migration-related pathways.

Identification of CKI components

CKI was fractionated and components were selectively recombined to create MJ and MN fractions (Fig. 2) as treatments for bioassays on cultured cells. Concentrations of the nine major compounds in CKI were measured using LC-MS/MS (see Methods). The concentrations of MJ components were determined (Additional files 2 and 3: FigureS2 and S3) from calibration curves of nine standard compounds as previously described [23] and summarized in Table 1. The total concentration of the nine major compounds in CKI was 9.99 mg/ml which accounted for approximately 40 % of the dry mass of CKI, and the total concentration of the nine compounds in MJ was 8.62 mg/ml, indicating that the major compounds were clearly fractionated from CKI, and that MJ and MN components were well separated.

Impairment of cell migration by CKI and fractionated mixtures

Effects of CKI on two-dimensional cell migration were assessed using a circular wound healing assay (Fig. 3a). Percent wound closure after 20 hours was calculated based on the initial wound area. CKI-based treatments were tested on eight different cancer cell lines *(*HT-29, SW-480, DLD-1*,* U-87 MG, U-251 MG and MDA-MB-231*)* and two non-cancerous cell lines (HEK-293 and HFF), at five doses ranging from 0 to 2 mg/ml (Fig. 3b). In all cell lines, net migration rates were inhibited more by CKI than by MN or MJ treatments alone, except in HEK-293 which showed low sensitivity to CKI. The retention of biological activity in the fractionated MJ and MN treatments was confirmed by demonstrating reconstituted CKI (in which MN and MJ were mixed together) was equally effective as CKI for blocking cell migration (Fig. 3b). The most sensitive cell lines were breast cancer (MDA-MB-231) and colon cancer (HT-29). DLD-1 and HEK-293 cell lines were the least sensitive.

In all the CKI-sensitive cell lines, the inhibition of migration by MN alone was greater than that seen with MJ alone (Fig. 3b), but neither treatment was as potent as CKI in any cell line. To determine if a single compound in MJ accounted for the enhanced inhibition seen with co-application of MJ and MN, each of the isolated major compounds alone was added in turn to 1 mg/ml MN, at a final concentration equal to its original concentration in 2 mg/ml CKI. Wound healing assays showed certain compounds added to MN produced a significantly greater inhibition than MN alone, but the effective compounds and levels of potency differed between cell lines (Fig. 4 and Additional file 4: FigureS4). Matrine was effective in MDA-MB-231, HT-29 and U-251 MG cell lines; sophocarpine was effective in HEK-293; trifolirhizin was effective in HT-29, SW-480 and U-251 MG; and adenine was effective in HT-29 cells, as determined by a significant decrease in migration as compared to MN alone. More than one compound in MJ appeared to contribute to the activity of CKI in blocking cell migration.

None of the CKI-based treatments induced significant cytotoxicity at 1 or 2 mg/ml, as assessed by Alamar Blue assays (Fig. 5a, b and c). The lack of cytotoxicity suggested that the observed impairment of the two-dimensional cell migration was not an indirect consequence of reduced cell viability. However, CKI at 2 mg/ml substantially increased apoptosis in MDA-MB-231 and moderately increased apoptosis in HEK-293 cells, without a significant effect on HFF (Fig. 5d, e, f and g). These data extend prior work which showed CKI increased apoptosis in MCF-7 breast cancer cells (Qu et al., 2016), and support the idea that multiple responses induced by CKI could contribute to its overall anti-cancer effects.

To quantify the effects of CKI on two-dimensional cell motility *in vitro* in more detail, trajectories of individual cells were monitored in real time using live cell imaging (Fig. 6). Vehicle-treated cells were compared with those treated with 2 mg/ml CKI, or 1 mg/ml MN or MJ (doses equal to their concentration in CKI). Data were compiled for representative cells from six cancer and two non-cancerous cell lines. Positions of individual cells as a function of time over 20 hours were determined by the location of the cell nucleus (Fig. 6a). Distances moved per unit time interval showed a Gaussian distribution; the peak position illustrates the mean distance travelled per increment. Significant displacement of the curve to the left (representing a decreased mean distance travelled per time interval) was evident for CKI treatment in all cell lines as compared to vehicle-treated controls (Fig. 6b, and Additional file 5: VideoS1). Significant reductions in mean distance by either MN or MJ were observed in HT-29 and SW-480 cells. Reductions in mean distance by MN but not MJ were seen in U-87 MG, MDA-MB-231 and HFF cells. U-251 MG and DLD-1 cancer cells responded only to whole CKI. The effectiveness of CKI in blocking migration depended on the simultaneous presence of multiple minor and major compounds, but the specific agents conferring anti-migration activity appeared to depend on the cell line.

Impairment of invasiveness by CKI treatments in cancer and non-cancer cell lines

A transwell Boyden chamber assay with ECM-coated filters was used to measure the invasiveness of cells in response to a serum chemoattractant gradient in vehicle control, CKI, MN, and MJ treatment conditions (Fig. 7). CKI treatment and the combined MN+MJ treatment (i.e., reconstituted CKI) both significantly reduced invasiveness in all cell types. Smaller but significant decreases in invasiveness were seen with MN alone in all cell types except SW-480 and were seen with MJ alone in all but SW-480 and MDA-MB-231 cell lines. These results suggested that a combination of major and minor components of CKI was required for maximal inhibition of invasiveness through extracellular matrix barriers.

Transcriptome analysis of MDA-MB-231 cells treated with CKI

Functional enrichment analysis was used to narrow the field of candidate mechanisms potentially associated with the anti-migratory effects of CKI. Perturbations of KEGG Pathways that were significantly over-represented in DE genes affected by CKI treatment were further analysed using SPIA (Fig. 8a and Additional file 7: DataS2). “Melanogenesis”, “TGF-β signaling pathway”, “focal adhesion”, “regulation of actin cytoskeleton”, “ErbB signaling pathway”, and “GnRH signaling pathway” were significantly perturbed based on 'global perturbation values' ($pG<0.05$), consistent with the results of the KEGG analysis. Together, these analyses provided evidence that CKI was likely to impair cell migration by altering both adhesion and motility (Fig. 8b and c). To explore this idea, genes from two strongly affected pathways (“focal adhesion” and “actin cytoskeleton”) were characterised by comparing three independent gene datasets: (i) a set containing 135 Tumor Alterations Relevant for Genomics driven Therapy (TARGET) genes; (ii) a set containing 140 migration related genes collected from published articles; and (iii) a set containing 1381 genes from KEGG pathways. We identified 14 clinically relevant DE genes, which were: *CTNNB1, CDH1, AKT1, AKT2, AKT3, CCND1, MAPK1, JAK2, APC, CDK4, RB1, PIK3CA,* and *PTEN*, all of which have been shown

to affect cell migration (Fig. 8d, Additional file 8: DataS3 and Additional file 10: TableS2), suggesting that the slowing of cell migration could be clinically relevant to CKI treatment outcomes.

CKI interrupts F-actin polymerization

The results of functional enrichment analysis highlighted the actin cytoskeleton and focal adhesion pathways as potential targets of CKI. As a result, we decided to examine the effect of CKI on F-actin polymerization, filopodia formation and lamellipodia extension using confocal microscopy in all eight cell lines (Fig. 9). Cells in all lines treated with CKI, MN and MJ (at doses equal to those in 2 mg/ml CKI) at 24 hours were smaller and lacked cellular processes such as lamellipodia as compared to vehicle control treated. Abundant lamellipodia seen in the control treatment were visibly diminished in the treatment groups. Comparing responses within the treatment groups, CKI disrupted the lamellipodia extensions more than was seen with MN or MJ alone. The impairment of F-actin polymerization was consistent with the idea that MN and MJ fractions both contribute slowing cell migration.

CKI and fractionated mixtures perturb the actin cytoskeleton

To validate the gene expression changes at the protein level, we performed flow cytometry analyses of four proteins; CTNNB1, AKT (1, 2, 3), CCND1, and ACTB, selected for their significant contributions in actin cytoskeleton and focal adhesion pathways in MDA-MB-231 and HEK-293 cell lines. Results shown in Fig. 10 indicated that CKI, MN and MJ significantly downregulated the protein expression, confirming the gene expression data. While there was prominent down-regulation of CTNNB1 expression in MDA-MB-231 by all treatments, AKT (1, 2, 3) was downregulated by CKI and MN but not MJ treatments. In HFF cells, all treatments downregulated ACTB and CCND1 significantly; CKI and MN significantly reduced AKT (1,

2, 3) expression whereas MJ caused significant increase. In contrast, in the HFF cell line, CTNNB1 protein expression was significantly increased by CKI and MN, but significantly downregulated by MJ. In HEK cells, CKI upregulated ACTB, AKT and CCND1, whereas MN upregulated ACTB and downregulated CCND1; MJ had no significant impact on these four proteins (Fig. 10). These results showed that CKI, MN and MJ significantly downregulated the four proteins in MDA-MB-231 cells, with similar although not identical results in the two non-cancer cell lines, providing additional support for the idea that CKI affects cancer cell migration by altering cytoskeletal structure.

Discussion

Natural compounds with anti-cancer activities have been suggested to include potential anti-metastatic agents [17, 21, 31, 32]. Clinical chemotherapeutics for cancers are targeted mainly to killing rapidly dividing cells [33], but cause serious side effects including immunosuppression, hair loss and infertility, without eliminating risks of secondary neoplasms [34]. Non-toxic treatments to reduce metastasis as adjuncts to primary cancer therapies are greatly needed. CKI increased apoptotic activity in breast cancer MCF-7 and hepatocellular carcinoma HCC cell lines [17, 21]. Results here showed that CKI also significantly slowed cell migration and invasion, an outcome consistent with its beneficial clinical effects. The complexity of TCM presents a challenge for identifying single active compounds. By separating components of CKI into major and minor groups, and by adding novel screens for migration and invasion into the analyses of CKI biological activity, we have shown that co-application of multiple compounds was far more effective in blocking cell migration than single agents alone, and that different compounds (serendipitously combined in CKI) are required for activity across diverse cell types.

Components of CKI have both anti-proliferation and anti-migration activities which differ between cell lines, suggesting that refinement of the TCM composition could enable customized management for different cancer types. A subset of the major compounds in CKI have been investigated previously. For example, oxymatrine impaired angiogenesis in mouse breast cancer *in vitro* and *in vivo,* by altering NF-κB pathway and VEGF signaling [35]. Matrine inhibited migration and proliferation of mouse lung adenocarcinoma *in vitro* and slowed xenograft growth *in vivo,* by reducing expression of a calcium-dependent chloride channel shown to be upregulated in multiple cancer types [36, 37]. Consistent with these findings, we found matrine added to the CKI minor fraction further impaired cancer cell migration (Fig. 4); however, in contrast, addition of oxymatrine to the CKI minor fraction did

not affect the control of migration in any of the cell lines we tested. Oxysophocarpine slowed metastasis of oral squamous cell carcinoma *in vitro* and *in vivo,* by altering transcription factor Nrf2 and stress protein signaling pathways [38]. In contrast, our results showed oxysophocarpine partially reversed the inhibition of migration observed with the CKI minor fraction. Work here showed that the major components trifolirhizin and adenine, not previously characterized, when added to CKI minor fraction further slowed cell migration, suggesting these agents merit further study as potential therapeutics, singly and in combination. Not all components of CKI enhance its anti-cancer activities; for example, depletion of three compounds (oxymatrine, oxysophocarpine and macrozamin) increased the anti-proliferative activity of CKI [23].

Rational analysis of the differential effects of agents in a TCM mixture can benefit from quantitative systems biology approaches. Transcriptomics has proven valuable for identifying altered patterns of global gene expression in response to complex agents such as CKI [18]. Our pathway analysis of the transcriptome of CKI-treated MDA-MB-231 cells revealed a strong association with genes linked to "TGF-β signaling", "focal adhesion", "GnRH signaling", and "regulation of actin cytoskeleton". These pathways are linked with migratory phenotype, actin polymerization and lamellipodia protrusion [39] [40] [41]. Focal adhesion sites are points of contact with extracellular matrix, anchoring actin filaments via protein complexes with transmembrane integrin receptors [42]. Matrine has been reported to disrupt actin filament organization in DLD-1 colorectal adenocarcinoma cells [43]. Work here is the first to show that treatment with whole CKI significantly perturbed "focal adhesion" and "regulation of actin cytoskeleton" pathways, and to confirm predictions of the transcriptomic results by showing CKI reduced lamellipodial abundance, length of extension, and area of F-actin polymerization.

Two striking outcomes of our pathway analyses were the significant negative perturbation of the cytokine Transforming growth factor beta (TGF-β) and positive perturbation of Gonadotropin-releasing hormone (GnRH) signaling pathways by CKI treatment. Multifunctional TGF-β promotes the process of epithelial-mesenchymal transition, which facilitates cell migration, invasion and metastasis [44, 45]. Reduced TGF-β signaling would be consistent with our findings of impaired invasion and migration with CKI treatment. Conversely, GnRH activity has been associated with attenuating migration of DU145 human prostatic carcinoma cells by remodelling the actin cytoskeleton [46]. Increased GnRH signaling would be consistent with beneficial effects of CKI treatment. Further work is needed to fully understand the mechanisms of action of CKI on cell migration and invasion, the signaling pathways involved, the synergistic effects of combined therapeutic agents, and the translational potential by extending these analyses to metastatic cancer cells *in vivo*.

Conclusions

The primary outcome of this study is the demonstration that cancer cell migration and invasion rates are significantly reduced by CKI, suggesting that therapeutic activity of CKI in human cancer patients may arise in part from downregulation of a panel of key molecular targets necessary for adhesion and motility in metastasis. The secondary outcome of this study is that multiple compounds in CKI, acting together, are responsible for this effect.

Notes

Saeed Nourmohammadi and Thazin Nwe Aung contributed equally to this work.

Abbreviations

Compound Kushen Injection (CKI),

Major (MJ)

Minor (MN)

Traditional Chinese Medicine (TCM)

Human Foreskin Fibroblast (HFF)

Dulbecco Modified Eagle Medium (DMEM)

Fetal Bovine Serum (FBS)

Liquid Chromatography-Mass Spectrometry (LC-MS/MS)

High Performance Liquid Chromatography (HPLC)

Gene Ontology (GO)

5-fluoro-2'-deoxyuridine (FUDR)

RNA-sequencing (RNA-seq)

phosphate-buffered saline (PBS)

Kyoto Encyclopedia of Genes and Genomes (KEGG)

Signaling Pathway Impact Analysis (SPIA)

Extracellular matrix (ECM)

β-actin (ACTB)

Protein kinase B (AKT1, 2, 3)

β-catenin (CTNNB1)

Cyclin D1 (CCND1)

Tumor Alterations Relevant for Genomics driven Therapy (TARGET)

Transforming growth factor beta (TGF-β)

Gonadotropin-releasing hormone (GnRH)

Acknowledgements

The authors acknowledge Dr. Eric Smith for providing HFF cell line and Dr. Mohamad Kourghi, and Pak Hin Chow for valuable discussions. We also thank Dr. Agatha Labrinidis and Dr. Jane Sibbons for the facilities of Adelaide University Microscopy and technical assistance.

Author contributions

S.N, T.N.A, D.L.A and A.J.Y designed the study, analysed the data and wrote the manuscript. S.N and T.N.A conducted the experiments and J.C, J.V.P, M.L.D, Y.H-L and Z.Q assisted with the experiments and analysis.

Conflict of interest

The authors declare no conflicts of interest.

Funding

This work was supported by the special international corporation project of traditional Chinese medicine (GZYYGJ2017035); Australian Research Council (grant DP160104641); and The University of Adelaide, Zhendong Australia China Centre for Molecular Chinese Medicine.

References:

1. Steeg PS: **Targeting metastasis.** *Nature reviews cancer* 2016, **16:**201.
2. Hanahan D, Weinberg RA: **Hallmarks of cancer: the next generation.** *cell* 2011, **144:**646-674.
3. Riihimäki M, Hemminki A, Sundquist J, Hemminki K: **Patterns of metastasis in colon and rectal cancer.** *Scientific reports* 2016, **6:**29765.
4. Weigelt B, Peterse JL, Van't Veer LJ: **Breast cancer metastasis: markers and models.** *Nature reviews cancer* 2005, **5:**591.
5. Chaffer CL, Weinberg RA: **A perspective on cancer cell metastasis.** *Science* 2011, **331:**1559-1564.
6. Fife C, McCarroll J, Kavallaris M: **Movers and shakers: cell cytoskeleton in cancer metastasis.** *British journal of pharmacology* 2014, **171:**5507-5523.
7. Chowdhury FA, Hossain MK, Mostofa A, Akbor MM, Sayeed B, Shahdaat M: **Therapeutic Potential of Thymoquinone in Glioblastoma Treatment: Targeting Major Gliomagenesis Signaling Pathways.** *BioMed research international* 2018, **2018**.
8. Roth P, Weller M: **Challenges to targeting epidermal growth factor receptor in glioblastoma: escape mechanisms and combinatorial treatment strategies.** *Neuro-oncology* 2014, **16:**viii14-viii19.
9. Ratajczak MZ, Suszynska M, Kucia M: **Does it make sense to target one tumor cell chemotactic factor or its receptor when several chemotactic axes are involved in metastasis of the same cancer?** *Clinical and translational medicine* 2016, **5:**28.
10. Reid R, Steel A, Wardle J, Trubody A, Adams J: **Complementary medicine use by the Australian population: a critical mixed studies systematic review of utilisation, perceptions and factors associated with use.** *BMC complementary and alternative medicine* 2016, **16:**176.

11. Gall A, Leske S, Adams J, Matthews V, Anderson K, Lawler S, Garvey G: **Traditional and Complementary Medicine Use Among Indigenous Cancer Patients in Australia, Canada, New Zealand, and the United States: A Systematic Review.** *Integrative cancer therapies* 2018**:**1534735418775821.

12. Guo Z, Jia X, Liu JP, Liao J, Yang Y: **Herbal medicines for advanced colorectal cancer.** *Cochrane Database of Systematic Reviews* 2012.

13. Chung VC, Wu X, Hui EP, Ziea ET, Ng BF, Ho RS, Tsoi KK, Wong SY, Wu JC: **Effectiveness of Chinese herbal medicine for cancer palliative care: overview of systematic reviews with meta-analyses.** *Scientific reports* 2015, **5:**18111.

14. Li X, Yang G, Li X, Zhang Y, Yang J, Chang J, Sun X, Zhou X, Guo Y, Xu Y: **Traditional Chinese medicine in cancer care: a review of controlled clinical studies published in Chinese.** *PloS one* 2013, **8:**e60338.

15. Wang L, Zhou G-B, Liu P, Song J-H, Liang Y, Yan X-J, Xu F, Wang B-S, Mao J-H, Shen Z-X: **Dissection of mechanisms of Chinese medicinal formula Realgar-Indigo naturalis as an effective treatment for promyelocytic leukemia.** *Proceedings of the National Academy of Sciences* 2008, **105:**4826-4831.

16. Pan X, Han H, Wang L, Yang L, Li R, Li Z, Liu J, Zhao Q, Qian M, Liu M: **Nitidine chloride inhibits breast cancer cells migration and invasion by suppressing c-Src/FAK associated signaling pathway.** *Cancer letters* 2011, **313:**181-191.

17. Qu Z, Cui J, Harata-Lee Y, Aung TN, Feng Q, Raison JM, Kortschak RD, Adelson DL: **Identification of candidate anti-cancer molecular mechanisms of compound kushen injection using functional genomics.** *Oncotarget* 2016, **7:**66003.

18. Aung TN, Qu Z, Kortschak RD, Adelson DL: **Understanding the effectiveness of natural compound mixtures in cancer through their molecular mode of action.** *International journal of molecular sciences* 2017, **18:**656.

19. Ma Y, Gao H, Liu J, Chen L, Zhang Q, Wang Z: **Identification and determination of the chemical constituents in a herbal preparation, Compound Kushen injection, by HPLC and LC-DAD-MS/MS.** *Journal of Liquid Chromatography & Related Technologies* 2014, **37:**207-220.

20. Wang W, You R-l, Qin W-j, Hai L-n, Fang M-j, Huang G-h, Kang R-x, Li M-h, Qiao Y-f, Li J-w: **Anti-tumor activities of active ingredients in Compound Kushen Injection.** *Acta Pharmacologica Sinica* 2015.

21. Gao L, Wang K-x, Zhou Y-z, Fang J-s, Qin X-m, Du G-h: **Uncovering the anticancer mechanism of Compound Kushen Injection against HCC by integrating quantitative analysis, network analysis and experimental validation.** *Scientific reports* 2018, **8:**624.

22. Li X, Wu L, Liu W, Jin Y, Chen Q, Wang L, Fan X, Li Z, Cheng Y: **A network pharmacology study of Chinese medicine QiShenYiQi to reveal its underlying multi-compound, multi-target, multi-pathway mode of action.** *PloS one* 2014, **9:**e95004.

23. Aung TN, Nourmohammadi S, Qu Z, Harata-Lee Y, Cui J, Shen H, Yool AJ, Pukala T, Du H, Kortschak D: **FRACTIONAL DELETION OF COMPOUND KUSHEN INJECTION, A NATURAL COMPOUND MIXTURE, INDICATES CYTOKINE SIGNALING PATHWAYS ARE CRITICAL FOR ITS PERTURBATION OF THE CELL CYCLE.** *bioRxiv* 2018**:**462135.

24. De Ieso ML, Pei JV: **An Accurate and Cost-Effective Alternative Method for Measuring Cell Migration with the Circular Wound Closure Assay.** *Bioscience Reports* 2018**:**BSR20180698.

25. O'brien J, Wilson I, Orton T, Pognan F: **Investigation of the Alamar Blue (resazurin) fluorescent dye for the assessment of mammalian cell cytotoxicity.** *European journal of biochemistry* 2000, **267:**5421-5426.

26. Schindelin J, Arganda-Carreras I, Frise E, Kaynig V, Longair M, Pietzsch T, Preibisch S, Rueden C, Saalfeld S, Schmid B: **Fiji: an open-source platform for biological-image analysis.** *Nature methods* 2012, **9:**676.

27. Yu G, Wang L-G, Han Y, He Q-Y: **clusterProfiler: an R package for comparing biological themes among gene clusters.** *Omics: a journal of integrative biology* 2012, **16:**284-287.

28. Tarca AL, Draghici S, Khatri P, Hassan SS, Mittal P, Kim J-s, Kim CJ, Kusanovic JP, Romero R: **A novel signaling pathway impact analysis.** *Bioinformatics* 2008, **25:**75-82.

29. Luo W, Brouwer C: **Pathview: an R/Bioconductor package for pathway-based data integration and visualization.** *Bioinformatics* 2013, **29:**1830-1831.

30. Hu Y, Yan C, Hsu C-H, Chen Q-R, Niu K, Komatsoulis GA, Meerzaman D: **OmicCircos: a simple-to-use R package for the circular visualization of multidimensional omics data.** *Cancer informatics* 2014, **13:**CIN. S13495.

31. Zhu H, Hao J, Niu Y, Liu D, Chen D, Wu X: **Molecular targets of Chinese herbs: a clinical study of metastatic colorectal cancer based on network pharmacology.** *Scientific reports* 2018, **8:**7238.

32. De Ieso ML, Yool AJ: **Mechanisms of Aquaporin-Facilitated Cancer Invasion and Metastasis.** *Frontiers in Chemistry* 2018, **6**.

33. Gerber DE: **Targeted therapies: a new generation of cancer treatments.** *American family physician* 2008, **77**.

34. Brydøy M, Fosså SD, Dahl O, Bjøro T: **Gonadal dysfunction and fertility problems in cancer survivors.** *Acta Oncologica* 2007, **46:**480-489.

35. Chen H, Zhang J, Luo J, Lai F, Wang Z, Tong H, Lu D, Bu H, Zhang R, Lin S: **Antiangiogenic effects of oxymatrine on pancreatic cancer by inhibition of the NF-κB-mediated VEGF signaling pathway.** *Oncology reports* 2013, **30:**589-595.

592 36. Guan L, Song Y, Gao J, Gao J, Wang K: **Inhibition of calcium-activated chloride**
593 **channel ANO1 suppresses proliferation and induces apoptosis of epithelium**
594 **originated cancer cells.** *Oncotarget* 2016, **7:**78619.
595 37. Guo S, Chen Y, Pang C, Wang X, Shi S, Zhang H, An H, Zhan Y: **Matrine is a novel**
596 **inhibitor of the TMEM16A chloride channel with antilung adenocarcinoma**
597 **effects.** *Journal of cellular physiology* 2018.
598 38. Liu R, Peng J, Wang H, Li L, Wen X, Tan Y, Zhang L, Wan H, Chen F, Nie X:
599 **Oxysophocarpine Retards the Growth and Metastasis of Oral Squamous Cell**
600 **Carcinoma by Targeting the Nrf2/HO-1 Axis.** *Cellular Physiology and Biochemistry*
601 2018, **49:**1717-1733.
602 39. Li S, Butler P, Wang Y, Hu Y, Han DC, Usami S, Guan J-L, Chien S: **The role of the**
603 **dynamics of focal adhesion kinase in the mechanotaxis of endothelial cells.**
604 *Proceedings of the National Academy of Sciences* 2002, **99:**3546-3551.
605 40. Yamaguchi H, Condeelis J: **Regulation of the actin cytoskeleton in cancer cell**
606 **migration and invasion.** *Biochimica et Biophysica Acta (BBA)-Molecular Cell*
607 *Research* 2007, **1773:**642-652.
608 41. Janet MT, Cheng G, Tyrrell JA, Wilcox-Adelman SA, Boucher Y, Jain RK, Munn LL:
609 **Mechanical compression drives cancer cells toward invasive phenotype.**
610 *Proceedings of the National Academy of Sciences* 2012, **109:**911-916.
611 42. Chorev DS, Moscovitz O, Geiger B, Sharon M: **Regulation of focal adhesion**
612 **formation by a vinculin-Arp2/3 hybrid complex.** *Nature communications* 2014,
613 **5:**3758.
614 43. Zhang B, Wang X, Li Y, Wu M, Wang S-Y, Li S: **Matrine is identified as a novel**
615 **macropinocytosis inducer by a network target approach.** *Frontiers in*
616 *pharmacology* 2018, **9:**10.

44. Heldin C-H, Vanlandewijck M, Moustakas A: **Regulation of EMT by TGFβ in cancer.** *FEBS letters* 2012, **586:**1959-1970.

45. Tan E-J, Olsson A-K, Moustakas A: **Reprogramming during epithelial to mesenchymal transition under the control of TGFβ.** *Cell adhesion & migration* 2015, **9:**233-246.

46. Enomoto M, Utsumi M, Park MK: **Gonadotropin-releasing hormone induces actin cytoskeleton remodeling and affects cell migration in a cell-type-specific manner in TSU-Pr1 and DU145 cells.** *Endocrinology* 2006, **147:**530-542.

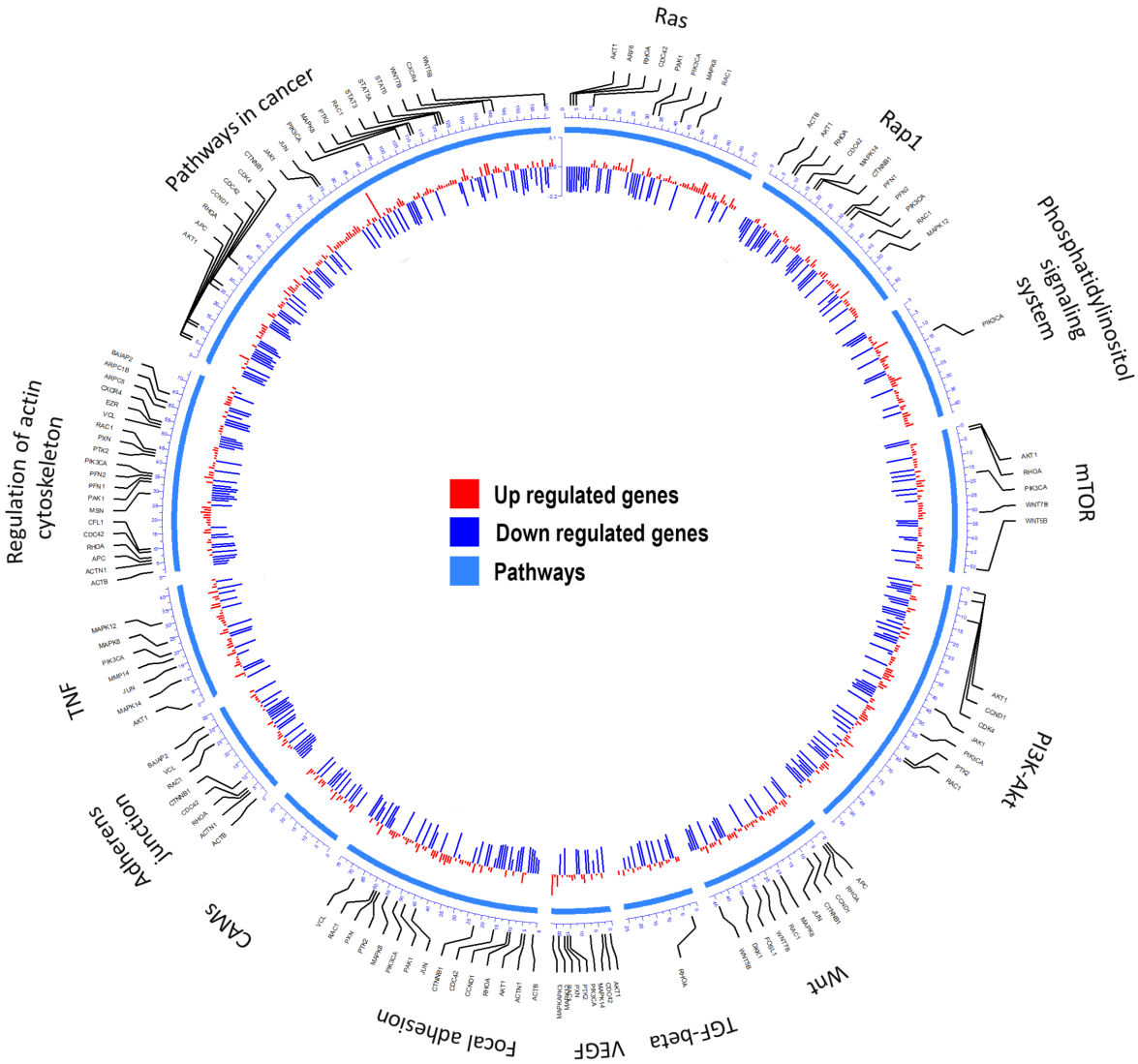

626

627 **Fig. 1**: Summary of the KEGG analyses of over-represented pathways for differentially
628 expressed genes after CKI treatment in MDA-MB-231 cells. From outer to inner, the first circle
629 indicates the pathways; the second shows the genes involved; and the third summarizes
630 significant changes in expression for transcript levels that were upregulated (red) or
631 downregulated (blue) following CKI treatment. P-value cutoff for KEGG analysis was 0.05.

632

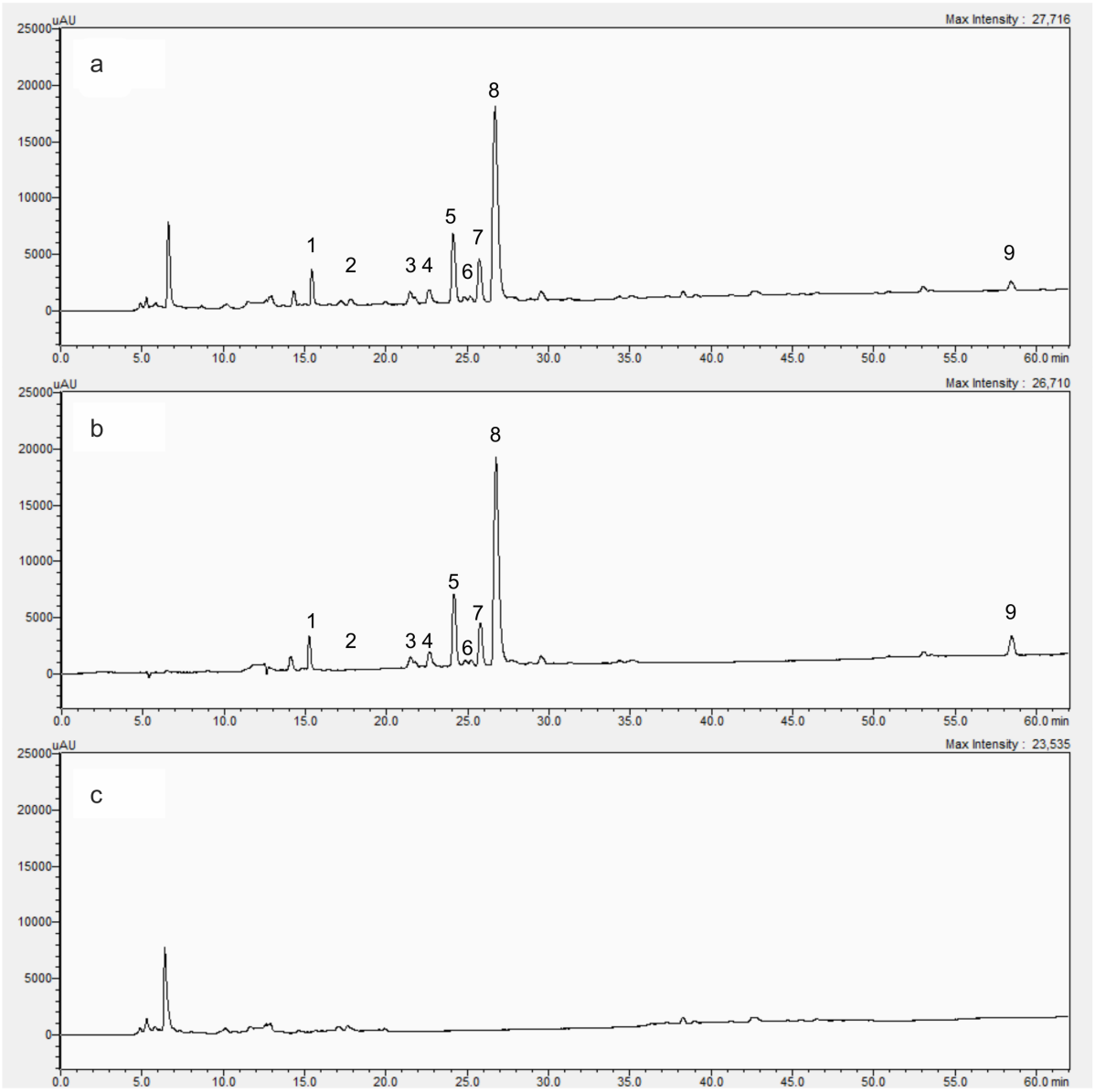

Fig. 2: HPLC profiles of the components present in (a) CKI, (b) MJ and (c) MN fractions. Samples (50 µl at 1 mg/ml) were run through a C18 semi-preparative column. Numbers indicate the nine major compounds; 1: macrozamin, 2: adenine, 3: n-methylcytisine, 4: sophoridine, 5: matrine, 6: sophocarpine, 7: oxysophocarpine, 8: oxymatrine, and 9: trifolirhizin.

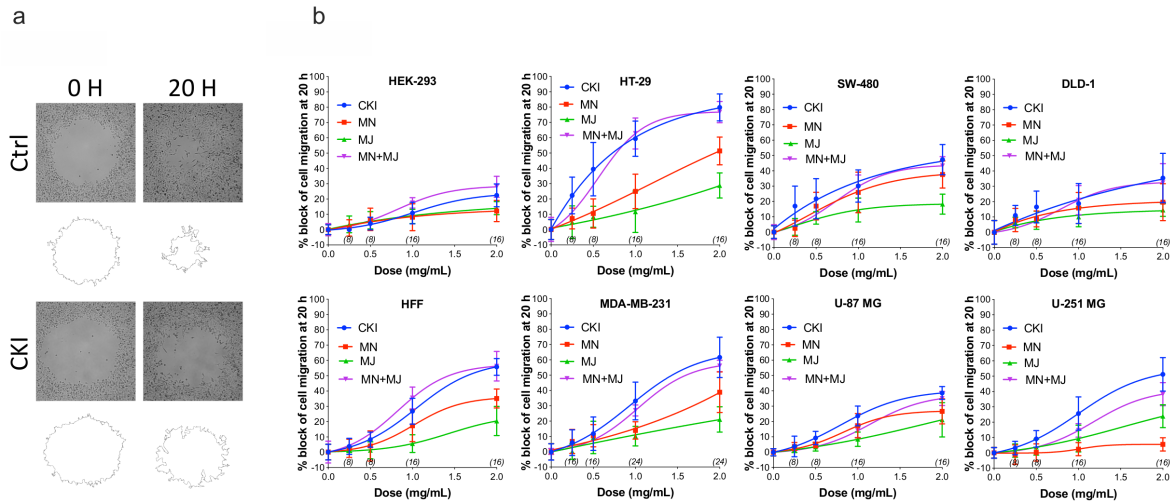

640

641 **Fig. 3**: Dose-dependent inhibition of cell migration by CKI, MJ and MN fractions in eight cell
642 lines, measured by wound closure assays. (a) Wound areas were imaged at 0 hour (initial) and
643 after 20 hours of treatment. (b) Graphs show percent inhibition of cell migration standardized
644 to the initial wound area, as a function of dose for treatments with CKI (blue), MJ (green), MN
645 (red), and reconstituted CKI with major and minor fractions combined (MN+ MJ; purple).

646

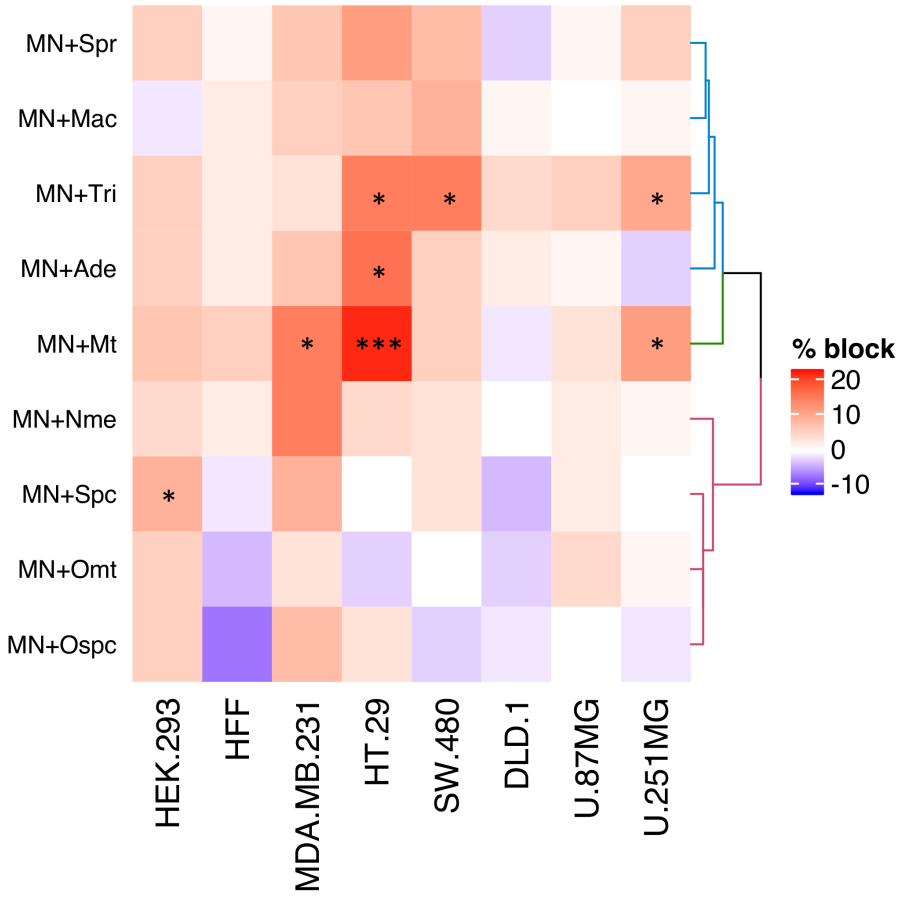

Fig. 4: Combinatorial analysis of effects on wound closure for the MN fraction tested in combination with each of nine individual major compounds of CKI, summarized as a heatmap. Data were normalized to values for percentage of migration blocked with MN alone at 0.5 mg/ml. Boxes display the net effects of added single major compounds, as no change (white), increased percentage block (red), or reduced percentage of migration blocked (blue). Statistically significant differences are shown as $p < 0.05$ (*), $p < 0.01$ (**), and $p < 0.001$ (***). No symbol in a box indicates the response was not significantly different from that with MN alone.

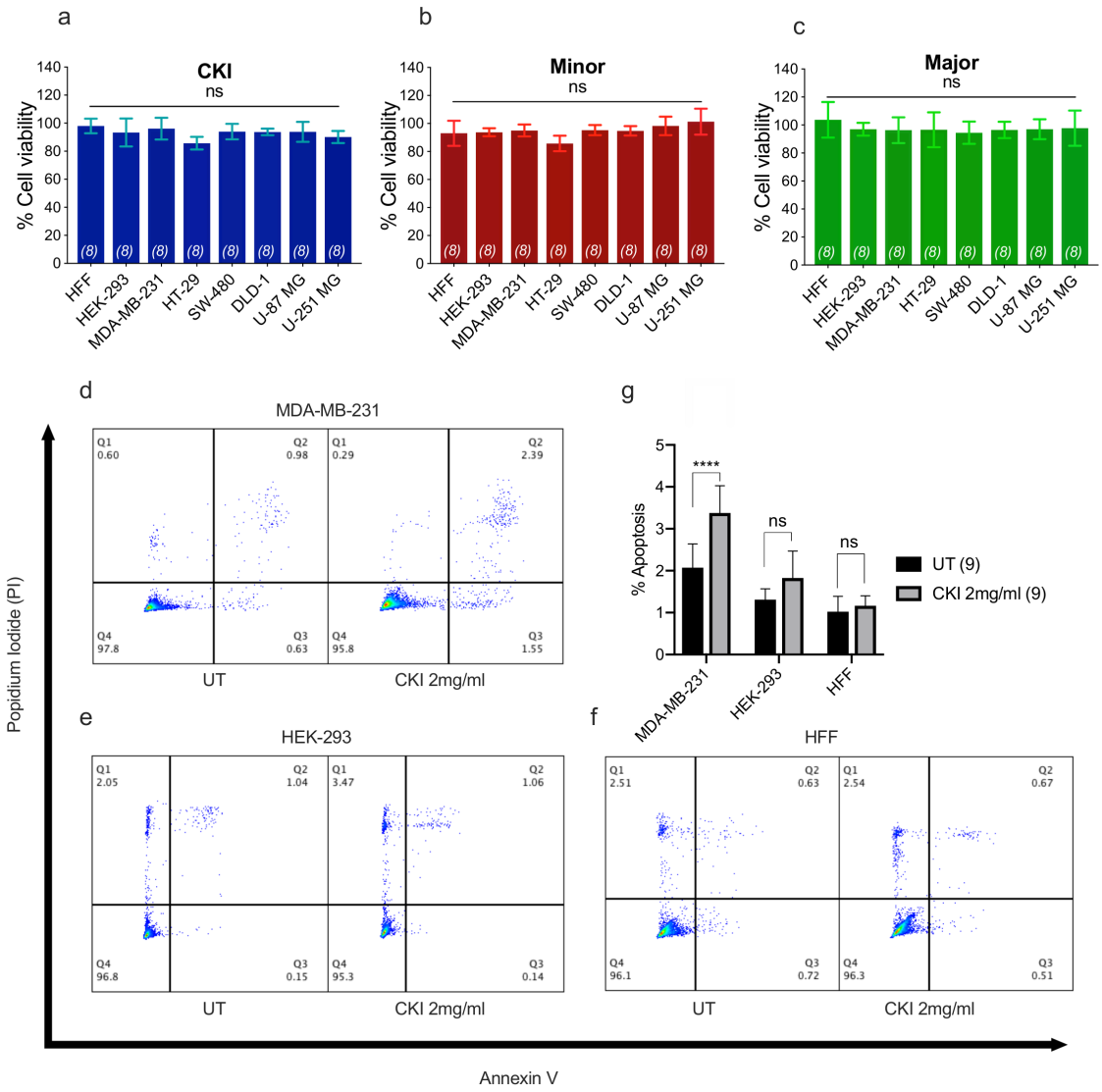

Fig. 5: Assessment of the effects of CKI and fractions on cell viability and incidence of apoptosis. Viability was measured by Alamar Blue assay in eight cell lines treated with (a) CKI, (b) MN or (c) MJ fractions (at doses present in 2 mg/ml CKI). Cell viability responses standardized as a percentage to mean values for vehicle control were not significantly different (ns) in any condition, based on repeated experiments with 8 replicates total. Apoptosis was compared in three cell lines with and without CKI treatment, for (d) MDA-MB-231, (e) HEK-293, and (f) HFF cells, analyzed by flow cytometry (see Methods for details). Pseudo-color plots illustrate the percentages of cells in the late (quadrant Q2) and early (Q3) stages of apoptosis. (g) Histogram summarizing compiled data (mean ± SD) depicting percentage apoptosis in three cell lines with and without CKI treatment.

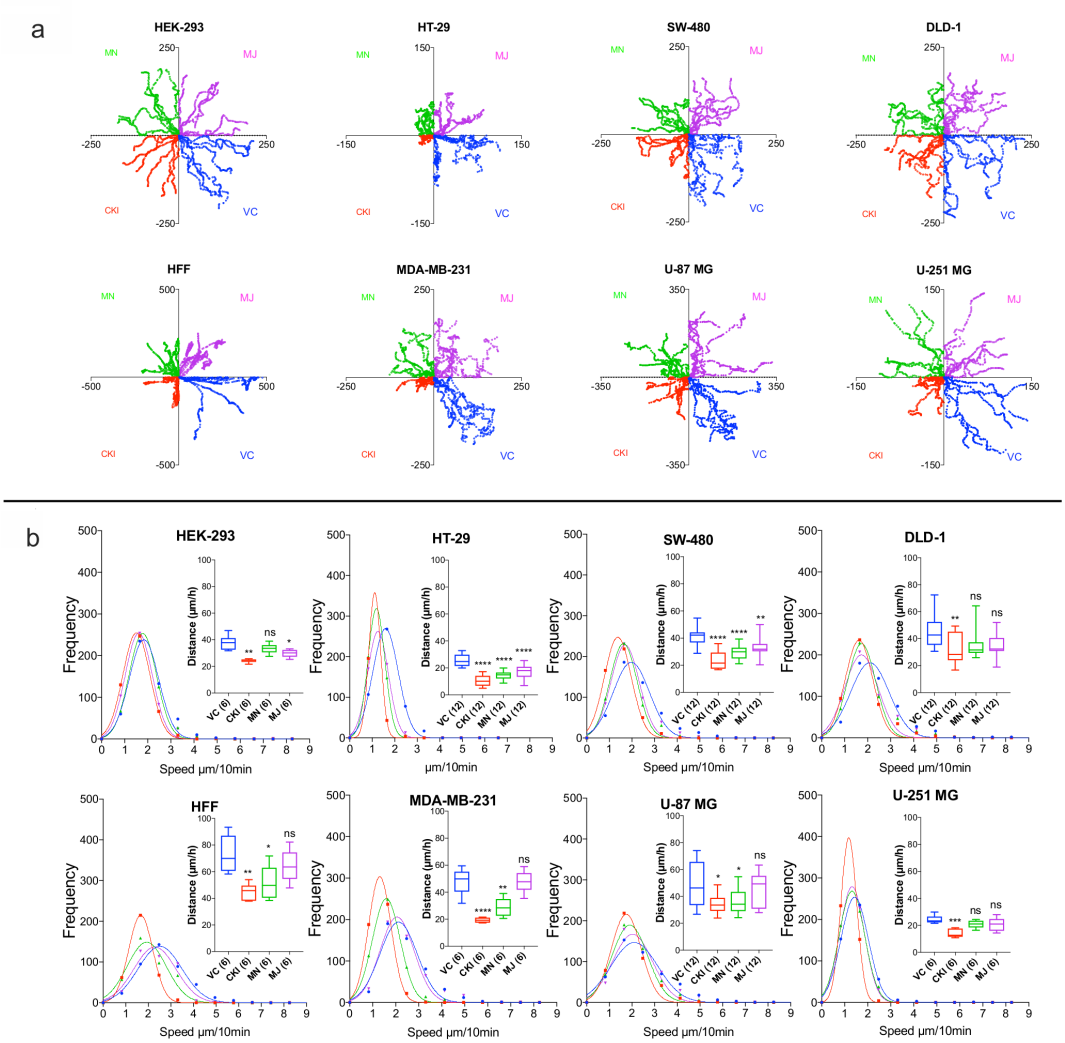

Fig. 6: Live-cell imaging of individual cell migration trajectories, with and without the treatments in eight cell lines. Six representative cells located near wound boundaries were selected at time zero and tracked by time-lapse imaging at 10-minute intervals for 20 hours by the positions of cell nuclei. (a) Trajectory plots of individual cells, starting at the graph origin at time 0, were assigned in quadrants based on treatment groups: VC (vehicle control, blue), CKI (red), MN (green), and MJ (violet). X and Y axis values are in µm. (b) Frequency histograms of distances moved by individual cells per 10-minute interval over 20 hours. Colours indicate treatment groups, as above. Total cumulative distances moved per cell are collated in box plots (insets). Boxes enclose 50 % of values; error bars show the full range; and horizontal lines are median values. Statistically significant difference is indicated as $p < 0.05$ (*), $p < 0.01$ (**), and $p < 0.001$ (***).

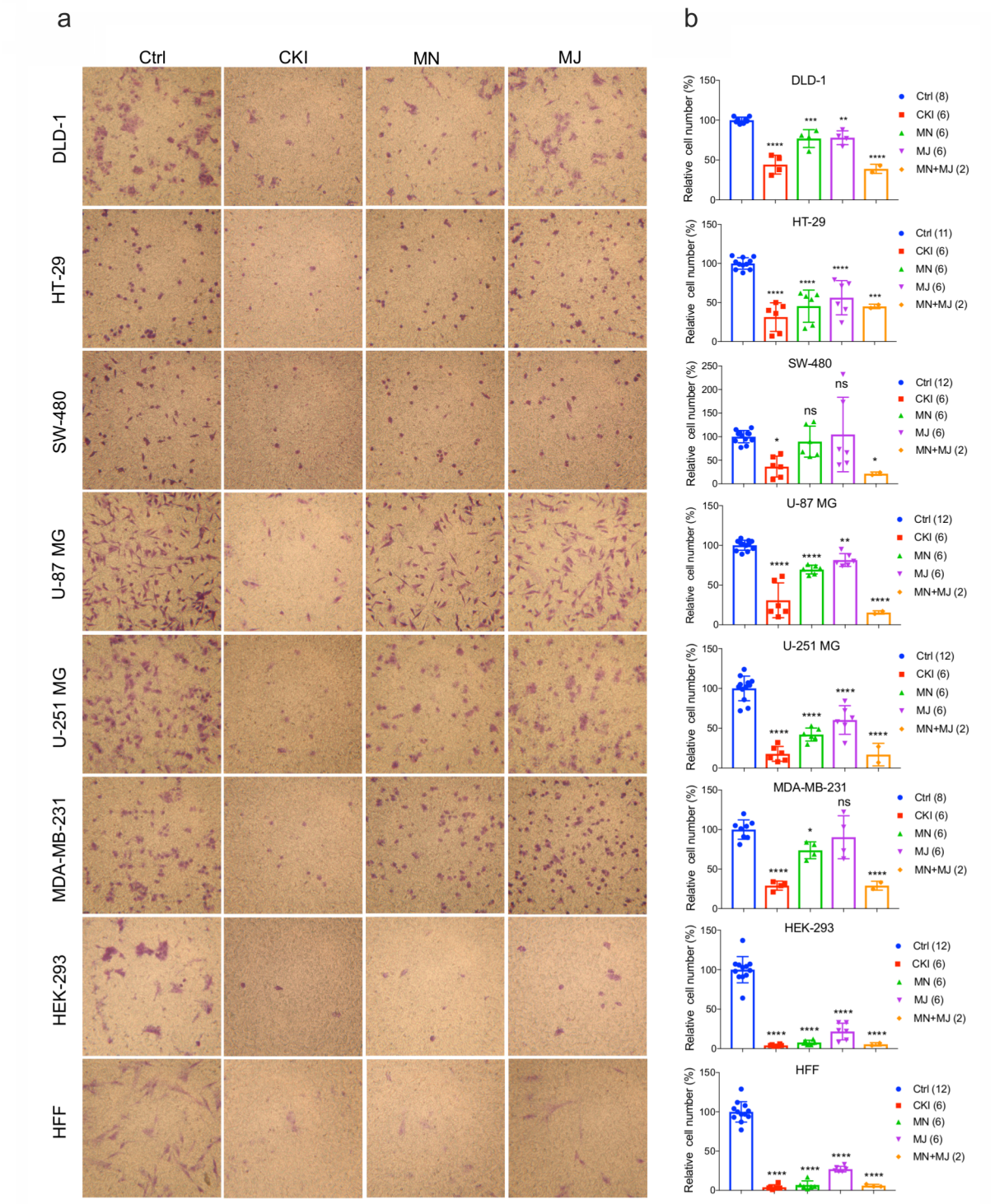

680

681 **Fig. 7**: Effects of CKI and fractions on cell invasiveness in eight cell lines. Migration
682 efficiencies of cells across an extracellular matrix barrier after treatment with CKI, minor
683 (MN), major (MJ), or combined (MN+MJ) fractions were measured by transwell invasion
684 assays. (a) Images show stained cells that had passed through the filter to reach the opposite
685 side of the transwell membrane. CKI, MN and MJ were applied at doses equal to those present

686 in 2 mg/ml CKI; Ctrl is vehicle control. (b) Compiled results are shown in histograms; n-values
687 are in italics in corresponding figure key. Statistically significant differences compared to
688 vehicle control are indicated as $p < 0.01$ (**), $p < 0.001$ (***), and $p < 0.0001$ (****); ns is not
689 significant.
690

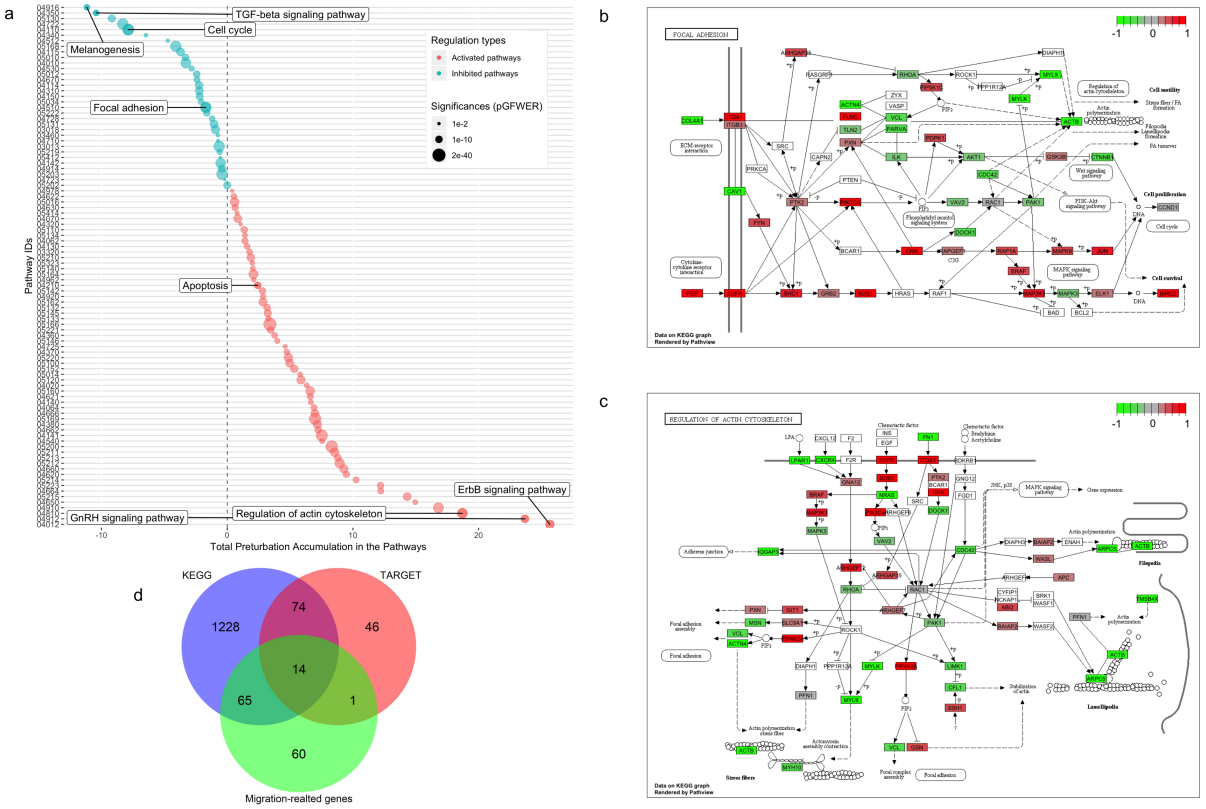

691

692 **Fig. 8**: Identification of significantly perturbed pathways using SPIA analysis. (a) 101
693 significantly perturbed pathways in MDA-MB-231 treated by CKI 2 mg/ml were observed.
694 Total perturbation values are shown on the x-axis, and pathway IDs are on the y-axis. The
695 global perturbation P value ($pG < 0.05$) was used. (b) Significantly perturbed "focal adhesion"
696 pathway in MDA-MB-231 treated by CKI 2 mg/ml. (c) Significantly perturbed "regulation of
697 actin cytoskeleton" pathway in MDA-MB-231 treated by CKI 2 mg/ml. Up- and down-
698 regulated genes are shown in red and green respectively and genes that were not affected by
699 CKI treatment are shown in white or grey. (d) 14 "core genes" that are found across three
700 different datasets (see Methods).

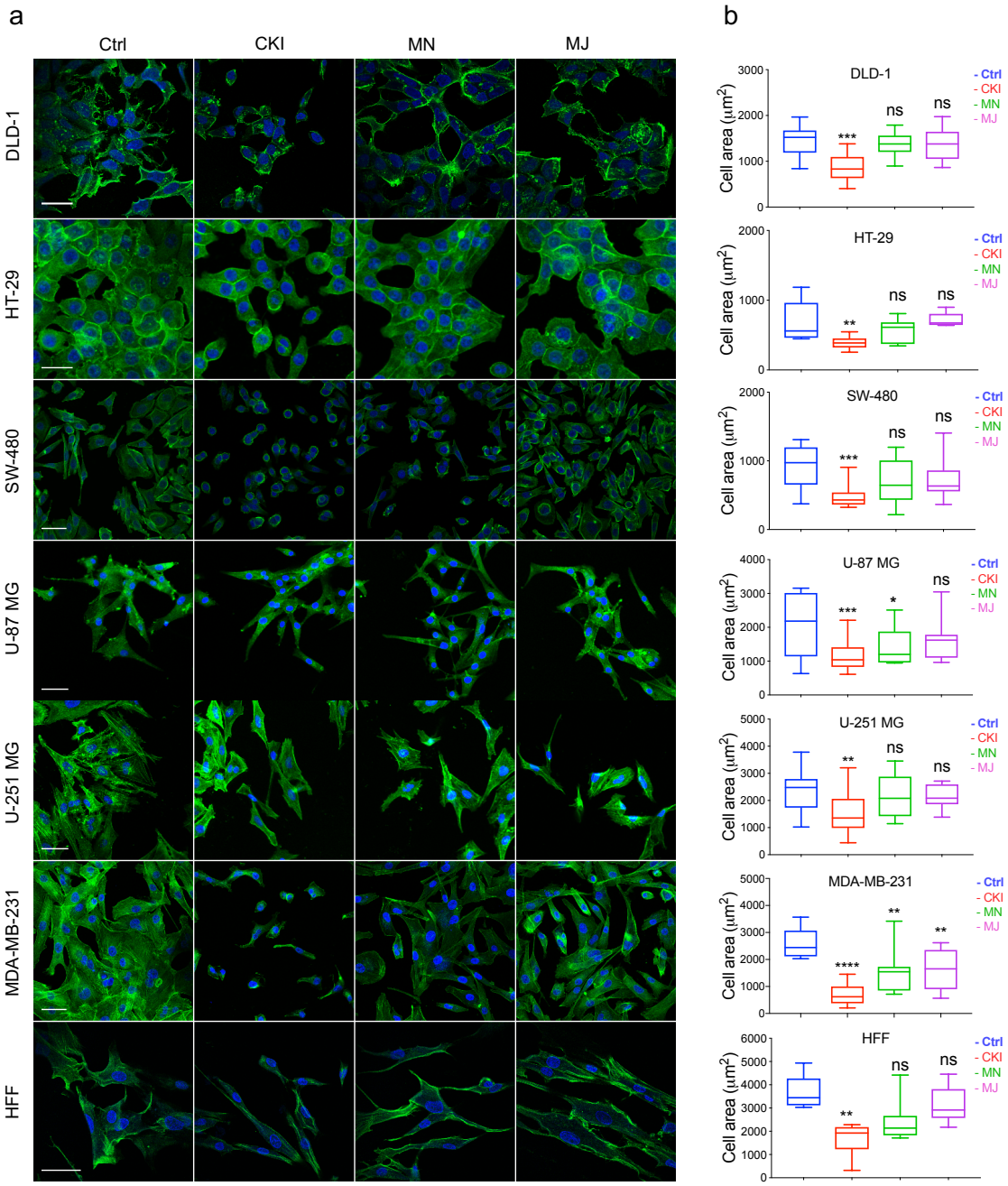

Fig. 9: Patterns of distribution of polymerized F-actin after CKI-based treatments in eight cell lines, visualized by confocal microscopy. (a) F-actin was labelled with phalloidin (green), and nuclei with Hoechst (blue), for treatment groups (from left to right): vehicle control (Ctrl), CKI, minor and major fractions at doses present in 2 mg/ml CKI. Scale bars are 50 µm. (b) Areas (µm2) of F-actin staining per cell are summarized in box plots. Statistically significant results are shown as $p < 0.05$ (*), $p < 0.01$ (**), $p < 0.001$ (***), $p < 0.0001$ (****) and (ns) for not significant.

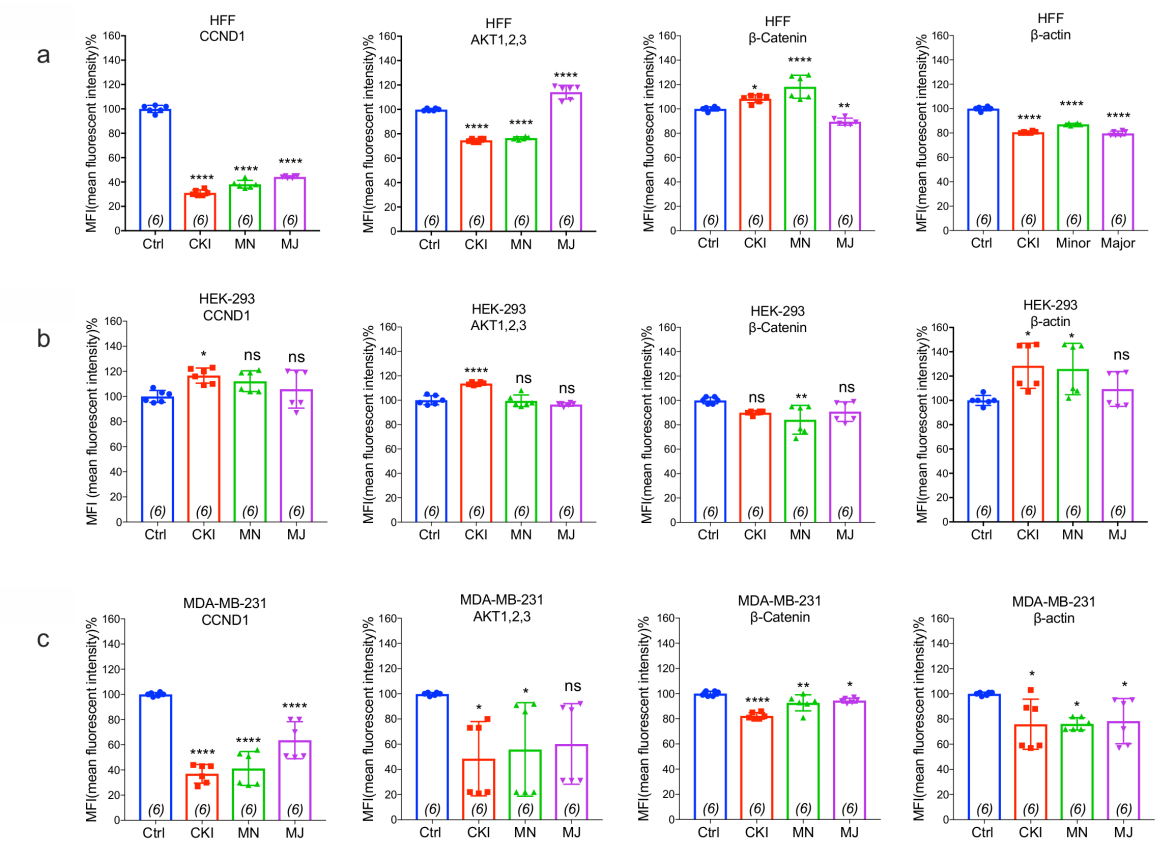

Fig. 10: Flow cytometry analyses of four proteins: CTNNB1, AKT (1, 2, 3), CCND1, and ACTB compared in three cell lines with and without CKI-based treatments. The levels of protein expression for four genes predicted by transcriptomic analysis to be significantly down-regulated were evaluated by FACS in three cell lines (a) MDA-MB-231, (b) HEK-293, and (c) HFF. Statistically significant differences compared to vehicle controls were analysed using one-way ANOVA and post hoc tests and are shown as $p < 0.05$ (*), $p < 0.01$ (**), $p < 0.001$ (***), $p < 0.0001$ (****), and not significant (ns).

Table 1: Concentration of 9 major compounds in CKI (Batch No:20151139) and MJ. Total alkaloid content in CKI (Batch No:20151139) = 25 mg/ml based on manufacturer's assay. Regression line for the calculation of compounds has previously been described (Aung et al., 2018).

Mixtures	Compounds	concentration (mg/mL)	%Contribution
CKI	Macrozamin	1.1 ± 0.07	4.4
	Adenine	0.04 ± 0.03	1.6
	N-methylcytisine	0.2 ± 0.04	0.8
	Sophoridine	0.3 ± 0.19	1.2
	Matrine	1.7 ± 0.17	6.8
	Sophocarpine	0.5 ± 0.03	2
	Oxysophocarpine	1.2 ± 0.18	4.8
	Oxymatrine	5.6 ± 0.66	22.4
	Trifolirhizin	0.12 ± 0.01	0.4
	Total	**11.1**	**44.4**
MJ	Macrozamin	1.2 ± 0.17	4.8
	Adenine	0.2 ± 0.01	0.8
	N-methylcytisine	0.2 ± 0.04	0.8
	Sophoridine	0.4 ± 0.12	1.4
	Matrine	1.5 ± 0.6	6
	Sophocarpine	0.3 ± 0.003	1.4
	Oxysophocarpine	1.1 ± 0.14	4.3
	Oxymatrine	5.9 ± 0.7	23.6
	Trifolirhizin	0.05 ± 0.01	0.2
	Total	**10.8**	**43.3**

*Total alkaloid content in CKI (Batch No:20151139) = 25 mg/ml based on manufacturer's assay. Regression line for the calculation of compounds have been previously described (Aung et.al).

Chapter 4

Identification of Candidate Anti-cancer Molecular Mechanisms of Compound Kushen Injection Using Functional Genomics

CKI has been used clinically as a complementary medicine for cancer treatment together with chemo- and radio-therapy over 15 years. By analysing the transcriptome of MCF-7 breast cancer cells treated by CKI, we mapped the effects CKI to specific pathways such as the cell-cycle pathway based on altered gene expression profiles in a cell-based assay. Reconstruction of co-expression networks in this study showed that CKI downregulated lncRNA H19, a molecule known to be upregulated in cancer. This chapter is in the format of the manuscript that was published in *Oncotarget*.

Statement of Authorship

Title of Paper	Identification of candidate anti-cancer molecular mechanisms of Compound Kushen Injection using functional genomics
Publication Status	☑ Published ☐ Accepted for Publication ☐ Submitted for Publication ☐ Unpublished and Unsubmitted w ork w ritten in manuscript style
Publication Details	Zhipeng Qu, Jian Cui, Yuka Harata-Lee, Thazin Nwe Aung, Qianjin Feng, Joy M.Raison, Robert Daniel Kortschak, David L. Adelson. "Identification of candidate anti-cancer molecular mechanisms of Compound Kushen Injection using functional genomics". Oncotarget. 2016; 7:66003-66019. https://doi.org/10.18632/oncotarget.11788

Principal Author

Name of Principal Author (Candidate)	Thazin Nwe Aung		
Contribution to the Paper	Assisted with experiments and data analysis.		
Overall percentage (%)	20%		
Certification:	This paper reports on original research I conducted during the period of my Higher Degree by Research candidature and is not subject to any obligations or contractual agreements with a third party that would constrain its inclusion in this thesis. I am the primary author of this paper.		
Signature		Date	5/11/2018

Co-Author Contributions

By signing the Statement of Authorship, each author certifies that:

i. the candidate's stated contribution to the publication is accurate (as detailed above);

ii. permission is granted for the candidate in include the publication in the thesis; and

iii. the sum of all co-author contributions is equal to 100% less the candidate's stated contribution.

Name of Co-Author	Zhipeng Qu		
Contribution to the Paper	Designed and carried out the experiments, analysed data and wrote the manuscript.		
Signature		Date	5/11/2018

Name of Co-Author	Jian Cui		
Contribution to the Paper	Experimental design, assisted with experiments, assisted with data analysis and wrote the manuscript.		
Signature		Date	5/11/2018

Please cut and paste additional co-author panels here as required.

Name of Co-Author	Yuka Harata-Lee		
Contribution to the Paper	Experimental design, assisted with experiments, assisted with data analysis and wrote the manuscript.		
Signature		Date	5/11/2018

Name of Co-Author	Qianjin Feng		
Contribution to the Paper	Assisted with experimental design, assisted with experiments		
Signatur		Date	2018.10.27

Name of Co-Author	Joy M. Raison		
Contribution to the Paper	Experimental design		
Signature		Date	27/10/18

Name of Co-Author	Robert Danial Kortschak		
Contribution to the Paper	Experimental design		
Signature		Date	5/11/2018

Name of Co-Author	David L. Adelson		
Contribution to the Paper	Supervised the research, assisted the research with the funding, experimental design and wrote the manuscript.		
Signature		Date	5/11/18

Research Paper

Identification of candidate anti-cancer molecular mechanisms of Compound Kushen Injection using functional genomics

Zhipeng Qu[1], Jian Cui[1,*], Yuka Harata-Lee[1,*], Thazin Nwe Aung[1], Qianjin Feng[2], Joy M. Raison[1], Robert Daniel Kortschak[1], David L. Adelson[1]

[1]Department of Genetics and Evolution, School of Biological Sciences, The University of Adelaide, Adelaide, South Australia 5005, Australia

[2]Shanxi Modern Chinese Medicine Engineering Laboratory, Shanxi University of Traditional Chinese Medicine, Shanxi 030619, China

[*]These authors contributed equally to this work

Correspondence to: *David L. Adelson,* ***email:*** *david.adelson@adelaide.edu.au*

Keywords: *systems biology, traditional Chinese medicine, lncRNA, transcriptome*

Received: *March 02, 2016* ***Accepted:*** *August 24, 2016* ***Published:*** *September 01, 2016*

ABSTRACT

Compound Kushen Injection (CKI) has been clinically used in China for over 15 years to treat various types of solid tumours. However, because such Traditional Chinese Medicine (TCM) preparations are complex mixtures of plant secondary metabolites, it is essential to explore their underlying molecular mechanisms in a systematic fashion. We have used the MCF-7 human breast cancer cell line as an initial *in vitro* model to identify CKI induced changes in gene expression. Cells were treated with CKI for 24 and 48 hours at two concentrations (1 and 2 mg/mL total alkaloids), and the effect of CKI on cell proliferation and apoptosis were measured using XTT and Annexin V/Propidium Iodide staining assays respectively. Transcriptome data of cells treated with CKI or 5-Fluorouracil (5-FU) for 24 and 48 hours were subsequently acquired using high-throughput Illumina RNA-seq technology. In this report we show that CKI inhibited MCF-7 cell proliferation and induced apoptosis in a dose-dependent fashion. We integrated and applied a series of transcriptome analysis methods, including gene differential expression analysis, pathway over-representation analysis, *de novo* identification of long non-coding RNAs (lncRNA) as well as co-expression network reconstruction, to identify candidate anti-cancer molecular mechanisms of CKI. Multiple pathways were perturbed and the cell cycle was identified as the potential primary target pathway of CKI in MCF-7 cells. CKI may also induce apoptosis in MCF-7 cells via a p53 independent mechanism. In addition, we identified novel lncRNAs and showed that many of them might be expressed as a response to CKI treatment.

INTRODUCTION

The complexity of carcinogenesis at the genetic level has been investigated more and more deeply by leveraging fast-developing omics-related techniques in the past decades [1–3]. Novel genetic mutations and molecular markers are now comprehensively identified in cancer genome sequencing projects. More importantly, whole transcriptome analyses are much more widely used to identify novel cancer-related transcripts or regulatory elements, such as long non-protein-coding RNAs (lncRNAs) and alternative splicing, and are also used to characterise the underlying molecular mechanisms based on global gene expression changes in different types of cancers *in vivo* or *in vitro* [4–6]. The current challenge is to integrate these new techniques to discover or evaluate novel cancer therapies [7].

Traditional Chinese Medicines (TCMs) are experience-based remedies derived from hundreds or thousands of years of clinical use in China. Most TCMs are extracted from one or more medicinal herbs. The existence of multiple bioactive ingredients makes many TCMs potential novel resources for the discovery of new cancer drugs, such as multi-targeted cancer drugs [8]. Compound Kushen Injection (CKI, also known as Yanshu injection) is a State Administration of Chinese Medicine-

approved TCM formula used in the clinical treatment of various types of cancers in China [9, 10]. It is extracted from the roots of two medicinal herbs, Kushen (*Radix Sophorae Flavescentis*) and Baituling (*Rhizoma smilacis Glabrae*), using modern standardised Good Manufacturing Processes (GMP) [11, 12]. The chemical fingerprint of CKI contains at least 8 different components, with primary compounds Matrine and Oxymatrine [12]. This indicates that multiple compounds in CKI may deliver an integrated anti-tumor effect through multiple targets and their associated molecular pathways.

By detecting the expression of key genes or proteins in single molecular pathways, the anti-tumor effects of Matrine or Oxymatrine, including the inhibition of cell proliferation and induction of apoptosis, have been demonstrated in various types of cancer [13–17]. The molecular mechanisms of CKI as a system have also been recently explored [11, 18]. Quantitative detection of expression changes of key regulators, including *beta-catenin*, *CyclinD1* and *c-Myc*, of the canonical Wnt/beta-catenin pathway, have shown that CKI can suppress the stem cells in MCF-7 cells by down-regulating this signalling pathway [11]. In addition, other studies suggest that CKI can inhibit mouse sarcoma growth and reduce tumor-induced hyperalgesia via the AKT and TRPV1 signalling pathways by reducing the phosphorylation of ERK and AKT kinases and BAD [18].

The main goal of modern pharmacology is to elucidate the molecular mechanisms that can be targeted by therapeutic compounds. Analyses using purified single components of TCM can be somewhat useful, but are limited when it comes to identifying integrated systemic effects resulting from a multi-compound formula. Furthermore, previous studies attempting to understand the mode of action of CKI have only focused on single or a few molecular pathways by assessing the expression of key regulators in these pathways. We have therefore, taken advantage of high throughput whole transcriptome analyses, and applied these to explore the system wide molecular mechanisms targeted by TCM. We have identified a comprehensive list of expressed genes perturbed by CKI, and used gene expression data to characterise molecular pathways potentially targeted by CKI in MCF-7 human breast cancer cells. Our results show that CKI can alter the expression of many cancer relevant genes and lncRNAs, correlated with the inhibition of cell proliferation through cell cycle arrest and the induction of apoptosis via p53 independent pathways.

RESULTS

CKI inhibits MCF-7 cell proliferation and induces cell apoptosis

To characterise the effect of CKI on proliferation of MCF-7 breast cancer cells, we used the XTT assay to measure cell viability after treating with different doses of CKI. The proliferation of MCF-7 cells was dramatically inhibited when treated with a high dose of CKI (2 mg/mL, based on the total alkaloid concentration in CKI) and showed a dose-dependent effect (Figure 1A and Supplementary Figure 1A). An Annexin V/Propidium Iodide (PI) assay was used to quantify cell apoptosis when MCF-7 cells were treated with CKI. Percentage of apoptotic cells, particularly at the higher dose of CKI, was increased at both time points compared with untreated cells, indicating that apoptosis was induced in cells treated with CKI (Figure 1B and 1C). The caspase3/7 colorimetric assay also showed that there was increased caspase3/7 activity in cells treated with CKI (Supplementary Figure 1B). Altogether, these results showed that CKI could inhibit growth and induce apoptosis of MCF-7 cells *in vitro*.

Global gene expression changes in MCF-7 cells treated with CKI

To further investigate the underlying molecular mechanisms of CKI on MCF-7 cells, we performed high-depth next generation sequencing using an Illumina HiSeq 2500. In total, more than 732 million stranded 100 basepairs (bp) paired-end reads were sequenced from 9 groups of MCF-7 cells treated with two doses of CKI or one dose of chemotherapy drug 5-Fluorouracil (5-FU) for 24 and 48 hours along with untreated cells (Supplementary Table 1) (GSE78512). The global gene expression profiles of CKI treated cells, particularly in cells treated with high dose CKI (2 mg/mL), were clearly different from the profile of 5-FU treated cells compared with untreated cells (Supplementary Figure 2). We then used edgeR to identify the statistically significant differentially expressed (DE) genes for the pairwise comparisons between cells treated with 1 mg/mL CKI, 2 mg/mL CKI and 5-FU for 24 or 48 hours respectively (Figure 2 and Supplementary Table 2). Compared with untreated cells, fewer than 200 genes had significantly altered expression in cells treated with low dose CKI (1 mg/mL) for 24 or 48 hours (Figure 2A and 2B). However, many more DE genes (1,826 genes for 24 hours and 2,904 for 48 hours) were identified in cells treated with high dose CKI (2 mg/mL). Interestingly, when comparing the number of DE genes in cells treated with high dose CKI with low dose CKI, we observed almost twice as many genes down-regulated but only a small number of genes (828 to 791) up-regulated (Figure 2A and 2B). Furthermore, we compared DE genes in cells treated with high dose CKI and in cells treated with 5-FU (Supplementary Figure 3). For up-regulated genes in cells treated with high dose CKI for 24 hours, approximately half (396 out of 791) of these were also identified as DE genes, with most (384) being up-regulated in 5-FU treated cells as well. 459 down-regulated genes were also shown as DE genes with most of these (424 out of 459) also being down-regulated in cells treated with 5- FU for 24 hours (Supplementary Figure 3A). After cells were treated with CKI or 5-FU for 48 hours, the number

of DE genes decreased dramatically in 5-FU treated cells, but greatly increased in cells treated with 2 mg/mL CKI (Supplementary Figure 3B). The common DE genes altered by CKI or 5-FU showed consistent expression changes at 48 hours (Supplementary Figure 3B).

To validate the gene expression changes from transcriptome analysis, we performed quantitative PCR (qPCR) for 6 genes and acquired overall consistent results (Figure 2C, Supplementary Figure 4 and Supplementary Table 2).

Annotation of the molecular pathways altered by CKI in MCF-7 cells

Since CKI likely contains multiple bioactive ingredients, we used a number of systems biology methods to explore the molecular mechanisms of CKI.

The over-represented Gene Ontology (GO) terms for all DE genes identified in cells treated with high dose CKI (2 mg/mL) for 24 hour and 48 hours are shown in Figure 3A and 3B. Based on their functional similarity, these GO terms were clustered into several primary categories, including "Regulation of biological process, cellular process and metabolic process", "Cell differentiation, development", "Transport, localisation", "Chromatin organisation, organelle organisation", "Cell motility and migration" and "Secondary metabolic processes and reactive oxygen species metabolic". Interestingly, we found that the majority of cell growth or proliferation related GO terms included more down-regulated genes, while GO terms associated with "Secondary metabolic processes and reactive oxygen species metabolic" showed enrichment of more up-regulated genes (Figure 3A). In MCF-7 cells treated with CKI for 48 hours, similar categories of over-represented GO terms seen at 24 hours were also observed, such as "Metabolic process", "Regulation of metabolic process" and "Localization". In addition, cell proliferation related terms, including "Cell cycle", "Cell growth" and "Cell death" were also over-represented in DE genes from cells treated with CKI for 48 hours (Figure 3B). Furthermore, we compared the over-representation of GO terms of the 200 most significantly

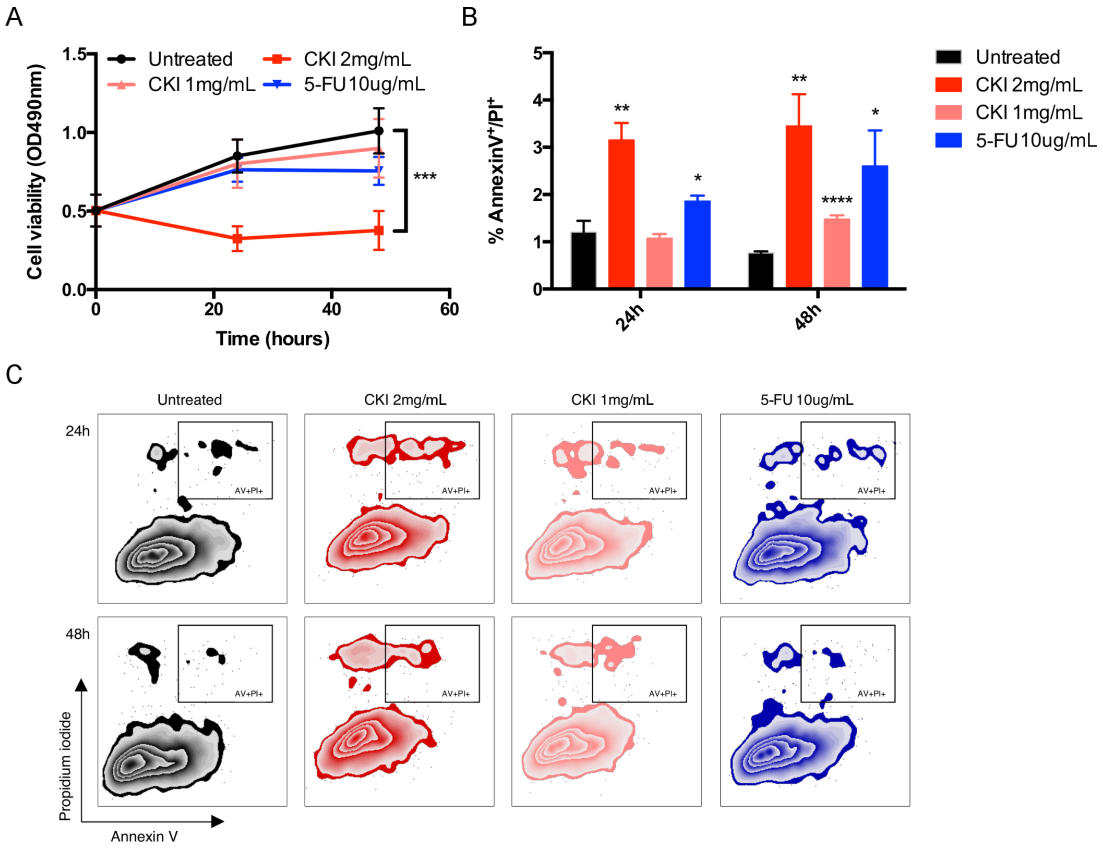

Figure 1: CKI inhibits proliferation and induces apoptosis of MCF-7 cells. A. Inhibition of MCF-7 cell proliferation with CKI treatment. The level of viability of cells under different treatments was measured using XTT:PMS. Data are represented as mean ±SEM (n=6). **B.** and **C.** Induction of apoptosis in MCF-7 cells with CKI treatment. The level of apoptosis was determined by measuring the levels of Annexin V and PI staining: B) Percentages of Annexin V^+/PI^+ cells, and C) representative plots of Annexin V and PI staining. Data are represented as mean ±SEM (n=6). Statistical analyses were performed using A) two-way ANOVA or B) t-test comparing with "untreated" (*p<0.05, **p<0.01, ****p<0.0001).

DE genes in cells treated with CKI or 5-FU for 24 hours or 48 hours (Figure 3C and 3D). In cells treated with CKI or 5-FU for 24 hours, over-represented GO terms were generally divided into two clusters with respect to the different expression status of the genes that contributed to each term. Terms such as "Cellular hormone metabolic process" and "Pigment metabolic process" were dominated by up-regulated genes, which were mainly DE genes from CKI treated cells only. On the other hand, terms represented by "Chromosome segregation", "Cell cycle",

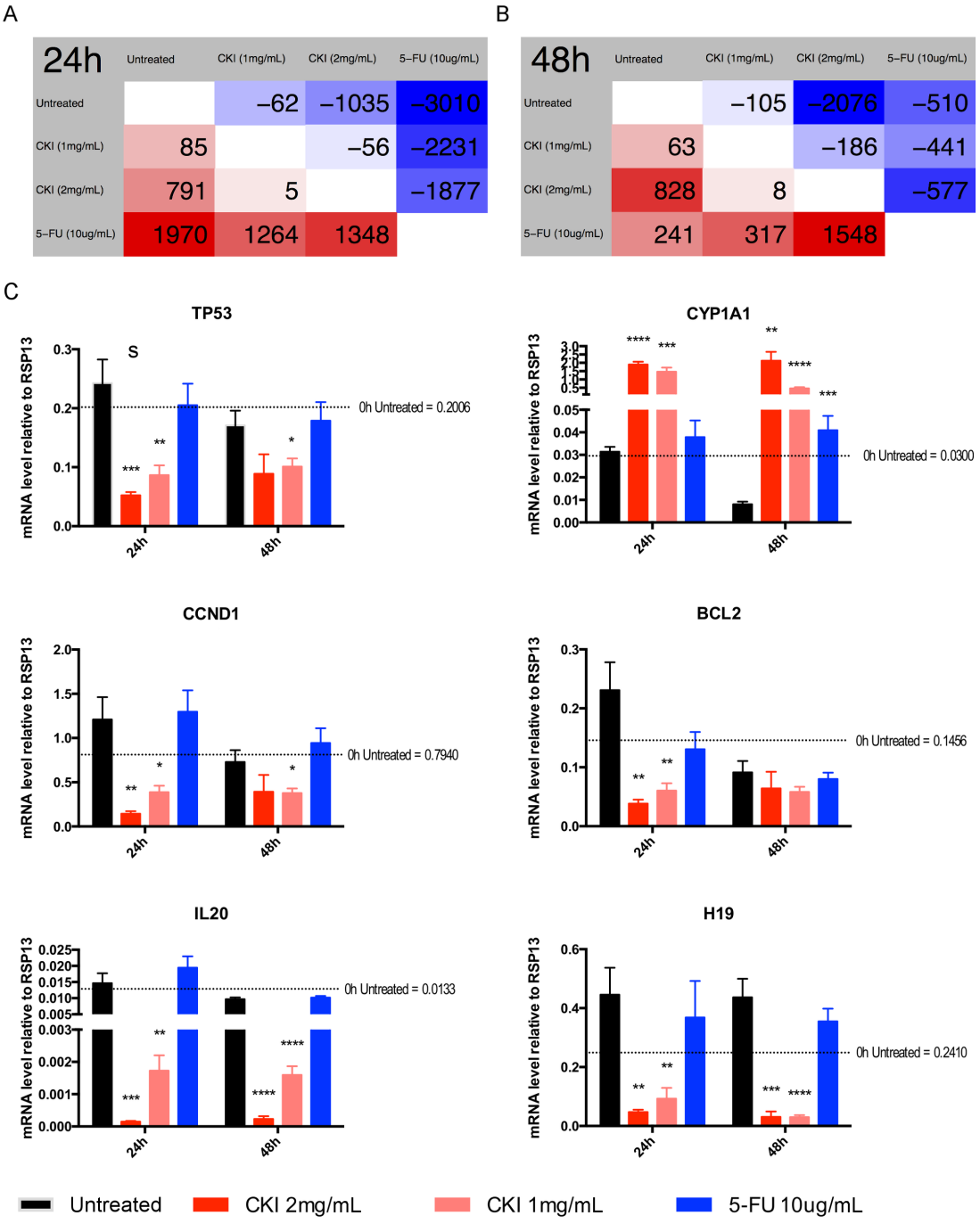

Figure 2: Differential gene expression in MCF-7 cells treated with CKI or 5-FU for 24 and 48 hours. Numbers of DE genes (FDR < 0.05 according to edgeR) between different groups at **A.** 24 hours or **B.** 48 hours time. Comparison is based on row against column. Therefore, cells with a red background show numbers of up-regulated genes and cells with a blue background show numbers of down-regulated genes. **C.** Validation of transcriptome sequencing. Total of 6 DE genes (*TP53*, *CCND1*, *CYP1A1*, *BCL2*, *IL-20* and *H19*) identified by transcriptome sequencing were selected and were subjected to validation analysis by qPCR. Data are represented as mean ±SEM (n=9). Statistical analyses were performed using t-test comparing with "untreated" (*p<0.05, **p<0.01, ***p<0.001, ****p<0.0001).

"Meiotic nuclear division" and "Somatic diversification of immune receptors", were mainly contributed by down-regulated genes, particularly DE genes from 5-FU treated cells. After 48 hours, the same over-represented GO terms in cells treated with CKI or 5-FU for 24 hours were found, but the proportions of DE genes from cells treated with CKI were increased for most of these terms, particularly for "Chromosome segregation" related terms. In addition, more significantly over-represented GO terms were found in cells treated with CKI or 5-FU for 48 hours compared to those in 24 hours, such as "Regulation of viral process" and "Negative regulation of intracellular transport", and the majority of DE genes that contributed to these terms were down-regulated in cells treated with CKI.

In order to further characterise the potential functional pathways altered by CKI, we performed over-representation analysis of Kyoto Encyclopedia of Genes and Genomes (KEGG) pathways for all DE genes in cells treated with high dose CKI. Metabolic pathways represented by "Steroid hormone biosynthesis", and including "Pentose and glucuronate interconversions" and "Drug metabolism" and so on, were over-represented based on DE genes in cells treated with CKI for 24 hours (Figure 4A). The majority of DE genes that contributed to these terms were up-regulated (Figure 4A). Over-represented cell growth related pathways, such as "Cell cycle" and "DNA replication", were also observed (Figure 4A). In addition, cancer-related pathways, such as "Prostate cancer", "Bladder cancer" and "MicroRNA in cancer", were also shown as over-represented pathways. It is also interesting to note that DE genes that contributed to cell growth and cancer related pathways were generally

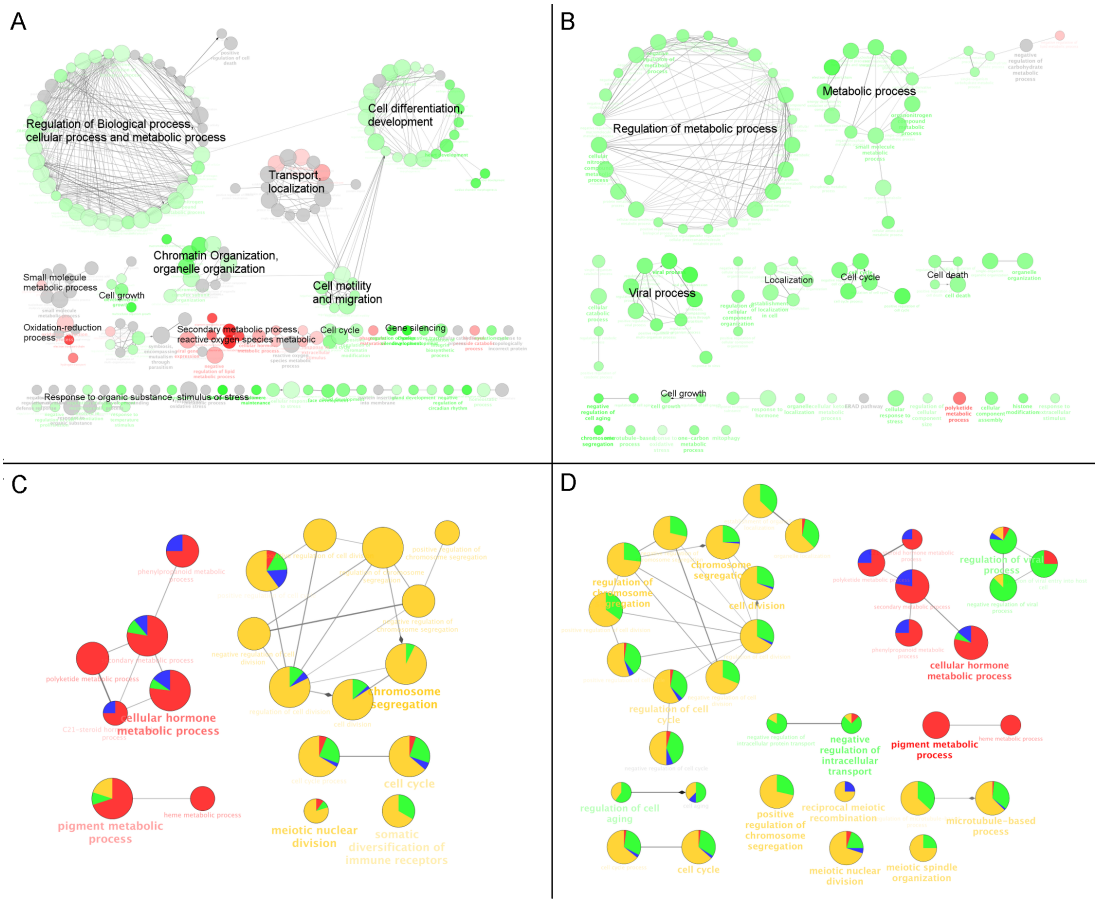

Figure 3: GO functional annotation of DE genes in CKI treated cells. *Over-represented GO terms (Biological Process at 3rd level) for DE genes identified from comparison of CKI treated cells against untreated cells for* **A.** *24 hours or* **B.** *48 hours.* Red coloured nodes mean more than 60% of DE genes that contributed to a term were up-regulated and green coloured nodes mean more than 60% of DE genes that contributed to a term were down-regulated. The colour gradient represents the proportion of up- or down- regulated genes between these cut offs, and the node size is proportional to the significance of over-representation. Terms with similar functional classifications are connected with edges and the most significant term in each cluster is shown in bold. *Comparison of over-represented GO terms for the top 200 significant DE genes in cells treated with 2 mg/mL CKI or 5-FU for* **C.** *24 hours or* **D.** *48 hours.* Four different colours were used to represent the proportion of DE genes from up- or down- regulated genes. For CKI (red = up-regulated and green = down-regulated) or 5-FU (blue = up-regulated and yellow = down-regulated). Node size is proportional to the significance of over-representation and terms with similar functional classifications are connected with edges and the most significant term in each cluster is shown in bold.

down-regulated in cells treated with CKI (Figure 4A). After cells were treated with CKI for 48 hours, most of the over-represented pathways found at 24 hours were still shown as significantly over-represented. However, some over-represented metabolic pathways and disease-related pathways at 48 hours were not shown as significantly over-represented pathways in cells treated with CKI for 24 hours. These pathways included "Arginine and proline metabolism", "Pyrimidine metabolism", "Fructose and mannose metabolism", "Parkinson's disease" and "Alzheimer's disease". In contrast to over-represented metabolic or disease related pathways in cells treated with CKI for 24 hours, these 48-hours-only significant over-represented metabolic or disease pathways were mostly a function of down-regulated DE genes (Figure 4B). Next, we compared the over-represented KEGG pathways based on the top 200 significantly DE genes in cells treated with CKI or 5-FU. Consistent with the results in Figure 4A and 4B, metabolic related pathways were primarily contributed by CKI up-regulated genes. Cell growth and cancer related pathways were also over-represented, and were mostly contributed by down-regulated genes in cells treated with CKI or 5-FU (Figure 4C and 4D). More significantly over-represented cancer-related pathways were found in cells treated with CKI or 5-FU after 48 hours, and DE genes in these pathways were mainly down-regulated (Figure 4D).

Many pathways perturbed by CKI in MCF-7 cells were inhibited

From the above gene set enrichment analysis, we observed that many over-represented GO terms or KEGG

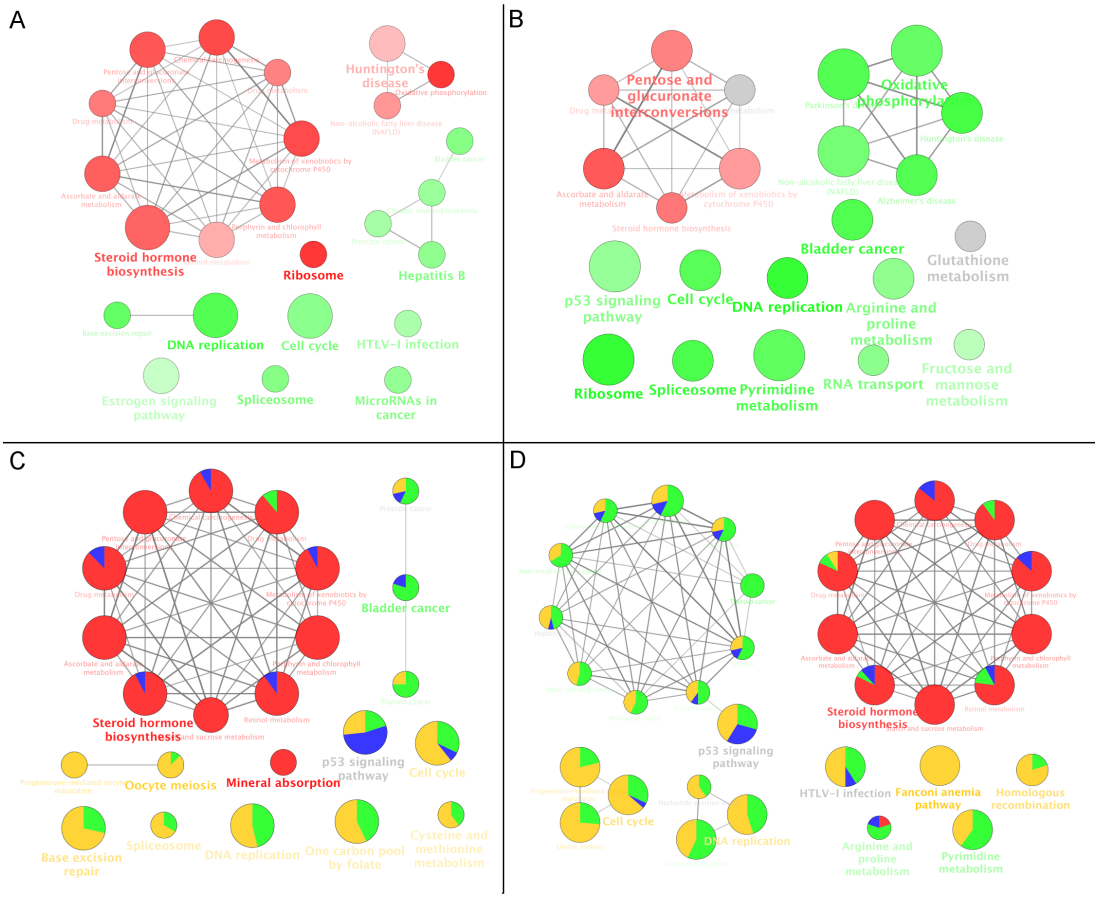

Figure 4: KEGG functional annotation of DE genes in cells treated with CKI. *Over-represented KEGG pathways for all DE genes identified from comparison of CKI treated cells with untreated cells for* **A.** *24 hours or* **B.** *48 hours.* Red coloured nodes mean that more than 60% of DE genes that contributed to this pathway were up-regulated and green coloured nodes mean that more than 60% of DE genes that contributed to this pathway were down-regulated. The colour gradient represents the proportion of up- or down- regulated genes between these two cut offs, and node size is proportional to the significance of over-representation. Pathways with similar functional classifications are connected with edges and the most significant term in each cluster is shown in bold. *Comparison of over-represented KEGG pathways for the top 200 significant DE genes in cells treated with 2 mg/mL CKI or 5-FU for* **C.** *24 hours or* **D.** *48 hours.* Four different colours were used to represent the proportion of DE genes from up- or down- regulated genes. For CKI (red = up-regulated and green = down-regulated) or 5-FU (blue = up-regulated and yellow = down-regulated). Node size represents the significance of over-representation and terms with similar functional classifications are connected with edges and the most significant term in each cluster is shown in bold.

pathways were enriched in down-regulated genes from cells treated with CKI. We used Signalling Pathway Impact Analysis (SPIA) to identify significantly perturbed functional pathways when integrating gene expression information with signalling pathway topology [19]. 21 KEGG pathways were identified as significantly perturbed in cells treated with high dose CKI (2 mg/mL) after 24 hours, and the majority of these pathways (16 out of 21) were shown as inhibited (Supplementary Table 3). In cells treated with 5-FU for 24 hours, more KEGG pathways (75) were identified as significantly perturbed, but only 22 of these were shown as inhibited (Supplementary Table 3). We then compared these significantly perturbed pathways in cells treated with CKI or 5-FU. Interestingly, all significantly altered pathways in cells treated with CKI were also shown as significantly perturbed in cells treated with 5-FU (Figure 5A). This suggests that at 24 hours, CKI and 5-FU perturbed some of the same pathways. However, the perturbation status of these common altered pathways in cells treated with CKI or 5-FU was quite different. The majority of inhibited pathways in cells treated with CKI were shown as activated in cells treated with 5-FU (Figure 5A). Although the perturbation status indicated by SPIA is just suggestive, it still provides some clues that CKI might target different genes even though it might perturb the same pathway as 5-FU. After cells were treated with CKI or 5-FU for 48 hours, 11 significantly perturbed pathways were identified in each of treatment group, but only 3 of these were shown as significantly perturbed pathways in both cells treated with CKI or 5-FU (Figure 5B).

In order to examine the perturbation of CKI on KEGG pathways at the individual gene level, we mapped the expression status of DE genes in cells treated with CKI or 5-FU on the cell growth and death related pathway "Cell cycle" as an example (Figure 6). Consistent with what we observed in the above KEGG over-representation analyses, the majority of DE genes in the "Cell cycle" pathway were down-regulated both in cells treated with CKI or 5-FU. Many essential regulators, such as *Cyclin-dependent kinase 2* (*CDK2*), *Transcription Factor Dp-1* (*DP-1*), *Origin recognition complex* (*ORC*) and *Minichromosome maintenance protein complex* (*MCM*) families, which are important in regulation of the G1/S transition [20, 21], were significantly down-regulated both in cells treated with CKI or 5-FU. However, some key regulators in this "Cell cycle" pathway had different expression status in cells treated with CKI or 5-FU. For example, *CCND1*, which encodes Cyclin-D1 (a member of the CycD protein family), was significantly down-regulated in cells treated with CKI compared with untreated cells. In contrast, *CCND3*, encoding Cyclin-D3 which also belongs to the CycD protein family, was significantly up-regulated in cells treated with 5-FU. Interestingly, as an important pro-apoptosis modulator, the expression of *p53* was opposite in cells treated with CKI (down-regulated) or 5-FU (up-regulated) compared to untreated cells. In addition, the protein levels of p53 were significantly decreased in cells treated with CKI for 24 hours and showed no significant change at 48 hours. In contrast p53 increased in cells treated with 5-FU for both 24 and 48 hours (Figure 6C). Taken together the results of down-regulated p53 mRNA and protein levels (Figure 2C and 6C) but elevated apoptosis activity (Figure 1B) in MCF-7 cells treated with CKI, suggest that CKI may induce cell apoptosis in a p53 independent fashion. In cells treated with CKI or 5-FU for 48 hours, essential genes for G1/S transition (as discussed above) were still shown as significantly down-regulated. In addition, more genes, such as *Cyclin A1* (*CCNA1*, encoding CycA), *Cyclin B1 and B2* (*CCNB1* and *CCNB2*, encoding CycB), *Mitotic Arrest Deficient 1* (*MAD1*, encoding mad1) and *Mitotic Arrest Deficient 2* (*MAD2*, encoding mad2), which are important regulators of G2 or M phase, were shown as significantly down-regulated in cells treated with CKI for 48 hours.

The cell cycle assay using flow cytometry indicated that proportions of cells in G1 and S phases were significantly lower in MCF-7 cells treated with high dose CKI (2 mg/mL), while significantly higher in G2/M phase, indicating a cell cycle arrest at G2/M phase by CKI in MCF-7 cells (Supplementary Figure 5). In summary, possible p53 independent apoptosis together with perturbation of other cancer cell growth associated pathways, such as "Cell cycle", probably contribute the anti-cancer effect of CKI.

The expression of many clinically relevant cancer genes was altered in MCF-7 cells treated with CKI

To investigate the potential molecular targets of CKI in MCF-7 cells, we examined the changes in expression of 135 genes in a curated database of Tumour Alterations Relevant for Genomics-driven Therapy (TARGET) from The Broad Institute (https://www.broadinstitute.org/cancer/cga/target). These genes are directly linked to a clinical outcome when somatically altered in cancer. Many genes showed similar expression changes in cells treated with CKI or 5-FU, and this confirmed what we observed in the pathway analysis (see above) (Figure 7A). However, the expression of some genes was either of a higher degree or in a different direction in cells treated with CKI compared with cells treated with 5-FU. For example, *ETS translocation variant 4* (*ETV4*), whose overexpression is oncogenic in prostate cells [22], was greatly down-regulated in cells treated with CKI compared with cells treated with 5-FU. On the other hand, *Cyclin-Dependent Kinase Inhibitor 1A* (*CDKN1A*, also named as *p21*) was highly up-regulated in 5-FU treated cells but not in CKI treated cells. We then examined how many significantly DE genes in cells treated with CKI or 5-FU were also in this TARGET gene list. In total, 27 DE genes in cells treated with CKI for 24 hours were in the TARGET gene

list, and more up-regulated genes (18 compared to 2) in cells treated with 5-FU for 24 hours were in the TARGET gene list (Figure 7B). In cells treated with CKI or 5-FU for 48 hours, 28 DE genes were in the TARGET list from cells treated with CKI, while only 6 of the DE genes from cells treated with 5-FU for 48 hours were in this list (Figure 7C).

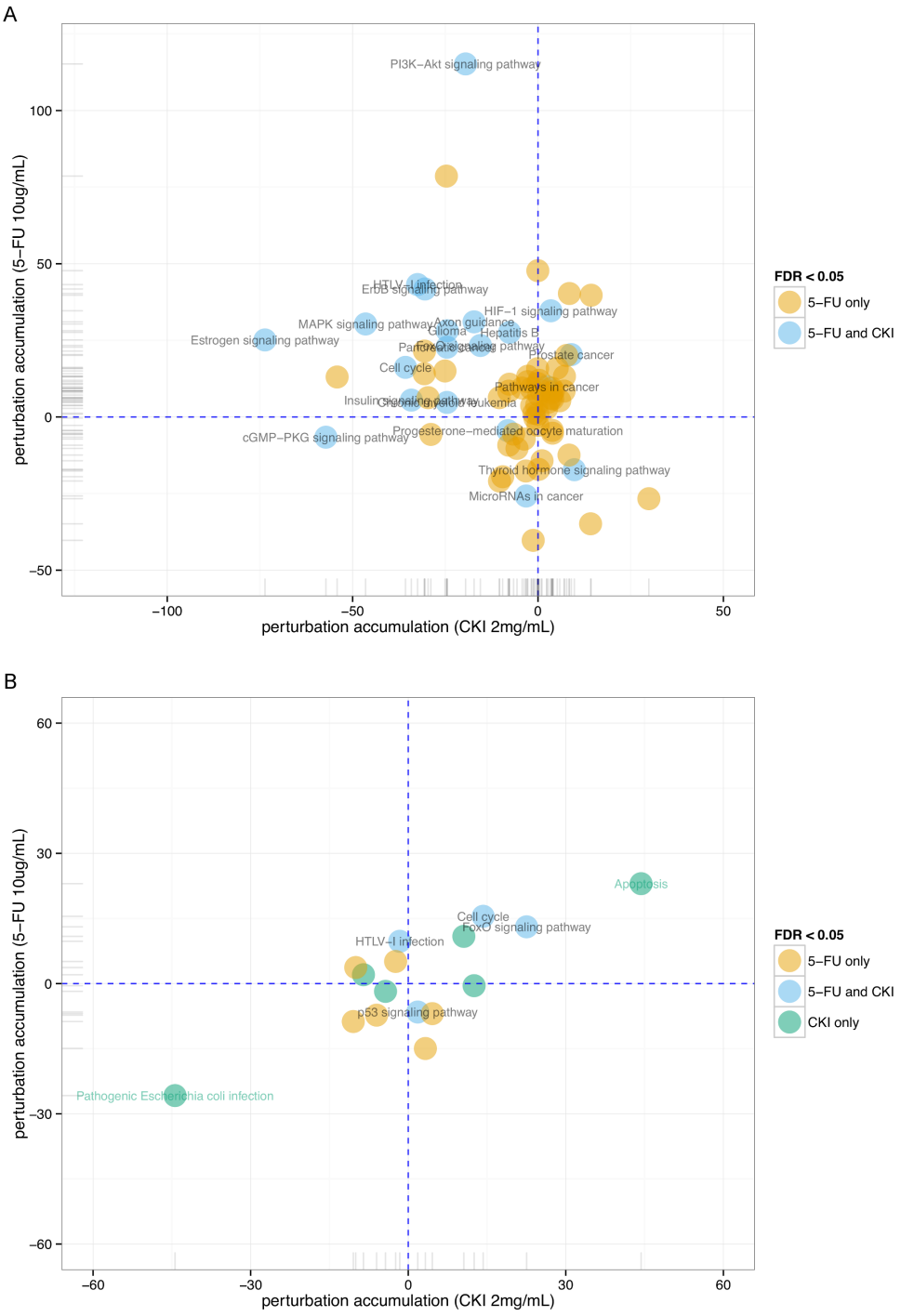

Figure 5: Perturbation of KEGG pathways in cells treated with CKI or 5-FU for A. 24 hours or **B.** 48 hours inferred with SPIA. Perturbation accumulation and significance of perturbation for each KEGG pathway were calculated based on the fold changes of expression of DE genes compared to untreated cells, integrated with the topology information in this pathway. Positive perturbation accumulation values mean this pathway is activated and *vice versa*. "5-FU only" or "CKI only" represent pathways that are only significantly perturbed in one condition not in the other.

Reconstruction of non-coding and protein-coding RNA co-expression networks altered by CKI

The differential expression analysis of refGenes showed that lncRNA, *H19*, was significantly down-regulated after cells were treated with CKI (Figure 2C and Supplementary Table 2). In order to better understand the potential expression change of lncRNAs in response to CKI in MCF-7 cancer cells, we carried out *de novo* identification of lncRNAs from this transcriptome dataset. In total, 2,576 lncRNA transcripts, which are from 2,287 unique genomic loci, were identified (Supplementary Figure 6). We also found that the majority of these lncRNAs were novel by comparing the genomic coordinates of these lncRNAs with two well-annotated human lncRNA datasets (Figure 8A) [23, 24]. The expression of many lncRNAs was changed in cells treated with CKI or 5-FU (Figure 8B). The expression of lncRNAs in cells treated with CKI for 24 hours was quite different compared with cells treated with 5-FU for 24 hours. While at 48 hours, we observed more similar lncRNA expression in cells treated with CKI or 5-FU (Figure 8B). These results indicate that some of these lncRNAs may play specific regulatory roles responding to different reagent treatments.

In order to identify potential lncRNA candidates that were highly relevant to CKI treatment in MCF-7 cells, we reconstructed the co-expression networks for 15,115 detectable refGenes and 2,287 lncRNAs in 9 different samples. 53 co-expression modules were reconstructed based on the expression profiles of refGenes or lncRNAs across 9 samples (Supplementary Figure 7 and Supplementary Table 4). Upon examination of the eigengene expression patterns of these 53 modules, we found three modules with expression profiles that were consistent with CKI-specific modules (Figure 8C and Supplementary Figure 8). Centrality analysis of these

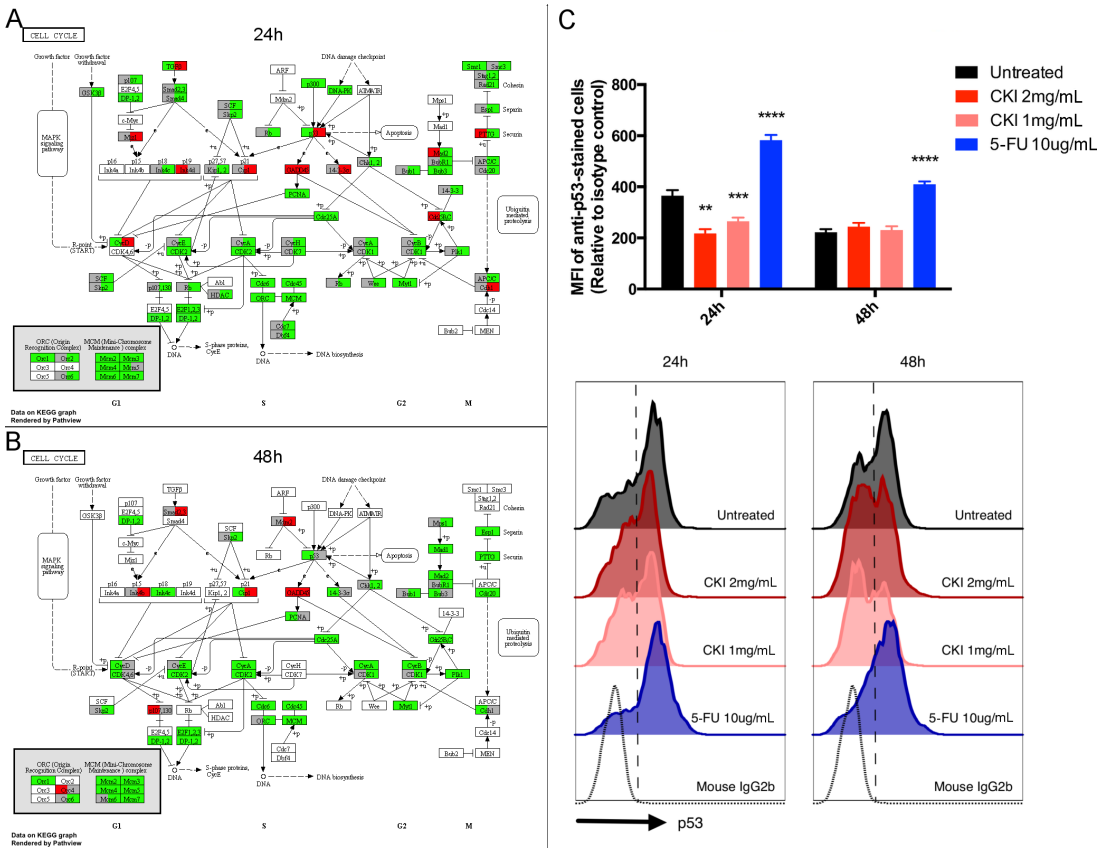

Figure 6: Comparison of individual gene expression change in MCF-7 cells treated with CKI (2 mg/mL) or 5-FU for A. 24 hours or **B.** 48 hours in the cell cycle pathway. Significant DE genes are coloured with red (up-regulated) or green (down-regulated). Each coloured box is separated into two parts, the left half represents the expression change status in cells treated with CKI and the right half represents the expression change status in cells treated with 5-FU. White or grey colours represent gene(s) that are not significantly differentially expressed. **C.** CKI caused down-regulation (24 hours) or no significant change (48 hours) of p53 protein level. The level of p53 protein present in cells treated with CKI was measured by flow cytometry. For the top panel, mean fluorescent intensity (MFI) of cells stained with anti-p53 where MFI of isotype control was subtracted. Data are represented as mean ±SEM (n=9). Statistical analyses were performed using t-test comparing with "untreated" (**p<0.01, ***p<0.001, ****p<0.0001). The bottom panel shows representative histograms of anti-p53 staining.

CKI-specific co-expression modules allowed us to identify "hub" nodes, many of which belonged to lncRNAs (Figure 8D and Supplementary Figure 8). These results showed that lncRNAs may be co-regulated or involved in the same regulatory pathways with protein-coding genes when MCF-7 cells are treated with CKI. We then performed GO and KEGG over-representation analysis for the protein-coding genes in these three CKI-specific modules, and "Cell proliferation" was identified as the most significantly over-represented functional term (Table 1). Interestingly, we also found genes in these CKI-specific co-expression modules are over-represented in functions involved in "intracellular signal cascade" and "second-messenger-mediated signaling" (Table 1), which might be triggered by the multiple molecular species present in CKI. In addition, we also identified three co-expression modules, which showed highly correlated co-expression profiles in both cells treated with CKI or 5-FU. We defined these as "CKI-5FU" modules (Supplementary Figure 9). These modules contained over-represented genes in "cell cycle", "DNA replication" and other cell growth related pathways (Supplementary Table 5). This result was consistent with what we observed in our DE analysis (see above).

DISCUSSION

Many TCMs or other herbal medicines, such as CKI used in this study, are extracted from multiple medicinal herbs. The fact that multiple potentially bioactive ingredients are present in these formulas suggests that they have multiple targets, and therefore perturb multiple biological pathways. Transcriptome analysis using high-throughput next generation sequencing technologies has been widely used in cancer biology for the identification of novel biomarkers, mutations and even novel transcripts, such as lncRNAs, in different cancer types [4, 5, 25, 26]. We have used whole transcriptome analysis to identify potential molecular mechanisms of CKI *in vitro*. We not only identified potential gene targets of CKI based

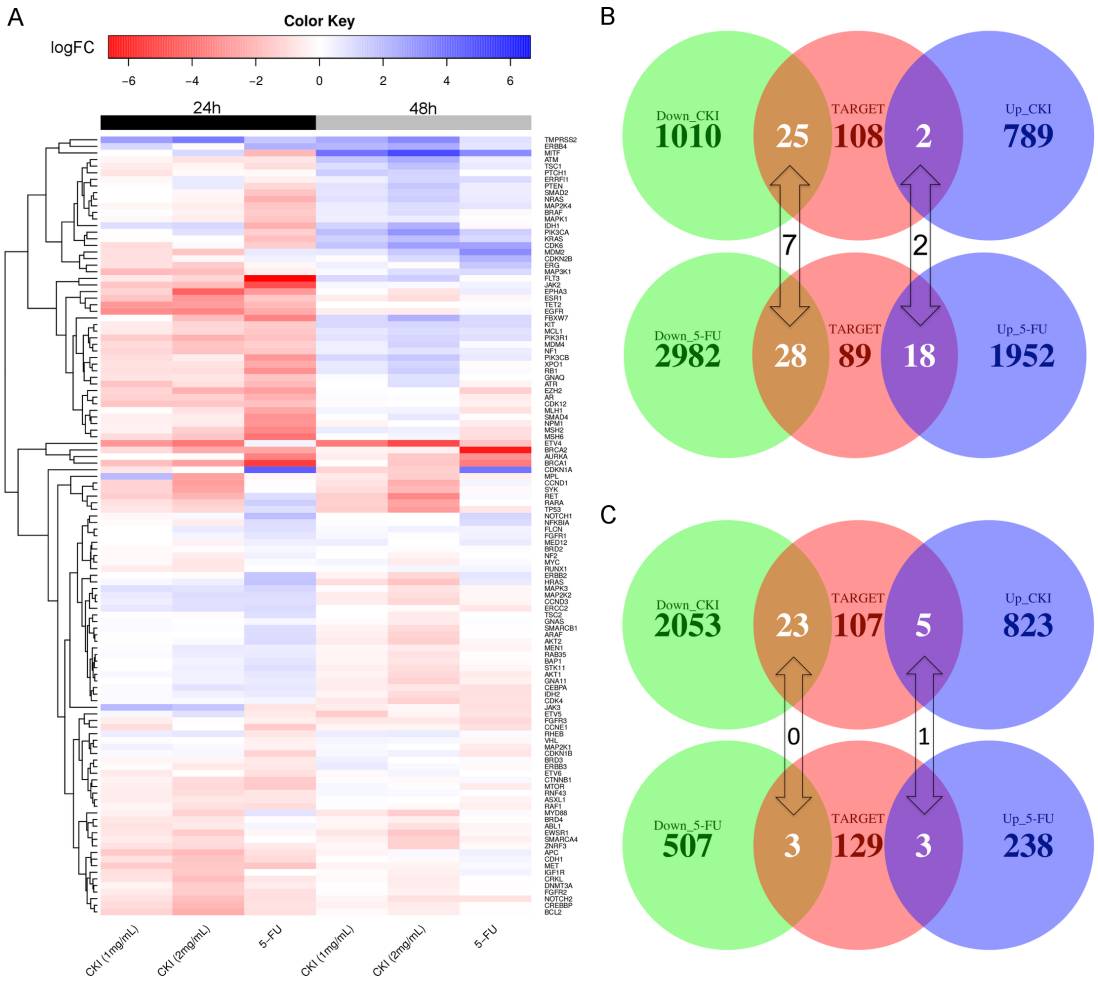

Figure 7: Expression change of clinically relevant cancer genes in cells treated with CKI or 5-FU. A. Heatmap showing the expression fold changes of cancer relevant genes from the TARGET database. Overlap of TARGET genes with DE genes in MCF-7 cells treated with 2 mg/mL CKI or 5-FU for **B.** 24 hours or **C.** 48 hours.

on differential gene expression, but also characterised potential biological pathways targeted by CKI. Although further experiments are required to validate these candidate targets, our results provide a very important starting point for subsequent experimental functional validation.

We have identified genes whose expression was significantly altered in MCF-7 cells treated with CKI. Consistent with the phenotypic analyses, the global gene expression changes in cells treated with CKI support a dose-dependent effect on MCF-7 cells, which had been

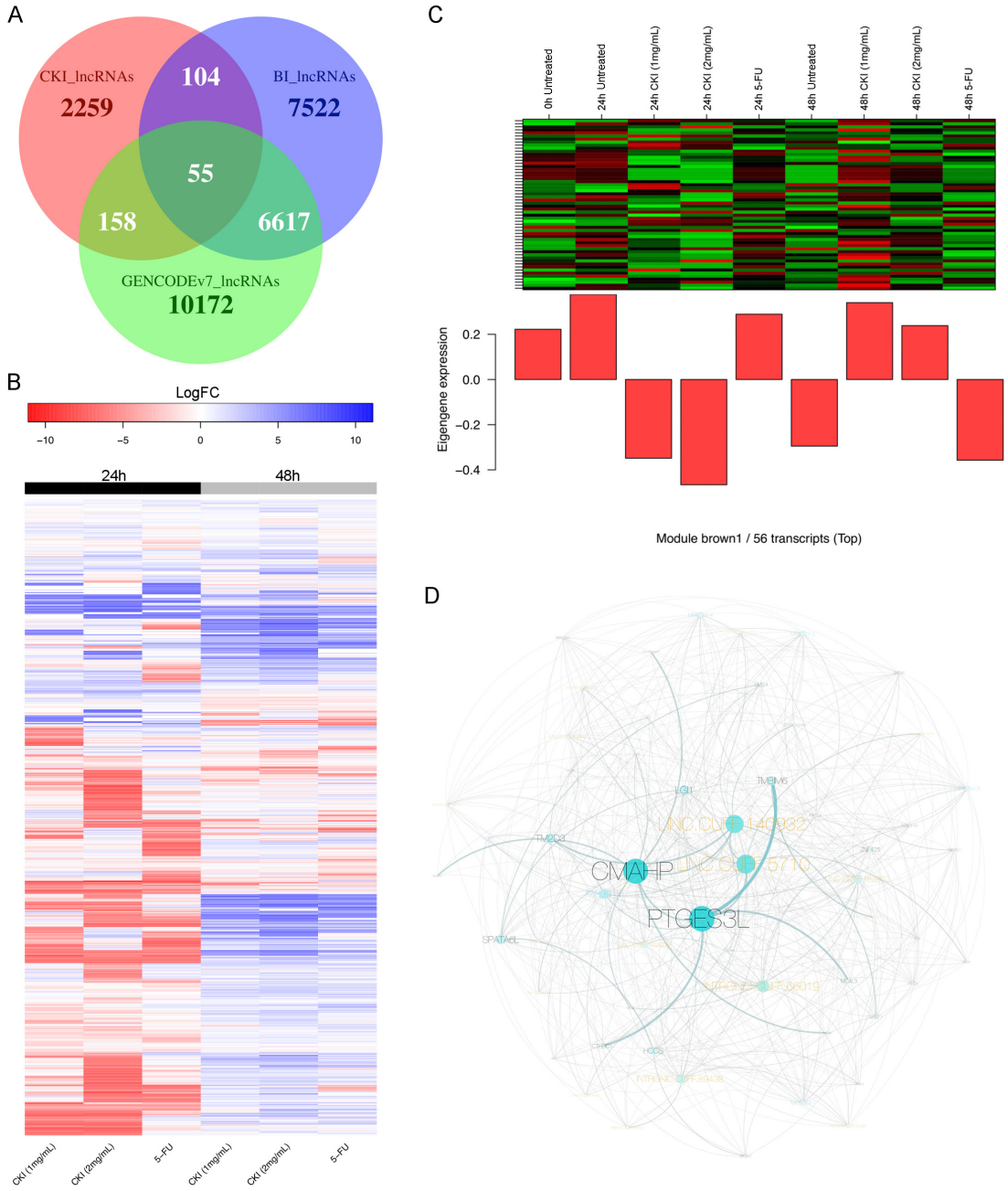

Figure 8: Expression change of *de novo* identified lncRNAs and an example of a CKI-specific co-expression module. **A.** Overlap of *de novo* identified lncRNAs (CKI_lncRNAs) with two annotated human lncRNA datasets: "BI_lncRNAs" as annotated lncRNAs from the Broad Institute and "GENCODEv7_lncRNAs" as lncRNAs from GENCODE version7. **B.** Heatmap showing expression fold change of 2,287 lncRNAs in 6 treated cell samples compared to corresponding untreated cells. **C.** Expression pattern of transcripts in CKI-specific module "brown1" is shown in top panel, and barplot in bottom panel shows the eigengene values in different samples. Green represents "under-expressed" and red represents "over-expressed" in the heatmap. The "eigengene value" is defined as the first principal component of this module, so it can be considered as a representative of the gene expression profiles in this module. **D.** Visualization of CKI-specific co-expression module "brown1". The black labels represent refGenes and gold labels represent lncRNAs. The size of the node/label and edge weight are proportional to between-ness betweeness centrality.

Table 1: Significantly over-represented GO and KEGG terms in protein-coding genes from three CKI-specific co-expression modules (count >4 and P-value < 0.05)

Category	Term	Count	Fold enrichment	P-value
GOTERM_BP_FAT	GO:0008283~cell proliferation	8	3.354	0.009
GOTERM_BP_FAT	GO:0010604~positive regulation of macromolecule metabolic process	11	2.346	0.016
GOTERM_BP_FAT	GO:0032989~cellular component morphogenesis	7	3.223	0.020
GOTERM_BP_FAT	GO:0048514~blood vessel morphogenesis	5	4.332	0.027
GOTERM_BP_FAT	GO:0035295~tube development	5	4.155	0.031
GOTERM_BP_FAT	GO:0007242~intracellular signaling cascade	13	1.892	0.036
GOTERM_BP_FAT	GO:0019932~second-messenger-mediated signaling	5	3.890	0.038
GOTERM_BP_FAT	GO:0000904~cell morphogenesis involved in differentiation	5	3.746	0.043
GOTERM_BP_FAT	GO:0000902~cell morphogenesis	6	3.081	0.043
GOTERM_BP_FAT	GO:0001568~blood vessel development	5	3.731	0.043
GOTERM_BP_FAT	GO:0001944~vasculature development	5	3.642	0.047
KEGG_PATHWAY	hsa05200:Pathways in cancer	7	3.391	0.013
KEGG_PATHWAY	hsa04020:Calcium signaling pathway	5	4.514	0.021

reported in MCF-7 stem cells and other types of cancer cells in previous studies [10, 11]. However, we have generated a far more comprehensive candidate gene list by considering CKI as a whole rather than looking at the effect of individual constituents. As expected, genes, including *Cytochrome P450 family 1* (*CYP1A1*), *Aldo-Keto Reductase Family 1*, *Member C2* (*AKR1C2*) and *Member C3* (*AKR1C3*), which are involved in xenobiotic compound metabolism, were significantly up-regulated when cells were treated with CKI [27, 28] but not with 5-FU. On the other hand, many genes involved in cell growth or used as biomarkers of carcinogenesis, such as *CCND1* [29], were significantly down-regulated. Interestingly, we observed one lncRNA *H19*, known to be over-expressed in several types of cancer [30, 31], was dramatically down-regulated in cells treated with CKI. Recently, many lncRNAs have been characterised as important gene regulators in various types or stages of carcinogenesis [32]. We hypothesise that lncRNAs may be also involved in the gene regulatory networks altered by CKI in MCF-7 cells. Whether lncRNAs are primary targets or secondary links to regulated pathway, still requires further study. Compared to traditional single-gene analyses used to understand the molecular mechanisms of TCM, transcriptome screening has significant advantages for identifying potential target genes.

Carcinogenesis is a complex cellular process involving multiple genetic alterations that perturb different biological processes or pathways [33]. By screening transcriptome-wide gene expression changes *in vitro*, one can do more than the mere identification of molecular markers for cancer diagnosis or therapy, one can also provide useful evidence to better characterise the underlying mechanisms of drug effects on cancer at pathway or network levels [34, 35]. Using whole transcriptome analysis, we identified multiple potential molecular pathways altered by CKI in MCF-7 cells. Cell growth related pathways, such as cell cycle, cell division, DNA replication and so on, were significantly altered in MCF-7 cells treated with CKI. By integrating the expression data and topologic information of genes involved in these pathways, it appears that cell cycle arrest might be one of the primary anti-tumour mechanisms of CKI in MCF-7 cells. As expected, 5-FU also significantly altered these cell growth related pathways, as reported in previous studies [36, 37]. However, when we consider the expression change of individual genes in these pathways, we found that many different genes were significantly altered by CKI or 5-FU, but the overall perturbation status of these pathways was consistent. We also noticed that CKI and 5-FU had opposite effects on some pathways, such as the p53 signalling pathway. Although the expression of the key *p53* gene in the p53 signalling pathway was significantly down-regulated in cells treated with CKI, we still observed changes in the expression of down-stream genes in the apoptosis pathway, such as *Bcl-2*. *Bcl-2* is an important anti-apoptotic gene [38], which was significantly down-regulated in CKI treated cells,

indicating that MCF-7 cells still underwent apoptosis when treated with CKI. The down-regulation of *Bcl-2* had been reported in other types of cancer cells treated with Matrine or Oxymatrine, two of the major components of CKI [16, 39–41]. Taking into account the results from the apoptosis assay, we propose that CKI may induce MCF-7 cell apoptosis via p53 independent pathways. As CKI is normally clinically used in combination with other cancer chemotherapies, our results also provide primary molecular evidence for this potential simultaneous effect in clinical usage [11].

Advances in omics technologies have allowed the development of new cancer therapies [42]. Improved gene therapies, such as targeted cancer therapies or precision medicine, are attracting more and more attention as a result of improved abilities to characterise cancer mechanisms in individual patients [42, 43]. On the other hand, therapies involving whole body system modulation, such as immunotherapy [44] and multiply-targeted therapies [45], are also proposed as potentially effective or complementary weapons for cancer treatment [46]. The nature of many TCMs or ancient medicines that include multiple bioactive ingredients, suggests that they can be a rich resource for identifying or developing multi-targeted cancer drugs [47]. However, most TCMs or ancient medicines are experience-based medicines developed from a long history of clinical use and little is known of their molecular modes of action. Classical pharmacology has used a reductionist strategy of purification and testing of single components from TCM, but this limits our understanding of the potential interaction or cumulative effects of multiple components on a functional system. The application of systems biology techniques, such as whole transcriptome analyses, is a good starting point to understand the functional system effects of TCMs, as a basis for further improvement and optimisation of existing TCMs in the context of evidence based medicine.

Studies have confirmed that many lncRNAs play important regulatory roles in cancer [32]. Our *de novo* identification of lncRNAs showed that some of these may contribute to regulatory networks, and even be specifically or differentially expressed in MCF-7 cancer cells treated by CKI. By integrating lncRNAs with protein-coding RNAs to reconstruct co-expression networks, we showed that this can be used as another powerful tool to understand global transcription changes potentially sensitive to TCM. We were able to confirm that "Cell cycle" and other cell growth related pathways might be the primary target pathways of CKI in MCF-7 cell line as shown in DE analysis, but were able to do this in a more general sense, because we included all expression detectable transcripts during the reconstruction of co-expression networks. In addition, we also showed co-expression networks may be useful in identifying potential co-expressed "hub" transcripts, including both protein-coding RNAs and lncRNAs, for further functional experiments [48]. In conclusion, we applied and integrated multiple transcriptome analysis tools to describe and analyse the complexity of molecular mechanisms altered by CKI in MCF-7 breast cancer cells, and we hope that this can be useful to harness the "magic power" of TCM.

MATERIALS AND METHODS

Cell culture and drugs

MCF-7 cells were purchased from ATCC (HTB-22™, VA, USA) and were cultured in DMEM medium (Thermo Fisher Scientific, MA, USA) supplemented with 10% fetal bovine serum (Thermo Fisher Scientific) and 0.01 mg/mL human recombinant insulin (Thermo Fisher Scientific) at 37°C with 5% CO_2. CKI (total alkaloids concentration of 20.8 mg/mL) was obtained from ZhenDong pharmaceutical Co.Ltd (Shanxi, China), and 5-FU was ordered from Sigma-Aldrich (MO, USA). For all *in vitro* experiments performed in this study, CKI was used at dilution of final concentration of either 1 mg/mL or 2 mg/mL of total alkaloids, and 5-FU was used at a final concentration of 10 ug/mL.

For cell culture in 6-well trays used for cell apoptosis assay, cell cycle assay, p53 protein staining assay and RNA extraction, each well was seeded with 5×10^5 cells in 2 mL of medium and cultured overnight. On the following day, 1 mL of either medium, CKI or 5-FU was added to the cells. After 24 and 48 hours of treatment, cells were harvested and used in the above assays.

Cell viability assay

The wells of 96-well trays were seeded with 1×10^4 cells in 50 µL of medium and cultured overnight. On the following day, 50 µL of either medium, CKI or 5-FU were added to the cells. Viability of the cells was measured at 0, 24 and 48 hours after the treatment by adding XTT:PMS (50:1; Sigma-Aldrich). After 4-hour incubation at 37°C optical density (OD) of each well was read at 490 nm. The background OD was also measured and the average was subtracted from the OD readings of appropriate wells.

Apoptosis assay by annexin V/PI staining

Cells were cultured in 6-well trays and treated with drugs as described above. After 24 and 48 hours of treatment, cells were harvested and the rate of apoptosis was measured using Annexin V-FITC detecton kit (Biotool, TX, USA) according to the manufacturer's instructions. The stained cells were sorted and data acquired on an LSRII (BD Biosciences, NJ, USA) and the data were analysed using FlowJo software (TreeStar Inc., OR, USA).

Caspase 3/7 colorimetric assay

Caspase 3/7 activity in cells was measured with a Caspase-3/7 Colorimetric Assay Kit (BioVision, CA, USA). Cells were cultured in 6-well trays and treated with drugs as described above. After 24 and 48 hours of treatment, cells were harvested and proteins from cells were extracted according to the manufacturer's instructions and concentrations were determined with a Nanodrop 2000 (Thermo Scientific). Caspase-3/7 activity was then measured according to the manufacturer's instructions.

Cell cycle assay

Cells were cultured in 6-well trays and treated with drugs as described above. After 24 and 48 hours of treatment, cells were harvested and subjected to cell cycle analysis by PI staining as described previously [49] and the stained cells were sorted and the data acquired on LSRII and the data were analysed using FlowJo software.

Intranuclear/intracellular staining for p53

Cells were cultured in 6-well trays and treated with drugs as described above. After 24 and 48 hours of treatment, cells were fixed and permeabilised using Nuclear Factor Fixation and Permeabilization Buffer Set (Biolegend, CA, USA) according to the manufacturer's instructions. 2×10^5 cells were labelled either with anti-p53-PE or mouse IgG2b-PE (1 μg/mL; Biolegend) and the cells were sorted and the data were acquired on an LSRII, and the data were analysed using FlowJo software.

RNA extraction and sequencing

Cells were cultured in 6-well plates with a seeding density of 5×10^5 cells/well and treated with CKI or 5-FU for 24 and 48 hours as above. Total RNA was isolated with the mirVana PARIS Kit (Thermo Fisher Scientific) according to the manufacturer's protocol. RNA samples were sent to the Cancer Genome Facility of the Australian Cancer Research Foundation (SA, Australia) for sequencing. The quality of the total RNA was verified on a Bioanalyzer ensuring all samples had RINs >7.0. Starting with 1 ug of total RNA, the polyA fraction was enriched using a NEBNext(r) Poly(A) mRNA Magnetic Isolation Module. Stranded mRNA libraries for Illumina sequencing were prepared using the NEBNext(r) Ultra Directional RNA kits from New England Biolabs, Inc. according to the manufacturer's protocol (Version 2.0 July 2013). Actinomycin D was added during cDNA synthesis to ensure high levels of strand specificity. All libraries were run on a Bionanalyzer to confirm library size and yield. Barcoded libraries were normalized and pooled based on concentrations determined by qPCR with Library Quantification kits from KAPA Biosystems. Libraries were sequenced using an Illumina HiSeq 2500 across 5 lanes with stranded paired-end 100 base pair reads. Raw and processed data were deposited at the Gene Expression Omnibus (GEO) data repository (GSE78512).

Data processing and functional annotation

Low quality and adaptor sequences in raw reads were trimmed using Trim_galore (v0.3.7, Babraham Bioinformatics) with the following parameters: --stringency 6 --paired. Then cleaned reads were aligned to the reference genome (hg19, UCSC) using STAR_2.4.0j with the following parameters: --outSAMstrandField intronMotif --outSAMattributes All --outFilterMismatchNmax 10 --seedSearchStartLmax 30 [50]. Differential expression analysis was performed with edgeR and DE genes were selected with a False Discovery Rate (FDR) < 0.05 [51].

GO and KEGG over-representation analyses were performed using ClueGO with the following settings: biological process at 3rd level (for GO); right-sided hypergeometric test for enrichment analysis; p values were corrected for multiple testing according to the Benjamini-Hochberg method. Over-represented terms/pathways were visualised with Cytoscape v3.2.1 [52, 53]. Signalling Pathway Impact Analysis (SPIA) was performed with SPIA package in R [19]. Gene expression status mapping in KEGG pathways was visualised with the R Pathview package [54].

Transcriptome validation with qPCR

Cells were cultured in 6-well trays and treated with drugs as described above. Untreated cells as well as cells treated for 24 and 48 hours were harvested and the cell pellets were snap-frozen in liquid nitrogen. Total RNA was extracted using PureLink RNA Mini Kit (Thermo Fisher Scientific) and treated with TURBO DNA-Free (Thermo Fisher Scientific) according to the manufacturer's instructions. cDNA synthesis was performed using High Capacity cDNA Reverse Transcription Kit (Thermo Fisher Scientific) according to the manufacturer's instructions.

qPCR reactions were set up with PowerUp SYBR Green Master Mix where forward and reverse primers were added at a final concentration of 400 nM each. Reactions were run on the StepOne Plus Real-Time PCR system and the data were analysed using its software v2.3 (Thermo Fisher Scientific). Relative levels of target mRNAs were calculated as $1/2^{\Delta CT}$, where ΔCT=CT of target − CT of *RSP13*. The sequences of all primers used in this study are provided in Supplementary Table 6.

LncRNA identification

The flowchart for lncRNA identification is shown in Supplementary Figure 6. In summary, short reads were mapped against the genome and assembled into

longer transcripts, and then transcripts shorter than 200 nucleotides (nt) were removed. Genomic coordinates of long transcripts were checked against refGenes from UCSC and classified into "refGene transcripts", "intergenic transcripts", "intronic transcripts" and "antisense transcripts". The latter three classes of transcripts were selected to filter unannotated protein-coding potential transcripts by following two steps: 1) Sequence similarity search against the Swiss-Prot protein database; 2) Predict Open Reading Frame(s) (ORF). In order to get a more reliable lncRNA dataset, we selected transcripts with expression higher than 1 count per million (CPM, normalised using the TMM method in edgeR) in at least 2 of 27 individual samples.

Reconstruction of co-expression networks

RefGenes were pre-filtered by expression (> 1 CPM in at least 2 of 27 individuals). Expression matrices for all pre-filtered refGenes and lncRNAs were merged to reconstruct co-expression networks with WGCNA [55]. "16" was selected as the soft thresholding power according to the protocol of WGCNA. Co-expression modules were visualized with Cytoscape v3.2.1. Betweenness centrality was used to select "hub" nodes. GO and KEGG over-representation analyses were performed with DAVID (Database For Annotation, Visualization and Integrated Discovery) [56].

ACKNOWLEDGMENTS

The Authors would like to thank Adriana Caon for technical help in cell culture and Seyyed Hani Moussavi Nik for technical help in RNA isolation.

CONFLICTS OF INTEREST

The authors declare no conflicts of interest.

REFERENCES

1. Berger MF, Lawrence MS, Demichelis F, Drier Y, Cibulskis K, Sivachenko AY, Sboner A, Esgueva R, Pflueger D, Sougnez C, Onofrio R, Carter SL, Park K, et al. The genomic complexity of primary human prostate cancer. Nature. 2011; 470: 214-20. doi: 10.1038/nature09744.
2. Pleasance ED, Cheetham RK, Stephens PJ, McBride DJ, Humphray SJ, Greenman CD, Varela I, Lin ML, Ordonez GR, Bignell GR, Ye K, Alipaz J, Bauer MJ, et al. A comprehensive catalogue of somatic mutations from a human cancer genome. Nature. 2010; 463: 191-6. doi: 10.1038/nature08658.
3. Saadatpour A, Lai S, Guo G, Yuan GC. Single-Cell Analysis in Cancer Genomics. Trends Genet. 2015; 31: 576-86. doi: 10.1016/j.tig.2015.07.003.
4. Barrett CL, DeBoever C, Jepsen K, Saenz CC, Carson DA, Frazer KA. Systematic transcriptome analysis reveals tumor-specific isoforms for ovarian cancer diagnosis and therapy. Proc Natl Acad Sci U S A. 2015; 112: E3050-7. doi: 10.1073/pnas.1508057112.
5. White NM, Cabanski CR, Silva-Fisher JM, Dang HX, Govindan R, Maher CA. Transcriptome sequencing reveals altered long intergenic non-coding RNAs in lung cancer. Genome Biol. 2014; 15: 429. doi: 10.1186/s13059-014-0429-8.
6. Prensner JR, Iyer MK, Balbin OA, Dhanasekaran SM, Cao Q, Brenner JC, Laxman B, Asangani IA, Grasso CS, Kominsky HD, Cao X, Jing X, Wang X, et al. Transcriptome sequencing across a prostate cancer cohort identifies PCAT-1, an unannotated lincRNA implicated in disease progression. Nat Biotechnol. 2011; 29: 742-9. doi: 10.1038/nbt.1914.
7. Simon R, Roychowdhury S. Implementing personalized cancer genomics in clinical trials. Nat Rev Drug Discov. 2013; 12: 358-69. doi: 10.1038/nrd3979.
8. Hsiao WL, Liu L. The role of traditional Chinese herbal medicines in cancer therapy--from TCM theory to mechanistic insights. Planta Med. 2010; 76: 1118-31. doi: 10.1055/s-0030-1250186.
9. Sun M, Cao H, Sun L, Dong S, Bian Y, Han J, Zhang L, Ren S, Hu Y, Liu C, Xu L, Liu P. Antitumor activities of Kushen: literature review. Evid Based Complement Alternat Med. 2012; 2012: 373219. doi: 10.1155/2012/373219.
10. Zhao Z, Fan H, Higgins T, Qi J, Haines D, Trivett A, Oppenheim JJ, Wei H, Li J, Lin H, Howard OM. Fufang Kushen injection inhibits sarcoma growth and tumor-induced hyperalgesia via TRPV1 signaling pathways. Cancer Lett. 2014; 355: 232-41. doi: 10.1016/j.canlet.2014.08.037.
11. Xu W, Lin H, Zhang Y, Chen X, Hua B, Hou W, Qi X, Pei Y, Zhu X, Zhao Z, Yang L. Compound Kushen Injection suppresses human breast cancer stem-like cells by down-regulating the canonical Wnt/beta-catenin pathway. J Exp Clin Cancer Res. 2011; 30: 103. doi: 10.1186/1756-9966-30-103.
12. Ma Y, Gao HM, Liu J, Chen LM, Zhang QW, Wang ZM. Identification and Determination of the Chemical Constituents in a Herbal Preparation, Compound Kushen Injection, by Hplc and Lc-Dad-Ms/Ms. Journal of Liquid Chromatography & Related Technologies. 2014; 37: 207-20. doi: 10.1080/10826076.2012.738623.
13. Yu P, Liu Q, Liu K, Yagasaki K, Wu E, Zhang G. Matrine suppresses breast cancer cell proliferation and invasion via VEGF-Akt-NF-kappaB signaling. Cytotechnology. 2009; 59: 219-29. doi: 10.1007/s10616-009-9225-9.
14. Liu T, Song Y, Chen H, Pan S, Sun X. Matrine inhibits proliferation and induces apoptosis of pancreatic cancer cells *in vitro* and *in vivo*. Biol Pharm Bull. 2010; 33: 1740-5.

15. Chen H, Zhang J, Luo J, Lai F, Wang Z, Tong H, Lu D, Bu H, Zhang R, Lin S. Antiangiogenic effects of oxymatrine on pancreatic cancer by inhibition of the NF-kappaB-mediated VEGF signaling pathway. Oncol Rep. 2013; 30: 589-95. doi: 10.3892/or.2013.2529.

16. Ling Q, Xu X, Wei X, Wang W, Zhou B, Wang B, Zheng S. Oxymatrine induces human pancreatic cancer PANC-1 cells apoptosis via regulating expression of Bcl-2 and IAP families, and releasing of cytochrome c. J Exp Clin Cancer Res. 2011; 30: 66. doi: 10.1186/1756-9966-30-66.

17. Zhang Y, Piao B, Zhang Y, Hua B, Hou W, Xu W, Qi X, Zhu X, Pei Y, Lin H. Oxymatrine diminishes the side population and inhibits the expression of beta-catenin in MCF-7 breast cancer cells. Med Oncol. 2011; 28: S99-107. doi: 10.1007/s12032-010-9721-y.

18. Guo YM, Huang YX, Shen HH, Sang XX, Ma X, Zhao YL, Xiao XH. Efficacy of Compound Kushen Injection in Relieving Cancer-Related Pain: A Systematic Review and Meta-Analysis. Evid Based Complement Alternat Med. 2015; 2015: 840742. doi: 10.1155/2015/840742.

19. Tarca AL, Draghici S, Khatri P, Hassan SS, Mittal P, Kim JS, Kim CJ, Kusanovic JP, Romero R. A novel signaling pathway impact analysis. Bioinformatics. 2009; 25: 75-82. doi: 10.1093/bioinformatics/btn577.

20. Bertoli C, Skotheim JM, de Bruin RA. Control of cell cycle transcription during G1 and S phases. Nat Rev Mol Cell Biol. 2013; 14: 518-28. doi: 10.1038/nrm3629.

21. Schaarschmidt D, Ladenburger EM, Keller C, Knippers R. Human Mcm proteins at a replication origin during the G1 to S phase transition. Nucleic Acids Res. 2002; 30: 4176-85.

22. Pellecchia A, Pescucci C, De Lorenzo E, Luceri C, Passaro N, Sica M, Notaro R, De Angioletti M. Overexpression of ETV4 is oncogenic in prostate cells through promotion of both cell proliferation and epithelial to mesenchymal transition. Oncogenesis. 2012; 1: e20. doi: 10.1038/oncsis.2012.20.

23. Cabili MN, Trapnell C, Goff L, Koziol M, Tazon-Vega B, Regev A, Rinn JL. Integrative annotation of human large intergenic noncoding RNAs reveals global properties and specific subclasses. Genes Dev. 2011; 25: 1915-27. doi: 10.1101/gad.17446611.

24. Derrien T, Johnson R, Bussotti G, Tanzer A, Djebali S, Tilgner H, Guernec G, Martin D, Merkel A, Knowles DG, Lagarde J, Veeravalli L, Ruan X, et al. The GENCODE v7 catalog of human long noncoding RNAs: analysis of their gene structure, evolution, and expression. Genome Res. 2012; 22: 1775-89. doi: 10.1101/gr.132159.111.

25. Lin KT, Shann YJ, Chau GY, Hsu CN, Huang CY. Identification of latent biomarkers in hepatocellular carcinoma by ultra-deep whole-transcriptome sequencing. Oncogene. 2014; 33: 4786-94. doi: 10.1038/onc.2013.424.

26. Liu J, Lee W, Jiang Z, Chen Z, Jhunjhunwala S, Haverty PM, Gnad F, Guan Y, Gilbert HN, Stinson J, Klijn C, Guillory J, Bhatt D, et al. Genome and transcriptome sequencing of lung cancers reveal diverse mutational and splicing events. Genome Res. 2012; 22: 2315-27. doi: 10.1101/gr.140988.112.

27. Walsh AA, Szklarz GD, Scott EE. Human cytochrome P450 1A1 structure and utility in understanding drug and xenobiotic metabolism. J Biol Chem. 2013; 288: 12932-43. doi: 10.1074/jbc.M113.452953.

28. Jin Y, Penning TM. Aldo-keto reductases and bioactivation/detoxication. Annu Rev Pharmacol Toxicol. 2007; 47: 263-92. doi: 10.1146/annurev.pharmtox.47.120505.105337.

29. Baldin V, Lukas J, Marcote MJ, Pagano M, Draetta G. Cyclin D1 is a nuclear protein required for cell cycle progression in G1. Genes Dev. 1993; 7: 812-21.

30. Hibi K, Nakamura H, Hirai A, Fujikake Y, Kasai Y, Akiyama S, Ito K, Takagi H. Loss of H19 imprinting in esophageal cancer. Cancer Res. 1996; 56: 480-2.

31. Adriaenssens E, Dumont L, Lottin S, Bolle D, Lepretre A, Delobelle A, Bouali F, Dugimont T, Coll J, Curgy JJ. H19 overexpression in breast adenocarcinoma stromal cells is associated with tumor values and steroid receptor status but independent of p53 and Ki-67 expression. Am J Pathol. 1998; 153: 1597-607. doi: 10.1016/S0002-9440(10)65748-3.

32. Huarte M. The emerging role of lncRNAs in cancer. Nat Med. 2015; 21: 1253-61. doi: 10.1038/nm.3981.

33. Vogelstein B, Papadopoulos N, Velculescu VE, Zhou S, Diaz LA, Jr., Kinzler KW. Cancer genome landscapes. Science. 2013; 339: 1546-58. doi: 10.1126/science.1235122.

34. Klijn C, Durinck S, Stawiski EW, Haverty PM, Jiang Z, Liu H, Degenhardt J, Mayba O, Gnad F, Liu J, Pau G, Reeder J, Cao Y, et al. A comprehensive transcriptional portrait of human cancer cell lines. Nat Biotechnol. 2015; 33: 306-12. doi: 10.1038/nbt.3080.

35. Abaan OD, Polley EC, Davis SR, Zhu YJ, Bilke S, Walker RL, Pineda M, Gindin Y, Jiang Y, Reinhold WC, Holbeck SL, Simon RM, Doroshow JH, et al. The exomes of the NCI-60 panel: a genomic resource for cancer biology and systems pharmacology. Cancer Res. 2013; 73: 4372-82. doi: 10.1158/0008-5472.CAN-12-3342.

36. Yoshikawa R, Kusunoki M, Yanagi H, Noda M, Furuyama JI, Yamamura T, Hashimoto-Tamaoki T. Dual antitumor effects of 5-fluorouracil on the cell cycle in colorectal carcinoma cells: a novel target mechanism concept for pharmacokinetic modulating chemotherapy. Cancer Res. 2001; 61: 1029-37.

37. Hernandez-Vargas H, Ballestar E, Carmona-Saez P, von Kobbe C, Banon-Rodriguez I, Esteller M, Moreno-Bueno G, Palacios J. Transcriptional profiling of MCF7 breast cancer cells in response to 5-Fluorouracil: relationship with cell cycle changes and apoptosis, and identification of novel targets of p53. Int J Cancer. 2006; 119: 1164-75. doi: 10.1002/ijc.21938.

38. Czabotar PE, Lessene G, Strasser A, Adams JM. Control of apoptosis by the BCL-2 protein family: implications for

physiology and therapy. Nat Rev Mol Cell Biol. 2014; 15: 49-63. doi: 10.1038/nrm3722.

39. Chang C, Liu SP, Fang CH, He RS, Wang Z, Zhu YQ, Jiang SW. Effects of matrine on the proliferation of HT29 human colon cancer cells and its antitumor mechanism. Oncol Lett. 2013; 6: 699-704. doi: 10.3892/ol.2013.1449.
40. Zhang Y, Zhang H, Yu P, Liu Q, Liu K, Duan H, Luan G, Yagasaki K, Zhang G. Effects of matrine against the growth of human lung cancer and hepatoma cells as well as lung cancer cell migration. Cytotechnology. 2009; 59: 191-200. doi: 10.1007/s10616-009-9211-2.
41. Liu J, Yao Y, Ding H, Chen R. Oxymatrine triggers apoptosis by regulating Bcl-2 family proteins and activating caspase-3/caspase-9 pathway in human leukemia HL-60 cells. Tumour Biol. 2014; 35: 5409-15. doi: 10.1007/s13277-014-1705-7.
42. Al-Lazikani B, Banerji U, Workman P. Combinatorial drug therapy for cancer in the post-genomic era. Nat Biotechnol. 2012; 30: 679-92. doi: 10.1038/nbt.2284.
43. Garman KS, Nevins JR, Potti A. Genomic strategies for personalized cancer therapy. Hum Mol Genet. 2007; 16: R226-32. doi: 10.1093/hmg/ddm184.
44. Mahoney KM, Rennert PD, Freeman GJ. Combination cancer immunotherapy and new immunomodulatory targets. Nat Rev Drug Discov. 2015; 14: 561-84. doi: 10.1038/nrd4591.
45. Petrelli A, Giordano S. From single- to multi-target drugs in cancer therapy: when aspecificity becomes an advantage. Curr Med Chem. 2008; 15: 422-32.
46. Vanneman M, Dranoff G. Combining immunotherapy and targeted therapies in cancer treatment. Nat Rev Cancer. 2012; 12: 237-51. doi: 10.1038/nrc3237.
47. Wang Y, Fan X, Qu H, Gao X, Cheng Y. Strategies and techniques for multi-component drug design from medicinal herbs and traditional Chinese medicine. Curr Top Med Chem. 2012; 12: 1356-62.
48. Yang Y, Han L, Yuan Y, Li J, Hei N, Liang H. Gene co-expression network analysis reveals common system-level properties of prognostic genes across cancer types. Nat Commun. 2014; 5: 3231. doi: 10.1038/ncomms4231.
49. Riccardi C, Nicoletti I. Analysis of apoptosis by propidium iodide staining and flow cytometry. Nat Protoc. 2006; 1: 1458-61. doi: 10.1038/nprot.2006.238.
50. Dobin A, Davis CA, Schlesinger F, Drenkow J, Zaleski C, Jha S, Batut P, Chaisson M, Gingeras TR. STAR: ultrafast universal RNA-seq aligner. Bioinformatics. 2013; 29: 15-21. doi: 10.1093/bioinformatics/bts635.
51. Robinson MD, McCarthy DJ, Smyth GK. edgeR: a Bioconductor package for differential expression analysis of digital gene expression data. Bioinformatics. 2010; 26: 139-40. doi: 10.1093/bioinformatics/btp616.
52. Bindea G, Mlecnik B, Hackl H, Charoentong P, Tosolini M, Kirilovsky A, Fridman WH, Pages F, Trajanoski Z, Galon J. ClueGO: a Cytoscape plug-in to decipher functionally grouped gene ontology and pathway annotation networks. Bioinformatics. 2009; 25: 1091-3. doi: 10.1093/bioinformatics/btp101.
53. Shannon P, Markiel A, Ozier O, Baliga NS, Wang JT, Ramage D, Amin N, Schwikowski B, Ideker T. Cytoscape: a software environment for integrated models of biomolecular interaction networks. Genome Res. 2003; 13: 2498-504. doi: 10.1101/gr.1239303.
54. Luo W, Brouwer C. Pathview: an R/Bioconductor package for pathway-based data integration and visualization. Bioinformatics. 2013; 29: 1830-1. doi: 10.1093/bioinformatics/btt285.
55. Langfelder P, Horvath S. WGCNA: an R package for weighted correlation network analysis. BMC Bioinformatics. 2008; 9: 559. doi: 10.1186/1471-2105-9-559.
56. Huang da W, Sherman BT, Lempicki RA. Systematic and integrative analysis of large gene lists using DAVID bioinformatics resources. Nat Protoc. 2009; 4: 44-57. doi: 10.1038/nprot.2008.211.

Chapter 5

The Effect of Compound Kushen Injection on Cancer Cells: Integrated Identification of Candidate Molecular Mechanisms

In this chapter, the transcriptome analysis of two cell lines including MDA-MB-231 and HEPG2 were combined with the previous data from MCF-7 to compare the core and unique set of genes with respect to the responses to CKI treatment. A set of 363 core genes associated with cell cycle, energy metabolism, DNA replication/repair, and various cancer pathways were identified. This chapter is in the format of a manuscript that has been submitted to *Phytomedicine*.

Statement of Authorship

Title of Paper	The effect of Compound Kushen Injection on Cancer Cells: Integrated Identification of Candidate Molecular Mechanisms
Publication Status	☐ Published ☐ Accepted for Publication ☑ Submitted for Publication ☐ Unpublished and Unsubmitted w ork w ritten in manuscript style
Publication Details	

Principal Author

Name of Principal Author (Candidate)	Thazin Nwe Aung
Contribution to the Paper	Assisted with experiments
Overall percentage (%)	20%
Certification:	This paper reports on original research I conducted during the period of my Higher Degree by Research candidature and is not subject to any obligations or contractual agreements with a ird party that would constrain its inclusion in this thesis. I am the primary author of this paper.
Signature	Date 5/11/2018

Co-Author Contributions

By signing the Statement of Authorship, each author certifies that:

i. the candidate's stated contribution to the publication is accurate (as detailed above);

ii. permission is granted for the candidate in include the publication in the thesis; and

iii. the sum of all co-author contributions is equal to 100% less the candidate's stated contribution.

Name of Co-Author	Jian Cui
Contribution to the Paper	Designed and carried out the experiments, analysed data and wrote the manuscript.
Signature	Date 5/11/2018

Name of Co-Author	Zhipeng Qu
Contribution to the Paper	Experimental design, assisted with experiments, assisted with data analysis and wrote the manuscript.
Signature	Date 5/11/2018

Please cut and paste additional co-author panels here as required.

Name of Co-Author	Yuka Harata-Lee		
Contribution to the Paper	Experimental design, assisted with experiments, assisted with data analysis and wrote the manuscript.		
Signature		Date	5/11/2018

Name of Co-Author	Hanyuen Shen		
Contribution to the Paper	Assisted with experiments		
Signature		Date	6/11/2018

Name of Co-Author	Wei Wang		
Contribution to the Paper	Assisted with experimental design, assisted with experiments		
Signature		Date	30/10/2018

Name of Co-Author	Robert Danial Kortschak		
Contribution to the Paper	Experimental design		
Signature		Date	5/11/2018

Name of Co-Author	David L. Adelson		
Contribution to the Paper	Supervised the research, assisted the research with the funding, experimental design and wrote the manuscript.		
Signature		Date	5/11/18

The Effect of Compound Kushen Injection on Cancer Cells: Integrated Identification of Candidate Molecular Mechanisms.

Authors and affiliation:

Jian Cui[a], Zhipeng Qu[a], Yuka Harata-Lee[a], Hanyuan Shen[a], Thazin Nwe Aung[a], Wei Wang[a,b], R. Daniel Kortschak[a], and David L. Adelson[a,*]

[a]School of Biological Sciences, The University of Adelaide, South Australia, Australia, 5005.
[b]Zhendong Research Institute, Shanxi-Zhendong Pharmaceutical Co Ltd, Beijing, China

*Corresponding author:

David L. Adelson,

Room 261, The Braggs Bldg, School of Biological Sciences, the University of Adelaide, South Australia, 5005, AUSTRALIA

Ph: +61 8 8303 7555

Fax: +61 8 8303 5338

e-mail: david.adelson@adelaide.edu.au

Abstract

Background: Because TCM preparations are often combinations of multiple herbs containing hundreds of compounds, they have been difficult to study. Compound Kushen Injection (CKI) is a complex mixture cancer treatment used in Chinese hospitals for over twenty years.

Purpose: To demonstrate that a systematic analysis of molecular changes resulting from complex mixtures of bioactives from Traditional Chinese Medicine can identify a core set of differentially expressed (DE) genes and a reproducible set of candidate pathways.

Study Design: We used a cancer cell culture model to measure the effect of CKI on cell cycle phases, apoptosis and correlate those phenotypes with CKI induced changes in gene expression.

Methods: We treated cancer cells with CKI in order to generate and analyse high-throughput transcriptome data from two cancer cell lines. We integrated these differential gene expression results with previously reported results.

Results: CKI induced cell-cycle arrest and apoptosis and altered the expression of 363 core candidate genes associated with cell cycle, apoptosis, DNA replication/repair and various cancer pathways. Of these, 7 are clinically relevant to cancer diagnosis or therapy and 14 are cell cycle regulators, and most of these 21 candidates are downregulated by CKI. Comparison of our core candidate genes to a database of plant medicinal compounds and their effects on gene expression identified one-to-one, one-to-many and many-to-many regulatory relationships between compounds in CKI and DE genes.

Conclusions: By identifying promising candidate pathways and genes associated with CKI based on our transcriptome-based analysis, we have shown this approach is useful for the systematic analysis of molecular changes resulting from complex mixtures of bioactives.

Keywords:
Compound Kushen Injection, cancer cell, transcriptome, multiple targets, cell cycle, apoptosis

Abbreviations:

TCM, traditional Chinese medicine; CKI, compound Kushen injection; GO, Gene Ontology; DO, Disease Ontology; KEGG, Kyoto Encyclopedia of Gene and Genomes; PI, propidium iodide.

Introduction

The treatments of choice for cancer are often radiotherapy and/or chemotherapy, and while these can be effective, they can cause quite serious side-effects, including death. These side-effects have driven the search for adjuvant therapies to both mitigate side-effects and/or potentiate the effectiveness of existing therapies. Traditional Chinese Medicine (TCM) is one of the options for adjuvant therapies, particularly in China, but increasingly so in the West. While clinical trial data on the effectiveness of TCM is currently limited, it remains an attractive option because of its long history and because its potential effectiveness is believed to result from the cumulative effects of multiple compounds on multiple targets (Jiang, 2005). Because TCM often has not been subjected to rigorous evidence based assessment and because it is based on an alternative theoretical system compared to Western medicine, adoption of its plant derived therapeutics has been slow.

In this report, we continue to characterise the molecular effects of Compound Kushen Injection (CKI) on cancer cells. CKI has been approved by the State Food and Drug Administration (SFDA) of China for clinical use since 1995 (Shu et al., 2014) (State medical license no. Z14021231). CKI is an herbal extract from two TCM plants, Kushen (*Sophora flavescens*) and Baituling (*Smilax Glabra*) and contains more than 200 different chemical compounds. These compounds include alkaloids and flavonoids such as matrine, oxymatrine and kurarinol that have been reported to have anti-cancer activities (Shu et al., 2014; Wang et al., 2015; Zhang et al., 2013; Zhao et al., 2014). Some of these activities have been shown to influence the expression of TP*53, BAX, BCL2* and other key genes known to be important in cancer cell growth and survival (Liao et al., 2015; Ninomiya and Koketsu, 2013; Wu et al., 2015; Zhang et al., 2001).

We have previously characterised the effect of CKI on the transcriptome of MCF-7 breast carcinoma cells and in this report, we extend our previous results to two additional human

cancer cell lines (MDA-MB-231, breast carcinoma and HEPG2, hepatocellular carcinoma). Both cell lines have also been shown to undergo apoptosis in response to the ingredients of CKI (Wang et al., 2015; Wu et al., 2015; Zhang et al., 2010; Zhao et al., 2014). HEPG2 is one of the most sensitive cancer cell lines with respect to exposure to CKI (Yang et al., 2017) and CKI is often used in conjunction with Western chemotherapy drugs for the treatment of liver cancer patients in China. While the specific mechanism of action of CKI is unknown, several recent studies have reported that CKI or its primary compounds affect the regulation/expression of oncogene products including *β-catenin, TP53*, *STAT3* and *AKT* (Liu et al., 2014; Ma et al., 2016; Shu et al., 2014; Wang et al., 2015; Yu et al., 2009).

However, these and other reports did not evaluate the entire range of molecular changes from treatment with a multi-component mixture such as CKI (Gao et al., 2018; Hao and Xiao, 2014). Whilst several research databases and tools for TCM research have been developed (Cui et al., 2014; Song et al., 2013; Wang and Chen, 2013), they are limited by the fact that most of the studies that contribute to the *corpus* of these databases are from different experimental systems, use single compounds or measure effects based on one or a handful of genes/gene products.

In contrast to previous studies, our strategy was to carry out comprehensive transcriptome profiling and network reconstruction from cancer cells treated with CKI. Instead of focusing on specific genes or pathways in order to design experiments, we have linked phenotypic assessment and RNA-seq analysis to CKI treatment. This allows us to present an unbiased, comprehensive analysis of CKI specific responses of biological networks associated with cancer. Our results indicate that different cancer cell lines that undergo apoptosis in response to CKI treatment can exhibit different CKI induced gene expression profiles that nonetheless implicate similar core genes and pathways in multiple cell lines.

The current study presents the effects of CKI on gene expression in cancer cells with an aim to identify candidate pathways and regulatory networks that may be perturbed by CKI *in vivo*. To this end we primarily use concentrations of CKI higher than used *in vivo* in order to be able to detect effects in the short time frames available to tissue culture experiments. We also combine our current analysis with previously published data to focus on a shared, much smaller set of candidate genes and pathways.

Material and Methods

Cell culture and reagents

CKI (total alkaloids concentration of 25 mg/mL) in 5 ml ampoules was provided by Zhendong Pharmaceutical Co. Ltd. (Beijing, China). Chemotherapeutic agent, Fluorouracil (5-FU) was purchased from Sigma-Aldrich (MO, USA). A human breast adenocarcinoma cell line, MDA-MB-231 and a hepatocellular carcinoma cell line HEPG2 were purchased from American Type Culture Collection (ATCC, Manassas, VA). The cells were cultured in Dulbecco's Modified Eagle Medium (DMEM; Thermo Fisher Scientific, MA, USA) supplemented with 10% foetal bovine serum (Thermo Fisher Scientific). Both cell lines were cultured at 37℃ with 5% CO_2.

For all *in vitro* assays, $4x10^5$ cells were seeded in 6-well trays and cultured overnight before being treated with either CKI (at 1 mg/mL and 2 mg/mL of total alkaloids) or 5-FU (150 μg/ml for HEPG2 and 20 μg/ml for MDA-MB-231. As a negative control, cells were treated with medium only and labelled as “untreated”. After 24 and 48 hours of treatment, cells were harvested and subjected to the downstream experiments.

Cell cycle and apoptosis assay

The assay was performed as previously described (Qu et al., 2016). For each cell line, three operators replicated the assay twice in order to ensure reproducibility of the observations. The results were obtained by flow cytometry using either FACScanto or LSRII (BD Biosciences, NJ, US).

RNA isolation and sequencing

The treated cells were harvested and the cell pellets were snap frozen with liquid nitrogen and stored at −80 °C. Total RNA was isolated with PureLink™ RNA Mini Kit (Thermo Fisher Scientific) according to the manufacturer’s protocol. After quantified using a NanoDrop Spectrophotometer ND-1000 (Thermo Fisher Scientific), the quality of the total RNA was verified on a Bioanalyzer by Cancer Genome Facility (SA, Australia) ensuring all samples had RINs >7.0.

For both cell lines, the sequencing was performed in Ramaciotti Centre for Genomics (NSW, Australia). The sample preparation for each cell line was TruSeq Stranded mRNA-seq with dual indexed, on the NextSeq500 v2 platform. The parameter was 75bp paired-end High Output. The fastq files were generated and trimmed through Basespace with application "FASTQ Generation v1.0.0".

Bioinformatics analysis of RNA sequencing

The clean HEPG2 reads were aligned to reference genome (hg38) using STAR v2.5.1 with following parameters: --outFilterMultimapNmax 20 --outFilterMismatchNmax 10 --outSAMtype BAM SortedByCoordinate --outSAMstrandField intronMotif (Dobin et al., 2013). The clean MDA-MB-231 reads were aligned to reference genome (hg19) using TopHat2 v2.1.1 with following parameters: --read-gap-length 2 --read-edit-dist 2 (Kim et al., 2013). Differential expression analysis for reference genes was performed with edgeR and differentially expressed (DE) genes were selected with a False Discovery Rate (FDR) < 0.05 (Robinson et al., 2010).

The DE genes in common for both HEPG2 and MDA-MB-231 cell lines at 24 hours and 48 hours after CKI treatment were selected as "shared" genes. These shared genes were utilized to describe the major anti-cancer functions and principal mechanisms of CKI.

Gene Ontology (GO), and Kyoto Encyclopedia of Gene and Genomes (KEGG) over-representation analyses of both cell lines were carried out using the online database system ConsensusPathDB (Kamburov et al., 2008) with the following settings: "Biological process" (BP) at third level (for GO); q values (<0.01) were corrected for multiple testing with the system default settings. Disease ontology (DO) over-representation analyses of both cell lines were performed by using the Bioconductor R package clusterProfiler v3.5.1 (Yu et al., 2012). For the function analyses of shared/core genes, the method was as similar as our previous study (Qu et al., 2016) using ClueGO app 2.2.5 in Cytoscape v3.6.0. We enriched our GO terms in the biological process category level 3 and KEGG pathways, showing only terms/pathways with p values less than 0.01. Specific Over-represented terms/pathways and gene expression status mapping in KEGG pathways were visualised with the R package "Pathview" (Luo and Brouwer, 2013).

Gene expression-based investigation of bioactive components in CKI

To integrate with previous data from MCF-7 cells (Qu et al., 2016), all the shared DE genes regulated by CKI identified in all three cell lines using edgeR were mapped to the BATMAN-TCM database (Liu et al., 2016). The pharmacophore modelling method (Li et al., 2012) was used to generate the interaction network between the key genes and TCM components using R package igraph (Csardi and Nepusz, 2006).

Reverse transcription quantitative polymerase chain reaction (RT-qPCR)

RT-qPCR was performed as previously described (Qu et al., 2016). The list of target genes selected for this study and the sequences of all primers are shown in Additional file 1: Table S1.

Results

Effect of CKI on the cell cycle and apoptosis

In our previous study, CKI significantly perturbed/suppressed cancer cell target genes/networks. In the current study we present results that confirm and generalise our previous work. We observed in the MCF-7 study, low concentrations of CKI in our short-term cell assay showed no/little phenotypic effect within 48 hours, and very high doses resulted in excessive cell death at 48 hours precluding the isolation of sufficient RNA for transcriptome analysis (Qu et al., 2016). Therefore, in our current study with the two additional cell lines, to ensure consistency, we also selected 1 mg/ml and 2 mg/ml total alkaloid concentrations of CKI for our assays because they generated reproducible and significant phenotypic effects in our cell culture assay.

We used flow cytometric analysis of propidium iodide (PI) stained cells to assess both CKI induced alterations to the cell cycle and apoptosis. In HEPG2 cells, CKI treatment resulted in an overall increase in the proportion of cells in G1 phase and decrease in S phase (Fig. 1a and b). Similarly in MDA-MB-231 cells, although a consistent increase in G1 phase was not observed, CKI caused a decrease in S phase particularly at the 24-hour time point (Fig. 1a and b) indicating possible incidence of cell cycle arrest at G1 phase. Furthermore, at 2 mg/ml of total alkaloids, CKI consistently induced significantly higher level of apoptosis in both cell lines at both time points compared to untreated controls (Fig. 1c). These data together suggest that CKI has effects on the cell cycle by interfering with the transition

between G1 to S phase as well as by acting on the apoptosis pathway and promoting cell death.

CKI perturbation of gene expression

In order to elucidate the molecular mechanisms of action of CKI on these cancer cells, transcriptome analysis of CKI treated cells was performed. As mentioned above, RNA samples from two cell lines were sequenced with 2x75 bp paired-end reads. We had previously sequenced transcriptomes from CKI treated MCF-7 cells (Qu et al., 2016) and have included those results for comparison below. The samples from each cell line contained 7 groups at 3 time points (Fig. 2a), in triplicate for every group. In the multidimensional scaling (MDS) analysis, each cell line clustered independently and generally, within the cell line clusters, untreated cells clustered apart from treated cells (Additional file 2: Fig. S1).

With the mapping rate were around 90% (Additional file 3: Table S2), a P-value based ranked list of DE genes (compared to untreated from each time point) was generated for both cell lines (Additional file 4: Table S3, sheet 1-4). This list was used to select the shared DE genes. This analysis generated thousands of DE genes (Additional file 4: Table S3, sheet 5) across two cell lines.

Because for each cell line the respective treatment groups clustered together on the MDS plot, there were large numbers of shared genes between them. As a result, we identified a set of 6852 shared DE genes by identifying common DE genes from HEPG2 and MDA-MB-231 cell lines, at 24hours and 48 hours (Fig. 2b). These shared genes might predict a common molecular signature for CKI's activity. However, there were still a large number of DE genes that were not shared by both cell lines, as seen in the heatmap in Fig. 2c. The expression of the shared gene set in both HEPG2 and MDA-MB-231 is highly consistent. Interestingly, this consistency is with respect to treatment time, rather than with respect to cell line.

RT-qPCR validation and dose response of gene expression to CKI

Based on our previous results (Qu et al., 2016), and analysis below, we selected the 4 top ranked DE genes expressed in G1-S phase of the cell cycle (*TP53* and *CCND1* for expression level validation and *E2F2*and *PCNA* for low dose response), as well as the proliferation and differentiation relevant ras subfamily encoding gene (*RAP1GAP1*) for low dose response. We also selected a prominently expressed gene (*CYP1A1*) for validation because of its sensitivity to CKI treatment. *CYP1A1, TP53* and *CCND1* expression changes were validated with RT-qPCR with all three genes showing similar patterns of expression in the transcriptome data and RT-qPCR (Fig. 3a).

Because low dose treatment with CKI did not cause significant gross phenotypic effects in either cell line, we decided to use gene expression as a more sensitive measure of phenotype to look at the effect of lower doses of CKI. We used 0.125 mg/ml, 0.25 mg/ml, 0.5 mg/ml and 1mg/ml concentrations to look for dose dependency of gene expression. Our results showed an obvious dose-dependent expression trend (Fig. 3b) in both cell lines. Because the 0.125mg/ml concentration of CKI is equivalent to what cancer patients are treated with, our results are potentially clinically relevant.

Function enrichment analysis

To identify candidate mechanisms of action of CKI, we carried out functional enrichment analysis. We used ConsensusPathDB(Kamburov et al., 2008) and Clusterprofiler (Li et al., 2012) along with GO and KEGG pathways for over-representation analysis, along with disease ontology (DO) (Schriml et al., 2011) enrichment.

GO over-representation test was determined based on Biological Process level 3 and *q* value <0.01. The results for both cell lines at both time points were summarised and visualized based on semantic analysis of terms in Fig. 4a. From this result, it was obvious that there were a large proportion of enriched GO terms relating to cell cycle, such as “cell cycle checkpoint”, “negative/positive regulation of cell cycle process” and so on prominently featured for all data sets (Additional file 5: Fig. S2, Additional file 6: Table S4, sheet 1-4).

We then used KEGG pathways to determine the specific pathways altered by CKI in cancer. The most regulated over-representative KEGG pathways are summarized according to KEGG

Orthology (KO) (Fig. 4b). Cell cycle related pathways such as “cell cycle”, “DNA replication”, and “apoptosis” were also consistently seen in the KEGG enrichment results (Additional file 6: Table S4, sheet5-8) at both 24 and 48 hours. Moreover, in addition to the cell cycle relevant pathways, some cancer related pathways were also observed, such as “prostate cancer” and “chronic myeloid leukaemia”, and a large number of DE genes (283) from the two cell lines were relevant in “pathways in cancer”.

Because the KEGG enrichment revealed many pathways relating to diseases, most of which were cancers, we decided to explore the enrichment of DE genes with respect to DO terms (Fig. 4c). In the DO list (Additional file 6: Table S4, sheet 9-12), all top ranked terms listed are cancers. Interestingly, most cancer types listed are from the lower abdomen, for example “ovarian cancer”, “urinary bladder cancer “and “prostate cancer” etc. occurring in genitourinary organs (Additional file 6: Table S4, sheet 9-12). For both KEGG pathway and DO enrichment, the effects of CKI on both cell lines were similar.

In addition to cell line specific functional enrichment of DE genes, we also analysed the over-represented GO terms for shared DE genes (Fig. 5a). The most significant clusters were highly relevant to metabolic process, such as “cellular macromolecule metabolic process”, as well as the corresponding positive/negative regulatory biological process (Additional file 6: Table S4, sheet 13). Moreover, various signalling pathways, though not forming a large cluster, were also significant, for example, “regulation of signal transduction” and “intracellular receptor signalling pathway”. Finally, some “cell cycle” related terms constituted relatively large sub-clusters, including “cell division” and “mitotic cell cycle process”. The enriched GO analysis was consistent with the cell line specific enriched results, and with our previous analysis of MCF-7 cells (Qu et al., 2016). It is worth noting that for “cell cycle” related terms, most of the participating genes were down-regulated by CKI.

Similar results were observed from KEGG analysis (Fig. 5b, and Additional file 6: Table S4, sheet 14) of shared genes. Various pathways related to cancer, formed a large cluster. Pathways such as “DNA replication”, “Ribosome” and “cell cycle” were mostly down-regulated, while up-regulated pathways included “inositol phosphate metabolism” and “protein processing in endoplasmic reticulum”.

We also carried out over-representation analysis of DO terms (Fig. 5c) for all shared DE genes. The analysis results were consistent with the single cell line DO term analysis with mostly cancer related terms; in particular genitourinary or breast cancer terms. While this was also partially similar to the KEGG results for shared DE genes, there were some differences in the KEGG results for disease pathways compared to the DO results, such as "bacterial invasion of epithelial cells", "Fanconi anemia pathway" and "AGE-RAGE pathway in diabetic complications".

Regulation of specific pathways related to cancer

Specific to the therapeutic potential of CKI for cancer treatment, we applied our data set mapping to KEGG cancer pathways: pathways in cancer- homo sapiens (Additional file 7: Fig. S3). The R package Pathview (Luo and Brouwer, 2013) was used to integrate log fold change values of all the genes expression patterns into these target pathways. Within the 21 pathways in cancer, the "cell cycle" still featured prominently (Fig. 6a). The expression of almost every gene in the cell cycle pathway was affected by CKI, with most of them suppressed. We did not observe this kind of overall pathway suppression in any of the other pathways. We have displayed the summaries for the remaining 20 pathways in the heatmap in Fig. 6b. Although all the pathways were all perturbed by CKI, they include both over and under expressed genes in roughly equal proportions.

Collectively, these results suggest a direct anticancer effect of CKI, and implicate specific candidate mechanisms of action based on the perturbed molecular networks. The most obvious example is the cell cycle, where G1-S phase is significantly altered, resulting in the induction of apoptosis. The downstream process triggered by CKI is the suppression of gene expression of cell cycle regulators, including *P53* and *CCND1*. The other perturbed cancer pathways provide additional candidate mechanisms of action for CKI. In the following section we integrate these results with previous results reported in the literature to refine the core set of genes and pathways perturbed by CKI.

Discussion

Although HEPG2 (liver cancer – mesodermal tissue origin) and MDA-MB-231 (mammary epithelial adenocarcinoma – ectodermal tissue origin) are different cancer types, they shared a large number of CKI DE genes with similar expression profiles, presumably these

shared genes include CKI response genes that are essential to the apoptotic response triggered by CKI. However, the number of shared CKI DE genes is too high to allow straight forward identification of genes critical to the CKI response. We therefore decided to combine these data with previously reported CKI DE genes from MCF-7 cells (Qu et al., 2016) in order to reduce the number of core CKI response genes. The intersection of MCF-7 CKI DE genes with the shared CKI DE genes yielded 363 core CKI DE genes (Additional file 8: Fig. S4).

Among the 363 core CKI DE genes, cytochrome P450 family 1 subfamily A member 1 (*CYP1A1*) gene is the most over-expressed. This gene is consistently up-regulated by CKI in all three cell lines, and showed significant dose response. In liver cancer cells, over-expression of *CYP1A1* induced by plant natural products has been associated with Aryl-hydrocarbon Receptor transformation (Anwar-Mohamed and El-Kadi, 2009; Zhou et al., 2016). Furthermore, as a steroid-metabolizing enzyme, CYP1A1 is part of cancer metabolic processes relevant to steroid hormone responsive tumours, such as breast cancer, ovarian cancer and prostate cancer (Mitsui et al., 2016; Nandekar et al., 2016; Ou et al., 2016; Piotrowska-Kempisty et al., 2017). Therefore, *CYP1A1* may be of particular interest for understanding the mechanism of action of CKI on cancer cells.

Comparison of the 363 core genes to the 135 Tumour Alterations Relevant for Genomics-driven Therapy (TARGET) genes (version 3) from The Broad Institute (https://www.broadinstitute.org/ cancer/cga/target) identified 7 DE genes that were shared across the three cell lines and two time points (Fig. 7a). Of these seven genes, six (*TP53*, *CCND1*, *MYD88* (Myeloid differentiation primary response gene 88) , *EWSR1*, *TMPRSS2* and *IDH1* (isocitrate dehydrogenase 1)) were similarly regulated (either always over-expressed or under-expressed), while *CCND3* was over-expressed in all three cell lines at both time points except at 48 hours in MCF-7 cells, where it was under-expressed.

The *TP53* gene encodes a tumor suppressor protein, that can induce apoptosis (Harris and Levine, 2005). However, in all cell lines *TP53* was down-regulated, and all cell lines showed increased apoptosis. This suggests that CKI induced apoptosis was not *TP53*-dependent. Support for this comes from the fact that transcripts for *PCNA* (proliferating cell nuclear antigen), and a group of transcription factors: *MCM* (mini-chromosome maintenance)

complex and the *E2F* family are down-regulated. The *E2F* transcription factors regulate the cell cycle and *TP53*-dependent and -independent apoptosis (Hollern et al., 2014; Sun et al., 2013; Woods et al., 2007; Zaldua et al., 2016). In addition, other core genes present in the TARGET database have also been shown to induce apoptosis. For example, inhibition of *MYD88* induces apoptosis in both triple negative breast cancer and bladder cancer (Christensen et al., 2017; Zhang et al., 2016). The increased expression of *IDH1* may be important, as IDH1 is frequently mutated in cancers (Li et al., 2012) and when mutated, it causes loss of α–ketoglutarate production and may be important for the Warburg effect. *TMPRSS2* (transmembrane protease, serine 2) has also been shown to regulate apoptosis in cancer (Afar et al., 2001). Therefore, CKI may induce apoptosis through a variety of means.

In the GO (Fig. 7b) and KEGG (Fig. 7c) over-representation analysis of the 363 core genes yielded enrichment for cell cycle and cancer pathways. In the GO enriched genes, cell cycle and related pathways accounted for the majority of functional sub-clusters. In the KEGG enriched pathways, cell cycle and cancer pathways predominated in a single cluster. Most of the core genes in GO and KEGG clusters were down-regulated by CKI.

In addition to the cell cycle, CKI treatment also caused enrichment for terms or pathways related to cancer progression, such as “focal adhesion” and “blood vessel development”. (Additional file 6: Table S4, sheet 5-8). These developmental processes contribute to tumorigenesis and metastasis(Luo and Guan, 2010; Warren et al., 1995). It is tempting to speculate that CKI may alter these functions *in vivo*, possibly altering angiogenesis which is critical for tumours (Hanahan and Folkman, 1996). In addition, there were metabolic pathways and terms that were also identified as perturbed by CKI. Effects on many targets/pathways is one of the expected features of TCM drugs which likely hit multiple targets (Efferth et al., 2007).

We have examined the effect of a complex mixture of plant natural products (CKI) on different cancer cell lines and have identified specific, consistent effects on gene expression resulting from this mixture. However, the complexity of CKI makes it difficult to determine the mechanism of action of individual components, and often testing of individual components has resulted in either no effect or contradictory results in the research literature. In spite of this complexity, it is possible to map our results on to a pre-existing

corpus of work that links individual natural compounds to changes in gene expression. We have used BATMAN (Liu et al., 2016), an online TCM database of curated links between compounds and gene expression. Based on this resource, we have identified 14 components of CKI that have been linked to the regulation of 52 of our core genes (Fig. 7d). We can see from the network diagram in Fig. 7d that one to one, one to many and many to many relationships exist between CKI components and genes which is consistent with previous studies (Liu et al., 2014; Wu et al., 2015; Zhang and Yu, 2016). As more information becomes available for individual components, we will be able to construct a more comprehensive model of CKI mechanism based on network analysis.

Conclusions

Our systematic analysis of gene expression changes in cancer cells caused by a complex herbal extract used in TCM has proven to be effective at identifying candidate molecular pathways. CKI has consistent and specific effects on gene expression across multiple cancer cell lines and it also consistently induces apoptosis in vitro. These effects show that CKI can suppress the expression of cell cycle regulatory genes and other well characterized cancer related genes and pathways. Validation of a subset of DE genes at lower doses of CKI has shown a dose-response relationship that suggests that CKI may have similar effects in vivo at clinically relevant concentrations. Our results provide a molecular basis for further investigation of the mechanism of action of CKI.

Conflict of Interest

We wish to draw the attention of the Editor to the following facts which may be considered as potential conflicts of interest and to significant financial contributions to this work. While a generous donation was used to set up the Zhendong Centre by Shanxi Zhendong Pharmaceutical Co Ltd, they did not determine the research direction for this work or influence the analysis of the data. JC: no competing interests, ZQ: no competing interests, YHL: no competing interests, HS: no competing interests, TNA: no competing interests, WW: is an employee of Zhendong Pharma seconded to Zhendong Centre to learn bioinformatics

methods, RDK: no competing interests, DLA: Director of the Zhendong Centre which was set up with a generous donation from the Zhendong Pharmaceutical Co Ltd. Zhendong Pharmaceutical has had no control over these experiments, their design or analysis and have not exercised any editorial control over the manuscript.

403

404 Literature Cited

405

406 Afar, D.E., Vivanco, I., Hubert, R.S., Kuo, J., Chen, E., Saffran, D.C., Raitano, A.B., Jakobovits,
407 A., 2001. Catalytic cleavage of the androgen-regulated TMPRSS2 protease results in its
408 secretion by prostate and prostate cancer epithelia. Cancer research 61, 1686-1692.
409 Anwar-Mohamed, A., El-Kadi, A.O., 2009. Sulforaphane induces CYP1A1 mRNA, protein, and
410 catalytic activity levels via an AhR-dependent pathway in murine hepatoma Hepa 1c1c7 and
411 human HepG2 cells. Cancer letters 275, 93-101.
412 Christensen, A.G., Ehmsen, S., Terp, M.G., Batra, R., Alcaraz, N., Baumbach, J., Noer, J.B.,
413 Moreira, J., Leth-Larsen, R., Larsen, M.R., 2017. Elucidation of Altered Pathways in Tumor-
414 Initiating Cells of Triple-Negative Breast Cancer: A Useful Cell Model System for Drug
415 Screening. STEM CELLS.
416 Csardi, G., Nepusz, T., 2006. The igraph software package for complex network research.
417 InterJournal, Complex Systems 1695, 1-9.
418 Cui, M., Li, H., Hu, X., 2014. Similarities between "Big Data" and traditional Chinese medicine
419 information. Journal of Traditional Chinese Medicine 34, 518-522.
420 Dobin, A., Davis, C.A., Schlesinger, F., Drenkow, J., Zaleski, C., Jha, S., Batut, P., Chaisson, M.,
421 Gingeras, T.R., 2013. STAR: ultrafast universal RNA-seq aligner. Bioinformatics 29, 15-21.
422 Efferth, T., Li, P.C., Konkimalla, V.S.B., Kaina, B., 2007. From traditional Chinese medicine to
423 rational cancer therapy. Trends in molecular medicine 13, 353-361.
424 Gao, L., Wang, K.-x., Zhou, Y.-z., Fang, J.-s., Qin, X.-m., Du, G.-h., 2018. Uncovering the
425 anticancer mechanism of Compound Kushen Injection against HCC by integrating
426 quantitative analysis, network analysis and experimental validation. Scientific reports 8, 624.
427 Hanahan, D., Folkman, J., 1996. Patterns and emerging mechanisms of the angiogenic
428 switch during tumorigenesis. cell 86, 353-364.
429 Hao, D.C., Xiao, P.G., 2014. Network pharmacology: a Rosetta Stone for traditional Chinese
430 medicine. Drug development research 75, 299-312.
431 Harris, S.L., Levine, A.J., 2005. The p53 pathway: positive and negative feedback loops.
432 Oncogene 24, 2899.
433 Hollern, D.P., Honeysett, J., Cardiff, R.D., Andrechek, E.R., 2014. The E2F transcription
434 factors regulate tumor development and metastasis in a mouse model of metastatic breast
435 cancer. Molecular and cellular biology 34, 3229-3243.
436 Jiang, W.-Y., 2005. Therapeutic wisdom in traditional Chinese medicine: a perspective from
437 modern science. Trends in pharmacological sciences 26, 558-563.
438 Kamburov, A., Wierling, C., Lehrach, H., Herwig, R., 2008. ConsensusPathDB—a database for
439 integrating human functional interaction networks. Nucleic acids research 37, D623-D628.
440 Kim, D., Pertea, G., Trapnell, C., Pimentel, H., Kelley, R., Salzberg, S.L., 2013. TopHat2:
441 accurate alignment of transcriptomes in the presence of insertions, deletions and gene
442 fusions. Genome Biol 14, R36.
443 Li, X., Xu, X., Wang, J., Yu, H., Wang, X., Yang, H., Xu, H., Tang, S., Li, Y., Yang, L., 2012. A
444 system-level investigation into the mechanisms of Chinese Traditional Medicine: Compound
445 Danshen Formula for cardiovascular disease treatment. PloS one 7, e43918.
446 Liao, C.-Y., Lee, C.-C., Tsai, C.-c., Hsueh, C.-W., Wang, C.-C., Chen, I., Tsai, M.-K., Liu, M.-Y.,
447 Hsieh, A.-T., Su, K.-J., 2015. Novel investigations of flavonoids as chemopreventive agents
448 for hepatocellular carcinoma. BioMed research international 2015.

Liu, Y., Xu, Y., Ji, W., Li, X., Sun, B., Gao, Q., Su, C., 2014. Anti-tumor activities of matrine and oxymatrine: literature review. Tumor Biology 35, 5111-5119.
Liu, Z., Guo, F., Wang, Y., Li, C., Zhang, X., Li, H., Diao, L., Gu, J., Wang, W., Li, D., 2016. BATMAN-TCM: a Bioinformatics Analysis Tool for Molecular mechANism of Traditional Chinese Medicine. Scientific reports 6.
Luo, M., Guan, J.-L., 2010. Focal adhesion kinase: a prominent determinant in breast cancer initiation, progression and metastasis. Cancer letters 289, 127-139.
Luo, W., Brouwer, C., 2013. Pathview: an R/Bioconductor package for pathway-based data integration and visualization. Bioinformatics 29, 1830-1831.
Ma, X., Li, R.-S., Wang, J., Huang, Y.-Q., Li, P.-Y., Wang, J., Su, H.-B., Wang, R.-L., Zhang, Y.-M., Liu, H.-H., 2016. The therapeutic efficacy and safety of compound kushen injection combined with transarterial chemoembolization in unresectable hepatocellular carcinoma: an update systematic review and meta-analysis. Frontiers in pharmacology 7.
Mitsui, Y., Chang, I., Kato, T., Hashimoto, Y., Yamamura, S., Fukuhara, S., Wong, D.K., Shiina, M., Imai-Sumida, M., Majid, S., 2016. Functional role and tobacco smoking effects on methylation of CYP1A1 gene in prostate cancer. Oncotarget 7, 49107.
Nandekar, P.P., Khomane, K., Chaudhary, V., Rathod, V.P., Borkar, R.M., Bhandi, M.M., Srinivas, R., Sangamwar, A.T., Guchhait, S.K., Bansal, A.K., 2016. Identification of leads for antiproliferative activity on MDA-MB-435 human breast cancer cells through pharmacophore and CYP1A1-mediated metabolism. European journal of medicinal chemistry 115, 82-93.
Ninomiya, M., Koketsu, M., 2013. Minor flavonoids (chalcones, flavanones, dihydrochalcones, and aurones), Natural Products. Springer, pp. 1867-1900.
Ou, C., Zhao, Y., Liu, J.-H., Zhu, B., Li, P.-Z., Zhao, H.-L., 2016. Relationship Between Aldosterone Synthase CYP1A1 MspI Gene Polymorphism and Prostate Cancer Risk. Technology in cancer research & treatment, 1533034615625519.
Piotrowska-Kempisty, H., Klupczyńska, A., Trzybulska, D., Kulcenty, K., Sulej-Suchomska, A.M., Kucińska, M., Mikstacka, R., Wierzchowski, M., Murias, M., Baer-Dubowska, W., 2017. Role of CYP1A1 in the biological activity of methylated resveratrol analogue, 3, 4, 5, 4′-tetramethoxystilbene (DMU-212) in ovarian cancer A-2780 and non-cancerous HOSE cells. Toxicology letters 267, 59-66.
Qu, Z., Cui, J., Harata-Lee, Y., Aung, T.N., Feng, Q., Raison, J.M., Kortschak, R.D., Adelson, D.L., 2016. Identification of candidate anti-cancer molecular mechanisms of Compound Kushen Injection using functional genomics. Oncotarget 7, 66003-66019.
Robinson, M.D., McCarthy, D.J., Smyth, G.K., 2010. edgeR: a Bioconductor package for differential expression analysis of digital gene expression data. Bioinformatics 26, 139-140.
Schriml, L.M., Arze, C., Nadendla, S., Chang, Y.-W.W., Mazaitis, M., Felix, V., Feng, G., Kibbe, W.A., 2011. Disease Ontology: a backbone for disease semantic integration. Nucleic acids research 40, D940-D946.
Shu, G., Yang, J., Zhao, W., Xu, C., Hong, Z., Mei, Z., Yang, X., 2014. Kurarinol induces hepatocellular carcinoma cell apoptosis through suppressing cellular signal transducer and activator of transcription 3 signaling. Toxicology and applied pharmacology 281, 157-165.
Song, Y.-N., Zhang, G.-B., Zhang, Y.-Y., Su, S.-B., 2013. Clinical applications of omics technologies on ZHENG differentiation research in traditional Chinese medicine. Evidence-Based Complementary and Alternative Medicine 2013.
Sun, H.X., Xu, Y., Yang, X.R., Wang, W.M., Bai, H., Shi, R.Y., Nayar, S.K., Devbhandari, R.P., He, Y.z., Zhu, Q.F., 2013. Hypoxia inducible factor 2 alpha inhibits hepatocellular carcinoma

growth through the transcription factor dimerization partner 3/E2F transcription factor 1–dependent apoptotic pathway. Hepatology 57, 1088-1097.
Wang, P., Chen, Z., 2013. Traditional Chinese medicine ZHENG and Omics convergence: A systems approach to post-genomics medicine in a global world. Omics: a journal of integrative biology 17, 451-459.
Wang, W., You, R.-l., Qin, W.-j., Hai, L.-n., Fang, M.-j., Huang, G.-h., Kang, R.-x., Li, M.-h., Qiao, Y.-f., Li, J.-w., 2015. Anti-tumor activities of active ingredients in Compound Kushen Injection. Acta Pharmacologica Sinica 36, 676-679.
Warren, R.S., Yuan, H., Matli, M.R., Gillett, N.A., Ferrara, N., 1995. Regulation by vascular endothelial growth factor of human colon cancer tumorigenesis in a mouse model of experimental liver metastasis. The Journal of clinical investigation 95, 1789-1797.
Woods, K., Thomson, J.M., Hammond, S.M., 2007. Direct regulation of an oncogenic micro-RNA cluster by E2F transcription factors. Journal of Biological Chemistry 282, 2130-2134.
Wu, C., Huang, W., Guo, Y., Xia, P., Sun, X., Pan, X., Hu, W., 2015. Oxymatrine inhibits the proliferation of prostate cancer cells in vitro and in vivo. Molecular medicine reports 11, 4129-4134.
Yang, X., Huang, M., Cai, J., Lv, D., Lv, J., Zheng, S., Ma, X., Zhao, P., Wang, Q., 2017. Chemical profiling of anti-hepatocellular carcinoma constituents from Caragana tangutica Maxim. by off-line semi-preparative HPLC-NMR. Natural product research 31, 1150-1155.
Yu, G., Wang, L.-G., Han, Y., He, Q.-Y., 2012. clusterProfiler: an R Package for Comparing Biological Themes Among Gene Clusters. OMICS : a Journal of Integrative Biology 16, 284-287.
Yu, P., Liu, Q., Liu, K., Yagasaki, K., Wu, E., Zhang, G., 2009. Matrine suppresses breast cancer cell proliferation and invasion via VEGF-Akt-NF-κB signaling. Cytotechnology 59, 219-229.
Zaldua, N., Llavero, F., Artaso, A., Gálvez, P., Lacerda, H.M., Parada, L.A., Zugaza, J.L., 2016. Rac1/p21‐activated kinase pathway controls retinoblastoma protein phosphorylation and E2F transcription factor activation in B lymphocytes. FEBS journal 283, 647-661.
Zhang, H., Ye, Y., Li, M., Ye, S., Huang, W., Cai, T., He, J., Peng, J., Duan, T., Cui, J., 2016. CXCL2/MIF-CXCR2 signaling promotes the recruitment of myeloid-derived suppressor cells and is correlated with prognosis in bladder cancer. Oncogene.
Zhang, J.-Q., Li, Y.-M., Liu, T., He, W.-T., Chen, Y.-T., Chen, X.-H., Li, X., Zhou, W.-C., Yi, J.-F., Ren, Z.-J., 2010. Antitumor effect of matrine in human hepatoma G2 cells by inducing apoptosis and autophagy. World journal of gastroenterology: WJG 16, 4281.
Zhang, L.P., Jiang, J.K., Tam, J.W.O., Zhang, Y., Liu, X.S., Xu, X.R., Liu, B.Z., He, Y.J., 2001. Effects of Matrine on proliferation and differentiation in K-562 cells. Leukemia Research 25, 793-800.
Zhang, X., Yu, H., 2016. Matrine inhibits diethylnitrosamine-induced HCC proliferation in rats through inducing apoptosis via p53, Bax-dependent caspase-3 activation pathway and down-regulating MLCK overexpression. Iranian Journal of Pharmaceutical Research: IJPR 15, 491.
Zhang, X.-L., Cao, M.-A., Pu, L.-P., Huang, S.-S., Gao, Q.-X., Yuan, C.-S., Wang, C.-M., 2013. A novel flavonoid isolated from Sophora flavescens exhibited anti-angiogenesis activity, decreased VEGF expression and caused G0/G1 cell cycle arrest in vitro. Die Pharmazie-An International Journal of Pharmaceutical Sciences 68, 369-375.
Zhao, Z., Fan, H., Higgins, T., Qi, J., Haines, D., Trivett, A., Oppenheim, J.J., Wei, H., Li, J., Lin, H., 2014. Fufang Kushen injection inhibits sarcoma growth and tumor-induced hyperalgesia via TRPV1 signaling pathways. Cancer letters 355, 232-241.

543 Zhou, Y., Li, Y., Zhou, T., Zheng, J., Li, S., Li, H.-B., 2016. Dietary natural products for
544 prevention and treatment of liver cancer. Nutrients 8, 156.
545
546
547

Author contributions statement:

JC experimental design, carried out experiments, analysed data, wrote paper, ZQ experimental design, assisted with experiments, assisted with data analysis, wrote paper, YHL experimental design, assisted with experiments, assisted with data analysis, wrote paper, HS assisted with experiments, TNA assisted with experiments, WW assisted with experimental design, assisted with experiments, RDK experimental design, and DLA supervised the research, acquired funding for the experiments, experimental design, wrote paper.

Data Availability

All RNAseq data raw and processed data were deposited at the Gene Expression Omnibus (GEO) data repository (XXXXXXX).

Figure legends

Fig. 1

Effects of different treatment on cell cycle and apoptosis of HEPG2 and MDA-MB-231 cells. **A)** The apoptosis and cell cycle distribution of each cell line after 24- and 48-hour treatments with CKI or 5-Fu assessed PI staining. **B)** Percentages of cells in different phases of cell cycle resulting from treatment. **c** Percentage of apoptotic cells after treatment. Results shown are mean ±SEM (n=6). Statistically significant differences from untreated control were identified using two-way ANOVA (*p<0.05, **p<0.01, ****p<0.0001).

Fig. 2

570 DE genes shared in both cell lines at both time points. **A)** Work flow diagram showing
571 experimental design and sample collection. **B)** Venn diagram showing the number of shared
572 DE genes between HEPG2 and MDA-MB-231. **C)** Heatmap presenting the overall gene
573 expression pattern in both cell lines treated with CKI. Heatmap is split into four parts based
574 on gene content and expression pattern: 5442 differentially regulated genes with
575 expression not shared between the two cell lines, 3157 upregulated genes shared between
576 both cell lines, 3522 down-regulated genes shared between both cell lines, and 173
577 discordantly regulated genes with differential expression shared between both cell lines.

578 Fig. 3

579 Validation of gene expression and effects of low dose CKI using RT-qPCR. **A)** Comparison of
580 DE genes between RNA-seq results (left) and RT-qPCR validation (right) for each cell line at 2
581 time-points. Three DE genes (*CYP1A1, TP53* and *CCND1*) were chosen for validation. Gene
582 expression was generally consistent between transcriptome data and qPCR data. **B)** Dose
583 response of CKI using a subset of genes with conserved expression in HEPG2 (left), and
584 MDA-MB-231 (right) from 0 mg/ml to 1 mg/ml of total alkaloids. Six genes (*CYP1A1, TP53,*
585 *CCND1, Rap2GAP1, E2F2* and *PCNA*) were selected based on their relevance to important
586 pathways perturbed by CKI. RT-qPCR results are presented as expression relative to RPS13.
587 Data are represented as mean ±SEM (n>3). A t-test was used to compare CKI doses with
588 "untreated" (*p<0.05, **p<0.01, ***p<0.001, ****p<0.0001).

589 Fig. 4

590 Functional annotation of DE genes for each cell line as a result of CKI treatment. Summary of
591 over-represented **A)** GO terms for Biological Process, **B)** KEGG pathways and **C)** DO terms for
592 DE genes as a result of CKI treatment in each cell line at two time points. For GO semantic

593 and enrichment analysis, Lin's algorithm was applied to cluster and summarize similar
594 functions based on GO terms found in every treatment. Similarly, by back-tracing the
595 upstream categories in the KEGG Ontology, we were able to obtain a more generalized
596 summary of KEGG pathways for each treatment. The size of each bubble represents the
597 number of GO terms/pathways, and the colour shows the statistical significance of the
598 relevant function or pathways. The DO summary for each treatment was determined by
599 back-tracing to parent terms.

600 Fig. 5

601 Functional annotation of DE genes with shared expression in both cell lines as a result of CKI
602 treatment. Over-representation analysis was performed to determine **A)** GO terms for
603 Biological Process, **B)** KEGG pathways, and **C)** DO terms for DE genes shared in both cell
604 lines. In nodes for both GO terms and KEGG pathways, node size is proportional to the
605 statistical significance of over-representation. For DO terms, all the enriched terms are
606 statistically significant ($p<1x10^{-5}$) in each category, and the bar length represents the
607 number of expressed genes that map to the term.

608 Fig. 6

609 Comparison of shared genes expression in specific pathways across two cell lines. **A)** Cell
610 cycle pathways, where each coloured box is separated into 4 parts, from left to right
611 representing 24h CKI treated HEPG2, 48h CKI treated HEPG2, 24h CKI treated MDA-MB-231
612 as well as 48h CKI treated MDA-MB-231. **B)** Heatmap of pathways in cancer. The top two
613 heatmaps summarise the effects of CKI on HEPG2 cells for two time-points, and the bottom
614 two heatmaps show the effects of CKI on MDA-MB-231 cells. In addition to the cell cycle
615 pathway, there were 21 associated pathways in cancer that were perturbed by CKI. The

616 effects of CKI on both cell lines were similar, with changes in TARGET database genes
617 indicated by arrows. Compared to other pathways in cancer, the effects of CKI on the cell
618 cycle pathway showed overall down-regulation.

619 Fig. 7.

620 Analysis of CKI regulated core genes from this report combined with previous available data.
621 **A)** Fold changes of TARGET and cell cycle regulatory gene expression in MDA-MB-231,
622 HEPG2 and MCF-7(Qu et al., 2016) cell lines 24 and 48 hours after CKI treatment. Only seven
623 TARGET genes are affected by CKI in all three cell lines. Most of the 14 cell cycle regulatory
624 genes differentially expressed in all three cell lines are down-regulated. **B)** GO term
625 enrichment analysis of 363 core genes from MDA-MB-231, HEPG2 and MCF-7 cell lines. **C)**
626 KEGG pathway enrichment of 363 core genes from MDA-MB-231, HEPG2 and MCF-7 cell
627 lines. **D)** Some individual compounds present in CKI linked to genes they regulate that are
628 also found in this report and our previous study (add citation number Qu et al, 2016). Node
629 size is proportional to the number of related components/genes.

630

631

632 **Figures:**

633 Fig. 1

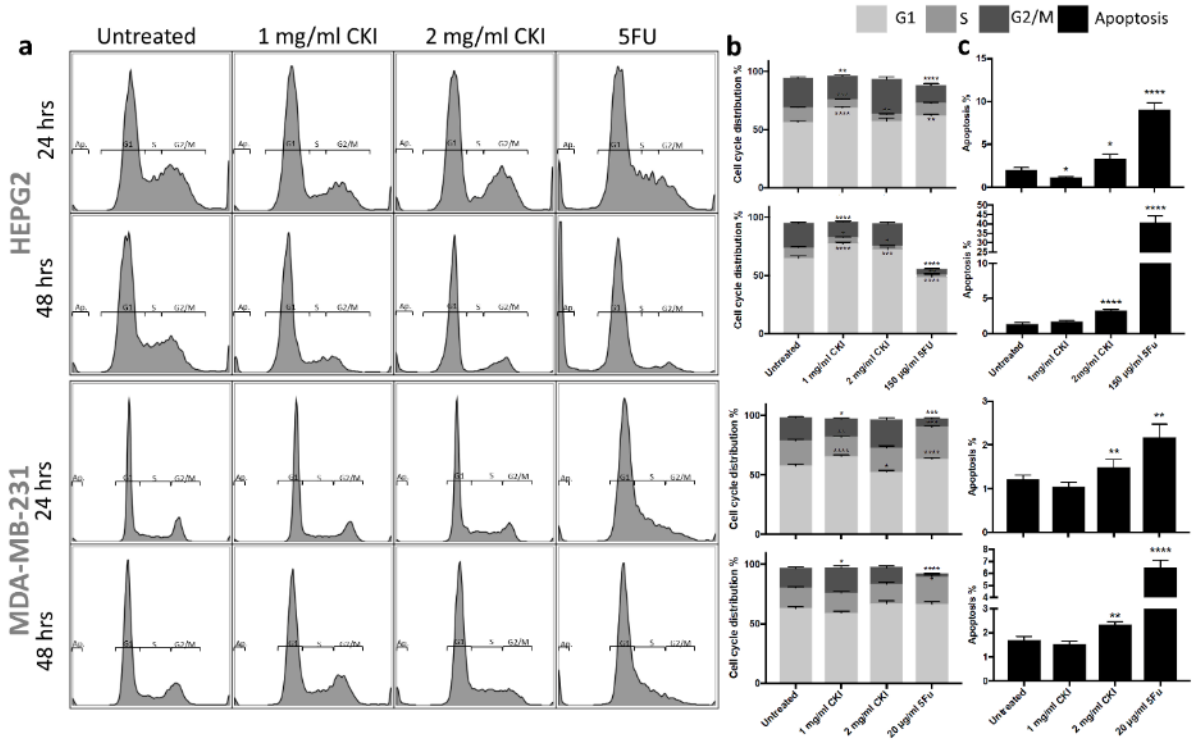

634

635

636 Fig. 2

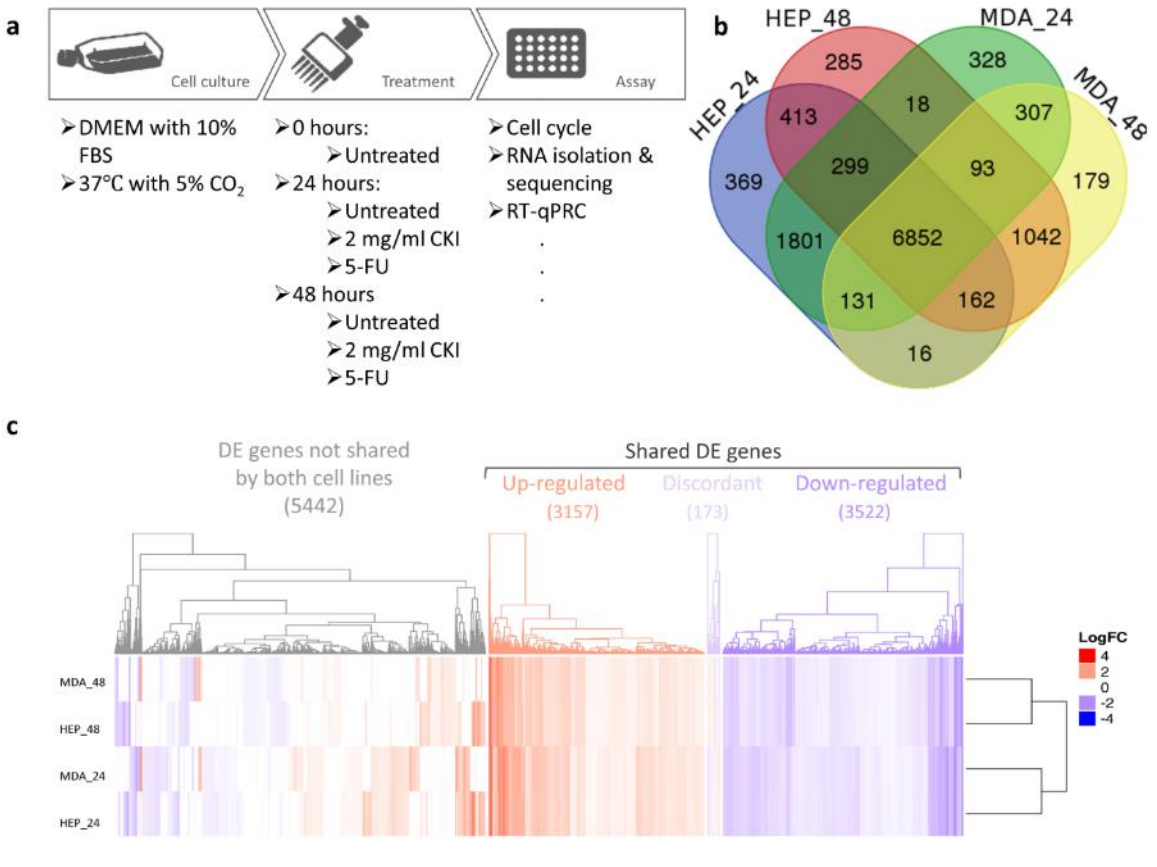

637

638

639 Fig. 3

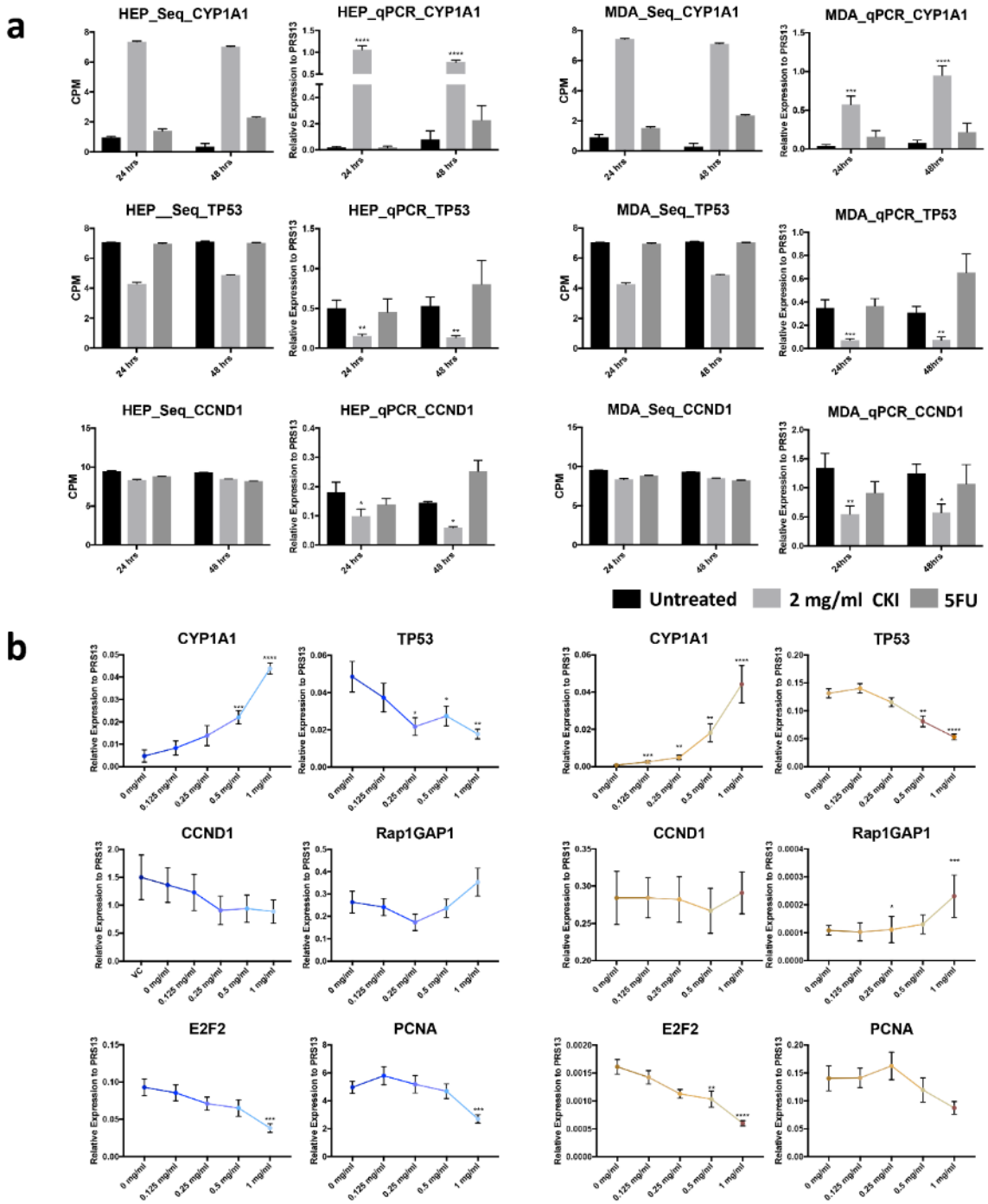

640

641

642 Fig. 4

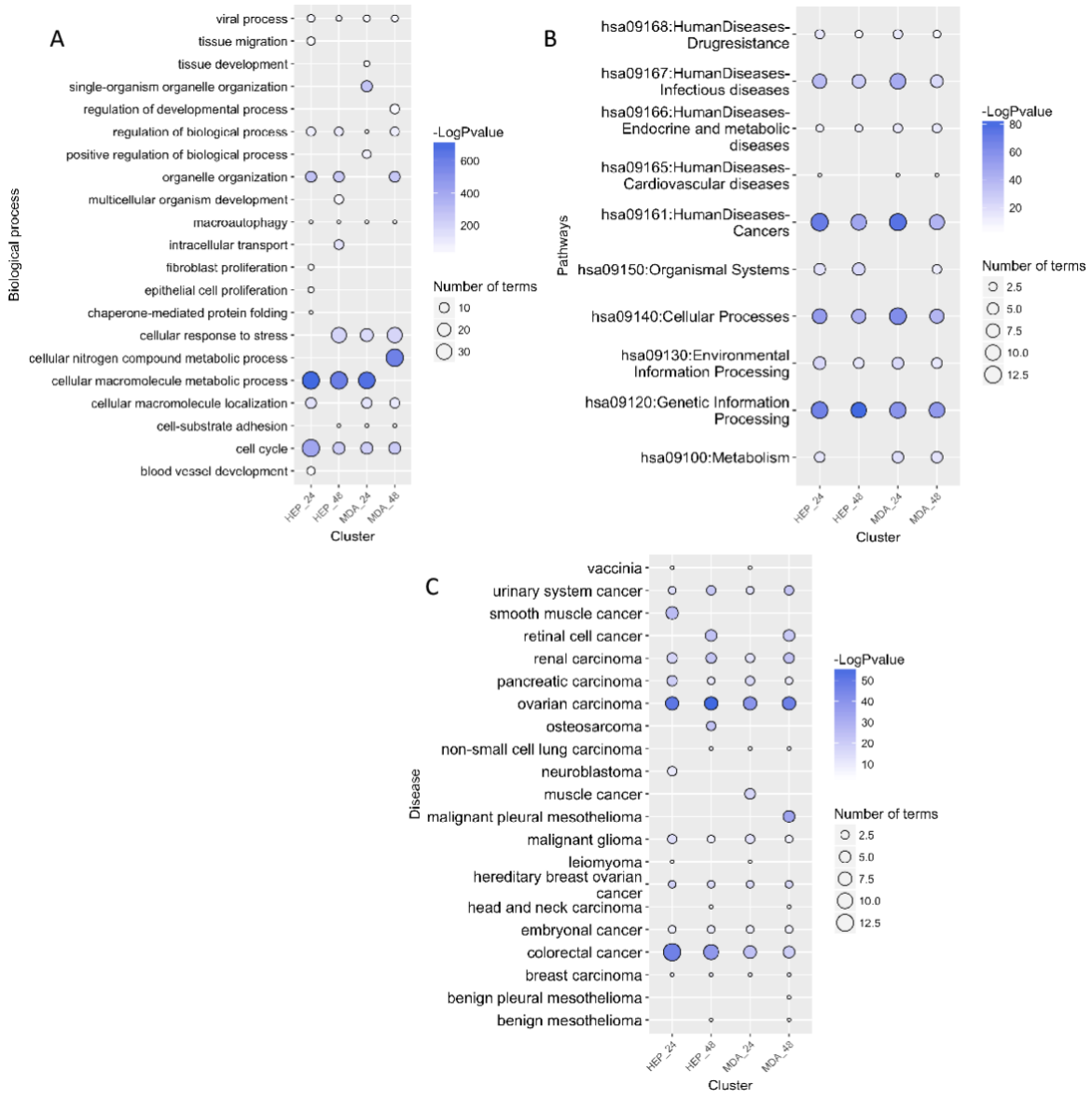

643

644

645 Fig. 5

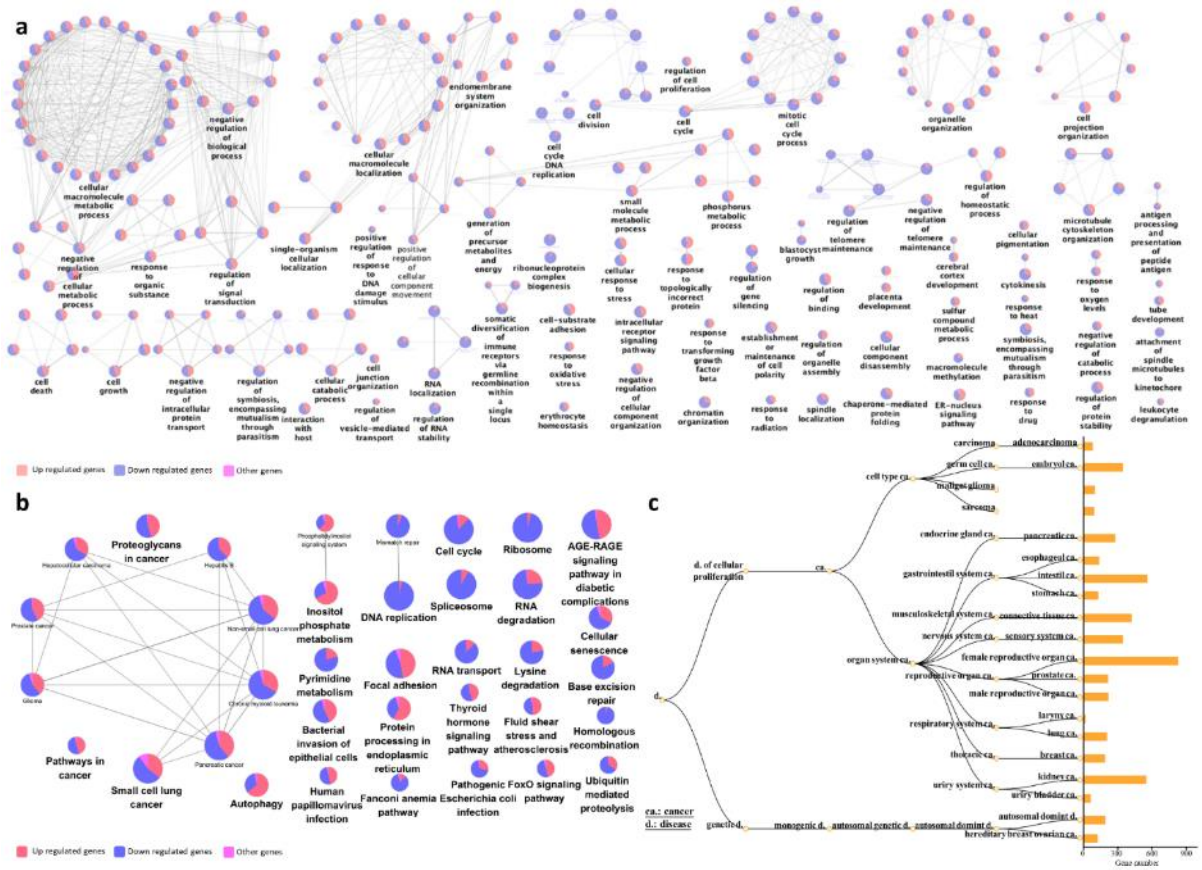

646

647

Fig. 6

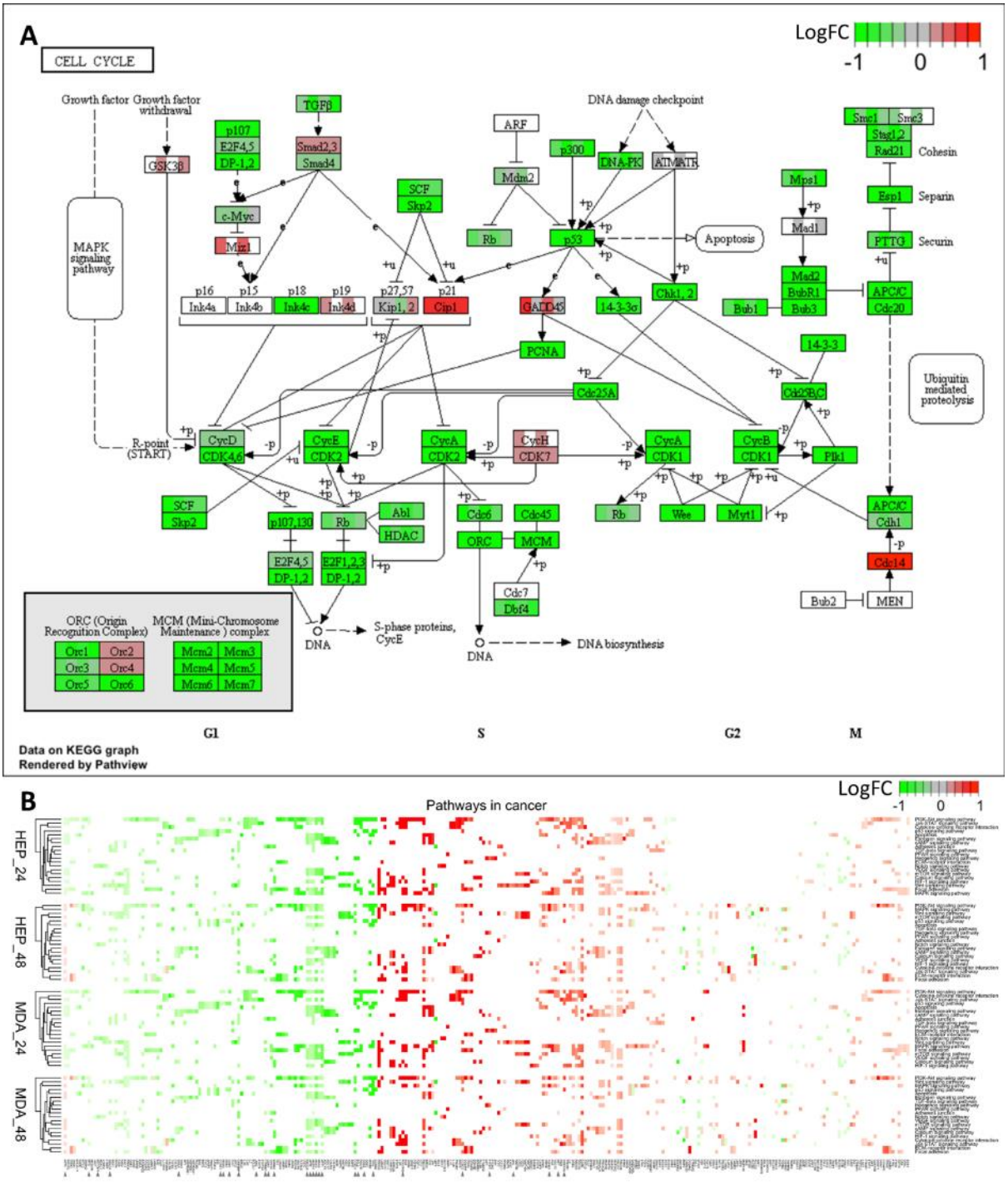
A
CELL CYCLE
LogFC
-1
0
1
Growth factor
Growth factor withdrawal
TGFβ
DNA damage checkpoint
ARF
Smc1
Smc3
Stag1,2
Rad21
Cohesin
p107
E2F4,5
DP-1,2
Smad2,3
Smad4
GSK3β
Mdm2
p300
DNA-PK
ATM/ATR
Mps1
Esp1
Separin
SCF
Skp2
c-Myc
Mxi1
Rb
p53
Apoptosis
Mad1
PTTG
Securin
MAPK signaling pathway
p16
Ink4a
p15
Ink4b
p18
Ink4c
p19
Ink4d
p27,57
Kip1, 2
p21
Cip1
GADD45
14-3-3σ
Chk1, 2
Bub1
Mad2
BubR1
Bub3
APC/C
Cdc20
PCNA
14-3-3
Ubiquitin mediated proteolysis
Cdc25A
Cdc25C
R-point
(START)
CycD
CDK4,6
CycE
CDK2
CycA
CDK2
CycH
CDK7
CycA
CDK1
CycB
CDK1
Plk1
SCF
Skp2
p107,130
Rb
Abl
HDAC
Cdc6
Cdc45
ORC
MCM
Rb
Wee
Myt1
APC/C
Cdh1
Cdc14
E2F4,5
DP-1,2
E2F1,2,3
DP-1,2
Cdc7
Dbf4
Bub2
MEN
ORC (Origin Recognition Complex)
Orc1
Orc2
Orc3
Orc4
Orc5
Orc6
MCM (Mini-Chromosome Maintenance) complex
Mcm2
Mcm3
Mcm4
Mcm5
Mcm6
Mcm7
DNA
S-phase proteins, CycE
DNA
DNA biosynthesis
G1
S
G2
M
Data on KEGG graph
Rendered by Pathview
B
Pathways in cancer
LogFC
-1
0
1
HEP_24
HEP_48
MDA_24
MDA_48

649

650

651 Fig. 7

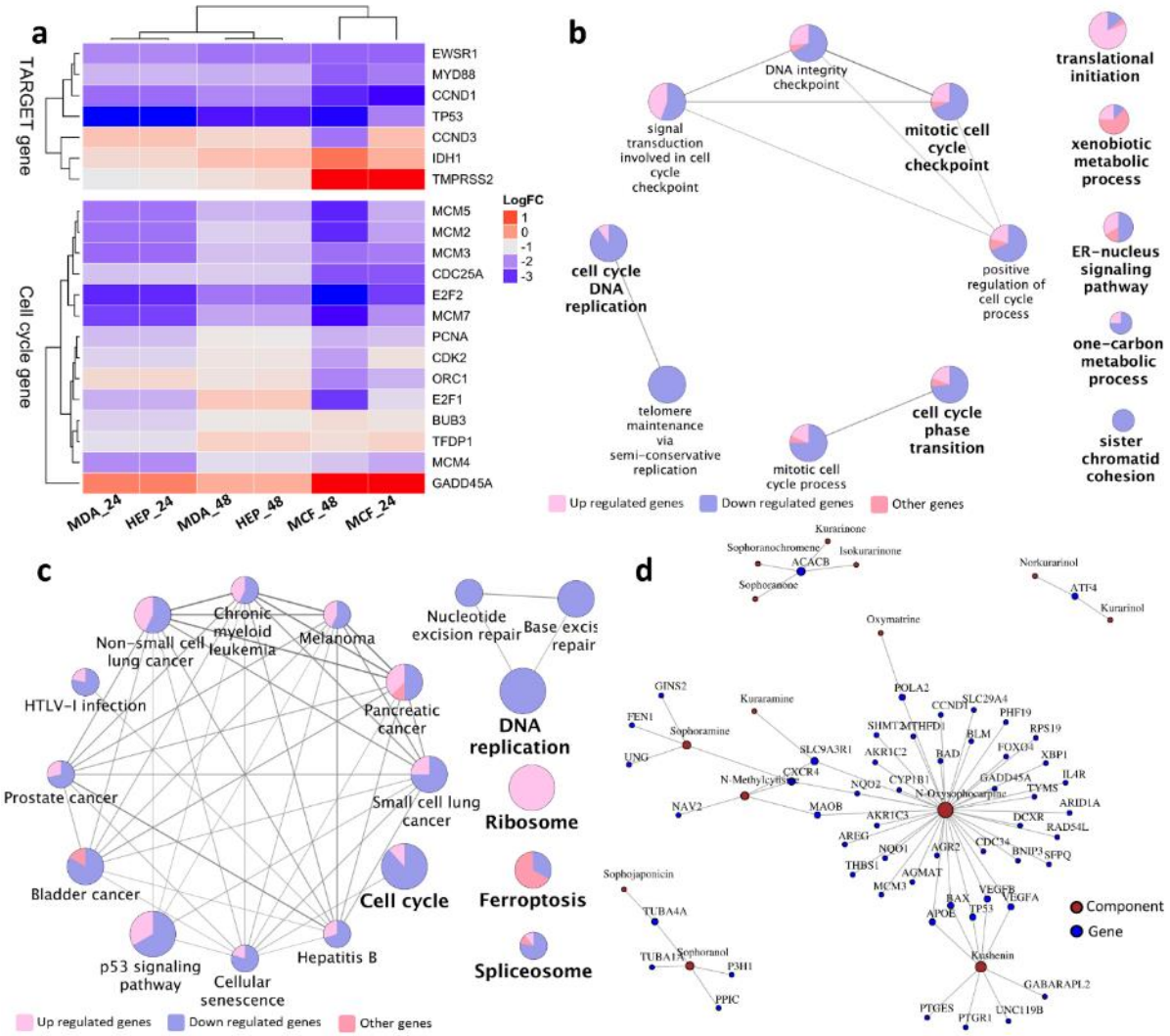

652

653

Chapter 6

Cell Cycle, Glycolysis and DNA Repair Pathways in Cancer Cells are Suppressed by Compound Kushen Injection

Previous work identified the cell cycle, energy metabolism and DNA replication/repair as candidate target pathways and they were selected for validation experiments. We carried out a series of experiments to validate the effects of CKI on energy charge, lactate production, glucose consumption, DNA double strand breaks (DSB) and the ku70/ku80 protein complex in DNA repair in MDA-MB-231 and HEPG2 cell lines. Decreased reduction in energy charge, increased lactate production and reduced glucose consumption along with decreased levels of proteins responsible for cell cycle regulation and DNA repair and increased levels of DSB were observed after treatment with CKI. This chapter is in the format of a manuscript accepted by *BMC Cancer*.

Statement of Authorship

Title of Paper	Cell Cycle, Glycolysis and DNA Repair pathways in Cancer Cells are Suppressed by Compound Kushen Injection
Publication Status	☐ Published ☐ Accepted for Publication ☑ Submitted for Publication ☐ Unpublished and Unsubmitted work written in manuscript style
Publication Details	Jian Cui, Zhipeng Qu, Yuka Harata-Lee, Thazin Nwe Aung, Hanyuen Shen, David L. Adelson. "Cell Cycle, Glycolysis and DNA Repair pathways in Cancer Cells are Suppressed by Compound Kushen Injection". doi: https://doi.org/10.1101/348102

Principal Author

Name of Principal Author (Candidate)	Thazin Nwe Aung		
Contribution to the Paper	Assisted with experiments		
Overall percentage (%)	25%		
Certification:	This paper reports on original research I conducted during the period of my Higher Degree by Research candidature and is not subject to any obligations or contractual agreements with a third party that would constrain its inclusion in this thesis. I am the primary author of this paper.		
Signature		Date	5/11/2018

Co-Author Contributions

By signing the Statement of Authorship, each author certifies that:

i. the candidate's stated contribution to the publication is accurate (as detailed above);

ii. permission is granted for the candidate in include the publication in the thesis; and

iii. the sum of all co-author contributions is equal to 100% less the candidate's stated contribution.

Name of Co-Author	Jian Cui		
Contribution to the Paper	Designed and carried out the experiments, analysed data and wrote the manuscript.		
Signature		Date	5/11/2018

Name of Co-Author	Zhipeng Qu		
Contribution to the Paper	Experimental design, assisted with experiments, assisted with data analysis and wrote the manuscript.		
Signature		Date	5/11/2018

Please cut and paste additional co-author panels here as required.

Name of Co-Author	Yuka Harata-Lee		
Contribution to the Paper	Experimental design, assisted with experiments, assisted with data analysis and wrote the manuscript.		
Signature		Date	5/11/2018

Name of Co-Author	Hanyuen Shen		
Contribution to the Paper	Assisted with experiments		
Signature		Date	6/11/2018

Name of Co-Author	David L. Adelson		
Contribution to the Paper	Supervised the research, assisted the research with the funding, experimental design and wrote the manuscript.		
Signature		Date	5/11/18

Cell Cycle, Energy Metabolism and DNA Repair Pathways in Cancer Cells are Suppressed by Compound Kushen Injection

Jian Cui[1,2], Zhipeng Qu[1,2], Yuka Harata-Lee[1,2], Thazin Nwe Aung[1,2] Hanyuan Shen[1,2] David L Adelson[1,2*],

1 Department of Molecular and Biomedical Science, The University of Adelaide, North Terrace, Adelaide, South Australia, Australia, 5005

2 Zhendong Australia - China Centre for Molecular Chinese Medicine, The University of Adelaide, North Terrace, Adelaide, South Australia, Australia, 5005

*Correspondence to: david.adelson@adelaide.edu.au

Abstract

In this report, we examine candidate pathways perturbed by Compound Kushen Injection (CKI) a Traditional Chinese Medicine (TCM) that we have previously shown to alter the gene expression patterns of multiple pathways and induce apoptosis in cancer cells. We have measured protein levels in Hep G2 and MDA-MB-231 cells for genes in the cell cycle pathway, DNA repair pathway and DNA double strand breaks (DSBs) previously shown to have altered expression by CKI. We have also examined energy metabolism by measuring [ADP]/[ATP] ratio (cell energy charge), lactate production and glucose consumption. Our results demonstrate that CKI can suppress protein levels for cell cycle regulatory proteins and DNA repair while increasing the level of DSBs. We also show that energy metabolism is reduced based on reduced glucose consumption and reduced cellular energy charge. Our results validate these pathways as important targets for CKI. We also examined the effect of the major alkaloid component of CKI, oxymatrine and determined that it had no effect on DSBs, a small effect on the cell cycle and increased the cell energy charge. Our results indicate that CKI likely acts through the effect of multiple compounds on multiple targets where the observed phenotype is the integration of these effects and synergistic interactions.

Keywords:
alkaloid, matrine, cyclin, Ku70, Ku80, cell-cycle

Abbreviations
DSBs, double strand breaks; Ku70/Ku80,the Ku heterodimer proteins

Introduction

Compound Kushen Injection (CKI) is a complex mixture of plant bioactives extracted from Kushen (*Sophora flavescens*) and Baituling (*Smilax Glabra*) that has been approved for use in China since 1995 by the State Food and Drug Administration (SFDA) of China (State medical license no. Z14021231). CKI is widely used in China as an adjunct for both radiotherapy and chemotherapy in cancer. While most of the data supporting its use have been anecdotal and there is little clinical trial data demonstrating its efficacy, it has been shown to be effective at reducing sarcoma growth and cancer pain in an animal model[1] and cancer pain in patients [2].

CKI contains over 200 chemical compounds including alkaloids and flavonoids such as matrine, oxymatrine and kurarinol, and has previously been shown to affect the cell cycle and induce apoptosis in cancer cells[1, 2, 3, 4, 5, 6, 7]. Furthermore, functional genomic characterization of the effect of CKI on cancer cells using transcriptome data indicated that multiple pathways were most likely affected by CKI [4]. These observations support a model wherein many/all of the individual compounds present in CKI can act on many single targets or on multiple targets to induce apoptosis.

Based on previously reported work [4] and our currently unpublished work (Cui *et al*)[8], specific pathways were selected for follow up experiments to validate their response to CKI in order to formulate more specific hypotheses regarding the mechanism of action of CKI on cancer cells. We had previously shown that CKI altered the cell cycle and induced apoptosis while altering the expression of many cell cycle genes in three cancer cell lines [4, 8]. We had also shown that DNA repair pathway genes were significantly down-regulated by CKI and that energy production related to NAD(P)H synthesis from glycolysis and oxidative phosphorylation was reduced by CKI. As a result, we focused on the following candidate pathways: cell cycle, DNA repair and glucose metabolism to validate their alteration by CKI. We used two cell lines for these validation experiments, one relatively insensitive to CKI (MDA-MB-231) and one sensitive to CKI (Hep G2). Furthermore, while the literature shows varying effects for major compounds present in CKI on cancer cells [9, 10], we also tested oxymatrine, the major alkaloid found in CKI and widely believed to be very important for the effects of CKI, on our selected pathways.

Materials and methods

Cell culture and chemicals

CKI with a total alkaloid concentration of 26.5 mg/ml in 5 ml ampoules was provided by Zhendong Pharmaceutical Co. Ltd. (Beijing, China). Cell culture methods have been previously described [4].

A human breast adenocarcinoma cell line, MDA-MB-231 and a hepatocellular carcinoma cell line Hep G2 were purchased from American Type Culture Collection (ATCC, Manassas, VA). The cells were cultured in Dulbecco's Modified Eagle Medium (DMEM; Thermo Fisher Scientific, MA, USA)

supplemented with 10% fetal bovine serum (Thermo Fisher Scientific). Both cell lines were cultured at 37℃ with 5% CO2. For all *in vitro* assays, cells were cultured overnight before being treated with either CKI (at 1 mg/ml and 2 mg/ml of total alkaloids). As a negative control, cells were treated with medium only and labeled as "untreated". After 24 and 48 hours of treatment, cells were harvested and subjected to the downstream experiments.

All the *in vitro* assays employed either 6-well plates or 96-well plates. The seeding density for 6-well plates for both cell lines was 4×10^5 cells and treatment methods were as previously described [4]. The seeding density of Hep G2 cells for 96 well plates was 4×10^3 cells per well and for MDA-MB-231 cells was 8×10^4 cells per well, and used the same treatment method as above: after seeding and culturing overnight, cells were treated with 2 mg/ml CKI diluted with complete medium for the specified time.

Glucose consumption assay

Glucose consumption was determined by using a glucose oxidase test kit (GAGO-20, Sigma, St. Louis, MO). After culturing for different durations (3, 6, 12, 24 and 48 hours), 50 μl of culture medium was collected from untreated groups and treated groups. The cells were trypsinized for cell number determination using trypan blue exclusion assay and the number of bright, viable cells were counted using a hemocytometer. Collected suspension, blank medium and 2 mg/ml CKI, were all filtered and diluted 100 fold with MilliQ water. The absorbance at 560 nm was converted to glucose concentration using a 5μg/ml glucose standard from the kit as a single standard. Glucose consumption was calculated by subtracting the blank medium value from treated/collected medium values. Glucose consumption per cell was calculated from the number of cells determined above.

Measurement of [ADP]/[ATP] ratio

Cells were cultured in white 96-well plates with clear bottoms. The [ADP]/[ATP] ratio of both cell lines was determined immediately after the incubation period (24 and 48 hours) using an assay kit (MAK135; Sigma Aldrich, USA) according to the manufacturer's instructions. Levels of luminescence from the luciferase-mediated reaction were measured using a plate luminometer (PerkinElmer 2030

multilabel reader, USA for CKI experiments or Promega, USA for oxymatrine experiments). The [ADP]/[ATP] ratio was calculated from the luminescence values using a formula provided by the kit manufacturer.

Lactate content assay

The concentration of lactate, the end product of glycolysis, was determined using a lactate colorimetric assay kit (Abcam, Cambridge, MA, USA). Cells were cultured in 6-well plates, and then harvested and deproteinized according to the manufacturer's protocol. The optical density was measured at 450 nm and a standard curve plot (nmol/well vs. OD 450 nm) was generated using serial dilutions of lactate. Lactate concentrations were calculated with the formula provided by the kit manufacturer.

Cell cycle assay

Cells were cultured in 6-well plates and treated with 2 mg/ml CKI or 0.5 mg/ml oxymatrine. After culturing for 3, 6, 12, 24 and 48 hours, cells were harvested and subjected to cell cycle analysis by Propidium Iodide staining as previously reported [4]. Data were obtained by flow cytometry using Accrui (BD Biosciences, NJ, US) and analysed using FlowJo software (Tree Star Inc, Ashland, Oregon, USA).

Microscopy

After culturing for 48 hours on 8 well chamber slides, control and treated cells were fixed in 1% paraformaldehyde for 10 minutes at room temperature, washed with Phosphate Buffered Saline three times and permeabilized with 0.5% Triton X-100 for 10 minutes. After fixation and permeabilization, cells were blocked with 5% Fetal Bovine Serum for 30 minutes. Permeabilized cells were stained with 5μg/ml of Alexa Fluor®594 conjugated anti-H2AX.X Phospho (red) (Biolegend, Ser139) in 5% Fetal Bovine Serum overnight followed with Alexa Fluor®488 conjugated Phalloidin (green) (Biolegend) staining for 20 minutes at 4℃.

Stained cells were mounted with 4',6-diamidino-2-phenylindole (DAPI) and visualized with an Olympus FV3000 (Olympus Corporation, Tokyo, Japan) confocal microscope using a 60× oil objective. Fluorescence intensity was quantified using Imaris software (Bitplane, Saint Paul, MN) and averaged using at least 10 cells in each experiment.

Flow-cytometry quantification of protein expression

Cells were cultured in 6-well plates and treated with CKI. After 24 and 48 hours, cells were harvested to detect intranuclear/intracellular levels of proteins involved in cell cycle and DNA DSBs pathways using the following antibodies; (cell cycle primary antibodies: (Cell Signaling Technologies, Danvers, MA, USA: P53 Rabbit mono-Ab, CCND1 Rabbit mono-Ab, CDK2 Rabbit mono-Ab) (Abcam, Cambridge, UK:CDK1 Rabbit mono-Ab), for these primaries, cell cycle isotype control: Cell Signaling Technologies: Rabbit igG, cell cycle secondary antibody Anti-rabbit (PE conjugated), additional primary antibody: CTNNB1 Rabbit mono-Ab (Alexa Fluor®647 conjugated) and isotype control: Rabbit IgG (Alexa Fluor®647 conjugated), both from Abcam)(DSBs antibody: Anti-H2AX (PE conjugated) primary antibody and isotype control: Mouse IgG1 (PE conjugated) both from BioLegend, San Diego, CA, USA) (DNA repair antibodies: primary antibodies - KU70 Rabbit mono-Ab (Alexa Fluor®647 conjugated) and KU80 Rabbit mono-Ab (Alexa Fluor®647 conjugated), Isotype control: Rabbit IgG (Alexa Fluor®647 conjugated), all from Abcam) Cells were sorted and the data acquired on a FACS Canto (BD Biosciences, NJ, US) or Accrui (BD Biosciences, NJ, US), and the data were analysed using FlowJo (Tree Star Inc.) software.

Cell cycle functional enrichment re-analysis

In order to identify the phases of the cell cycle affected by CKI, differentially expressed gene data from [4] was submitted to the Reactome database[11], and used to identify functionally enriched genes.

Statistical analysis

All measurements above were performed in triplicate and repeated at least three times. Statistical significance was determined by two-way ANOVA test; error bars represent standard deviation.

Results

Pathway validation

Based on our previous results indicating that CKI could suppress NAD(P)H synthesis [4] and (Supplementary Material, Figure S1), we examined the effect of CKI on energy metabolism by measuring glucose uptake, [ADP]/[ATP] ratio and lactate production. We measured glucose uptake in both CKI treated and untreated cells from 0 to 48 hrs after treatment and observed a reduction in glucose uptake (Fig. 1A). The growth curves for both cell lines were relatively flat after CKI treatment, in contrast to untreated cells. MDA-MB-231 cells, which are less sensitive to CKI in terms of apoptosis, had a higher level of glucose uptake than Hep G2 cells, which are more sensitive to CKI. Because the overall glucose uptake was consistent with the cell growth curves, the glucose consumption per million cells for each cell line under treatment was different. Untreated Hep G2 cells maintained a relatively flat rate of glucose consumption per million cells, while for CKI treated Hep G2 cells the rate of glucose consumption per million cells decreased with time, becoming significantly less towards 48 hrs. The glucose consumption variance for both untreated and treated MDA-MB-231 cells was high, but both overall glucose consumption and glucose consumption per million cells appeared to decrease over time.

Because changes in glucose consumption are mirrored by other aspects of energy metabolism, we assessed the energy charge of both CKI treated and untreated cells by measuring the [ADP]/[ATP] ratio at 24 and 48 hours after treatment (Fig. 1B). Hep G2 cells had a lower energy charge (higher [ADP]/[ATP] ratio) compared to MDA-MB-231 cells and after CKI treatment both cell lines showed a decrease in energy charge, consistent with our previous measurements using a 2,3-Bis(2-methoxy-4-nitro-5-sulfonyl)-2H-tetrazolium-5-carboxanilideinner salt (XTT) assay (Supplementary Material, Figure S1). However, the decrease in energy charge was earlier and much

more pronounced for Hep G2 cells compared to MDA-MB-231 cells.

The flip side of glucose consumption is the production of lactate via glycolysis, which is the initial pathway for glucose metabolism. We, therefore, measured lactate production in order to determine if the observed decreases in energy charge and glucose consumption were directly attributable to reduced glycolytic activity. We measured intracellular lactate concentration in both CKI treated and untreated cells at 24 and 48 hours after treatment (Fig. 1C) and found that lactate concentrations increased as a function of CKI treatment in both cell lines. This result is consistent with a build up of lactate due to an inhibition of the Tricarboxylic Acid (TCA) cycle leading to decreased oxidative phosphorylation and lower cellular energy charge. CKI must, therefore, inhibit cellular energy metabolism downstream of glycolysis, most likely at the level of the TCA cycle. Decreased energy charge can have widespread effects on a number of energy-hungry cellular processes involved in the cell cycle, such as DNA replication.

Having validated the effect of CKI on cellular energy metabolism, we proceeded to examine the perturbation of cell cycle and the expression of cell cycle proteins, as these are energy intensive processes. We had previously identified the cell cycle as a target for CKI based on transcriptome data from CKI treated cells [4, 8]. We carried out cell cycle profiling on CKI treated and untreated cells using Propidium Iodide staining and FACS (Fig. 2A) as described in Materials and Methods. The two cell lines displayed slightly different profiles to each other, but their response to CKI was similar in terms of an increase in the proportion of cells in G1-phase. For Hep G2 cells, CKI caused consistent reductions in the proportion of cells in S-phase accompanied by corresponding increases in the proportion of cells in G1-phase. This is indicative of a block in S-phase leading to accumulation of cells in G1-phase. For MDA-MB-231 cells, CKI did not promote a significant decrease in the proportion of cells in S-phase, but did cause an increase in the percentage of cells in G1 phase at 24hrs and a pronounced decrease in cells in G2/M phase at 12 hours.

We also examined the levels of key proteins involved in the cell cycle pathway (Cyclin D1:CCND1,Cyclin Dependent Kinase 1:CDK1, Cyclin Dependent Kinase 2:CDK2, Tumor Protein p53:TP53 and Catenin Beta 1:CTNNB1) at 24 and 48 hours after CKI treatment previously shown to have altered transcript expression by CKI (Fig. 2B). Both cell lines showed similar results for all five proteins, with decreased levels caused by CKI, and validated previous RNAseq data [4, 8]. CCND1 regulates the cell-cycle during G1/S transition. CDK-1 promotes G2-M transition, and

regulates G1 progress and G1-S transition. CDK-2 acts at the G1-S transition to promote the E2F transcriptional program and the initiation of DNA synthesis, and modulates G2 progression. TP53 acts to negatively regulate cell division. CTNNB1 acts as a negative regulator of centrosome cohesion. Down-regulation of these proteins is therefore consistent with cell cycle arrest/dysregulation and the cell cycle result in Fig. 2A. These results indicate that CKI alters cell cycle regulation consistent with cell cycle arrest. Cell cycle arrest is also an outcome that can result from DNA damage such as DSBs [12].

We had previously observed that DNA repair genes had lower transcript levels in CKI treated cells [4, 8], so hypothesised that this might result in increased numbers of DSBs. We measured the expression of γ-H2AX in both cell lines (Fig. 3A) and found that it was only over-expressed at 48 hours in CKI treated Hep G2 cells. We also carried out localization of γ-H2AX using quantitative immunofluorescence microscopy and determined that the level of γ-H2AX increased in nuclei of CKI treated cells in both cell lines (Fig. 3B). These results indicated an increase in DSBs as a result of CKI treatment. In order to confirm if reduced expression of DNA repair proteins was correlated with the increase in DSBs, we measured levels of Ku70/Ku80 proteins in CKI treated cells (Fig. 3C). In Hep G2 cells, Ku80, a critical component of the Non-Homologous End Joining (NHEJ) DNA repair pathway was significantly down regulated at both 24 and 48 hours after CKI treatment. In MDA-MB-231 cells, Ku70 expression was down-regulated at both 24 and 48 hours after CKI treatment, and Ku80 was down-regulated at 24 hours. Because Ku70/Ku80 are subunits of a required DNA repair complex, reduced expression of either subunit will result in decreased DNA repair. Our results, therefore, support a suppressive effect of CKI on DNA repair, likely resulting in an increased level of DSBs.

Effect of Oxymatrine, the principal alkaloid in CKI

Because CKI is a complex mixture of many plant secondary metabolites that may have many targets and there is little known about its molecular mode of action, we examined the effects of the most abundant single compound found in CKI, oxymatrine, on the most sensitive cell line, Hep G2. Oxymatrine is an alkaloid that has previously been reported to have effects similar to CKI, so we expected it might have an effect on one or more of our three validated pathways.

Oxymatrine, at 0.5 mg/ml which is equivalent to the concentration of oxymatrine in 2mg/ml CKI, did not have an equivalent effect on the cell cycle compared to CKI (Fig. 4A vs Fig. 2A). Oxymatrine caused only minor changes to the cell cycle with small but significant increases in the proportion of cells in G1-phase at 3 and 48 hours and a small but significant decrease in the proportion of cells in S1-phase at 48 hours. Oxymatrine also caused a significant increase in the proportion of cells undergoing apoptosis in Hep G2 cells, albeit at a lower level than CKI (Supplementary Material, Figure 2).

Oxymatrine had no effect on H2AX levels in Hep G2 cells (Fig. 4B). This was in stark contrast to the effect of CKI (Fig. 3A) at 48 hours and indicated that oxymatrine alone had no effect on the level of DSBs.

Surprisingly, oxymatrine had the opposite effect on energy metabolism compared to CKI, causing a decrease in [ADP]/[ATP] ratio indicating a large increase in the energy charge of the cells (Fig. 4C).

Integration of results

The effect of CKI on cancer cells was validated in all three of our candidate pathways: cell cycle, energy metabolism and DNA repair. Because these pathways are not isolated, but instead are integrated aspects of cell physiology CKI may act through targets in some or all of these three pathways or may act through other targets that either directly or indirectly suppress these pathways. CKI may also act through the synergistic effects of multiple compounds on multiple targets in our candidate pathways. This possibility is consistent with the partial and minor effects of oxymatrine on our candidate pathways.

Discussion

We have validated three pathways (cell cycle, energy metabolism and DNA repair) that are perturbed by CKI and that can be used as the focus for further investigations to identify specific molecular targets that mediate the perturbations.

Cell cycle perturbation by CKI

Our results show that CKI can perturb the cell cycle by altering the proportions of cells in G1-phase, S-phase and G2/M-phase. This result is similar to what we have observed before [4, 8], but has not been widely reported in the literature. The alkaloid oxymatrine, the most abundant compound present in CKI, has also been shown previously to perturb a number of signaling pathways [13] and alter/arrest the cell cycle in a variety of cancer cells [14, 15, 16, 17, 18] and we have confirmed this observation (Fig. 4A) in Hep G2 cells. Our results permit direct comparison with CKI because our experiments have been done using equivalent concentrations of oxymatrine alone or in CKI. While oxymatrine has an effect on the cell cycle, it is not as effective at perturbing the cell cycle as is CKI. This indicates that oxymatrine must interact with other compounds in CKI to have a stronger effect on the cell cycle.

Energy metabolism suppression by CKI

We have shown for the first time that CKI can inhibit energy metabolism as demonstrated by lower levels of NADH/NADPH and a higher [ADP]/[ATP] ratio. These results, combined with lower glucose utilisation and higher lactate levels indicate that this suppression was likely due to inhibition of the TCA cycle or oxidative phosphorylation. Previously, Gao *et al* [3] have reported that CKI significantly increased the concentration of pyruvate in the medium and this observation in combination with our results supports a decrease in metabolic flux through the TCA cycle as the likely cause of the reported suppression of energy metabolism. Interestingly, oxymatrine on its own had the opposite effect on [ADP]/[ATP] ratio compared to CKI, indicating that it can enhance energy metabolism and increase the energy charge of the cell.

DNA repair suppression by CKI

There is only one report in the literature of oxymatrine inducing DSBs [19] and no reports with respect to CKI. Our results show for the first time that not only does CKI induce DSBs, but that is also likely inhibits DNA repair by decreasing the expression of the Ku70/Ku80 complex required for NHEJ mediated DNA repair. It is worth noting, however, that the reported effect of oxymatrine on

DSBs [19] uses significantly higher (4-8 fold) concentrations of oxymatrine compared to our experiments. In our hands oxymatrine alone at 0.5mg/ml showed no effect on DSBs as judged by the level of γ-H2AX after 24 or 48 hours.

Conclusions

CKI causes suppression of energy metabolism and DNA repair along with altered cell cycle (summarized in Fig. 5). CKI has also previously been reported to induce apoptosis in cancer cells [4]. The overarching question is if CKI has independent effects on these three pathways or if the primary effect of CKI is through a single pathway that propagates effects to other, physiologically linked pathways. It may be that CKI suppresses energy metabolism thus disrupting downstream, energy-hungry processes such as DNA replication and DNA repair. Alternatively, there could be independent effects on DNA repair leading to checkpoint-induced cell cycle perturbation/arrest. Our results based on oxymatrine treatment of Hep G2 cells indicate that the cell-cycle is likely directly affected by oxymatrine and thus CKI. However, oxymatrine alone had no effect on DNA repair and boosted, rather than reduced the energy charge of the cell. Taken together, these results support a model of many compounds/many targets [20] for the mode of action of CKI, where multiple compounds affect multiple targets and the synergistic, observed effect is significantly different to that seen with individual components.

Acknowledgements

We would like to thank Prof. Frank Grutzner for providing DAPI, Adelaide Microscopy for training and equipment use and Jue Zhang, Bo Han and Dan Kortschak for helpful discussions.

Funding

This project is supported by The Special International Cooperation Project of Traditional Chinese Medicine (GZYYGJ2017035) and The University of Adelaide - Zhendong Australia - China Centre

for Molecular Chinese Medicine.

Availability of data and materials

All data analyzed in this study are available from the public source NCBI (https://www.ncbi.nlm.nih.gov/) and details can be found in the supplementary file.

Author's contributions

J.C, Z.Q., Y.H-L. and D.L.A. designed research; J.C., Y-H-L., Z.Q., T.N.A. and H.S. performed research; and J.C., Z.Q., Y.H-L. and D.L.A wrote the paper.

Ethics approval and consent to participate

Not applicable.

Consent for publication

Not applicable.

Competing interests

The authors declare that they have no competing interests.

References

1. Zhao Z, Fan H, Higgins T, Qi J, Haines D, Trivett A, et al. Fufang Kushen injection inhibits sarcoma growth and tumor-induced hyperalgesia via TRPV1 signaling pathways. Cancer Letters. 2014 Dec;355(2):232–241. Available from: http://dx.doi.org/10.1016/j.canlet.2014.08.037.

2. Wang W, You Rl, Qin Wj, Hai Ln, Fang Mj, Huang Gh, et al. Anti-tumor activities of active ingredients in Compound Kushen Injection. Acta Pharmacologica Sinica. 2015;36(6):676.

3. Gao L, Wang KX, Zhou YZ, Fang JS, Qin XM, Du GH. Uncovering the anticancer mechanism of Compound Kushen Injection against HCC by integrating quantitative analysis, network analysis and experimental validation. Sci Rep. 2018 Jan;8(1):624.

4. Qu Z, Cui J, Harata-Lee Y, Aung TN, Feng Q, Raison JM, et al. Identification of candidate anti-cancer molecular mechanisms of Compound Kushen Injection using functional genomics. Oncotarget. 2016 10;7(40):66003–66019.

5. Zhou SK, Zhang RL, Xu YF, Bi TN. Antioxidant and immunity activities of Fufang Kushen Injection Liquid. Molecules. 2012 May;17(6):6481–90.

6. Sun M, Cao H, Sun L, Dong S, Bian Y, Han J, et al. Antitumor activities of kushen: literature review. Evid Based Complement Alternat Med. 2012;2012:373219.

7. Xu W, Lin H, Zhang Y, Chen X, Hua B, Hou W, et al. Compound Kushen Injection suppresses human breast cancer stem-like cells by down-regulating the canonical Wnt/β-catenin pathway. J Exp Clin Cancer Res. 2011 Oct;30:103.

8. Cui J, Qu Z, Harata-Lee Y, Shen H, Aung TN, Wang W, et al. The Effect of Compound Kushen Injection on Cancer Cells: Integrated Identification of Candidate Molecular Mechanisms.;. (Manuscript submitted).

9. Ma X, Li RS, Wang J, Huang YQ, Li PY, Wang J, et al. The Therapeutic Efficacy and Safety of Compound Kushen Injection Combined with Transarterial Chemoembolization in Unresectable Hepatocellular Carcinoma: An Update Systematic Review and Meta-Analysis. Frontiers in Pharmacology. 2016 Mar;7. Available from: http://dx.doi.org/10.3389/fphar.2016.00070.

10. Zhongquan Z, Hehe L, Ying J. Effect of compound Kushen injection on T-cell subgroups and natural killer cells in patients with locally advanced non-small-cell lung cancer treated with concomitant radiochemotherapy. Journal of Traditional Chinese Medicine. 2016;36(1):14 – 18. Available from: http://www.sciencedirect.com/science/article/pii/S0254627216300024.

11. Fabregat A, Jupe S, Matthews L, Sidiropoulos K, Gillespie M, Garapati P, et al. The Reactome pathway knowledgebase. NUCLEIC ACIDS RESEARCH. 2018;46(D 1):D649–D655.

12. Shaltiel IA, Krenning L, Bruinsma W, Medema RH. The same, only different - DNA damage checkpoints and their reversal throughout the cell cycle. J Cell Sci. 2015 Feb;128(4):607–20.

13. Lu ML, Xiang XH, Xia SH. Potential Signaling Pathways Involved in the Clinical Application of Oxymatrine. Phytotherapy Research. 2016 May;30(7):1104–1112. Available from: http://dx.doi.org/10.1002/ptr.5632.

14. Li W, Yu X, Tan S, Liu W, Zhou L, Liu H. Oxymatrine inhibits non-small cell lung cancer via suppression of EGFR signaling pathway. Cancer Med. 2018 Jan;7(1):208–218.

15. He M, Jiang L, Li B, Wang G, Wang J, Fu Y. Oxymatrine suppresses the growth and invasion of MG63 cells by up-regulating PTEN and promoting its nuclear translocation. Oncotarget. 2017 Sep;8(39):65100–65110.

16. Li S, Zhang Y, Liu Q, Zhao Q, Xu L, Huang S, et al. Oxymatrine inhibits proliferation of human bladder cancer T24 cells by inducing apoptosis and cell cycle arrest. Oncol Lett. 2017 Jun;13(6):4453–4458.

17. Wu J, Cai Y, Li M, Zhang Y, Li H, Tan Z. Oxymatrine Promotes S-Phase Arrest and Inhibits Cell Proliferation of Human Breast Cancer Cells in Vitro through Mitochondria-Mediated Apoptosis. Biol Pharm Bull. 2017;40(8):1232–1239.

18. Ying XJ, Jin B, Chen XW, Xie J, Xu HM, Dong P. Oxymatrine downregulates HPV16E7 expression and inhibits cell proliferation in laryngeal squamous cell carcinoma Hep-2 cells in vitro. Biomed Res Int. 2015;2015:150390.

19. Wang Z, Xu W, Lin Z, Li C, Wang Y, Yang L, et al. Reduced apurinic/apyrimidinic endonuclease activity enhances the antitumor activity of oxymatrine in lung cancer cells. International journal of oncology. 2016;49(6):2331–2340.

20. Li FS, Weng JK. Demystifying traditional herbal medicine with modern approach. Nat Plants. 2017 Jul;3:17109.

Additional Files

Additional file 1 — Supplementary Information

Additional file contains supplementary figures and tables as referred to in the main body of the paper.

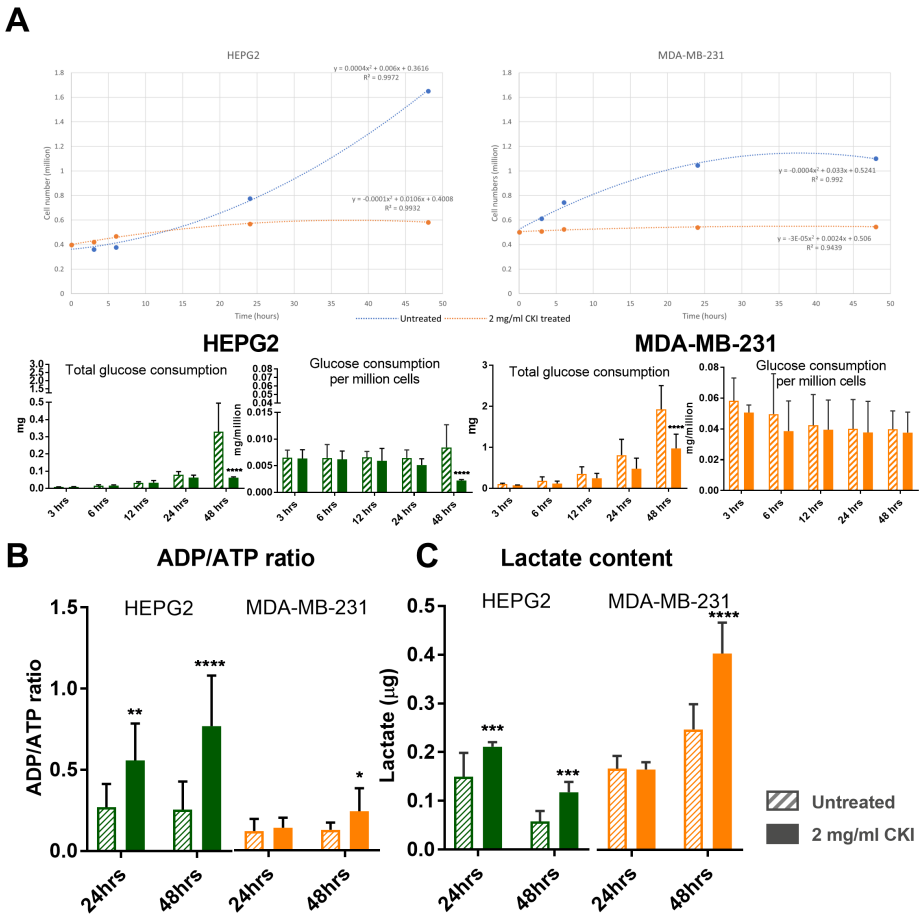

Figure 1. The energy metabolism determination assays in the two cell lines. A. Comparison of glucose consumption analysis between the two cell lines at 3, 6, 12, 24 and 48 hours. Overall glucose consumption is divided by cell number to calculate the consumption of glucose per million cells. B. [ATP]/[ADP] ratio assay result for the two cell lines at 24 and 48 hours. C. Lactate content detection for the two cell lines at 24 and 48 hours. Statistical analyses were performed using two-way ANOVA comparing treated with untreated (*p<0.05, **p<0.01, ***p<0.001, ****p<0.0001); bars show 1 standard deviation from the mean.

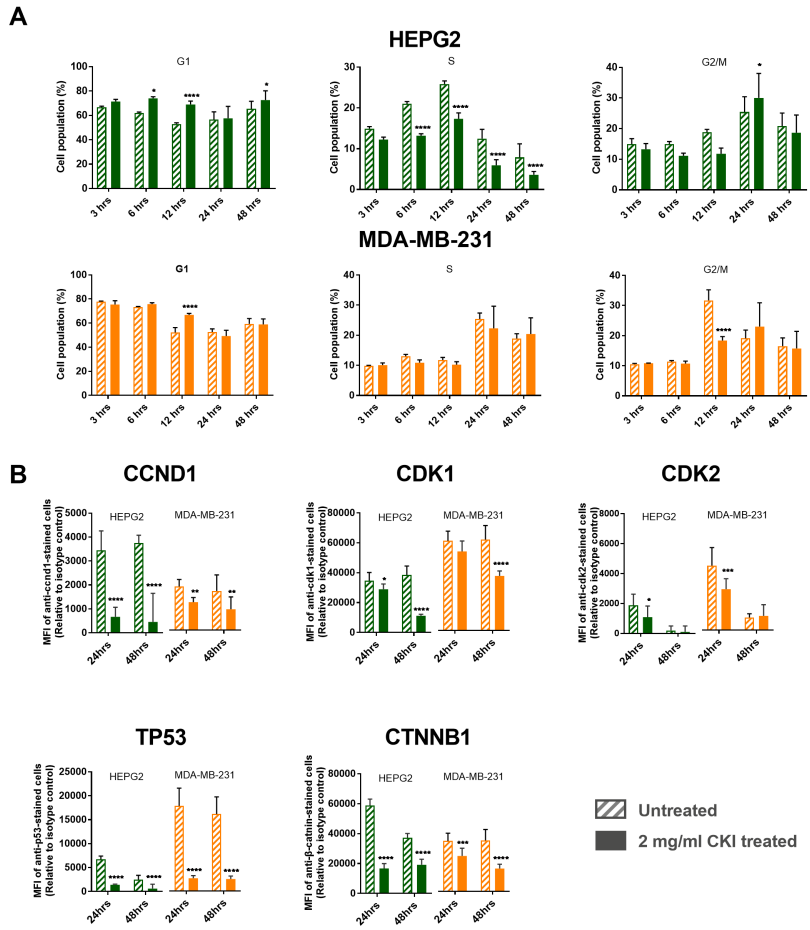

Figure 2. Cell cycle shift by CKI and undulating expression of the key proteins . A. Cell cycle shift regulated by CKI over 48 hours. In both cell lines, the earliest shifted cell cycle phase was S phase 6 hours after treatment. Compared to Hep G2, MDA-MB-231 showed delayed responses. B. Expression levels for 5 proteins (ccnd1, cdk1, cdk2, p53 and catenin β 1) as a result of CKI treatment at both 24 hours and 48 hours. Statistical analyses were performed using two-way ANOVA comparing with untreated (*p<0.05, **p<0.01, ***p<0.001, ****p<0.0001); bars show 1 standard deviation from the mean.

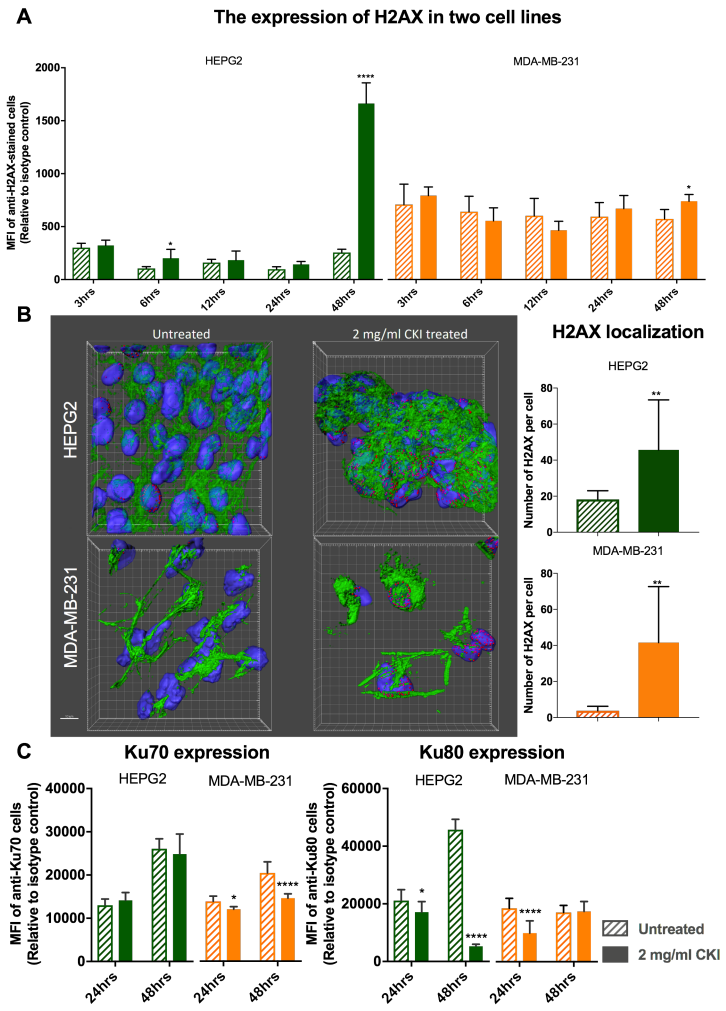

Figure 3. DSBs were increased by CKI treatment. A. γ-H2AX expression from 3 hours to 48 hours after treatment with 2 mg/ml CKI in two cell lines. B. Localization of γ-H2AX in two cell lines after CKI treatment for 48 hours. Green shows the cytoskeleton stained with an antibody to F-actin, blue is DAPI staining of nuclei, pink/red is staining of DSBs with antibody to γ-H2AX. The bar graph shows a quantification of the average number of γ-H2AX foci per cell detected in immunofluorescence images of 2 mg/ml CKI treated and untreated groups. At least 10 images of 3 independent replicate experiments were analyzed. C.Expression of DSBs repair proteins, Ku70 and Ku80, as a result of treatment with 2 mg/ml CKI in two cell lines. Statistical analyses were performed using two-way ANOVA comparing treated with untreated (*p<0.05, **p<0.01, ***p<0.001, ****p<0.0001); bars show 1 standard deviation from the mean.

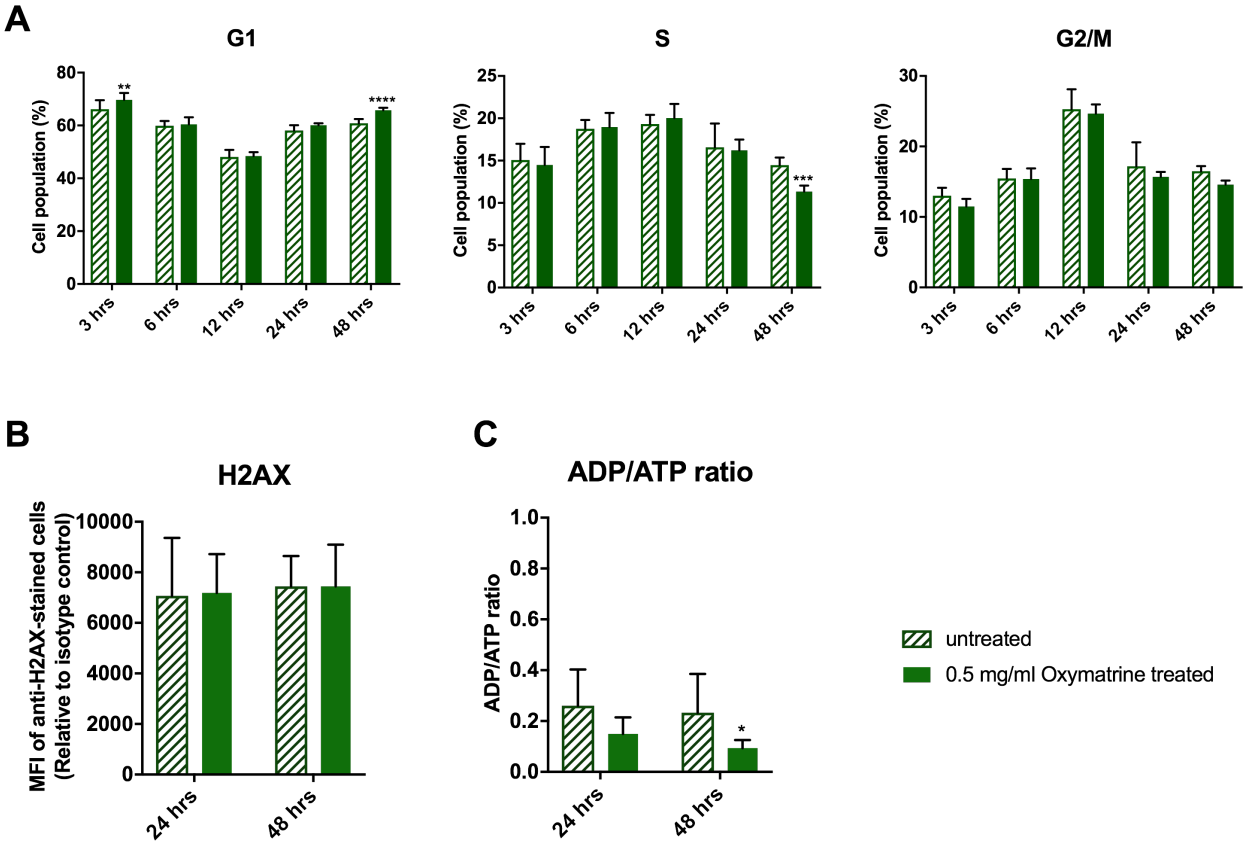

Figure 4. Effect of oxymatrine alone on validated pathways. Oxymatrine was tested at 0.5mg/mL which is equivalent to its concentration in CKI. A. Effect of oxymatrine on cell cycle in Hep G2 cells over 48 hours. B. Effect of oxymatrine on γ-H2AX (DSBs) levels after 24 and 48 hours. C. Effect of oxymatrine on [ADP]/[ATP] ratio after 24 and 48 hours. Statistical analyses were performed using two-way ANOVA comparing treated with untreated (*$p<0.05$, **$p<0.01$, ***$p<0.001$, ****$p<0.0001$); bars show 1 standard deviation from the mean.

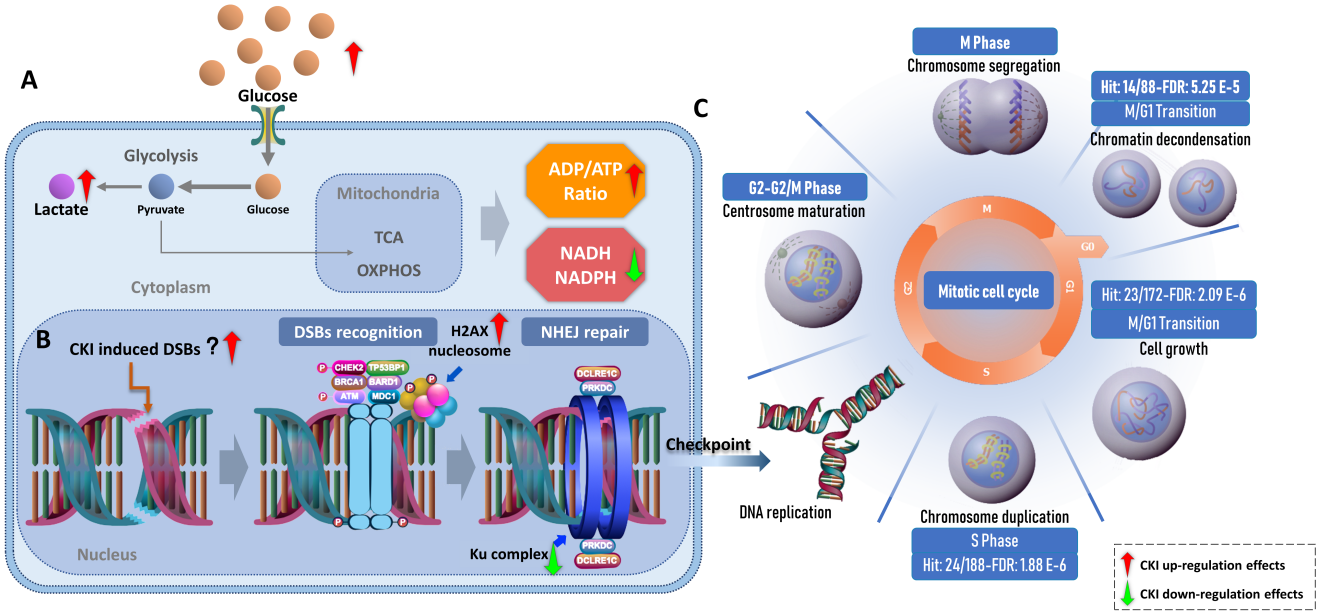

Figure 5. Integration of the three pathways altered by CKI. A. General presentation of energy metabolism affected by CKI. Glucose utilization is down-regulated by CKI. This is accompanied by increased lactate in the cytoplasm as CKI inhibits glucose metabolism downstream of glycolysis, leading to an increase in [ADP]/[ATP] and decrease in NADH/NADPH. B. Effects on DNA repair in cancer cells by CKI. CKI may be able to directly induce DSBs, but CKI may also indirectly induce DSBs by arresting checkpoint functions during the cell cycle. In addition, CKI may also inhibit NHEJ, the major repair mechanism for DSBs. C. Reactome functional enrichment of cell cycle genes based on shared differentially expressed (DE) genes from previous studies. From M/G1 to S phase, the shared DE genes from both cell lines were significantly enriched. Most of these DE genes, were down-regulated.

Chapter 7

Conclusions and Future Directions

For this dissertation, I have characterised the effects of CKI using various approaches. I have developed a novel research strategy for dissecting the molecular mode of action of components within CKI by associating phenotypic and global gene expression changes. The strategy is based on three approaches: 1) analytical chemistry approach to fractionate the components into different groups, 2) cellular approach that determines the phenotypic changes triggered by these fractionated mixtures, and 3) systems biology approach to identify their underlying molecular modes of action. In this study, oxymatrine and oxysophocarpine (Omt and Ospc) were the only two compounds that when depleted, caused measurable changes in the effects of CKI. Specifically, removal of N-OmtOspc paradoxically caused a significant increase in the ability of CKI to reduce viability and kill cells. It is worth noting that although compounds were well resolved using HPLC in this study, its detector has limited sensitivity for quantifying the molecular mass of the compounds, particularly when separating a compound mixture such as CKI which contains some structurally similar compounds that might potentially have isomers. On the other hand, MS determines the mass of each ion quantitatively and it is a relatively sensitive detection approach to detect the molecular mass of the compounds. The flip side of MS for analysing components from CKI is that multiple components in CKI not only are structurally similar but have same molecular mass and hence are difficulty to detect. Therefore, a combination of LC-MS technique would significantly enhance the detection and separation of CKI for future experiments. If it had been applied to this research, it would have provided more sensitivity and accuracy of the fractional deletion of the compounds from CKI. In this study, I have only applied LC-MS/MS to identify the nine known standard compounds in both original and fractionated mixtures and it has provided significant benefits for understanding the fractionated mixtures as compared to the original. Should further experiments be conducted using this fractional deletion approach, application of LC-MS/MS is highly recommended. By linking transcriptome analysis from different fractionated mixtures, changes of gene expression were mapped

with respect to changes in the phenotypes of the cells. In follow on work, the inhibition of cell migration/invasion by CKI was investigated in six cancer cell lines. By using HPLC separated major and minor components compared with CKI in cell migration/invasion assays, CKI was shown to be more inhibitory than either of the two fractions and that the minor peak fraction was more inhibitory than the major peak fraction. This suggests that the major and minor peaks/compounds may be synergistic in their contribution to the activity of CKI. Additional experiments showed that inhibition of migration and invasion probably occur through perturbation of the actin cytoskeleton, and impairment of lamellipodial extension via downregulation of gene products..

A prevailing view of TCM is that multiple components act on many targets in a many to many fashion, however, no hard evidence for this view has been published. Studies in this dissertation identify the complex and unpredictable interactions between components that make up CKI and support the notion that single compounds in TCM may often have no obvious effects but that combinations of such compounds can have significant effects on cancer cells. One possible effective mechanism that was beyond of the scope of this thesis was the possible effect of CKI treatment on tumor microenvironment (TME) which comprises various immune cells, fibroblasts, signaling molecules and ECM in the surrounding cellular environment of the tumor. TCM has been claimed to affect tumor microenvironment in several ways including inhibition of ECM degradation and angiogenesis and reversing immunosuppression. In our signaling pathway analyses, significant perturbation of ECM-receptor interaction, cytokine-cytokine receptor interaction and chemokine signaling pathways were observed as a result of CKI treatment suggesting its potential impact on the tumor microenvironment. The multiple *in vitro* cancer cell lines that we have examined in this study provided critical information of the mechanistic changes of the genes and signalling pathways as a result of CKI treatment in various cancers. The experiment conducted with the cell models was originally for the purpose of drug development and testing of developed anticancer drugs. Despite the fundamental data provided by the use of cancer cell lines, there is still an uncertainty on the fact whether or not these findings can be extrapolated to and translated into medical practice. As it has been stated above, an important fact when applying the herbal drug mixture to consider is the impurities of the extracted herbal medicine that have their own biological activities which may provide false positive signals of the molecules during drug screening. As a result, the observed effects of *in vitro* studies might have been associated with both anti-cancer activities and the on-target and off-target effects of CKI. Therefore, futher work on CKI to ensure better outcomes in cancer treatment will need appropriate preclinical *in vivo* models in follow-on experiments.

The major contribution of this study is the identification of a novel model for compound specific target gene identification that uses a subtractive fractionation approach. However, the specific protein targets for these compounds remain unknown. As future work, characterisation of the specific proteins that bind to compounds in CKI needs to be carried out. In order for a protein to have the potential as a drug target it must be druggable, i.e. have a conformation that favours interactions with small molecules. One approach to use for identifying these interactions could be the use of yeast two-hybrid screening, which is the most commonly used screening method to identify novel protein interactions, in the presence and absence of CKI in order to characterize specific protein-protein interactions that are perturbed by CKI. By comparing the interactions of tumor suppressors with oncoproteins as a result of CKI treatment, we might better characterise the genetic pathways leading to apoptosis and/or inhibition of metastasis. These interactions could be further explored by using subtractive fractions of CKI and individual compounds to map them to specific compounds or compound families. The yeast three-hybrid assay, where interactions between proteins and small molecules can be detected, which was developed based on the yeast two-hybrid method can be used to support the identification of specific compounds of CKI and their activities for drug screening.

Appendix A

Supplementary Tables, Data and Video

All the supplementary tables and data for chapters 2, 3, 4 and 5 can be obtained online: https://drive.google.com/open?id=1I9nQy4GzcALD3flYqgFHL9lJEm1C7a5w.

1. For chapter 2, there are one supplementary Data and one supplementary Table:

    a) Data 1. Calibration curve for the concentrations of known compounds in CKI and reconstituted subtractive fractions.

    b) Table 1. Summary of shared, differentially expressed (DE) genes across treatments. Similarity percentage calculated from total number of shared DE genes from all listed comparisons. To find the number of DE genes, CKI treatment was used as a baseline to compare all other fractionated treatments in order to emphasize the effect of depleted compounds and UT (untreated) was used as a base to calculate the DE genes for CKI treatment.

2. For chapter 3, there are three supplementary Data, one supplementary table and one supplementary video including:

    a) Data 1: Significantly over-represented functional GO terms, as determined by GO analysis of the transcriptome from CKI treated MDA-MB-231 cells. ($P < 0.05$).

    b) Data 2: Significantly perturbed pathways, as determined by SPIA analysis of the transcriptome from CKI treated MDA-MB-231 cells. ($pG < 0.05$).

    c) Data 3: Matching of genes in two strongly affected pathways (,Äúfocal adhesion,Äù and ,Äúactin cytoskeleton,Äù) against three independent gene datasets containing: (i) a set TARGET gene and (ii) migration related genes from published articles.

    d) Video: Live-cell imaging of the migration blocking effect of CKI in MDA-MB-231 cells in the wound closure migration assay. Videos show cell motility and wound closure rate in CKI at 2 mg/ml was reduced as compared to untreated control. Images were captured at 10-minute intervals for 20 hours.

    e) Table 1: Concentrations of Matrigel and number of cells used for each cell line in transwell invasion assay.

    f) Table 2: Fourteen clinically relevant DE genes from three independent gene datasets (see methods).

3. For chapter 4, there are six supplementary tables including:

    a) Table S1: Summary of RNA-seq datasets used in this study

    b) Table S2: Summary of significantly differentially expressed genes for different comparisons

    c) Table S3: Significantly perturbed KEGG pathways based on SPIA analysis

d) Table S4: Numbers of transcripts in 53 co-expression modules

e) Table S5: Significantly over-represented GO and KEGG terms in protein-coding genes from three CKI-5FU co-expression modules (count > 4 and P-value < 0.05)

f) Table S6: Primers used for qPCR

4. For chapter 5, there are four supplementary tables including:

a) Table S1. RT-qPCR target genes and their primer sequences.

b) Table S2. Mapping rate of each cell line.

c) Table S3. List of DE genes in each cell line at each time point.

d) Table S4. The summary of the functional analysis of both separate datasets and shared datasets.

i. Sheet 1-4: GO enrichment of each cell line at two time points. Selection standard: cut off p value<0.01, cut off q value<0.01.

ii. Sheet 5-8: KEGG enrichment of each cell line at two time points. Selection standard: cut off p value<0.01, cut off q value<0.01.

iii. Sheet 10-12: GO enrichment of each cell line at two time points. Selection standard: cut off p value<0.01, cut off q value<0.01.

iv. Sheet 13: GO enrichment of shared genes by both cell lines. Selection standard: cut off p value<0.01.

v. Sheet 14: KEGG enrichment of shared genes by both cell lines. Selection standard: cut off p value<0.01.

Appendix B

Supplementary Figures for Chapter 2

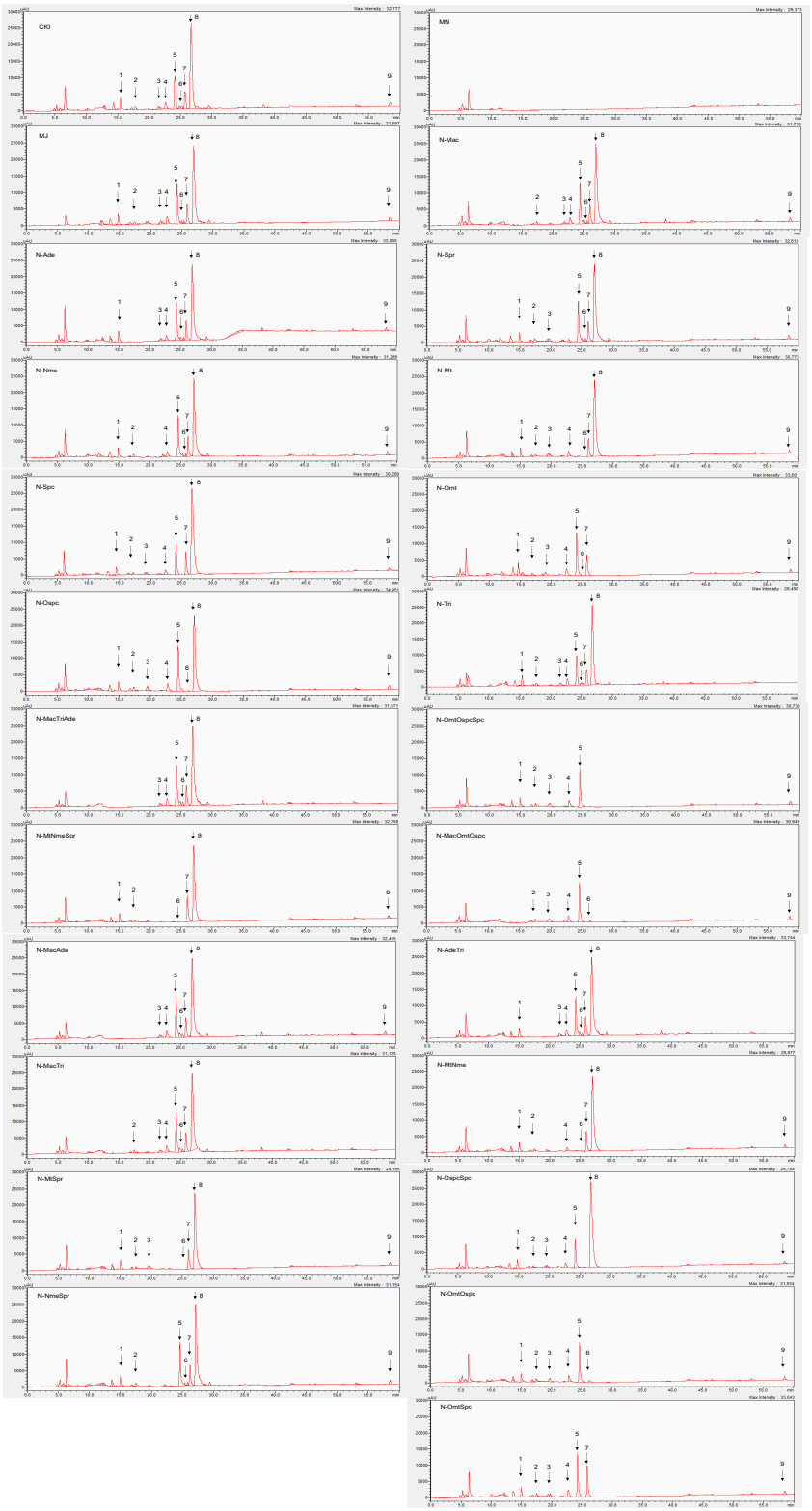

Sup. Fig. 1: HPLC profiles of 25 mixtures including CKI, MJ, MN, 9 (N-1), 4 (N-3), and 6 (N-2). Numbers represent compounds 1: Mac, 2: Ade, 3: Nme, 4: Spr, 5: Mt, 6: Spc, 7: Ospc, 8: Omt and 9: Tri. 50 µl of the samples at 1 mg/ml concentration was injected through the semi-preparative column to achieve the profiles.

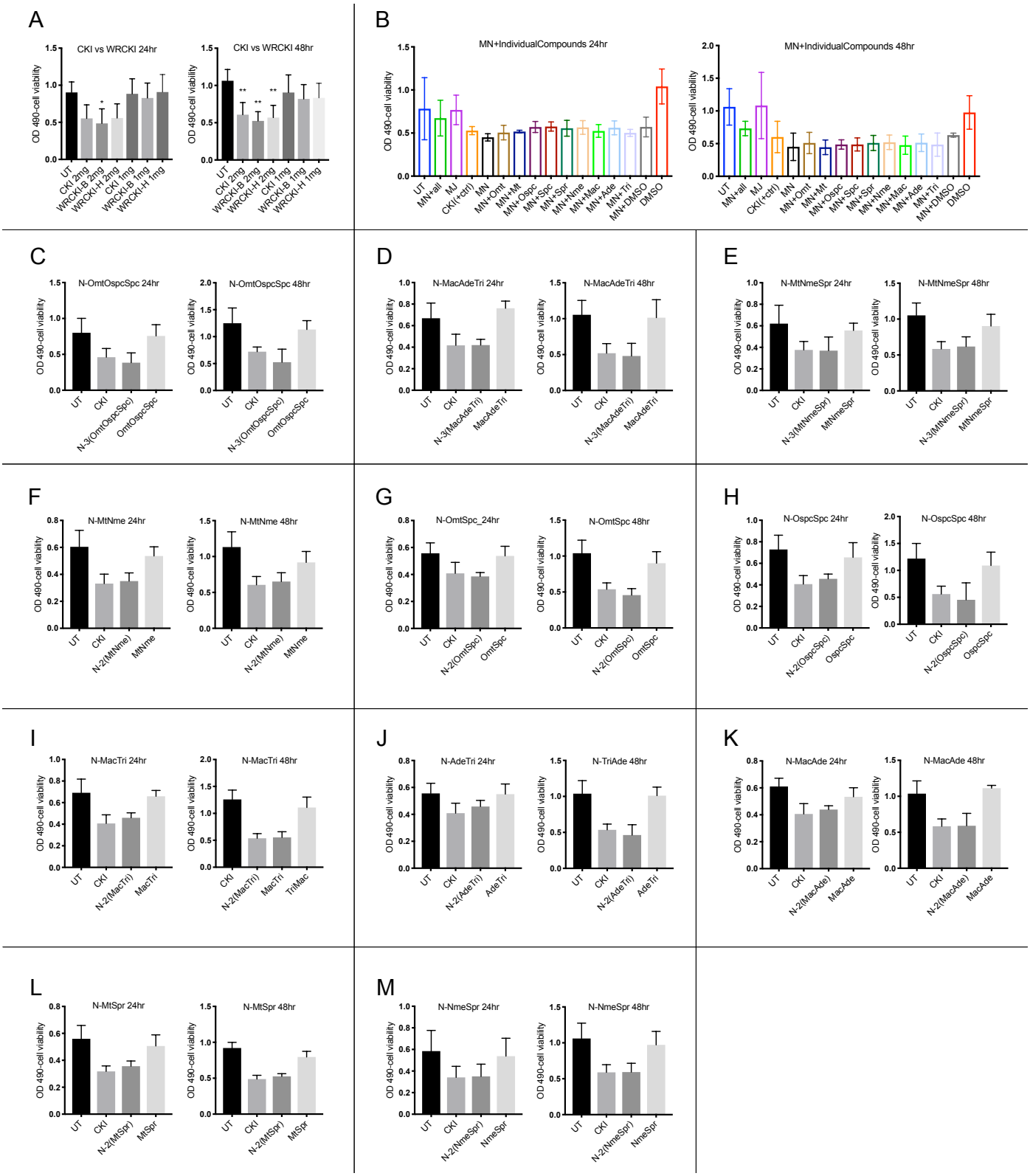

Sup. Fig. 2: XTT Cell viability assays of subtractive fractions in MDA-MB-231 cells at 24- and 48-hour timepoints treated with 1 mg/ml or 2 mg/ml of CKI and 2 mg/ml equivalent concentrations of all other treating agents. (A) Suppression of cell viability from the following treatments: CKI, WRCKI-

B (whole reconstituted CKI in buffer/vehicle control), and WRCKI-H (whole reconstituted CKI in milliQ H_2O) (B) assessment of the interaction effects of single MJ compounds by the addition to the MN subtractive fraction. Single major compounds were dissolved in either MilliQ H_2O or Dimethyl sulfoxide. Effect of subtractive fractions (C) N-OmtOspcSpc, (D) N-MacAdeTri, (E) N-MtNmeSpr, (F) N-MtNme, (G) N-OmtSpc, (H) N-OspcSpc, (I) N-MacTri, (J) N-AdeTri, (K) N-MacAde, (L) N-MtSpr, (M) NmeSpr. Statistically significant results shown as $p < 0.05$ (*) or $p < 0.01$ (**) $p < 0.001$ (***), or $p < 0.0001$ (****); ns (not significant). All data were shown as mean ± SD.

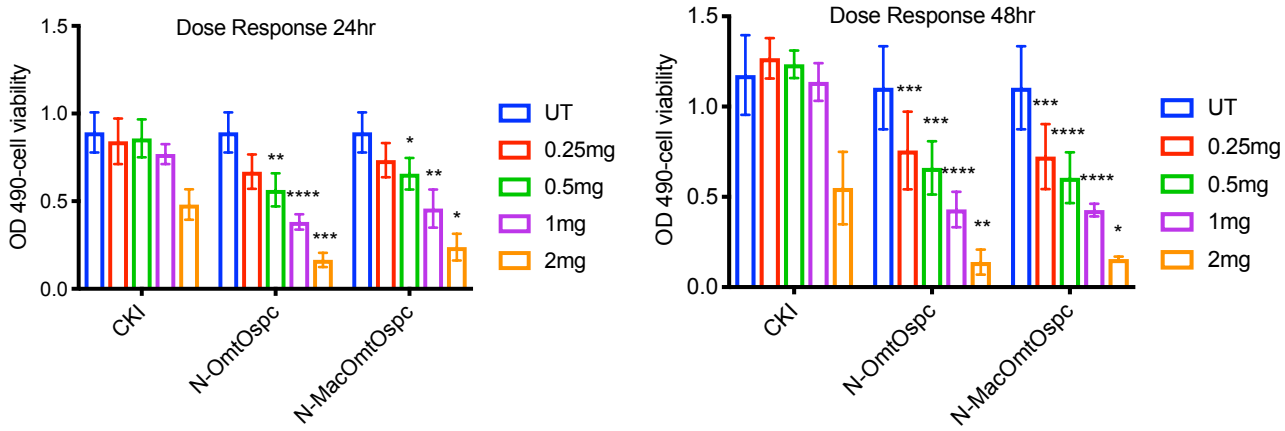

Sup. Fig. 3: XTT Cell viability assays of subtractive fractions N-OmtOspc and N-MacOmtOspc in MDA-MB-231 cells at 24- and 48-hour timepoints treated 4 different concentrations ranging from 0.25 mg/ml to 2 mg/ml of CKI and equivalent concentrations of two other agents. Statistically significant results shown as $p < 0.05$ (*) or $p < 0.01$ (**) $p < 0.001$ (***), or $p < 0.0001$ (****); ns (not significant). All data were shown as mean ± SD.

A

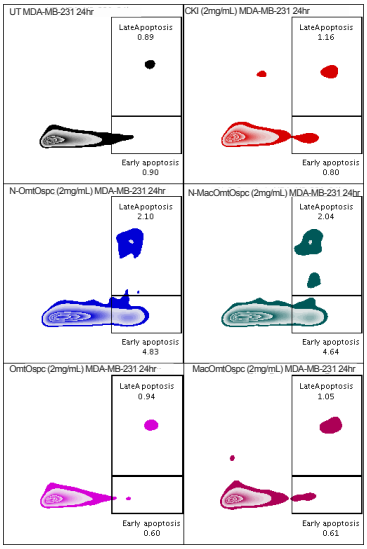

B

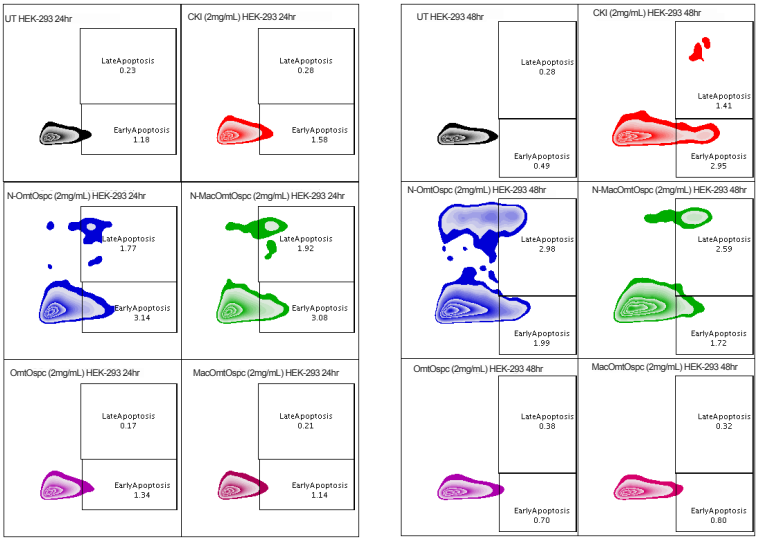

C

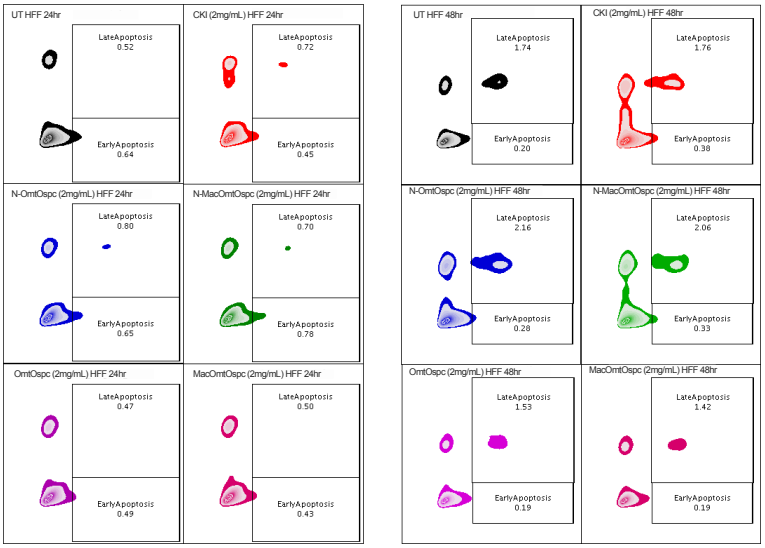

Sup. Fig. 4: Representative plots of Annexin V and PI staining in (A) MDA-MB-231, (B) HEK-293, and (C) HFF.

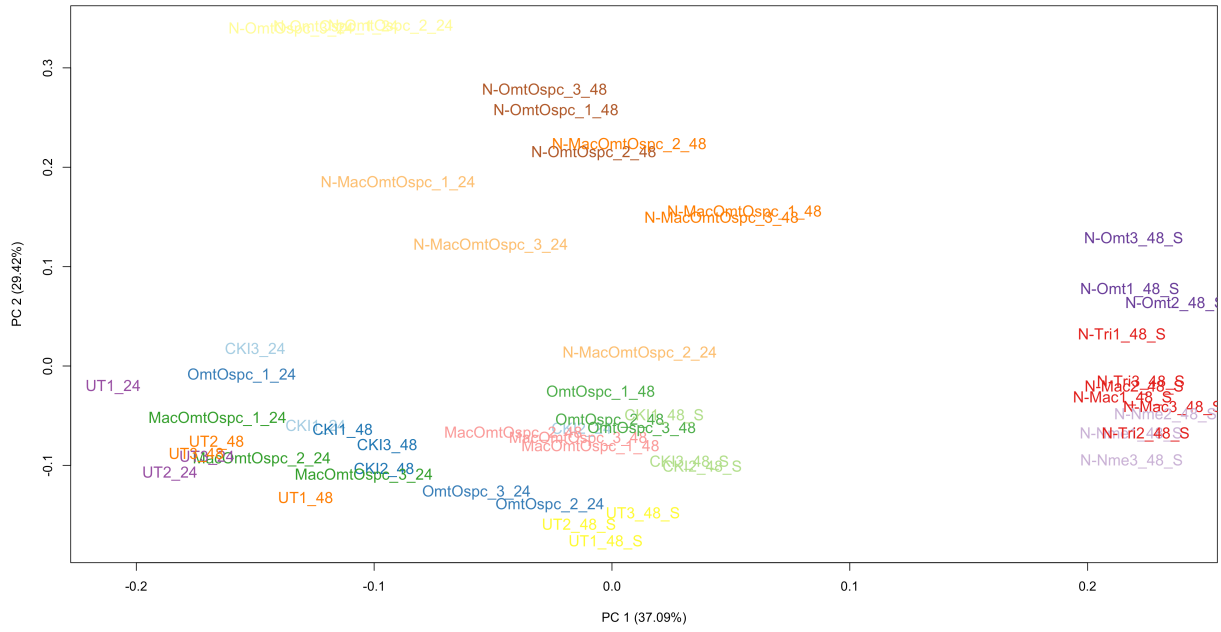

Sup. Fig. 5: Multiple dimensional scaling (MDS) plot for samples based on expression profiles of all genes before the removal of unwanted variance (RUVs) in R package.

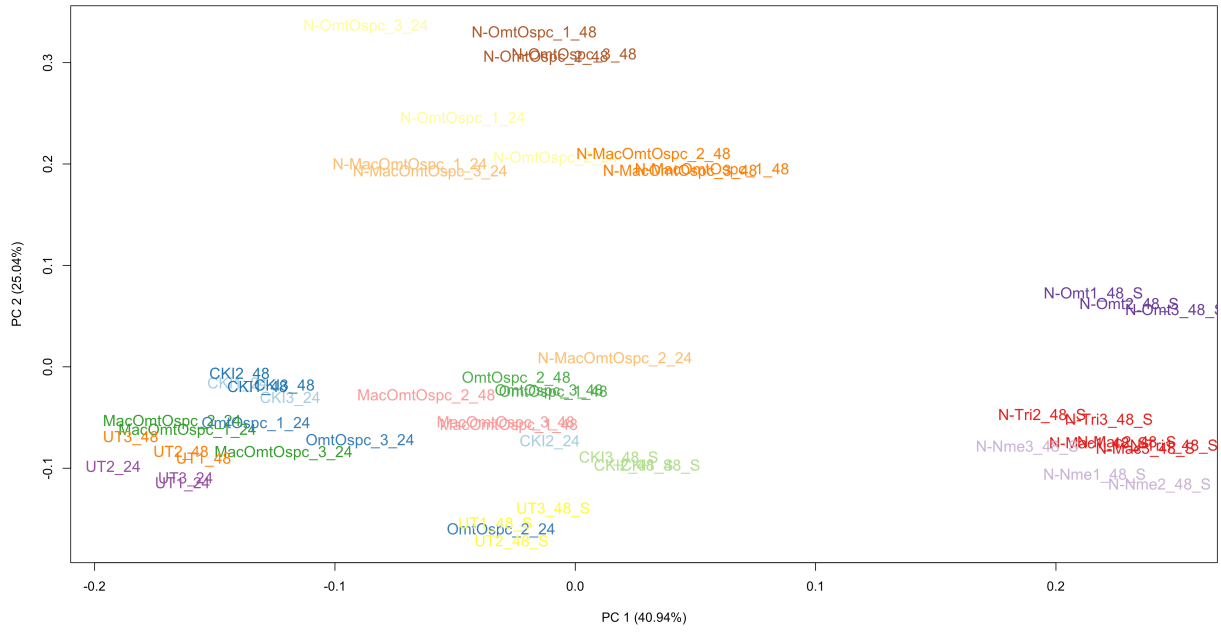

Sup. Fig. 6: MDS plot for samples based on expression profiles of all genes after the application of RUVs.

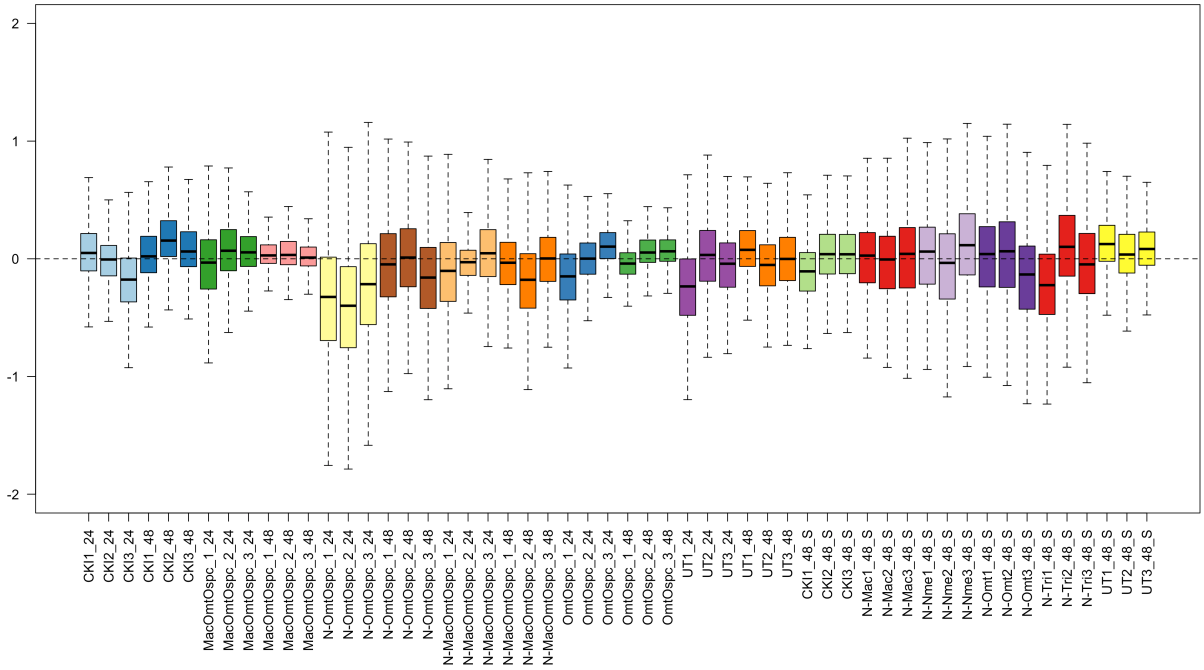

Sup. Fig. 7: Box plot for samples based on expression profiles of all genes before the application of RUVs.

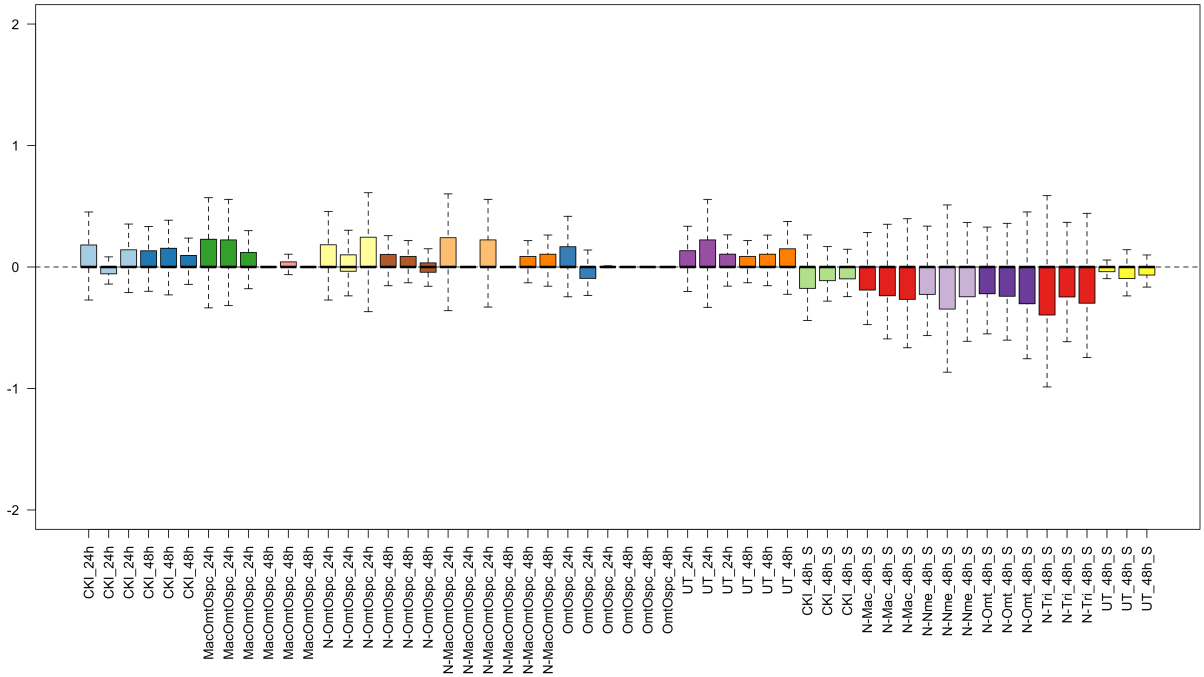

Sup. Fig. 8: Box plot for samples based on expression profiles of all genes after the application of RUVs.

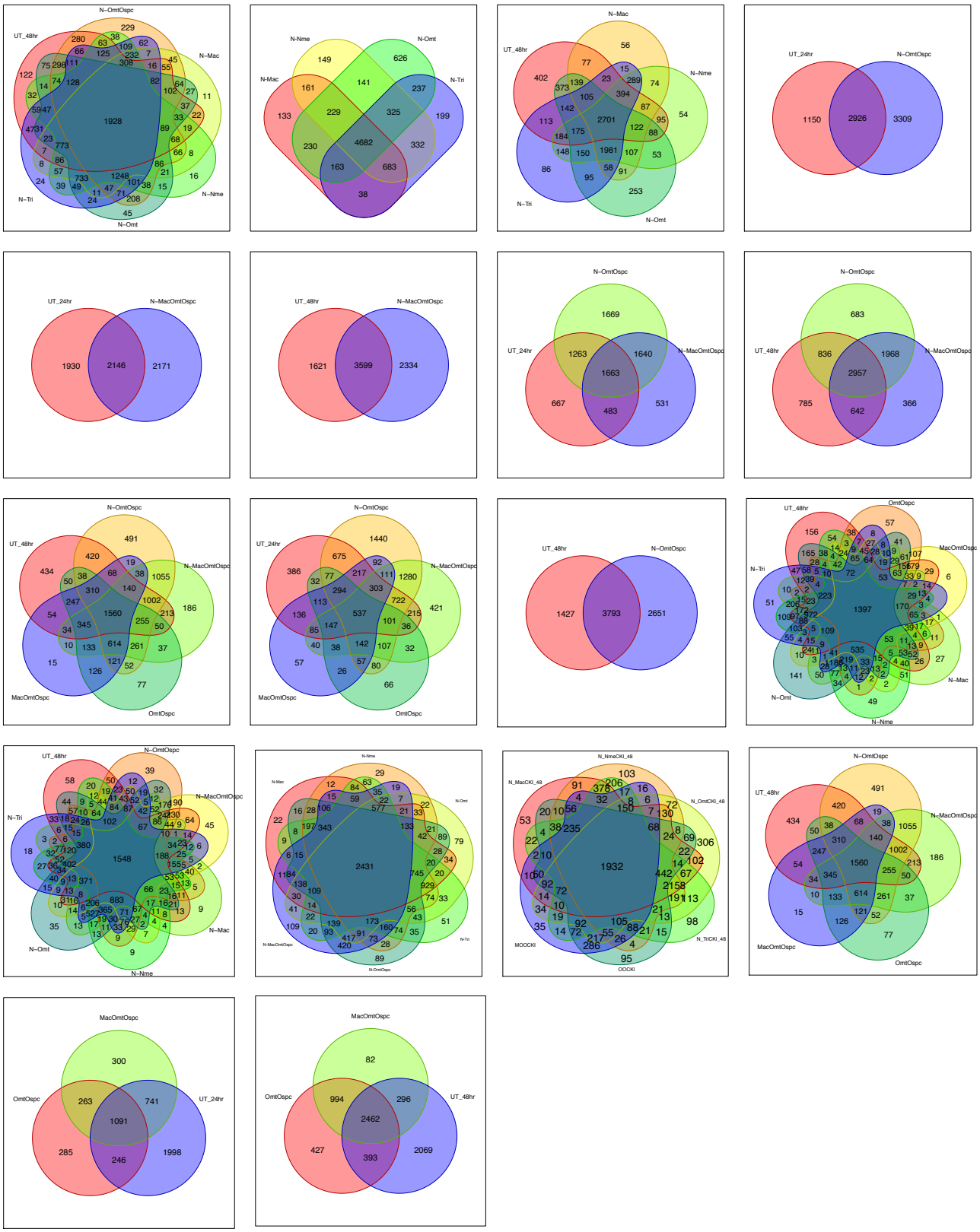

Sup. Fig. 9: Venn diagrams showing the number of overlaping DE genes between treatments at 24-hours and 48-hours.

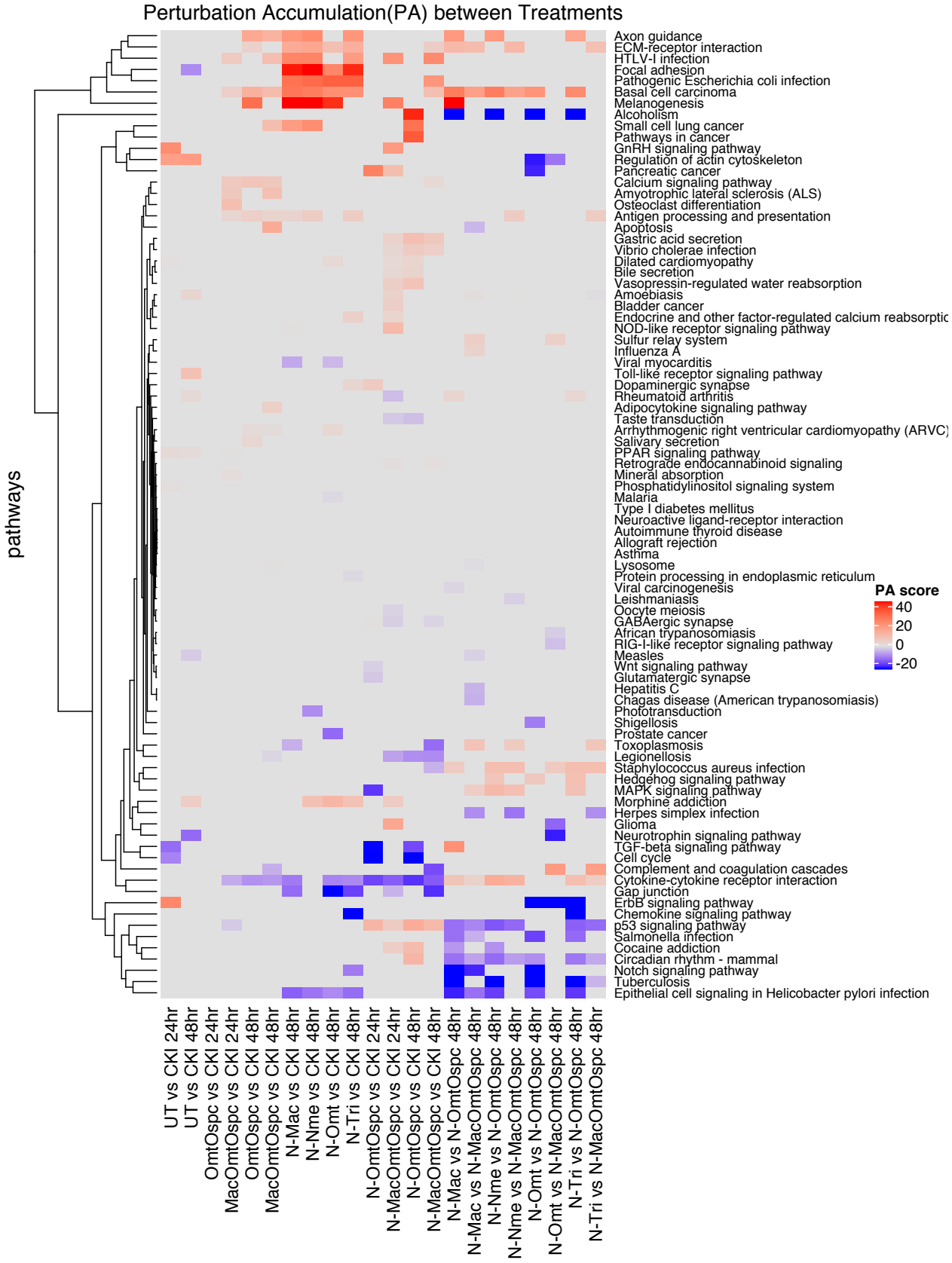

Sup. Fig. 10: Identification of significantly perturbed pathways using SPIA (pG< 0.05) analysis. Eighty-six significantly perturbed pathways from twenty-two comparisons were found.

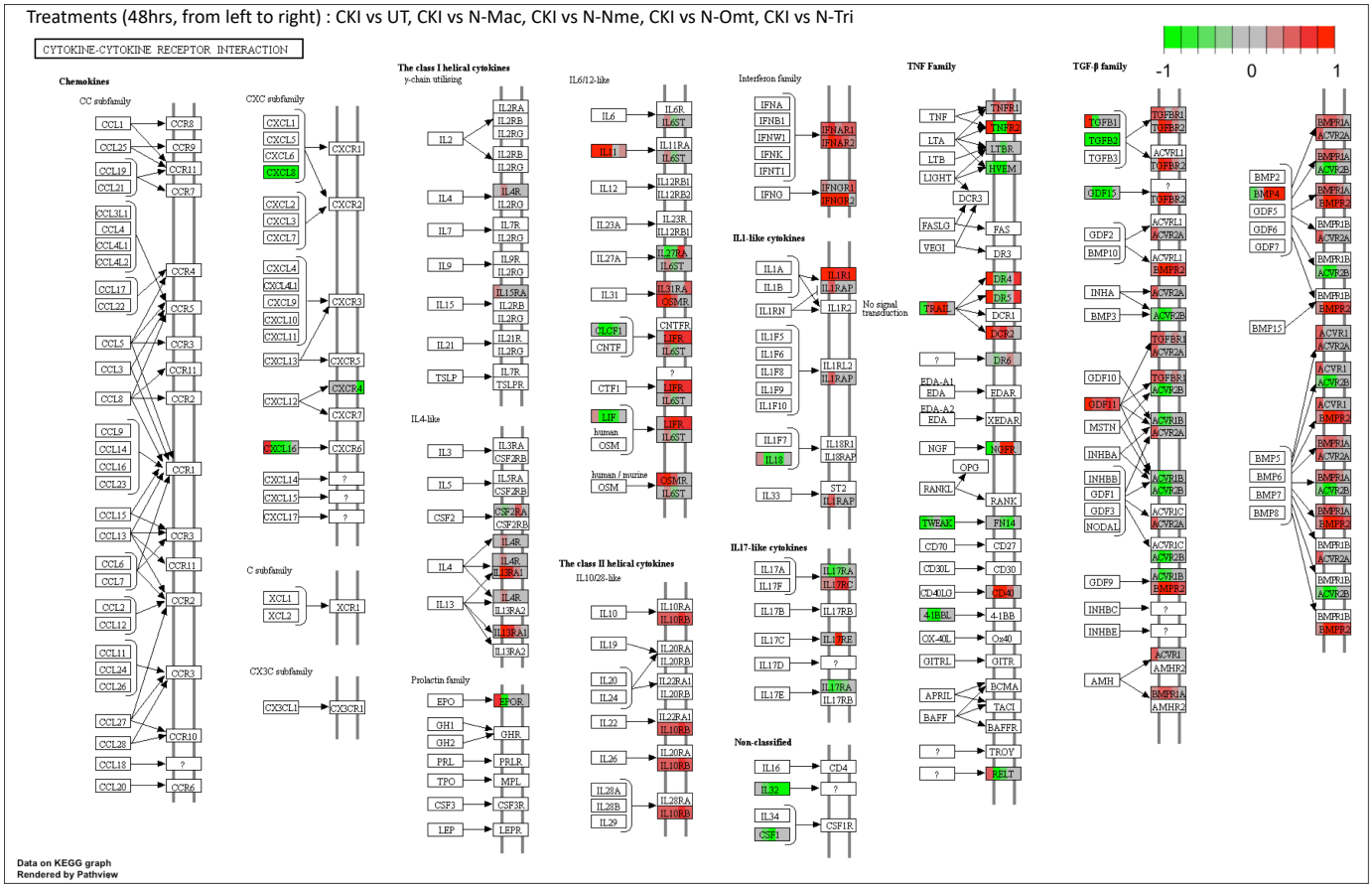

Sup. Fig. 11: DE genes from the following comparisons (CKI vs UT, CKI vs N-Mac, CKI vs N-Nme, CKI vs N-Omt and CKI vs N-Tri) shown in the "Cytokine-Cytokine Receptor Interaction pathway at 48-hours. Significantly up- and down-regulated DE genes were coloured red and green respectively. Each coloured box was separated into five parts according to treatments in this order: CKI vs UT, CKI vs N-Mac, CKI vs N-Nme, CKI vs N-Omt and CKI vs N-Tri. White or grey colours represented gene(s) that were not significantly differentially expressed by the treatments.

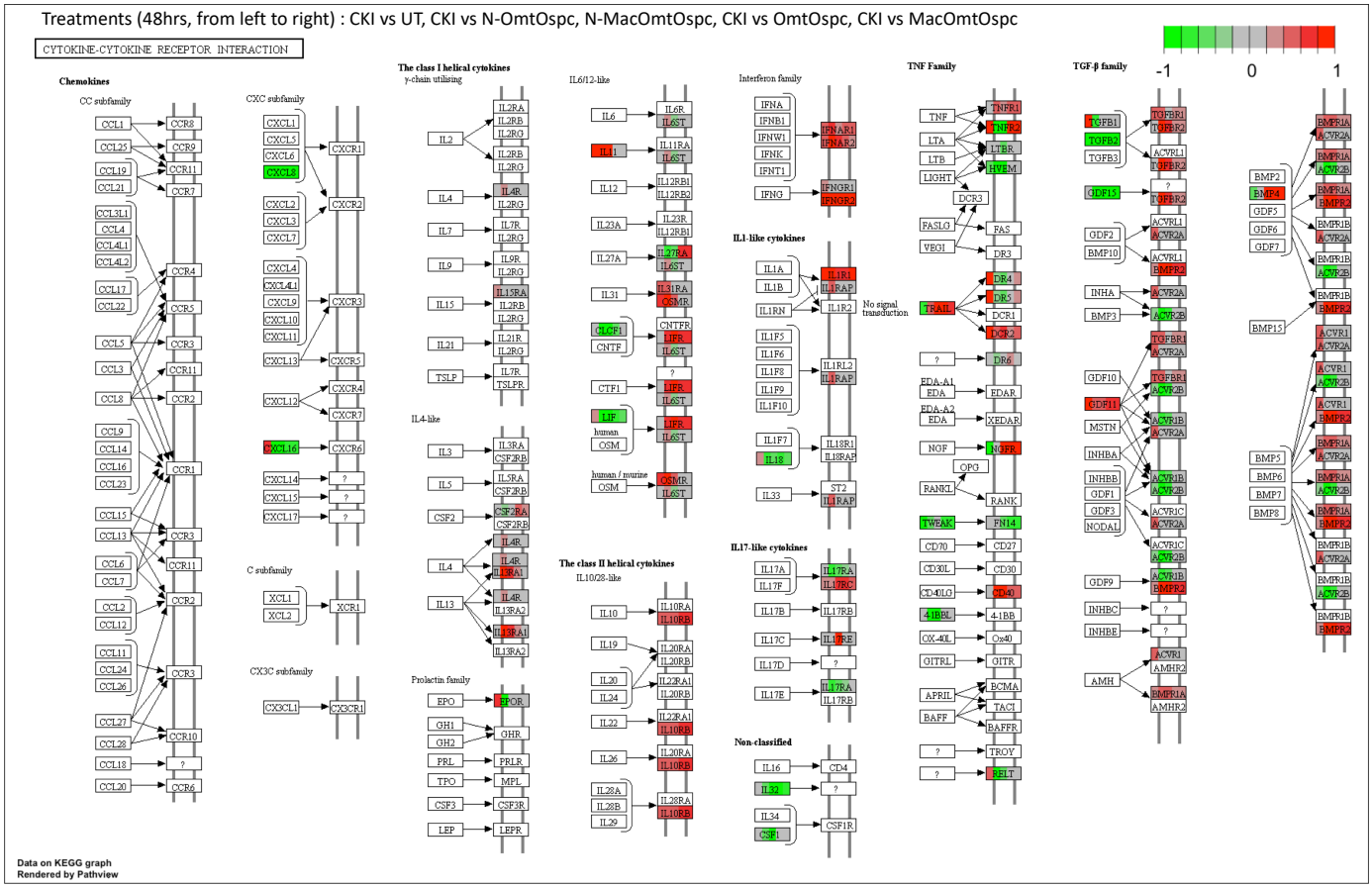

Sup. Fig. 12: DE genes from the following comparisons (CKI vs UT, CKI vs N-OmtOspc, CKI vs N-MacOmtOspc, CKI vs OmtOspc and CKI vs MacOmtOspc) shown in the Cytokine-Cytokine Receptor Interaction pathway at 48-hours. Significantly up- and down-regulated DE genes were coloured red and green respectively. Each coloured box was separated into five parts according to this order: CKI vs UT, CKI vs N-OmtOspc, CKI vs N-MacOmtOspc, CKI vs OmtOspc and CKI vs MacOmtOspc. White or grey colours represented gene(s) that were not significantly differentially expressed by the treatments.

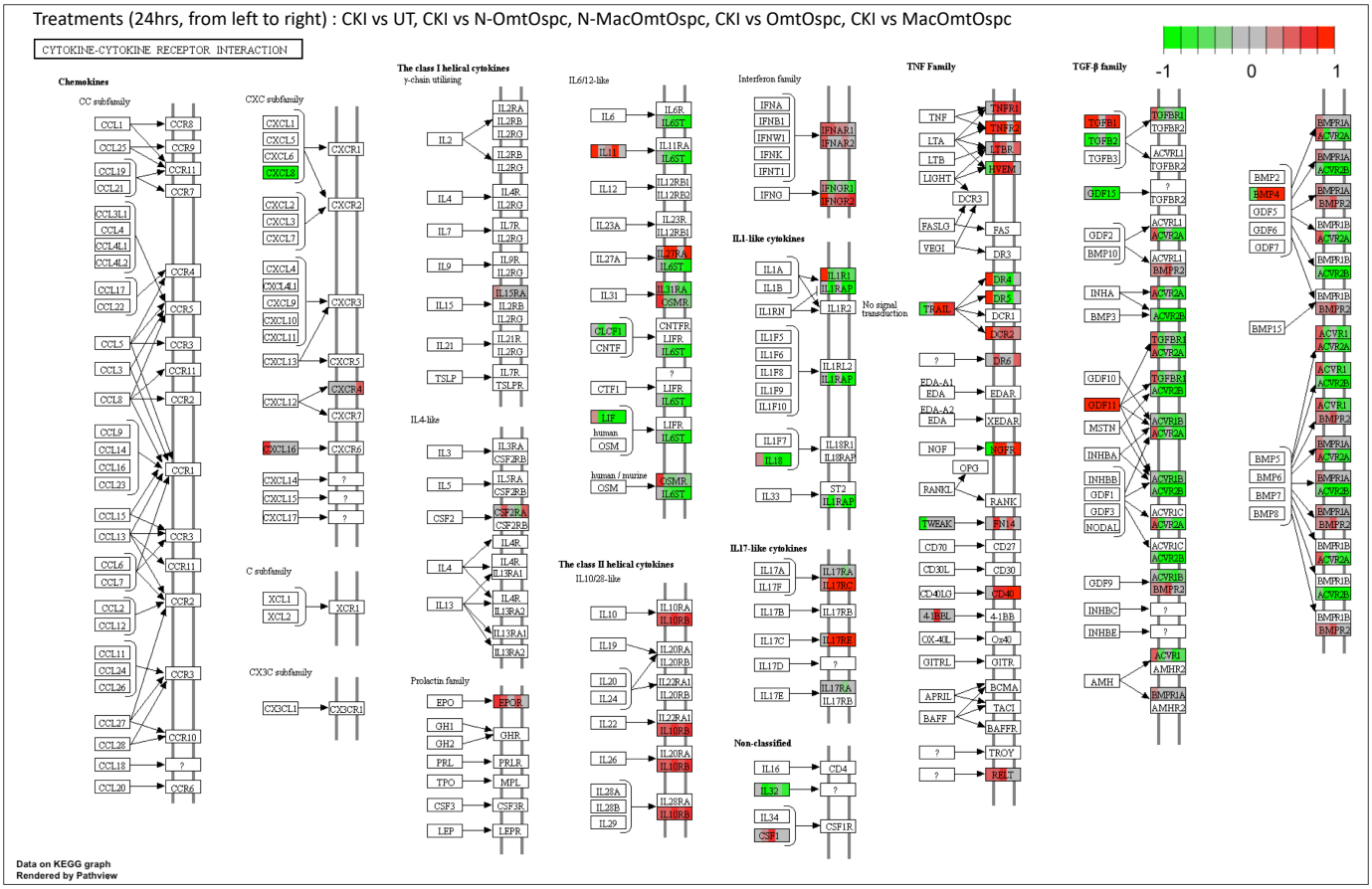

Sup. Fig. 13: DE genes from the following comparisons (CKI vs UT, CKI vs N-OmtOspc, CKI vs N-MacOmtOspc, CKI vs OmtOspc and CKI vs MacOmtOspc) shown in the Cytokine-Cytokine Receptor Interaction pathway at 24-hours. Significantly up- and down-regulated DE genes were coloured red and green respectively. Each coloured box was separated into five parts according to this order: CKI vs UT, CKI vs N-OmtOspc, CKI vs N-MacOmtOspc, CKI vs OmtOspc and CKI vs MacOmtOspc. White or grey colours represented gene(s) that were not significantly differentially expressed by the treatments.

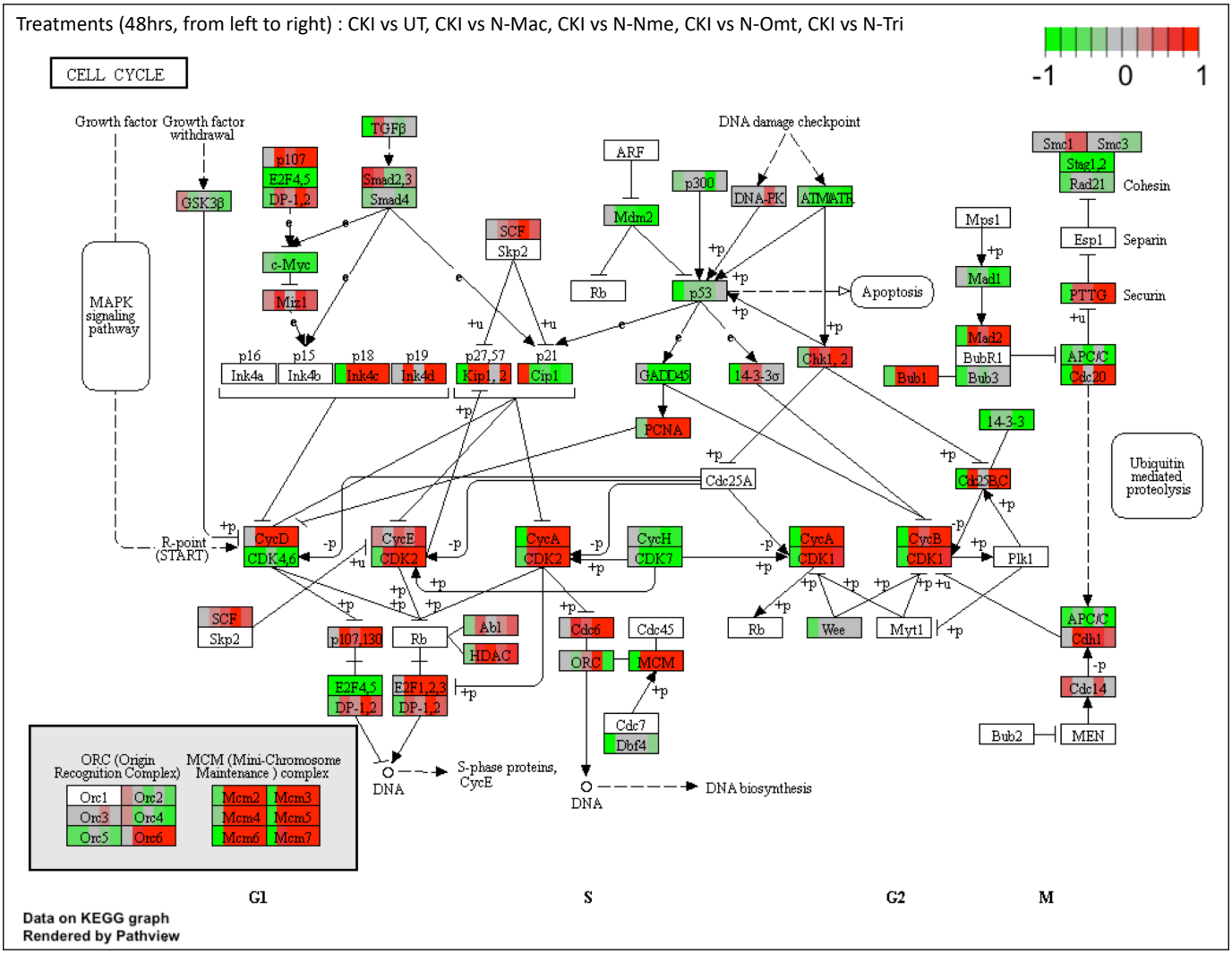

Sup. Fig. 14: DE genes from the following comparisons (CKI vs UT, CKI vs N-Mac, CKI vs N-Nme, CKI vs N-Omt and CKI vs N-Tri) shown in the Cell Cycle pathway at 48-hours. Significantly up- and down-regulated DE genes were coloured with red and green respectively. Each coloured box was separated into five parts according to this order: CKI vs UT, CKI vs N-Mac, CKI vs N-Nme, CKI vs N-Omt and CKI vs N-Tri. White or grey colours represented gene(s) that were not significantly differentially expressed by the treatments.

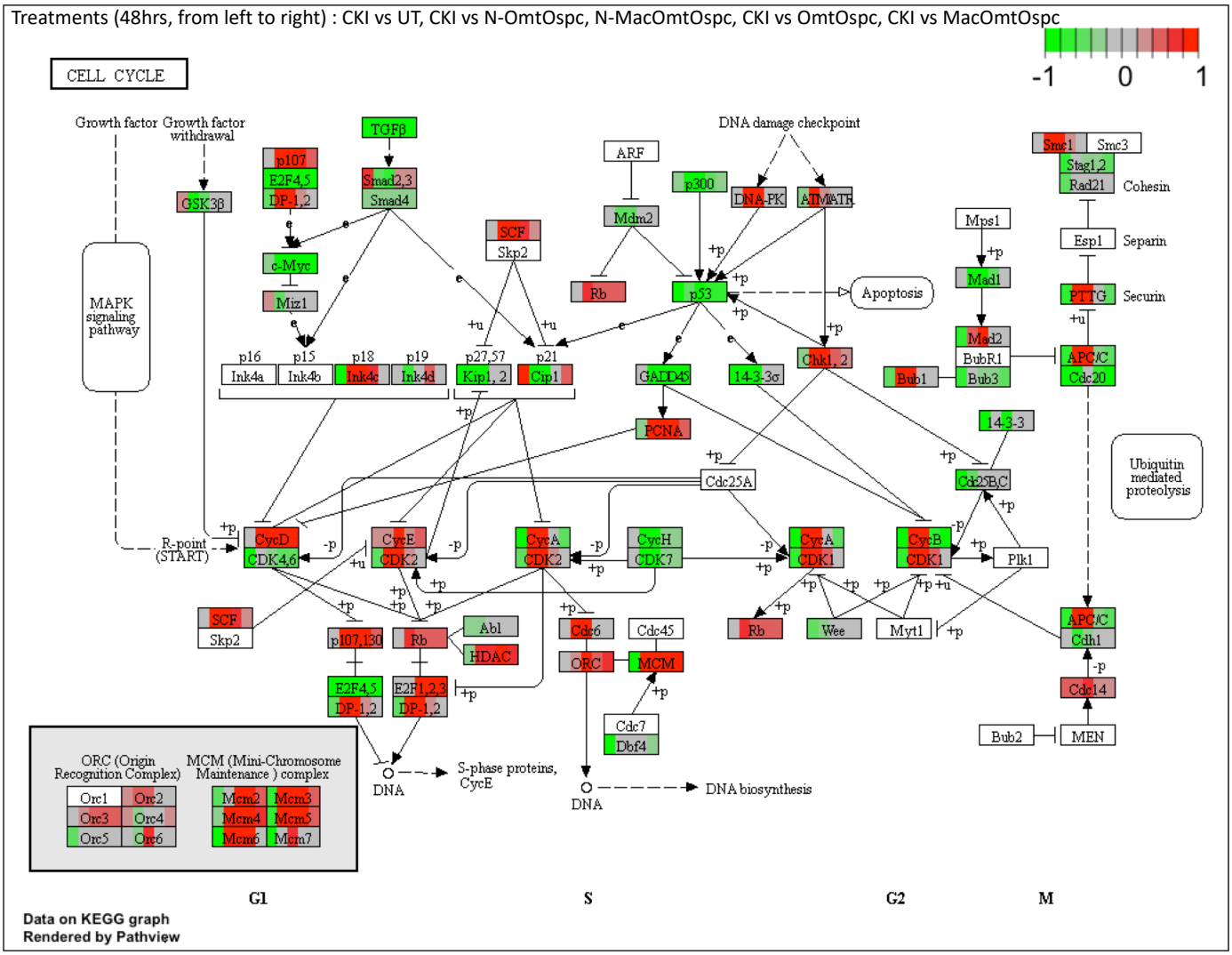

Sup. Fig. 15: DE genes from the following comparisons (CKI vs UT, CKI vs N-OmtOspc, CKI vs N-MacOmtOspc, CKI vs OmtOspc and CKI vs MacOmtOspc) shown in the Cell Cycle pathway at 48-hour treatments. Significantly up- and down-regulated DE genes were coloured red and green respectively. Each coloured box was separated into five parts according to this order: CKI vs UT, CKI vs N-OmtOspc, CKI vs N-MacOmtOspc, CKI vs OmtOspc and CKI vs MacOmtOspc. White or grey colours represented gene(s) that were not significantly differentially expressed by the treatments.

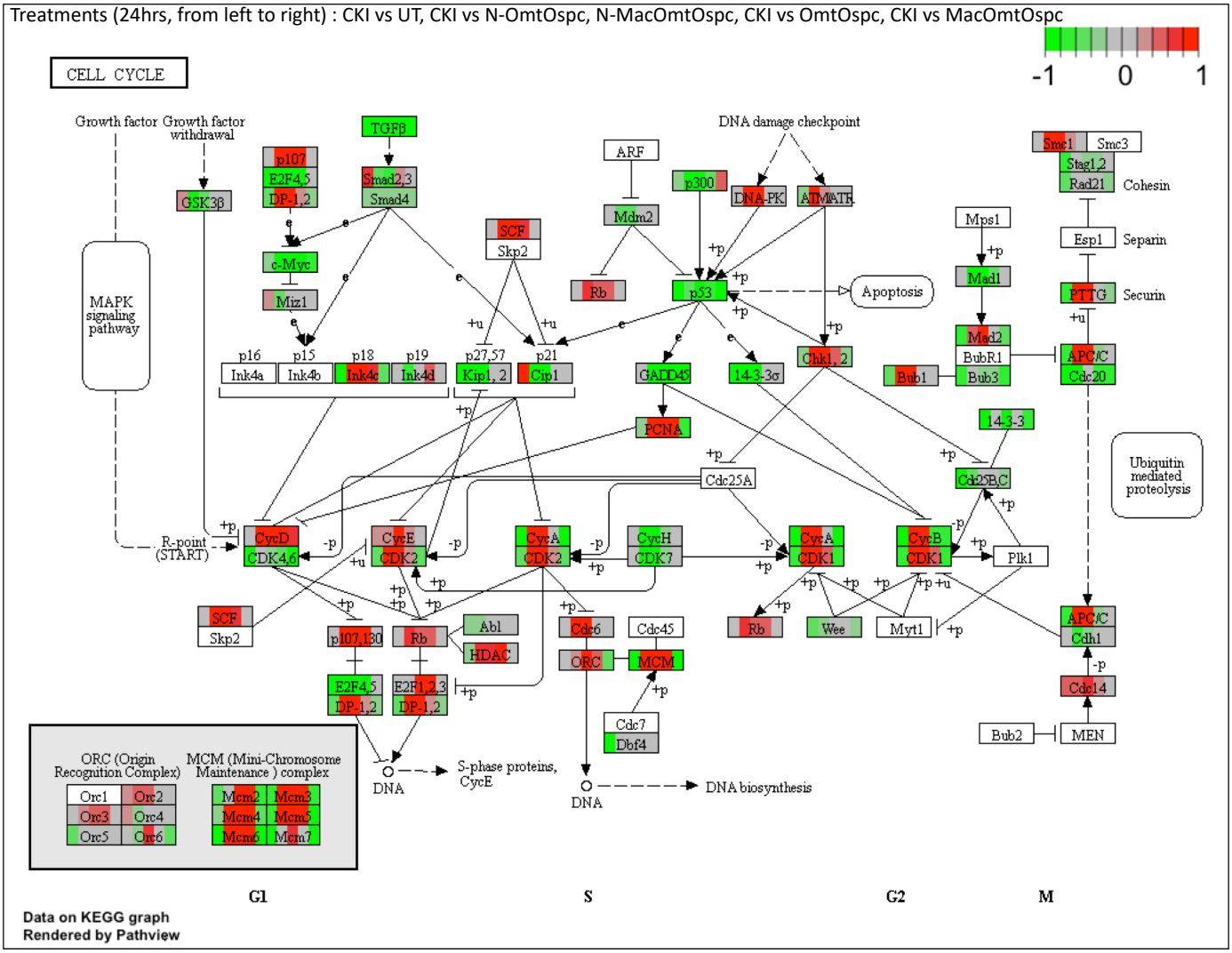

Sup. Fig. 16: DE genes from the following comparisons (CKI vs UT, CKI vs N-OmtOspc, CKI vs N-MacOmtOspc, CKI vs OmtOspc and CKI vs MacOmtOspc) shown in the Cell Cycle pathway at 24-hours. Significantly up- and down-regulated DE genes were coloured red and green respectively. Each coloured box was separated into five parts according to this order: CKI vs UT, CKI vs N-OmtOspc, CKI vs N-MacOmtOspc, CKI vs OmtOspc and CKI vs MacOmtOspc. White or grey colours represented gene(s) that were not significantly differentially expressed by the treatments.

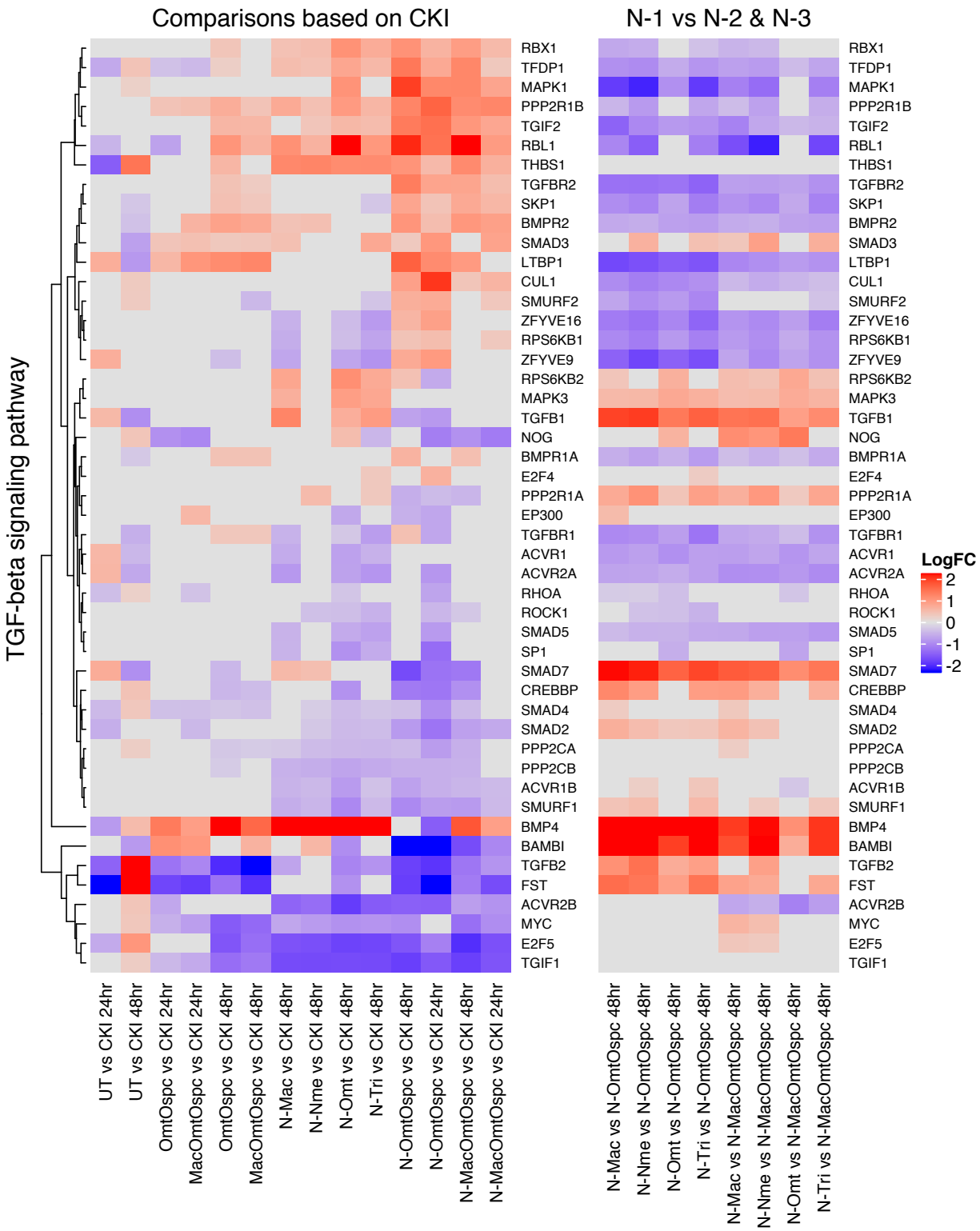

Sup. Fig. 17: Differential gene expression profiles of all treatments for TGF-ß signalling pathway: the left panel shows comparison of subtractive fraction treated cells against CKI treatment and the right panel shows comparison of single compound subtractive fraction treated cells against the treatments for two and three compound subtractive fractions.

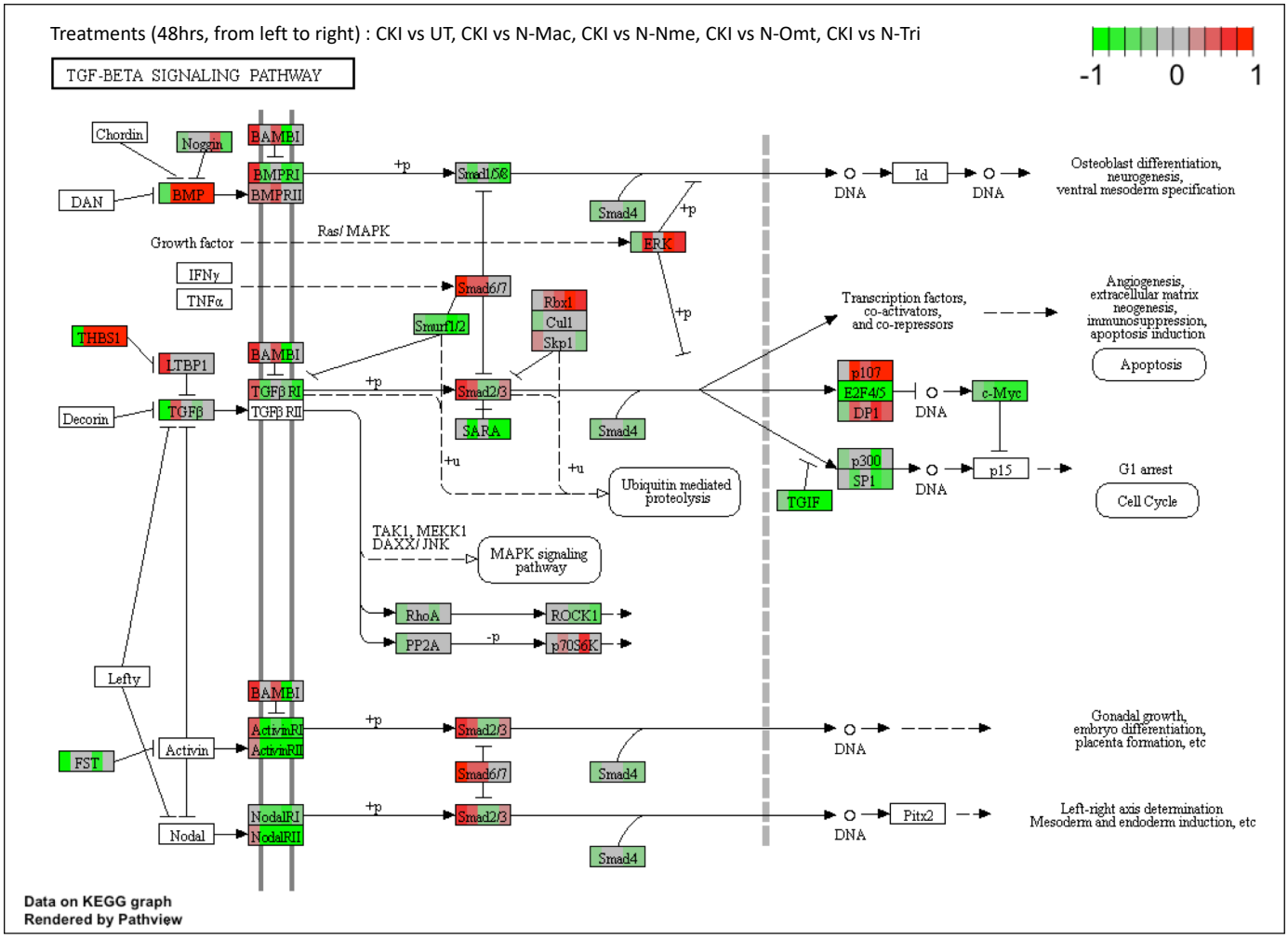

Sup. Fig. 18: DE genes from the following comparisons (CKI vs UT, CKI vs N-Mac, CKI vs N-Nme, CKI vs N-Omt and CKI vs N-Tri) shown in the TGF-ß signalling pathway at 48-hours. Significantly up- and down-regulated DE genes were coloured red and green respectively. Each coloured box was separated into five parts according to this order: CKI vs UT, CKI vs N-Mac, CKI vs N-Nme, CKI vs N-Omt and CKI vs N-Tri. White or grey colours represented gene(s) that were not significantly differentially expressed by the treatments.

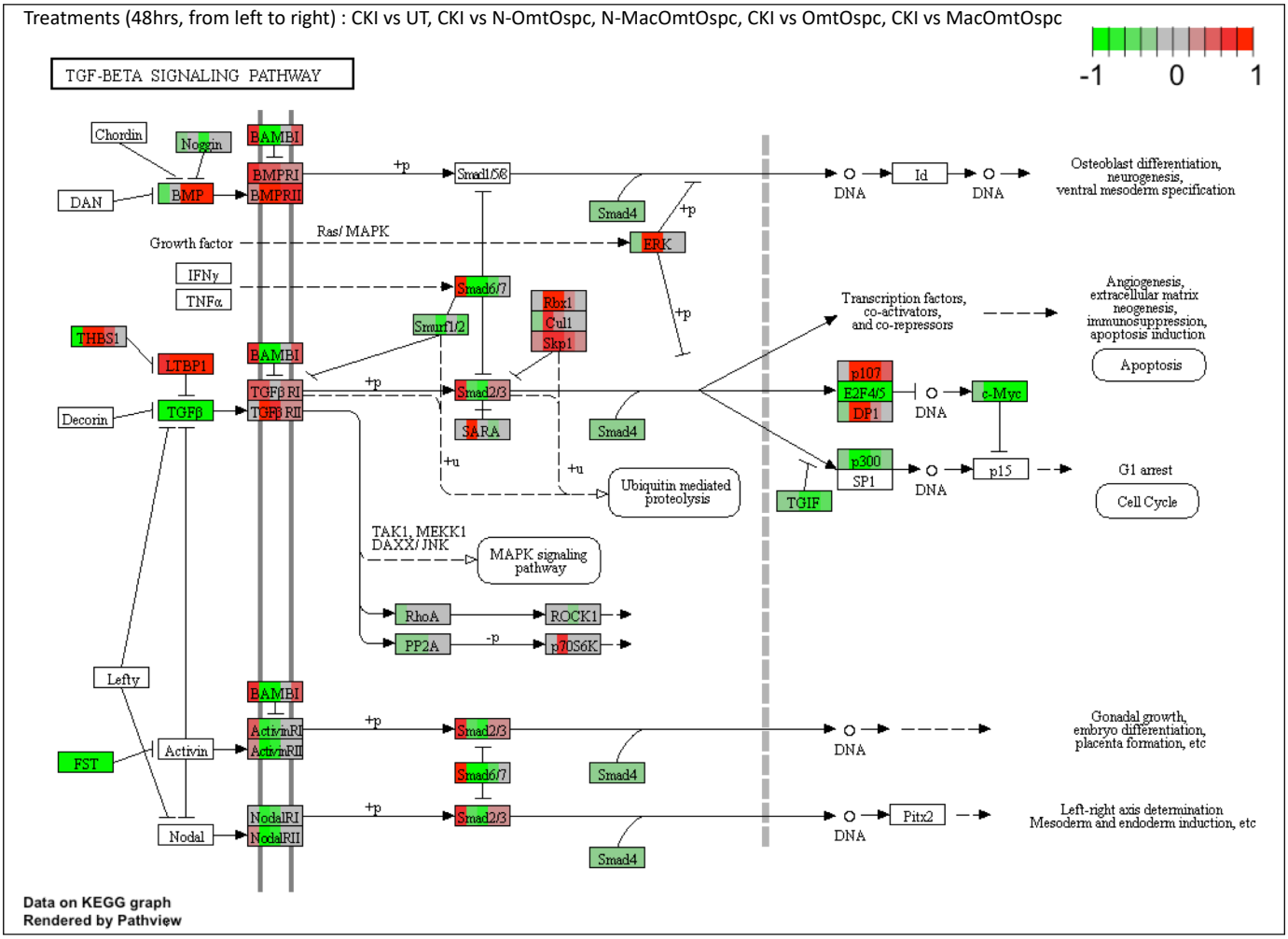

Sup. Fig. 19: DE genes from the following comparisons (CKI vs UT, CKI vs N-OmtOspc, CKI vs N-MacOmtOspc, CKI vs OmtOspc and CKI vs MacOmtOspc) shown in the TGF-ß signalling pathway at 48-hour treatments. Significantly up- and down-regulated DE genes were coloured red and green respectively. Each coloured box was separated into five parts according to this order: CKI vs UT, CKI vs N-OmtOspc, CKI vs N-MacOmtOspc, CKI vs OmtOspc and CKI vs MacOmtOspc. White or grey colours represented gene(s) that were not significantly differentially expressed by the treatments.

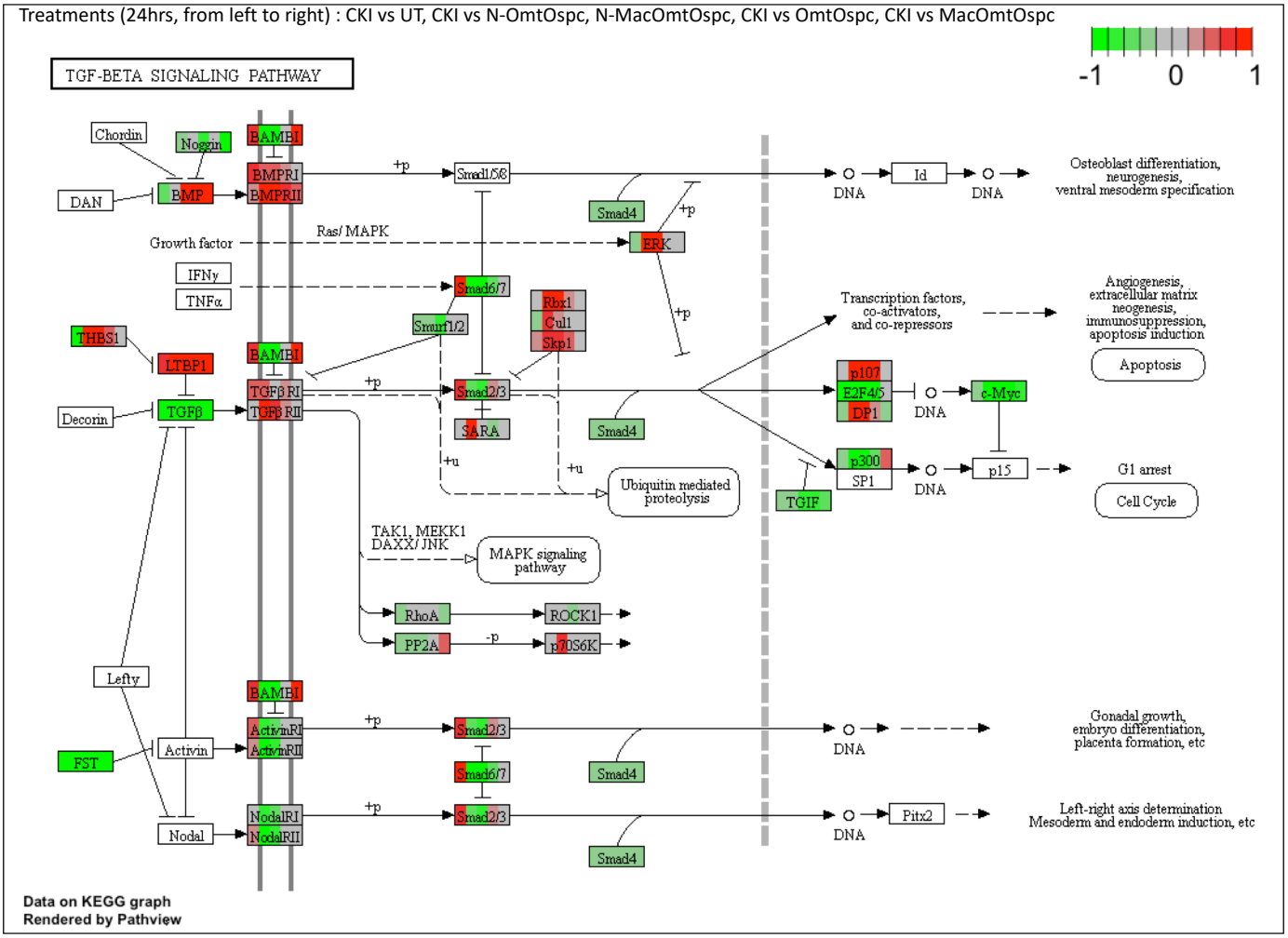

Sup. Fig. 20: DE genes from the following comparisons (CKI vs UT, CKI vs N-OmtOspc, CKI vs N-MacOmtOspc, CKI vs OmtOspc and CKI vs MacOmtOspc) shown in the TGF-ß signalling pathway at 24-hours. Significantly up- and down-regulated DE genes were coloured red and green respectively. Each coloured box was separated into five parts according to this order: CKI vs UT, CKI vs N-OmtOspc, CKI vs N-MacOmtOspc, CKI vs OmtOspc and CKI vs MacOmtOspc. White or grey colours represented gene(s) that were not significantly differentially expressed by the treatments.

Sup Table 1: Summary of shared, differentially expressed (DE) genes across treatments. Similarity (%) calculated from total number of shared DE genes from all listed comparisons. To find the number of DE genes, CKI treatment was used as a baseline to compare all other fractionated treatments in order to emphasize the effect of depleted compounds and UT (untreated) was used as a base to calculate the DE genes for CKI treatment.

Sup Data 1: Calibration curve for the concentrations of known compounds in CKI and reconstituted subtractive fractions.

Appendix C

Supplementary Figures for Chapter 3

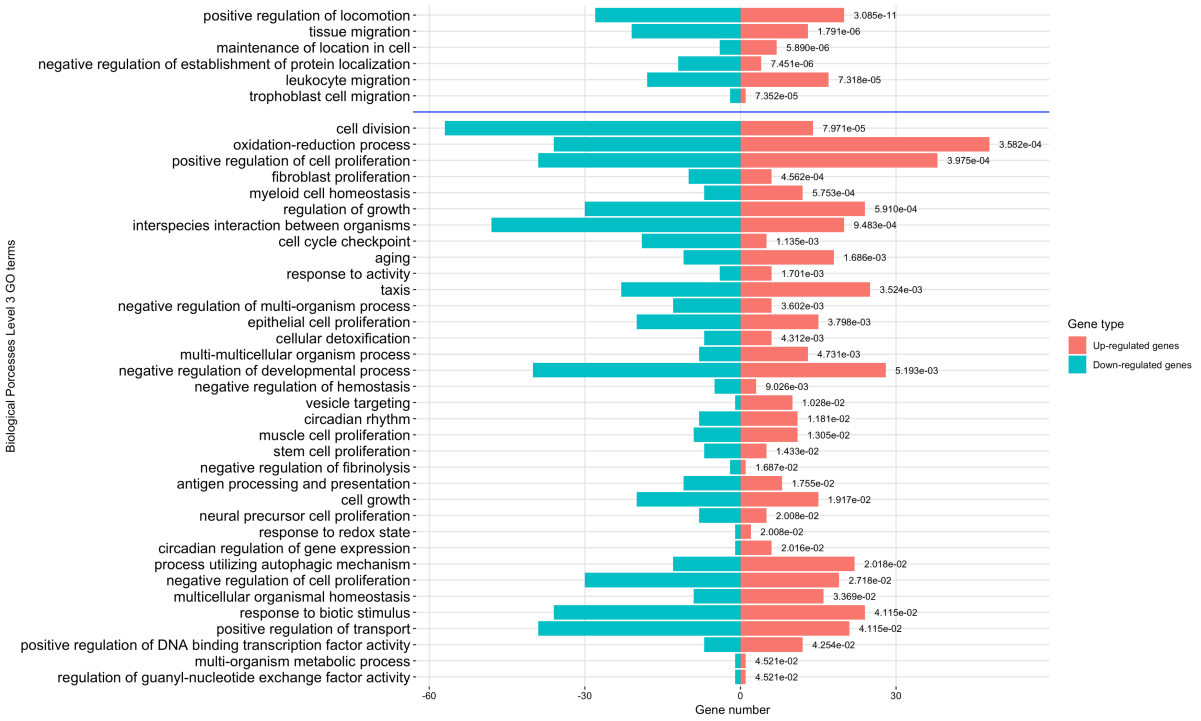

Additional file 1: FigureS1: (a) Total ion chromatogram (TIC) for CKI in 1 in 100 dilution from 25 mg/ml of stock concentration. Single peaks were extracted based on the molecular mass. (b) cytisine (spike in control), (c) macrozamin, (d) adenine, (e) n-methylcytisine, (f) sophoridine and matrine (similar molecular mass with different retention time) (g) oxysophocarpine, (h) oxymatrine, (i) sophocarpine and (j) trifolirhizin.

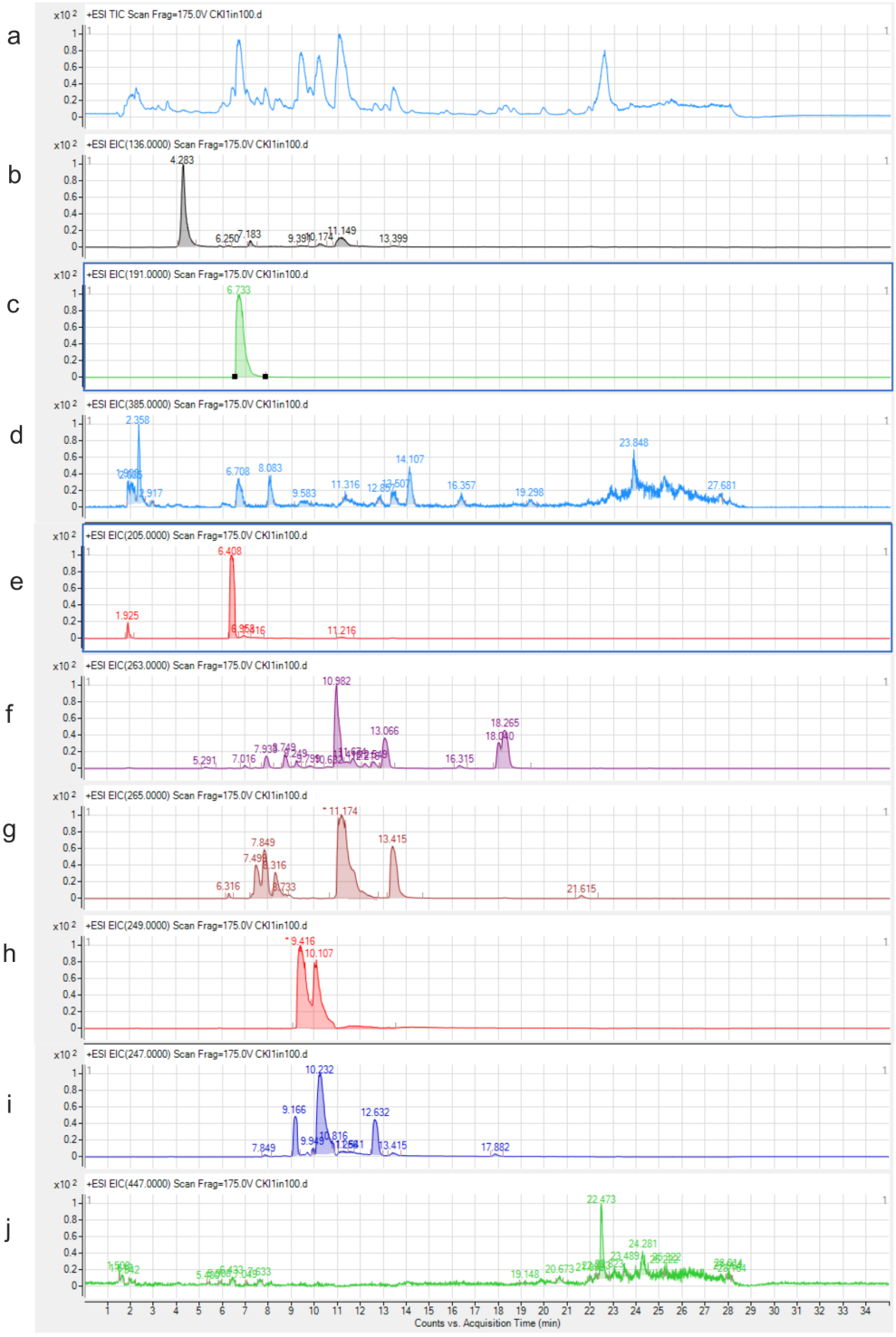

Additional file 2: **FigureS2**: (a) Total ion chromatogram (TIC) for MJ in 1 in 100 dilution from 25 mg/ml of stock concentration. Single peaks were extracted based on the molecular mass. (b) adenine, (c) cytisine (spike in control), (d) macrozamin, (e) n-methylcytisine, (f) sophoridine and matrine (similar molecular mass with different retention time) (g) oxysophocarpine, (h) oxymatrine, (i) sophocarpine and (j) trifolirhizin.

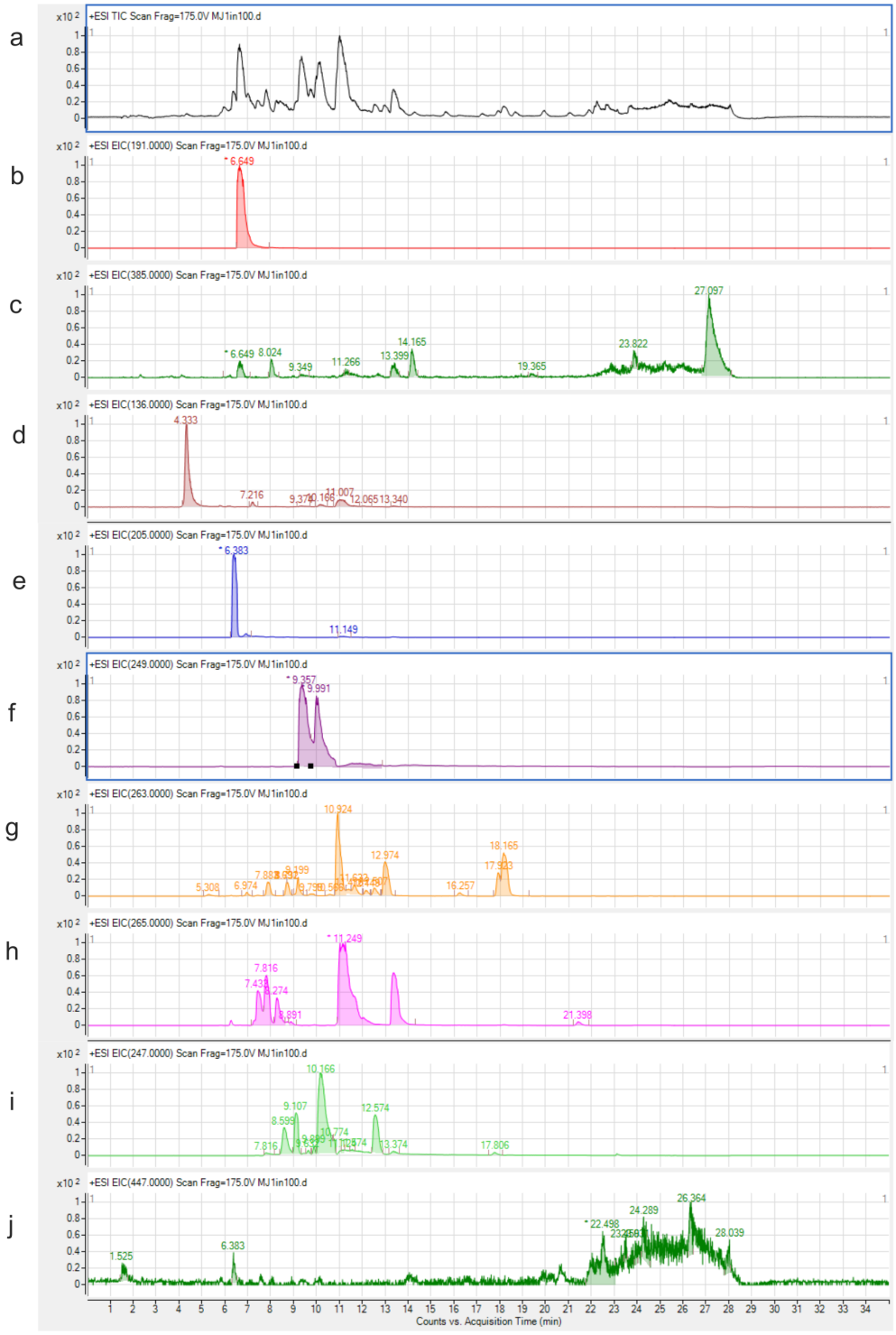

Additional file 3: **FigureS3**: Combinatorial analysis of the effects of MN with each of the nine major individual compounds, analyzed in eight cell lines with wound closure assays. Data were normalized to results with 0.5 mg/ml minor (MN) alone. Significantly increased or decreased percent block of migration resulting from the addition of major compounds is shown as $p < 0.05$ (*), $p < 0.01$ (**), $p < 0.001$ (***) and not significant (ns). Data are mean ± SD.

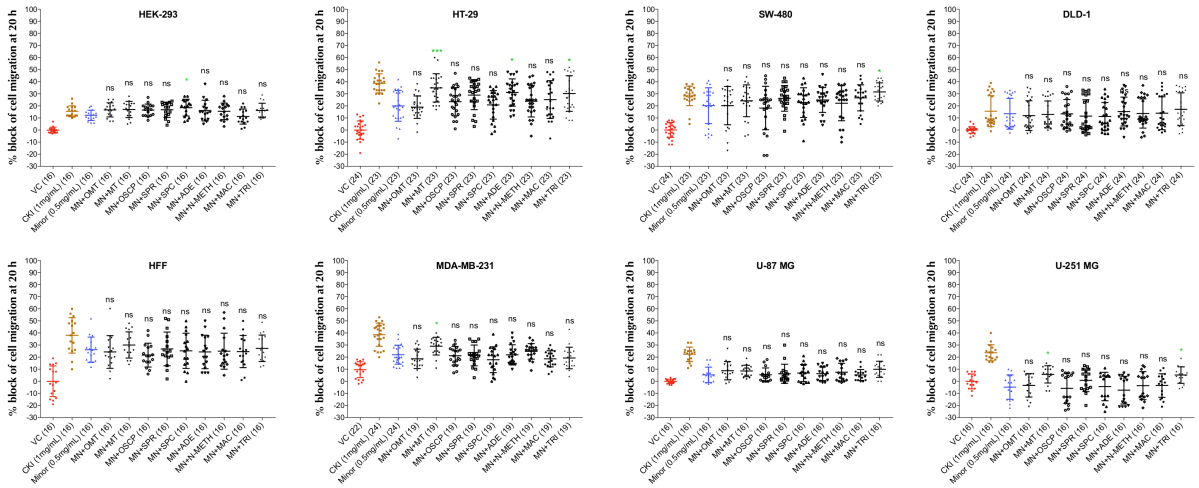

Additional file 4: **FigureS4**: Functional classification of genes by GO over-representation analyses. Over-represented GO terms (Biological Process, BP=3) for differentially expressed (DE) genes were identified from MDA-MB-231 cells treated by CKI. Upregulated and downregulated genes contained in each term were shown in red and green respectively. GO terms shown above the blue line were significant terms related to migration.

Additional file 5: **VideoS1**: Live-cell imaging of the migration blocking effect of CKI in MDA-MB-231 cells in the wound closure migration assay. Videos show cell motility and wound closure rate in CKI at 2 mg/ml was reduced as compared to untreated control. Images were captured at 10-minute intervals for 20 hours.

Additional file 6: **DataS1**: Significantly over-represented functional GO terms, as determined by GO analysis of the transcriptome from CKI treated MDA-MB-231 cells. ($P < 0.05$).

Additional file 7: **DataS2**: Significantly perturbed pathways, as determined by SPIA analysis of the transcriptome from CKI treated MDA-MB-231 cells. ($pG < 0.05$).

Additional file 8: **DataS3**: Matching of genes in two strongly affected pathways ("focal adhesion" and "actin cytoskeleton") against three independent gene datasets containing: (i) a

set TARGET gene and (ii) migration related genes from published articles. 14 core DE genes from three datasets including *CTNNB1, CDH1, AKT1, AKT2, AKT3, CCND1, MAPK1, JAK2, APC, CDK4, RB1, PIK3CA*, and *PTEN*, are known to have effects on cell migration.

Additional file 9: **TableS1**: Concentrations of Matrigel and number of cells used for each cell line in transwell invasion assay.

Additional file 10: **TableS2**: Fourteen clinically relevant DE genes from three independent gene datasets (see methods).

Appendix D

Supplementary Figures for Chapter 4

Identification of candidate anti-cancer molecular mechanisms of compound kushen injection using functional genomics

SUPPLEMENTARY FIGURES AND TABLES

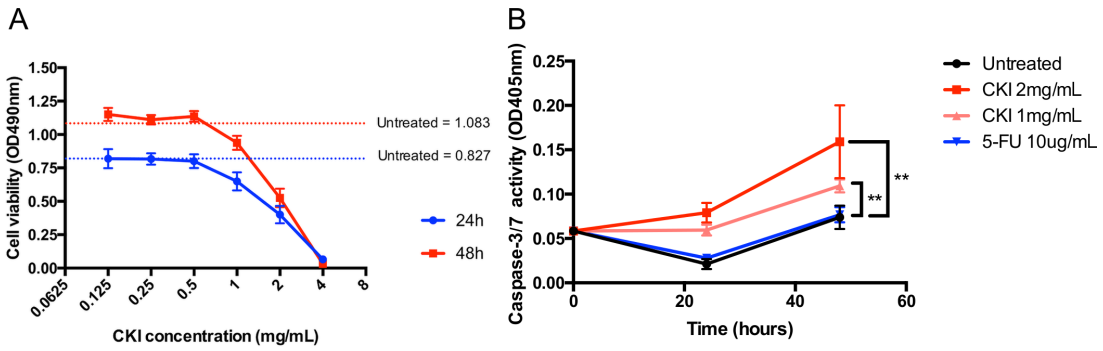

Supplementary Figure 1: CKI inhibited MCF-7 cell growth in a dose-dependent fashion and increased caspase-3/7 activity. A. The level of viability of cells after different treatments were measured using XTT:PMS. Data are represented as mean ±SEM (n=9). X-axis is log2 scaled. **B.** The level of caspase-3/7 activity in cells was measured with Caspase-3/7 Colorimetric Assay Kit. Data are represented as mean ±SEM (n=3). Statistical analyses were performed using two-way ANOVA (**p<0.01, ***p<0.001).

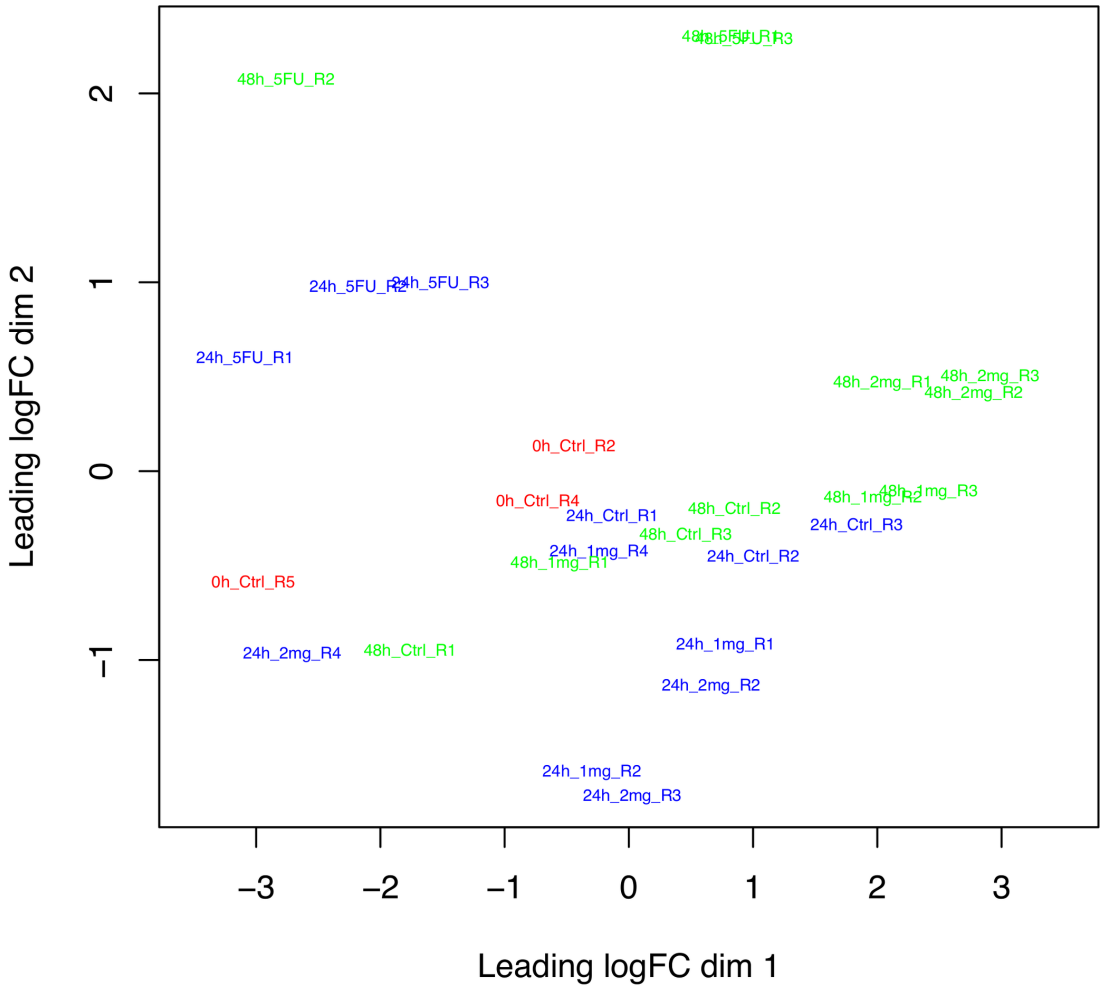

Supplementary Figure 2: Multiple dimensional scaling (MDS) plot for samples based on expression profiles of all genes.

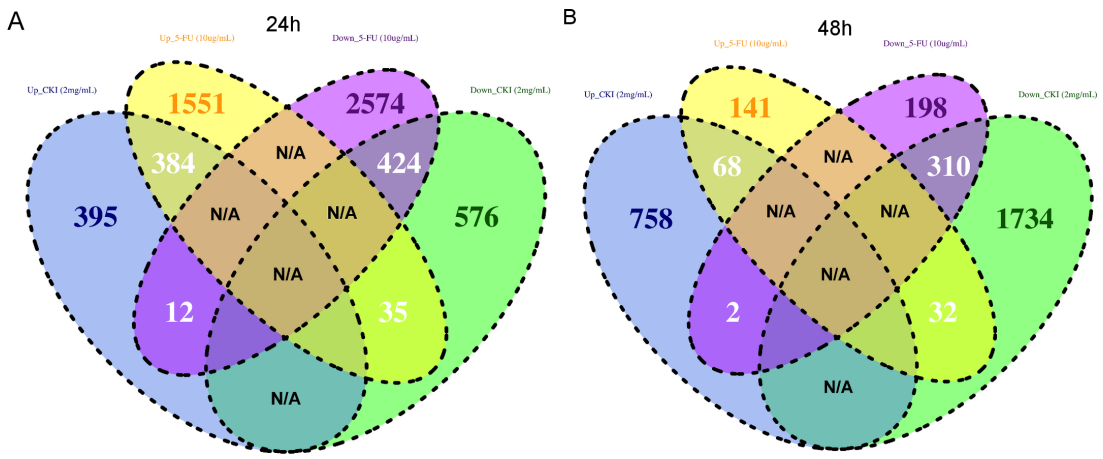

Supplementary Figure 3: Venn diagrams showing the overlap of DE genes in cells treated with CKI (2 mg/mL) or 5-FU for A. 24 hours or **B.** 48 hours.

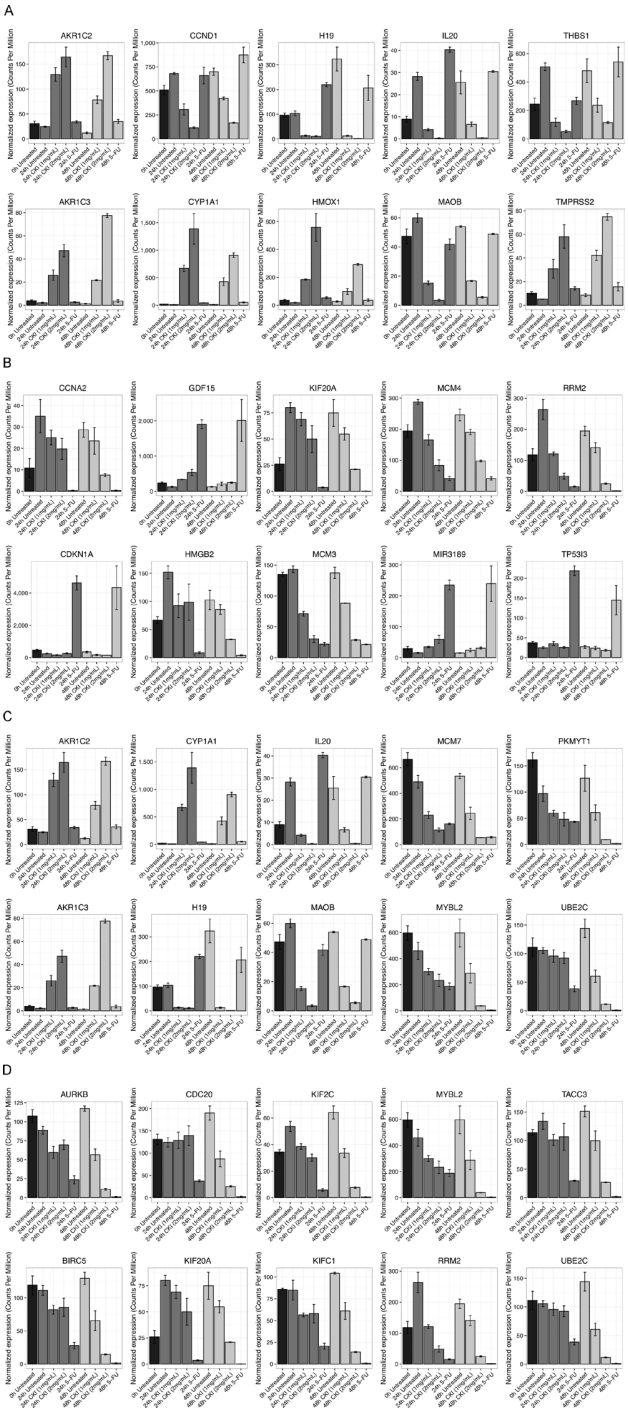

Supplementary Figure 4: Normalised expression values of the top10 significantly differentially expressed genes in cells treated with CKI (2 mg/mL) or 5-FU for 24 hours A. and **B.** or 48 hours **C.** and **D.**

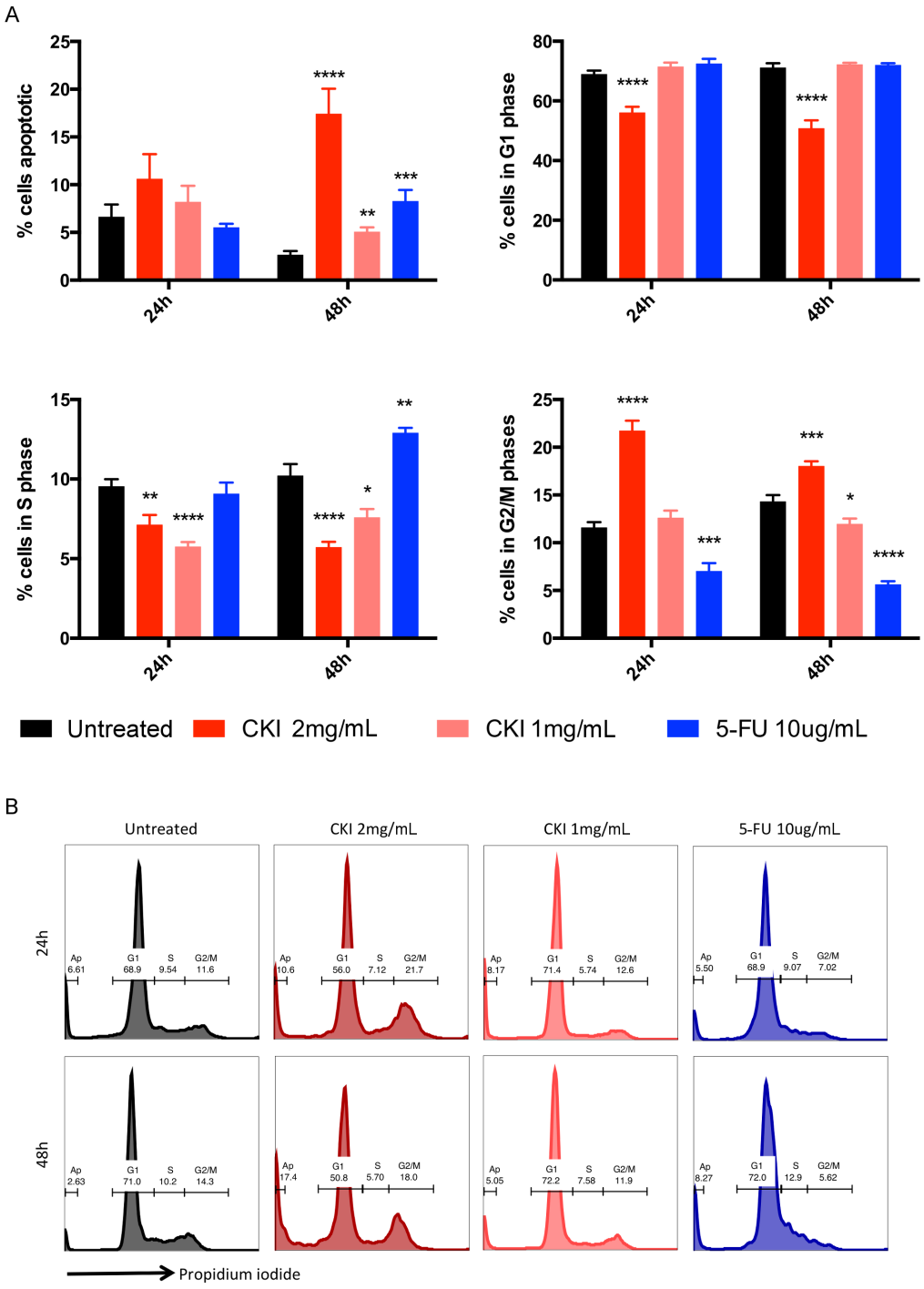

Supplementary Figure 5: Effect of CKI on cell cycle and apoptosis in MCF-7 cells. Proportions of cells in either apoptosis, G1, S or G2/M phase were determined by measuring the DNA contents of permeabilised cells stained with Propidium Iodide. **A.** Percentages of cells in each cell cycle phase. **B.** Representative histograms of PI staining with gating designation. Data are represented as mean ±SEM (n=9). Statistical analyses were performed using t-test comparing with "Untreated" (*p<0.05, **p<0.01, ***p<0.001, ****p<0.0001).

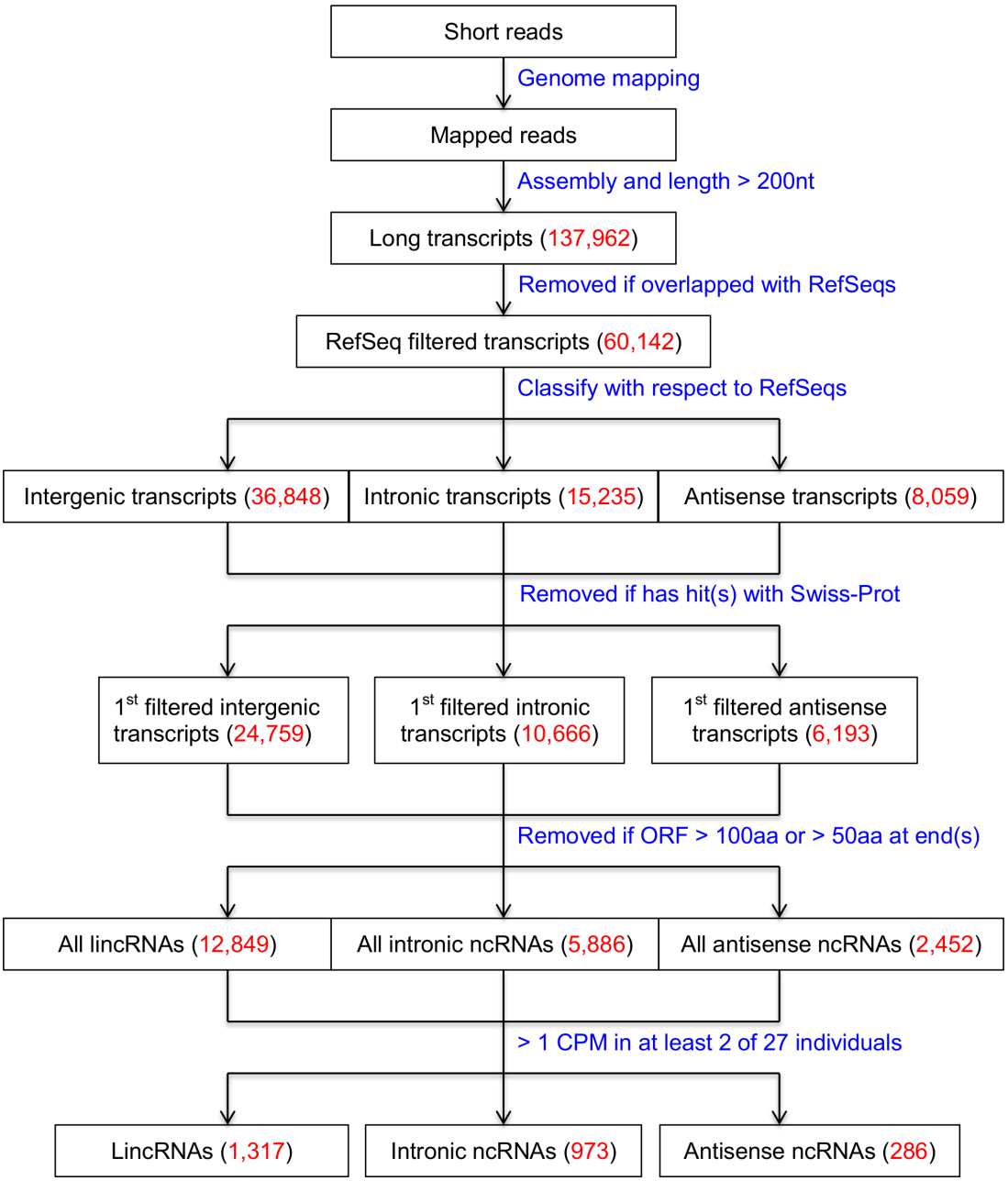

Supplementary Figure 6: Flowchart of *de novo* identification of lncRNAs from RNA-seq dataset. Digits in red colour represent the numbers of transcripts after corresponding data processing.

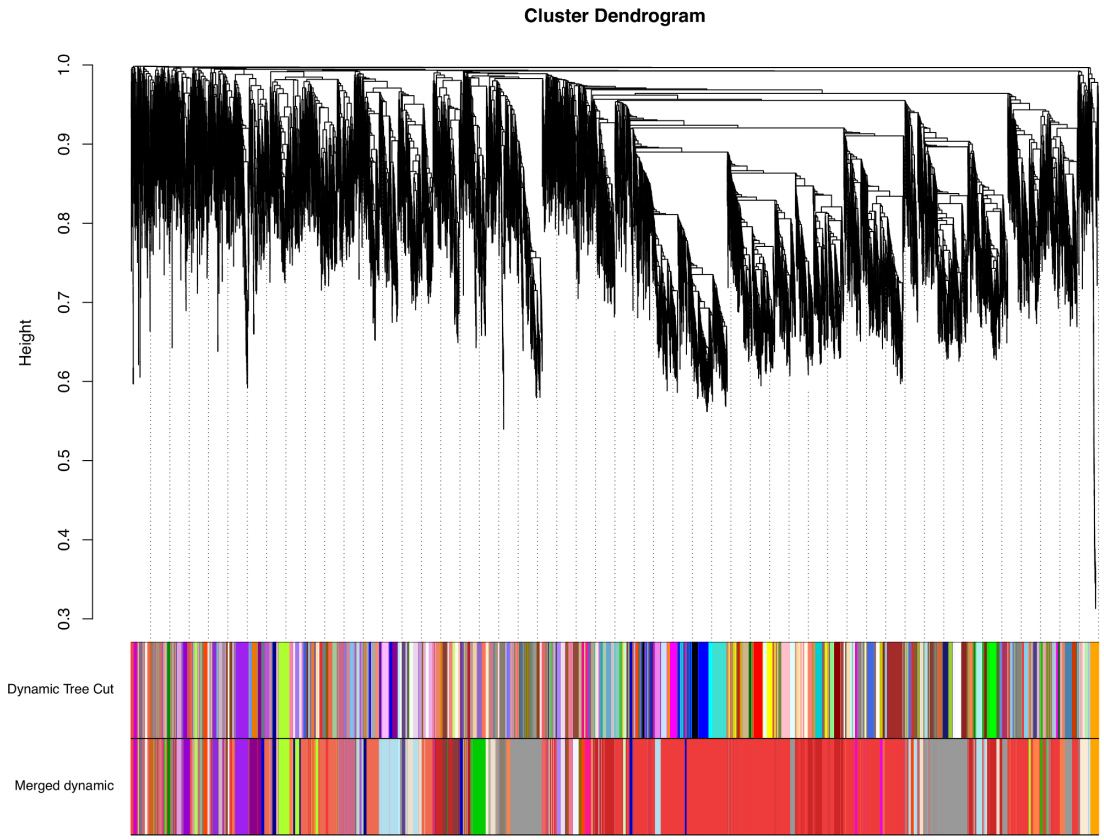

Supplementary Figure 7: Clustering dendrogram of genes, with dissimilarity based on topological overlap, together with co-expression module colors. Merged dynamic modules (lower color band) mean highly co-expressed modules are merged based on eigengene correlations in original clustered modules (upper color band).

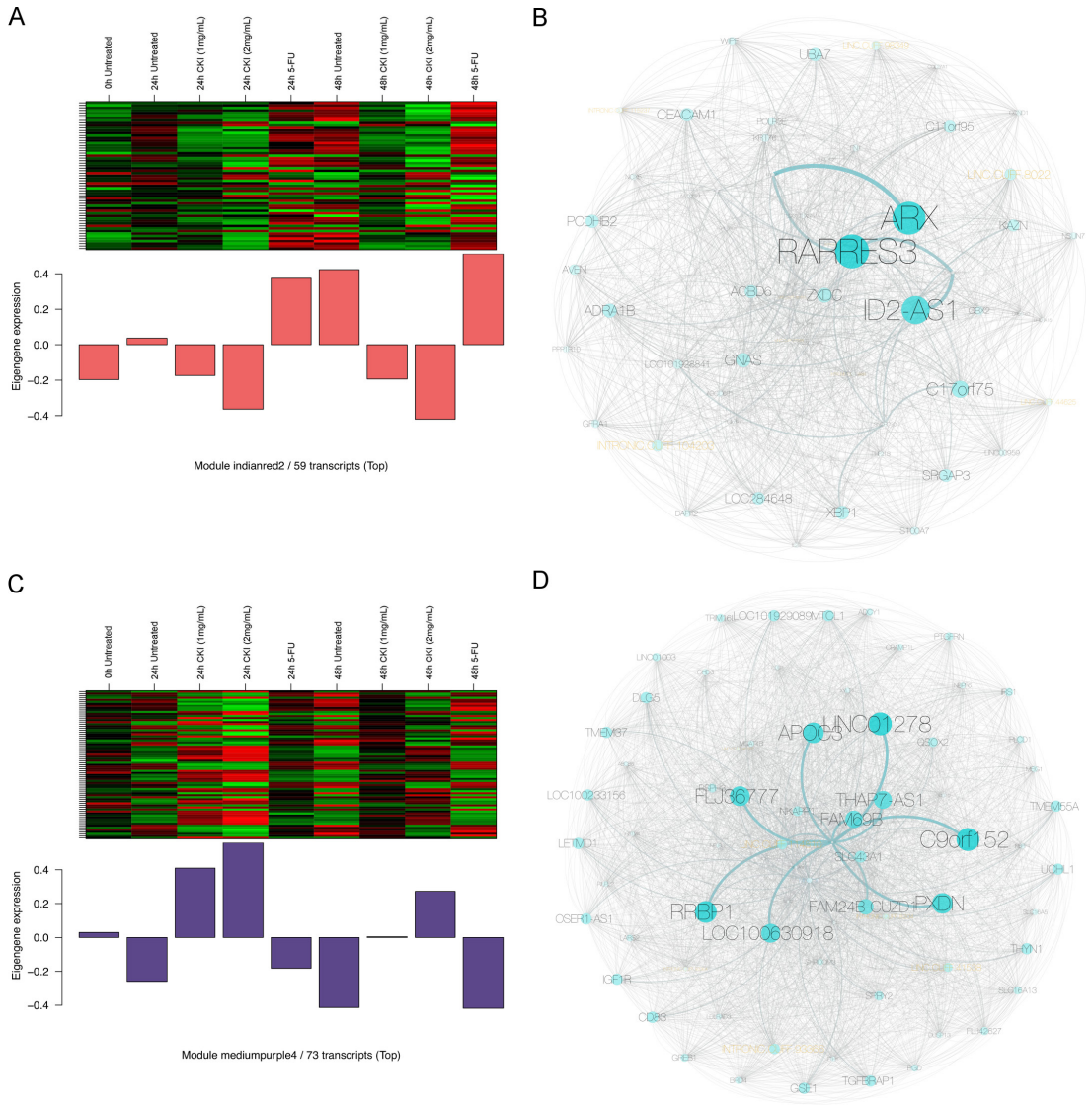

Supplementary Figure 8: Expression patterns of transcripts in CKI-specific modules "indianred2" and "mediumpurple2" are shown in the top panels A. and **C.** and the barplot in the bottom panels (A and C) shows the eigengene values for different samples. Green represents "under-expressed" and red represents "over-expressed" in the heatmap. The "eigengene value" is defined as the first principal component of this module, so it can be considered as representative of the gene expression profiles in this module. Visualization of CKI-specific modules "indianred2" and "mediumpurple2" **B.** and **D.** The black labels represent refGenes and gold labels represent lncRNAs. The size of the node/label and edge weight is proportional to betweenness centrality.

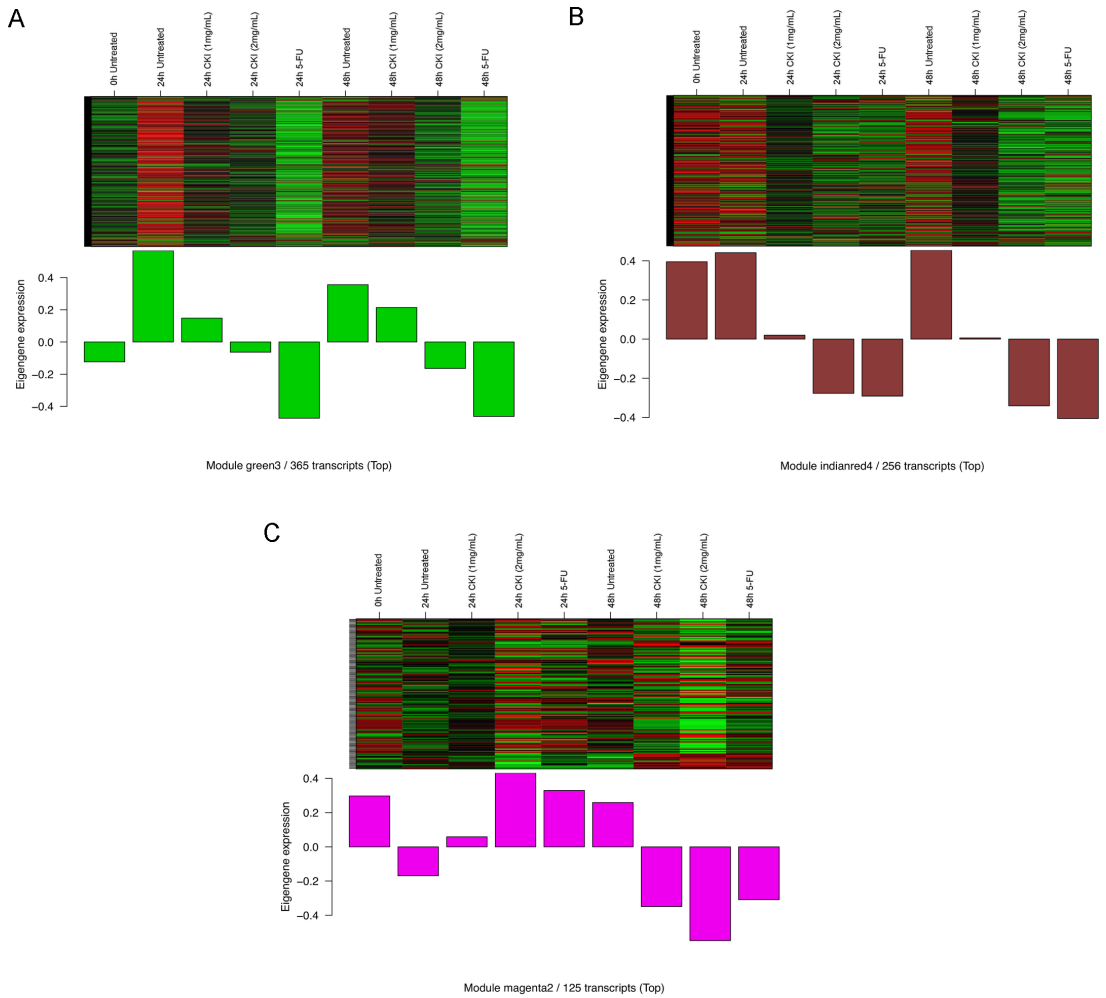

Supplementary Figure 9, Representative CKI-5FU co-expression modules. Expression patterns of transcripts in CKI-5FU modules **A.** "green3", **B.** "indianred4" and **C.** "magenta2" are shown in the top panels, and the barplot in the bottom panels show the eigengene values in different samples. Green represents "under-expressed" and red represents "over-expressed" in the heatmap. The "eigengene value" is defined as the first principal component of this module, so it can be considered as representative of the gene expression profiles in this module.

Supplementary Table 1: Summary of RNA-seq datasets used in this study

See Supplementary File 1

Supplementary Table 2: Summary of significantly differentially expressed genes for different comparisons

See Supplementary File 2

Supplementary Table 3: Significantly perturbed KEGG pathways based on SPIA analysis

See Supplementary File 3

Supplementary Table S4: Numbers of transcripts in 53 co-expression modules

See Supplementary File 4

Supplementary Table 5: Significantly over-represented GO and KEGG terms in protein-coding genes from three CKI-5FU co-expression modules (count > 4 and P-value < 0.05)

See Supplementary File 5

Supplementary Table 6: Primers used for qPCR

See Supplementary File 6

Appendix E

Supplementary Figures for Chapter 6

Supplementary Material: Cell Cycle, Energy Metabolism and DNA Repair Pathways in Cancer Cells are Suppressed by Compound Kushen Injection

Jian Cui, Zhipeng Qu, Yuka Harata-Lee, Thazin Nwe Aung, Hanyuan Shen and David L Adelson

The University of Adelaide, School of Biological Sciences, Dept of Molecular and Biomedical Sciences

1 SUPPLEMENTARY DATA

1.1 Methods

XTT assay: The wells of 96-well tray were seeded with 4×10^3 cells per well for HEPG2 cells and 8×10^4 cells per well for MDA-MB-231 cells in 50 μL of medium and cultured overnight. On the following day, 50 μL of either medium, CKI or 5-FU were added to the cells. Viability of the cells was measured at 0, 24 and 48 hours after the treatment by adding XTT:PMS (50:1; Sigma-Aldrich). After 4-hour incubation at 37C optical density (OD) of each well was read at 490nm. The background OD was also measured and the average was subtracted from the OD readings of appropriate wells.

1.2 Figures

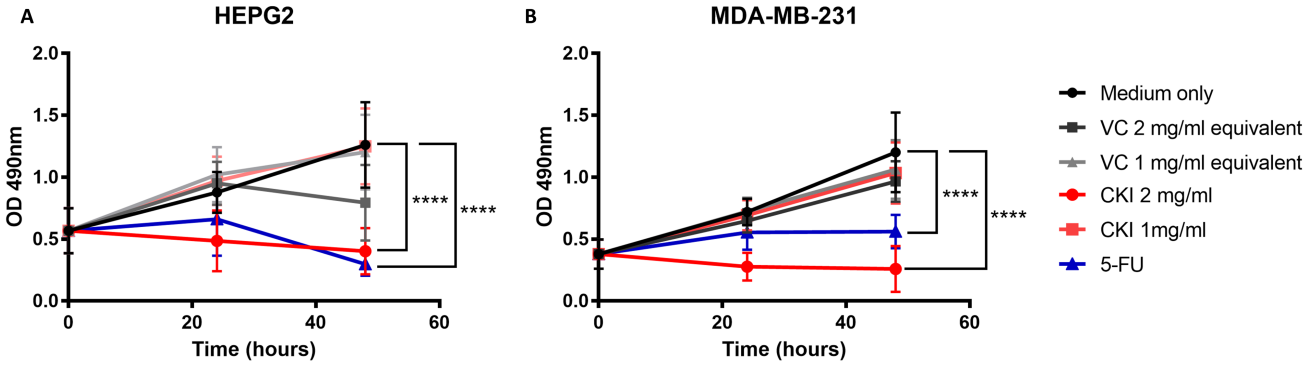

Figure S1. XTT assay result of HEPG2 and MDA-MB-231 cell lines. The XTT assay measures levels of NADH and NADPH by producing a formazan dye product that can be detected at 490nm. **A**. XTT assay result for HEPG2 cells. The assay was carried out at three time points: 0, 24, and 48 hours. 5 treatment groups were used and compared, 150 μg/ml 5-FU as a positive control for a cytotoxic agent, 1 mg/ml and 2 mg/ml CKI as well as the corresponding concentration of vehicle control (VC). CKI has a clear effect on the amount of formazan dye produced indicating a significant and marked suppression in the production of NADH and NADPH. **B**. XTT result of MDA-MB-231 cells. This test is with a low concentration of 5-FU (20 μg/ml). CKI has a clear and marked effect on the level of formazan dye produced indicating a significant and marked suppression in the production of NADH and NADPH. Statistical analyses were performed using two-way ANOVA comparing with untreated (****p$<$0.0001); bars show 1 standard deviation from the mean.

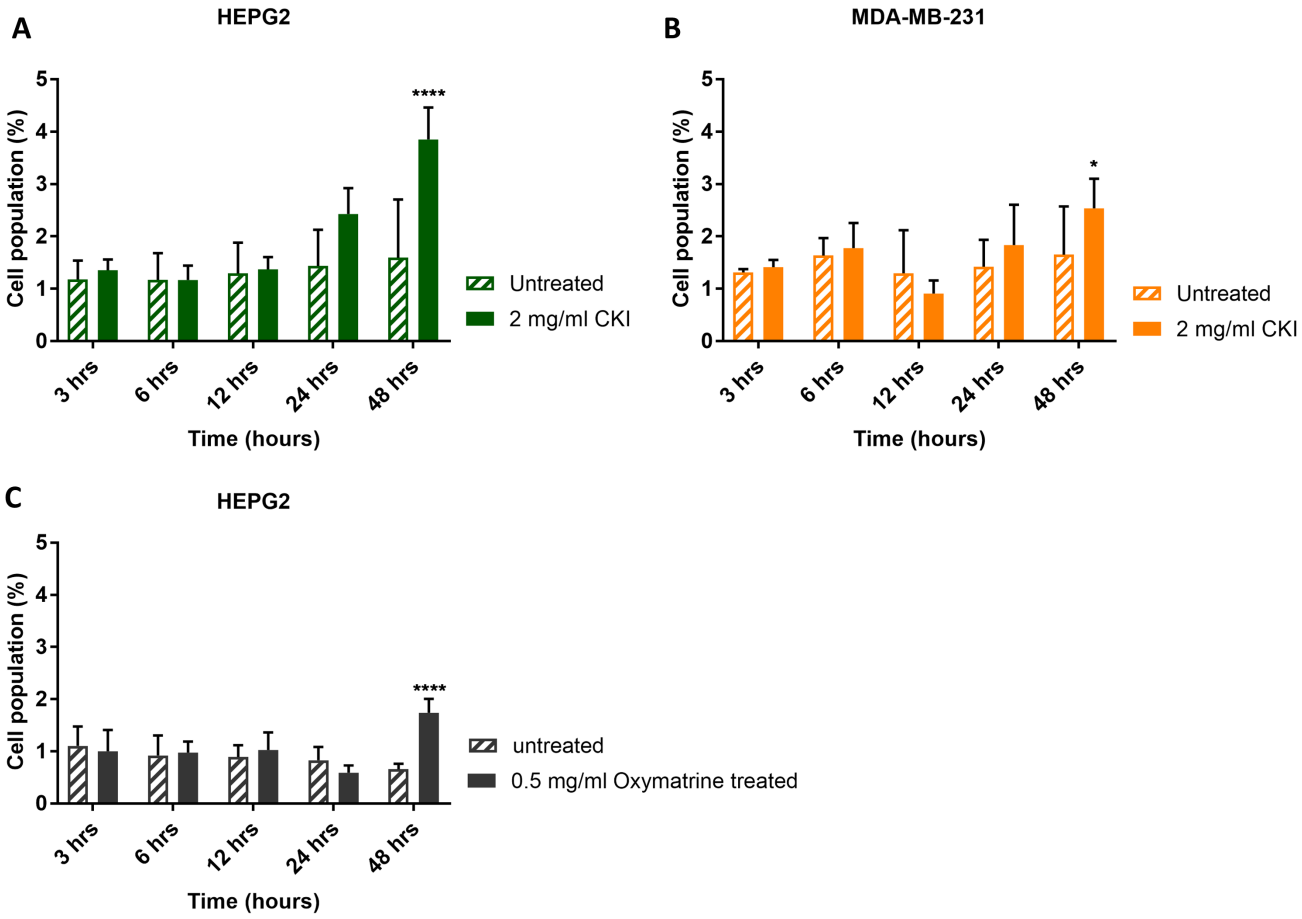

Figure S2. Cell apoptosis assay. A. Cell apoptosis in HEPG2 cells treated with CKI. The assay was carried out at 5 time points to detect apoptosis levels between untreated and 2 mg/ml CKI treated groups. From 3 to 12 hours, both groups maintained a baseline level of apoptosis. After 24 hour, apoptosis of CKI treated cells increased, with the difference attaining statistical significance at 48 hours. **B**. Cell apoptosis in MDA-MB-231 cells treated with CKI. From 3 to 24 hours, both groups show similar, if noisy results. By 48 hours apoptosis has increased and was statistically significantly different to the control. **C**. Cell apoptosis in HEPG2 cells treated with oxymatrine. We compare apoptosis levels between an untreated group and a group treated with 0.5 mg/ml oxymatrine. From 3 to 24 hours we observed a baseline level of apoptosis. By 48 hours apoptosis in the oxymatrine treated group is significantly greater than in the control group. Statistical analyses were performed using two-way ANOVA comparing with untreated (****$p<0.0001$); bars show 1 standard deviation from the mean.